

For my parents and Jackie

The characterization of the flavin-containing monooxygenase gene family of man

Azara Janmohamed

A thesis submitted in partial fulfilment of the requirements for the degree of
Doctor of Philosophy in the University of London

**Department of Biochemistry and Molecular Biology
University College London**

June 1998

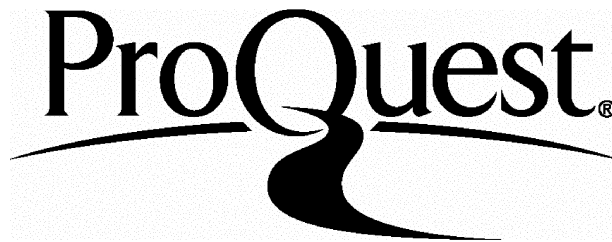
ProQuest Number: U643547

All rights reserved

INFORMATION TO ALL USERS

The quality of this reproduction is dependent upon the quality of the copy submitted.

In the unlikely event that the author did not send a complete manuscript and there are missing pages, these will be noted. Also, if material had to be removed, a note will indicate the deletion.



ProQuest U643547

Published by ProQuest LLC(2016). Copyright of the Dissertation is held by the Author.

All rights reserved.

This work is protected against unauthorized copying under Title 17, United States Code.
Microform Edition © ProQuest LLC.

ProQuest LLC
789 East Eisenhower Parkway
P.O. Box 1346
Ann Arbor, MI 48106-1346

Abstract

Flavin-containing monooxygenases (FMO) are a family of enzymes that metabolise a variety of foreign compounds such as pesticides, pharmaceuticals and toxicants. They are found in most tissues of all mammals. Five FMO isoforms (FMO1, 2, 3, 4 and 5) have been identified.

Analysis of human genomic DNA by Southern blot hybridization with cDNAs encoding the different FMO isoforms gave simple patterns of hybridization suggesting that a single gene encodes each protein.

Northern blot hybridization analyses and RNase protection assays showed that each FMO has a distinct tissue specific pattern of expression. This pattern differs between man and other species.

The skin is a major portal of entry for a variety of chemicals and environmental pollutants. FMOs 1, 3 and 5 were found to be the major forms present in human skin. *In situ* hybridization demonstrated that *FMOs 1, 3, 4 and 5* are expressed in the sebaceous gland and the epidermis.

Western blotting analysis of FMOs in whole skin homogenates and microsomes was unsuccessful due to a high degree of cross-reactivity of the polyclonal antibodies used with other skin proteins. The methimazole assay was used to determine the presence of FMO activity in skin.

The expression of FMOs in an immortalised human keratinocyte (HaCaT) cell line was also studied. These cells could offer an alternative system for biotransformation studies; this is possible only if HaCaT cells express a similar range of FMOs as the skin or primary human keratinocyte cultures. Primary cultures of human keratinocytes expressed *FMOs 1, 2, and 3* to varying degrees, whereas HaCaT cells, expressed only *FMOs 1, 4 and 5*.

An analysis of cytochromes P450 in whole human skin, primary keratinocyte cultures and HaCaT cells was undertaken. Regional localisation of CYP2As, CYP2B6 and CYP3As in the skin was the same as for FMOs.

Title.....	1
Abstract.....	2
Table of contents	3
List of tables.....	10
List of figures	12
Abbreviations	18
Acknowledgements.....	21
Introduction.....	23
1.1 Flavin containing monooxygenases (FMO).....	24
1.2 Catalytic cycle	24
1.3 FMO substrates	26
1.3.1 Amines.....	29
1.3.2 Organic sulphur compounds.....	30
1.4 Nomenclature of FMOs	32
1.4.1 FMO1	33
1.4.2 FMO2	35
1.4.3 FMO3	37
1.4.4 FMO4	39
1.4.5 FMO5	40
1.5 Fish odour syndrome/Trimethylaminuria.....	41
1.6 The Cytochrome P450-dependent monooxygenase system (CYP).....	43
1.7 CYP nomenclature and multiple forms.....	44
1.8 Importance of the CYPs.....	46
1.8.1 CYP1A subfamily.....	49
1.8.2 CYP1B subfamily.....	49
1.8.3 CYP2A subfamily:.....	51
1.8.4 CYP2B subfamily.....	52
1.8.5 CYP3A subfamily:.....	53

1.9 Metabolism of pesticides by FMOs and CYPs.....	54
1.10 The skin.....	56
1.10.1 The structure of the skin.....	57
1.10.1.1 The epidermis.....	60
1.10.1.2 The dermis.....	61
1.10.1.3 The subcutaneous layer.....	62
1.10.2 Metabolism of foreign compounds in the skin.....	63
1.10.2.1 Localisation of xenobiotic metabolising enzymes within the skin.....	63
1.10.3 FMOs in the skin.....	63
1.10.4 CYPs in the skin.....	65
1.11 Scope of thesis.....	70
Materials and Methods.....	72
2.1 Chemicals.....	73
2.2 Cell culture conditions.....	73
2.2.1 HaCaT cells.....	73
2.2.2 Primary cultures of normal human epidermal keratinocytes.....	75
2.2.2.1 Commercially obtained culture of proliferating keratinocytes.....	76
2.2.2.2 Establishment of primary cultures of human keratinocytes derived from full thickness skin.....	77
2.3 Plasmid propagation and manipulation.....	81
2.3.1 Transformation of competent E.coli cells.....	81
2.3.2 Small scale plasmid preparation and analysis.....	83
2.3.3 Restriction enzyme digestion.....	85
2.3.4 Large scale (Maxi prep) of plasmid DNA.....	86
2.3.5 Retrieval of DNA from Low Melting Point agarose gels.....	87

2.3.6 Preparation of radiolabelled probes for northern and Southern blot hybridization analysis	89
2.3.6.1 Measurement of the specific activity of the probe	91
2.4 Isolation of total RNA	93
2.4.1 Guanidine thiocyanate/lithium chloride precipitation	93
2.4.2 Ultraspec™ RNA isolation kit.....	96
2.4.3 Guanidine thiocyanate/guanidine hydrochloride extraction procedure	97
2.5 Northern blotting and hybridization analysis.....	99
2.5.1 Gel preparation.....	101
2.5.2 Sample preparation and gel electrophoresis	102
2.5.3 Northern blotting.....	102
2.5.4 Prehybridization and hybridization of northern blots.....	103
2.5.5 Washes.....	104
2.6 RNase protection assay (RPA).....	105
2.6.1 RNA transcription and transcript purification.....	108
2.6.1.1 In vitro transcription.....	109
2.6.1.2 DNase digestion.....	109
2.6.1.3 Hybridization.....	110
2.6.1.4 RNase digestion.....	111
2.6.1.5 Analysis of protected fragments	111
2.6.1.6 Standard curve.....	112
2.6.1.7 Calculation of specific radioactivity of probe.....	112
2.7 In situ hybridization	113
2.7.1 Specimen preparation.....	115
2.7.2 Slide preparation, sectioning and mounting.....	115
2.7.3 Prehybridization treatments.....	116
2.7.4 Probe preparation	117

2.7.5 Hybridization	118
2.7.6 Post-hybridization washes.....	119
2.7.7 Autoradiography.....	121
2.7.8 Development.....	121
2.8 Isolation of proteins from cell pellets derived from HaCaT cell cultures and primary keratinocyte cultures.....	122
2.8.1 Preparation of microsomes from whole skin samples.....	124
2.9 Determination of protein content.....	126
2.10 Western Blotting.....	126
2.10.1 SDS-Polyacrylamide gel preparation.....	128
2.10.2 Sample preparation and gel electrophoresis.....	129
2.10.3 Visualisation of proteins.....	130
2.10.4 Antigen detection	130
2.10.4.1 Transfer of Proteins	131
2.10.4.2 Antigen detection.....	131
2.11 Immunohistochemistry (IHC).....	133
2.11.1 IHC background and procedure.....	134
2.11.2 IHC on cultured cells	135
2.11.3 IHC on paraformaldehyde fixed tissue sections.....	137
2.11.3.1 Antigen unmasking.....	137
2.11.3.2 Antigen detection using IHC.....	138
2.12 Methimazole assay	139
2.13 Determination of P450 reductase activity	141
Results and Discussion.....	142
DNA Analysis	143
3.1 Southern blot hybridization analyses	144
3.1.1 FMO2	144
3.1.2 FMO3	145

3.1.3 FMO4	146
3.1.4 FMO5	147
3.2 Discussion.....	149
RNA Analyses	154
4.1 Detection of FMO mRNA using northern blot hybridization analyses.....	155
4.1.1 Extraction and integrity of RNA from various tissue and cell samples.....	155
4.2 Northern blot hybridization analyses	156
4.2.1 Expression of FMO1 mRNA.....	158
4.2.2 Expression of FMO2 mRNA.....	159
4.2.3 Expression of FMO3 mRNA.....	162
4.2.4 Expression of FMO4 mRNA.....	164
4.2.5 Expression of FMO5 mRNA.....	166
4.3 Summary of FMO mRNA expression	168
5.1 Detection of FMO mRNAs using RNase Protection Assays (RPAs)	171
5.2 Detection and quantification of FMO1 mRNA.....	171
5.3 Detection and quantification of FMO2 mRNA.....	176
5.3B Detection and quantification of FMO3 mRNA	181
5.4 Detection and quantification of FMO4 mRNA.....	185
5.5 Detection and quantification of FMO5 mRNA.....	188
5.6 Summary of results.....	192
Protein Analyses.....	196
6.1 Western blot analyses of cultured cells, microsomes and whole tissue proteins.....	197
6.1.1 Extraction of proteins	198
6.1.2 Sample viscosity.....	198
6.1.3 Antigen detection.....	201

6.1.4 Cross reactivity of antibodies to HaCaT and keratinocyte proteins.....	202
6.2 Western blot analyses on skin microsomes.....	203
7.1 Spectrophotometric assay of the Flavin containing monooxygenase.....	209
7.2 Results and discussion.....	212
7.2.1 Activity of heterologously expressed FMOs 1, 3 and 5.....	212
7.3 Measurement of FMO activity in whole skin microsomes.....	221
Cellular Localisation.....	229
8.1 Cell-type specific expression of FMOs in the human skin.....	230
8.2 Immunohistochemical localisation of FMOs in human skin.....	230
8.2.1 FMO1 localisation.....	231
8.2.2 FMO3 and 5 localisation.....	232
8.3 In situ hybridization analyses.....	235
8.3.1 Localisation of FMO mRNAs in human skin.....	236
8.4 Discussion.....	237
Cytochromes P450 in skin.....	259
9.1 Detection of CYPs in human skin and keratinocyte culture samples.....	260
9.2 CYP mRNAs.....	260
9.2.1 Detection of CYP2A.....	261
9.2.1.1 Northern blot hybridization analyses.....	261
9.2.1.2 RNase protection assays.....	261
9.2.2 Detection of CYP2B6.....	266
9.2.2.1 Northern blot hybridization analysis.....	266
9.2.2.2 RNase protection assay.....	269
9.2.3 Detection of CYP3A.....	273
9.2.3.1 Northern blot hybridization analysis.....	273

9.2.3.2 RNase protection assay.....	273
9.3 Localisation of CYP2A6, 2B6 and 3A4 mRNA in human skin.....	277
9.4 CYP protein expression.....	290
9.5 Discussion.....	296
<i>In vitro</i> systems for toxicological studies.....	299
10.1 In vitro systems for the study of foreign compound metabolism.....	300
10.2 Primary human epidermal keratinocytes.....	300
10.3 HaCaT cells.....	305
10.4 Discussion.....	308
11 Summary of results.....	310
Bibliography.....	317
Publications.....	340

List of tables

Table 1.1	List of some substrates metabolised by FMOs	25
Table 1.2	Reactions catalysed by the CYP system	45
Table 1.3	Summary of human CYP families and their roles	47
Table 1.4	Summary of human CYP families and subfamilies involved in foreign compound metabolism	50
Table 1.5	Examples of skin-mediated metabolic reactions	58
Table 1.6	Functional capacities of epidermal cells	57
Table 3.1	Lengths of fragments observed when human genomic DNA was digested with <i>EcoR</i> I, <i>Hind</i> III and <i>Bam</i> HI and hybridized to the cDNA encoding FMO2.	145
Table 3.2	Summary of hybridizing bands observed when human genomic DNA digested with <i>EcoRI</i> , <i>Hind</i> III and <i>Bam</i> HI was probed with the FMO3 cDNA	146
Table 3.3	Summary of fragment sizes obtained after hybridization of FMO4 cDNA to human genomic DNA digested with <i>EcoRI</i> , <i>Hind</i> III and <i>Bam</i> HI	147
Table 3.4	Summary of fragment sizes obtained when human genomic DNA was digested with <i>EcoRI</i> , <i>Hind</i> III and <i>Bam</i> HI and probed with FMO5 cDNA	148
Table 4.1	Summary of results obtained from northern blot hybridization analyses using full length cDNA clones from FMOs 1, 2, 3, 4 and 5.	170
Table 5.1	Amounts of FMOs 1, 2, 3, 4 or 5 mRNAs expressed in molecules of FMO mRNA/cell	195

Table 6.1	Summary of problems encountered during western blot analyses of proteins derived from human skin and cultured cells.	199
Table 7.1	Specific activities of FMO1, 3 or 5 expressed in insect cells, with 2mM MI as substrate	214
Table 7.2	Specific activity (nmole min ⁻¹ mg ⁻¹) of FMO1 in the presence of 0.2% Emulgen 911 and <i>n</i> -octylamine	218
Table 7.3	Summary of the specific activity (nmole min ⁻¹ mg ⁻¹) of P450-reductase in whole skin microsomes and rat liver microsomes	227

List of figures

	Page	
Fig 1.1	Major steps in the pig liver FMO catalytic cycle	27
Fig 1.2	<i>N</i> -Oxygenated products of amines	31
Fig 1.3	<i>S</i> -Oxygenated products of organic sulphur compounds	31
Fig 1.4	Summary of the oxidation products of phorate produced by CYPs and FMOs	55
Fig 1.5	Microscopic diagram of the skin	59
Fig 3.1	Human genomic DNA samples digested with <i>Eco</i> RI, <i>Hind</i> III and <i>Bam</i> HI and hybridized with the full length cDNAs encoding FMO2, FMO3, FMO4 or FMO5.	152
Fig 3.2	Structural organization of the human <i>FMO3</i> gene.	153
Fig 4.1.1	RNA samples extracted from human skin and primary cultures of human keratinocytes using the Ultraspec RNA isolation system.	157
Fig 4.1.2A	RNA samples from human tissues extracted using the guanidine thiocyanate/lithium chloride extraction procedure	157
Fig 4.1.2B	RNA samples extracted from whole skin using the guanidine thiocyanate/guanidine hydrochloride extraction procedure.	157
Fig 4.2.1	Northern blot hybridization analysis of FMO1 mRNA	160
Fig 4.2.2	Northern blot hybridization analysis of FMO1 mRNA	161

Fig 4.3	Northern blot hybridization analysis of FMO2 mRNA.	163
Fig 4.4	Northern blot hybridization analysis of FMO3 mRNA.	165
Fig 4.5	Northern blot hybridization analysis of FMO4 mRNA	167
Fig 4.6	Northern blot hybridization analysis of FMO5 mRNA	169
Fig 5.1.1	p8A1-6; construct used for FMO1 RPA analysis	172
Fig 5.1.2	pFMO2/2/15; construct used for FMO2 RPA analysis	172
Fig 5.1.3	pBSformII; construct used for FMO3 RPA analysis	173
Fig 5.1.4	2A1L-2; construct used for FMO4 RPA analysis	173
Fig 5.1.5	pIC1/1B/C; construct used for FMO5 RPA analysis	174
Fig 5.2.1	Analysis of FMO1 mRNA by RNase protection	177
Fig 5.2.2	Analysis of FMO1 and FMO2 mRNA by RNase protection	178
Fig 5.2.3	FMO1 mRNA concentrations in various tissue samples analysed	179
Fig 5.3.1	Analysis of FMO2 and FMO3 mRNAs by RNase protection	182
Fig 5.3.2	Analysis of FMO2 and/or FMO3 mRNAs by RNase protection	183
Fig 5.3.3	FMO2 mRNA concentration in various tissue samples analysed	184
Fig 5.4.1	Analysis of FMO3 and FMO5 mRNAs by RNase protection	186

Fig 5.4.2	FMO3 mRNA concentrations in various tissue samples analysed	187
Fig 5.5.1	Analysis of FMO4 and FMO5 mRNAs by RNase protection	189
Fig 5.5.2	Analysis of FMO4 and/or FMO5 mRNAs by RNase protection	190
Fig 5.5.3	FMO4 mRNA concentrations in various tissue samples analysed	191
Fig 5.6	FMO5 mRNA concentrations in various tissue samples analysed.	193
Fig 6.1	Western blot analyses with anti-FMO1, anti-FMO3 and anti-FMO3	206
Fig 6.2	Western blot analysis of heterologously expressed FMOs 1, 3 and 5 using an anti-FMO3 antibody	207
Fig 7.1	Oxygenation of methimazole by FMO	210
Fig 7.2	Oxidation of methimazole by FMO and reaction of the oxidised product with either MI or TNB	211
Fig 7.3	Activity of heterologously expressed FMO1, FMO3 and FMO5 towards MI	215
Fig 7.4	Summary of the activity of FMOs 1, 3 and 5 with methimazole as substrate	216
Fig 7.5	Activity of FMO1 in the presence of <i>n</i> -octylamine and/or Emulgen 911	219
Fig 7.6	Summary of the effects of <i>n</i> -octylamine and Emulgen 911 on the activity of FMO1	220

Fig 7.7	Activity of human skin microsomal membranes in the presence and absence of enhancers, with methimazole as a substrate	222
Fig 7.8	Activity of P450-reductase in rat liver microsomes	225
Fig 7.9	P450-reductase activity in human skin microsomes	226
Fig 8.1	Localisation of FMO1 to the proximal and distal tubules in the human kidney cortex	234
Fig 8.2	Localisation of FMO1 mRNA to the epidermis of human skin	239
Fig 8.3	Localisation of FMO1 mRNA to the sebaceous gland in human skin	241
Fig 8.4	Localisation of FMO3 mRNA to the epidermis of human skin	243
Fig 8.5	Localisation of FMO3 mRNA to the sebaceous gland of human skin	245
Fig 8.6	Localisation of FMO4 mRNA to the epidermis of human skin	247
Fig 8.7	Localisation of FMO4 mRNA to the sebaceous gland in human skin	249
Fig 8.8	Localisation of FMO5 mRNA to the epidermis of human skin	251
Fig 8.9	Localisation of FMO5 mRNA to the sebaceous gland of human skin (low magnification).	253
Fig 8.10	Localisation of FMO5 mRNA to the sebaceous gland of human skin (high magnification)	255
Fig 9.1.1	Northern blot hybridization analysis of CYP2A6 mRNA	262

Fig 9.1.2	pBS2A(288); construct used for CYP2A6 RPA analysis	263
Fig 9.1.3	Analysis of CYP2A6 and CYP3A4 mRNAs by RNase protection	264
Fig 9.1.4	CYP2A6 mRNA concentrations in various samples analysed	265
Fig 9.2.1	Northern blot hybridization analysis of CYP2B6 mRNA	267
Fig 9.2.2	Northern blot hybridization analysis of CYP2B6 mRNA	268
Fig 9.2.3	pBS2B(450); construct used for CYP2B6 RPA analysis	270
Fig 9.2.4	Analysis of CYP2B6 and CYP3A4 mRNAs by RNase protection	271
Fig 9.2.5	CYP2B6 mRNA concentrations in various samples analysed	272
Fig 9.3.1	Northern blot hybridization analysis of CYP3A4 mRNA	274
Fig 9.3.2	pBS3A(240); construct used for CYP3A4 RPA analysis	275
Fig 9.3.3	Sequence alignment of CYP3A4 with the corresponding regions of CYP3A3 and CYP3A5	275
Fig 9.3.4	CYP3A4 mRNA concentrations in various samples analysed	276
Fig 9.4	Localisation of CYP2A6 mRNA to the epidermis of human skin	279
Fig 9.5	Localisation of CYP2A6 mRNA to the sebaceous gland of human skin	281

Fig 9.6	Localisation of CYP2B6 mRNA to the epidermis of human skin	283
Fig 9.7	Localisation of CYP2B6 mRNA to the sebaceous gland of human skin	285
Fig 9.8	Localisation of CYP3A4 mRNA to the epidermis of the human skin	287
Fig 9.9	Localisation of CYP3A4 mRNA to the sebaceous gland of human skin	289
Fig 9.10	Localisation of CYP2A, 2B and 3A to the epidermis and sebaceous gland of human skin	293
Fig 9.11	Negative staining with sheep pre-immune serum	295
Fig 10.1	Northern blot hybridization analysis of P450-reductase mRNA	302
Fig 10.2	Confluent primary culture of human epidermal keratinocytes established from breast skin	307
Fig 10.3	Confluent culture of HaCaT cells	307

Abbreviations

A	Adenine
AHH	Aryl hydrocarbon hydroxylase
AP	Alkaline phosphatase
BCIP	5-bromo-4-chloro-3-indoyl phosphate
β NF	β -naphthoflavone
bp	base pairs
BPE	Bovine Pituitary Extract
C	Cytosine
cDNA	complementary DNA
Ci	Curie
cpm	counts per minute
CYP	Cytochrome P450
dATP	deoxyadenosine triphosphate
dCTP	deoxycytidine triphosphate
dGTP	deoxyguanosine triphosphate
DMEM	Dulbecco's Modified Eagles Medium
DNA	deoxyribonucleic acid
DNase I	Deoxyribonuclease I
dNTP	deoxynucleotide triphosphate
DTNB	5,5'-Dithio-bis(2-nitrobenzoic acid)
DTT	Dithiothreitol
dTTP	deoxythymidine triphosphate
<i>E. coli</i>	<i>Escherichia coli</i>
ECOD	7-ethoxycoumarin-O-dealkylase
EDTA	diaminoethanetetra-acetic acid, disodium salt
EGF	Epidermal Growth Factor
EMDM	erythromycin <i>N</i> -demethylase

EROD	7-ethoxyresorufin-O-dealkylase
FMO	Flavin-containing monooxygenase
G	Guanine
GSH	Glutathione
HEPES	N-2-hydroxyethylpiperazine-N-2-ethane sulphonic acid
HRP	Horseradish peroxidase
IAA	Isoamylalcohol
IHC	Immunohistochemistry
kb	kilobases
KGM	Keratinocyte Growth Medium
L-15	Leibowitz's L-15 medium
LB-medium	Luria-Bertani medium
MES	2-(N-morpholino)ethanesulphonic acid ^l
Methimazole	2-Mercapto-1-methylimidazole
MOPS	3-(N-morpholino) propanesulfonic acid
MPTP	1-Methyl-4-Phenyl-1,2,3,6-Tetrahydropyridine
mRNA	messenger RNA
NADH	β -Nicotinamide adenine dinucleotide, reduced form
NADPH	β -Nicotinamide adenine dinucleotide phosphate, reduced form
NBT	nitroblue 1-naphthol
NTP	nucleotide triphosphate
OD	Optical density
PAH	Polycyclic aromatic hydrocarbon
PB	Phenobarbital
PBS	Phosphate buffered saline
PIPES	Piperazine-N,N'-bis[2-ethanesulfonic acid]
PMSF	Phenylmethylsulfonyl fluoride
PROD	7-ethoxyresorufin O-deethylase
rATP	Adenosine triphosphate

rCTP	cytidine triphosphate
rGTP	guanosine triphosphate
RNA	ribonucleic acid
RNase A/T1	Ribonuclease A/T1
RPA	RNase Protection Assay
rRNA	ribosomal RNA
RT-PCR	Reverse transcriptase-polymerase chain reaction
rUTP	uridine triphosphate
SDS	Sodium dodecyl sulphate
T	Thymine
TCDD	2,3,7,8-tetrachlorodibenzo-p-dioxin
TEMED	N, N, N', N'-Tetramethylethylenediamine
TMA	Trimethylamine
TMAO	Trimethylamine N-oxide
TNB	nitro-5-thiobenzoate
TNS	Trypsin Neutralising solution
Tris	Tris(hydroxymethyl)aminoethane
tRNA	transfer RNA

Acknowledgments

During the course of this PhD, numerous people have helped me, both professionally and personally. Without their help and guidance this thesis would not have come to completion.

First and foremost, I would like to thank my supervisor, Professor Elizabeth Shephard. Although I turned up at her doorstep unexpectedly, she accepted me into her lab and from that time onwards has been more than just a supervisor. Thank you for your help, encouragement, for always being there to listen to me and for having faith in me.

For fear of sounding sentimental, although I have been away from my home and family, because of Professor Shephard and the present members of Lab 402, I have never felt far from family. For that I am and will always be extremely grateful.

I would like to thank Dr. Colin Dolphin for his help, advice and comments especially with the RNase protection and enzyme activity assays; Dr. Mike O'Hare and the members of his lab at the Department of Surgery, especially Sue and Catherine whose help with the primary cultures was invaluable; Prof. Jeremy Brockes and the members of his lab, especially Dr. Anoop Kumar, for their assistance with all the microscopic work; Dr. Sharon Hotchkiss for allowing me into her laboratory and the members of her laboratory for their time and patience in teaching me the microsome preparation procedure; Dr Richard M. Philpot and Dr. Patrick Maurel for providing me with the FMO and CYP antibodies; Professor Norbert Fusenig for his kind gift of the HaCaT cells; the Stephen Kirby Skin bank for the human skin samples; Mr. Neil Bilbe at the Department of Histopathology, UCL, for being so helpful with the slide preparation.

So many people in the Biochemistry Department of UCL and elsewhere have helped me in so many ways, these include, Professor Ian

Phillips, Dr. Mina Edwards, Professor Peter Campbell, Dr. Mike Rosemeyer, Michael, Paul and Tony (Biochemistry stores), Noreen, Lorraine, Dee and Julyan (Departmental office).

There are a group of people who have been a constant source of encouragement to me, without their help and support, I would never have reached this stage. These are Siew Cheng Wong, Marie Bootman, Shagufta Ahmed, Bina Bhamra, Roongsiri Muangmoonchai, Penny Smirlis and Helen Dell.

I owe a great debt of gratitude to Mr. Roshanali Merali and his family for their financial support which has enabled me to continue my studies in London; to A.A.L. for his initial financial commitment, were it not for him I would never have come to study in London; the Committee of Vice Chancellor and Principles of the UK (CVCP) for their funding assistance; Mr Philip Ransley, and of course Jackie, who has been so generous both financially and emotionally in the past years. You're the best sister one could ask for.

My parents have always been there for me, supporting me through thick and thin and having faith in me when nobody else did. Thank you for all the sacrifices you have made for me and for putting up with me.

Last but not least I would like to thank Peter Venables for his advice, support and understanding towards the end of this PhD. Thank you for being there for me during the worst and the best times.

INTRODUCTION

1.1 Flavin containing monooxygenases (FMO)

The flavin containing monooxygenases (FMOs) are a family of foreign compound metabolising enzymes found in the endoplasmic reticulum of most tissues of all mammals studied to date (Ziegler, 1988). The first FMO to be isolated was that from pig liver microsomal membranes (Ziegler and Mitchell, 1972, Pettit *et al.*, 1964, Masters and Ziegler, 1971). This protein is now known as FMO1 (Lawton *et al.*, 1994). The discovery of additional FMO forms in rabbit lung (Tynes *et al.*, 1985, Williams *et al.*, 1984), liver (Ozols, 1989) and in man (Dolphin *et al.*, 1992) have led to the description of at least five members in the *FMO* gene family.

Much of the catalytic data available on FMOs pertains to FMO1. However, recent studies with other FMO isoforms that have been expressed, via their cDNAs, in heterologous expression systems has led to further elucidation of the mode and mechanism of action of this family of enzymes.

FMOs catalyse the oxygenation of soft nucleophilic centres such as nitrogen, sulphur, phosphorous and selenium atoms in a large number of structurally diverse compounds (Ziegler, 1993). Some of the substrates metabolised by the FMOs are listed in Table 1.1. The broad substrate specificities of the FMOs are a consequence of the unusual features of their catalytic cycle.

1.2 Catalytic cycle (Ziegler, 1993)

The catalytic cycle of FMOs is based upon detailed kinetic and spectral studies carried out with FMO purified from pig liver microsomes (FMO1) and to a limited extent with FMO isolated from rabbit lung microsomes (FMO2) (Poulsen and Ziegler, 1979, Beaty and Ballou, 1980).

Functional group	Compound class	Example
$RSH \rightarrow RSSR$	<i>Sulfur Oxidation</i>	
$RSSR \rightarrow \begin{array}{c} O \\ \\ RSSR \end{array}$	Thiols	Cystamine \rightarrow cysteamine
$RSSR \rightarrow \begin{array}{c} O \\ \\ RSSR \end{array}$	Disulfides	
$RSR \rightarrow \begin{array}{c} O \\ \\ RSR \end{array} \rightarrow \begin{array}{c} O \\ \\ RSR \\ \\ O \end{array}$	Sulfides	Cimetidine, Aldicarb
$\begin{array}{c} SH \\ \\ -N-C-NH \\ \\ R \end{array} \rightarrow \begin{array}{c} S=O \\ \\ -N-C-NH_2 \\ \\ R \end{array} \rightarrow \begin{array}{c} SO_2H \\ \\ -N-C=NH \\ \\ R \end{array}$	Thiocarbamides	
$\begin{array}{c} S \\ \\ R-C-NH_2 \\ \\ R \end{array} \rightarrow \begin{array}{c} S=O \\ \\ R-C-NH_2 \\ \\ R \end{array} \rightarrow \begin{array}{c} SO_2H \\ \\ R-C=NH_2 \\ \\ R \end{array}$	Thioamides	Thioacetamide, thioacetamide
$\begin{array}{c} -N \\ \\ SH \\ \\ =N \\ \\ H \end{array} \rightarrow \begin{array}{c} -N \\ \\ \cdot SOH \\ \\ =N \\ \\ H \end{array} \rightarrow \begin{array}{c} -N \\ \\ SO_2H \\ \\ =N \\ \\ H \end{array}$	Mercaptopurines and pyrimidines	
	<i>Nitrogen Oxidation</i>	
<i>Acyclic</i> $\begin{array}{c} R_1 \\ \\ R-N \\ \\ R_2 \end{array} \rightarrow \begin{array}{c} OH \\ \\ R-N-R_2 \\ \\ R_1 \end{array}$	Tertiary amines	Chlorpromazine, cocaine, fluphenazine, nicotine
<i>Cyclic</i> $\begin{array}{c} R \\ \\ N \\ \\ CH_3 \end{array} \rightarrow \begin{array}{c} R \\ \\ N \\ \\ O^+ \\ \\ CH_3 \end{array}$		
$R-NH-R_1 \rightarrow \begin{array}{c} OH \\ \\ R-N-R_1 \end{array} \rightarrow \begin{array}{c} O \\ \\ R-N-R_1 \end{array}$	Secondary amines	Desipramine, N-methylamine
$\begin{array}{c} NH_2 \\ \\ R-N \\ \\ R_1 \end{array} \rightarrow R + \begin{array}{c} OH \\ \\ N-NH_2 \\ \\ R_1 \end{array}$	Hydrazines	Dimethylhydrazine, procarbazine, benzylhydrazine
$\begin{array}{c} \\ \\ \\ \\ N-R \\ \\ H \end{array} \rightarrow \begin{array}{c} \\ \\ \\ \\ N-R \\ \\ OH \end{array}$	N-Alkylarylamines	2-Acetylaminofluorene

Table 1.1 List of some substrates metabolised by FMOs (reproduced from Hayes 1994)

The most distinctive characteristic of the catalytic cycle is that unlike all other monooxygenases bearing flavin or other prosthetic groups, the substrate is not required for dioxygen reduction by NADPH. This is because FMO is present within cells in the very reactive 4a-hydroxyperoxyflavin form (FAD-OOH). Oxygen activation occurs before substrate addition and therefore any compound gaining access to the enzyme bound hydroperoxyflavin is a potential substrate. Any soft nucleophile that can make contact with this potent monooxygenating agent will be oxidised (fig 1.1). This is the only point (step 1) of contact between the xenobiotic and the terminal oxygen of the hydroperoxyflavin that is required for product formation. This unique property of FMOs is responsible for the broad substrate specificity of these flavoenzymes.

The product (SO), formed by oxygen transfer from the hydroperoxyflavin to the nucleophile, is released immediately. The intermediate steps (1, 2, 3, 4 and 5) regenerate the enzyme-bound oxygenating agent from NADPH and oxygen. The substrate is not required for any of these steps.

The energy required to drive the reaction is present in the enzyme before it encounters the xenobiotic, therefore the precise fit usually required to lower the energy of activation of an enzyme-catalyzed reaction is not necessary.

1.3 FMO substrates

The substrates for FMOs are various and include a number of pharmaceuticals, pesticides and toxicants. Substrates include secondary and tertiary amines (Ziegler and Mitchell, 1972), secondary hydroxylamines (Poulsen *et al.*, 1974b), hydrazines (Prough, 1973), thioamides,

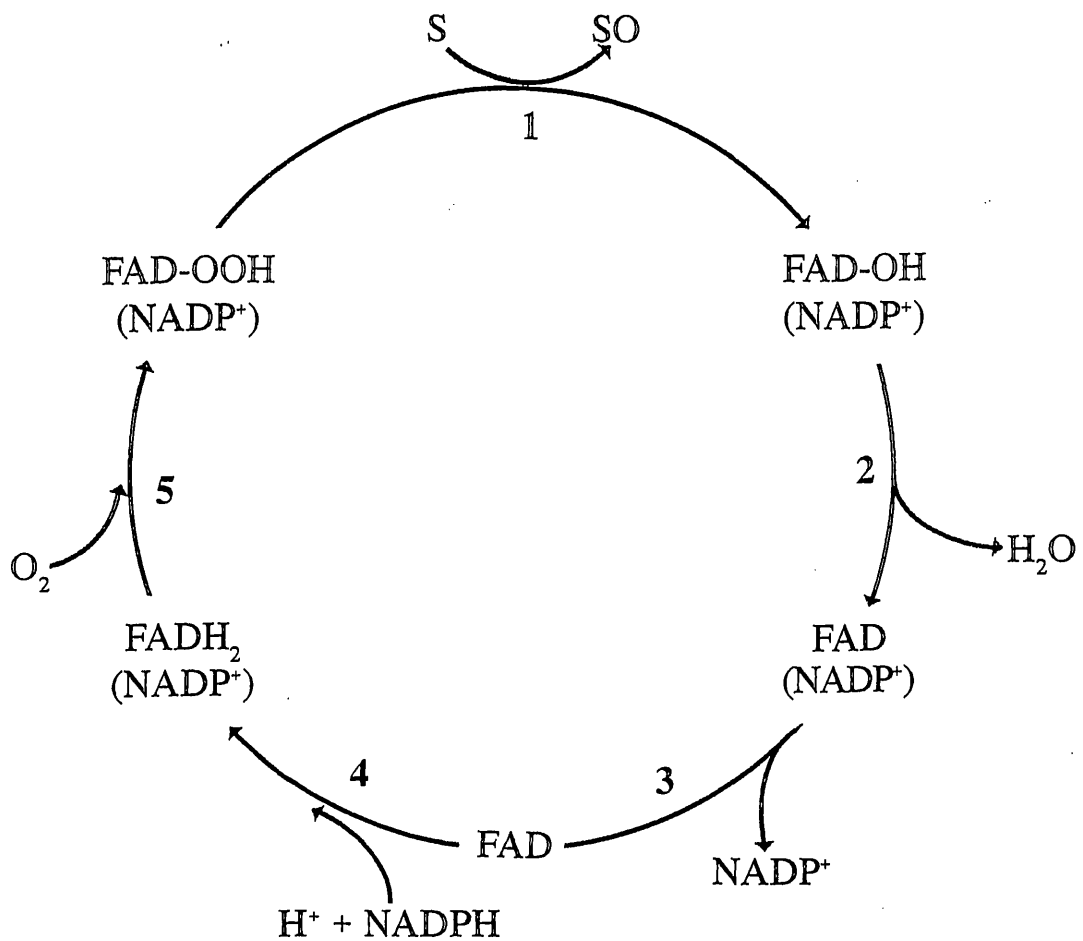


Fig 1.1 Major steps in the pig liver FMO catalytic cycle (from Ziegler, 1993)

Nucleophilic attack by the substrate (S) on the terminal oxygen of the enzyme bound hydroperoxyflavin, followed by heterolytic cleavage of the peroxide, forms the oxygenated product (SO).

thiocarbamides (Poulsen *et al.*, 1974a), sulphides, thiols and disulphides (Ziegler, 1980). Sulphoxidations catalysed by FMO appear to be a major route for the detoxification of drugs (Ziegler, 1988) and pesticides (Hajjar and Hodgson, 1980, Hajjar and Hodgson, 1982) bearing sulfide side chains.

The monooxygenase activity generally makes these compounds less toxic than the parent compounds, however, it converts some chemicals such as alkylhydrazines and aminoazobenzenes, to potentially toxic derivatives (Kadlubar *et al.*, 1976, Prough, 1973).

Of the functional groups bearing nitrogen, only amines, hydroxylamines and hydrazines are sufficiently nucleophilic to serve as substrates for FMO. Medicinal amines that fall into this categories include, antihistamines, monoamine oxidase inhibitors and tricyclic antipsychotic drugs with basic side-chains (Ziegler, 1988).

Neurotoxins such as the tertiary amine, MPTP (1-Methyl-4-Phenyl-1,2,3,6-Tetrahydropyridine), have been shown to be metabolised by FMOs. In mice (Chiba *et al.*, 1988, Chiba *et al.*, 1990) and rats (Di Monte *et al.*, 1988) the *N*-oxide is the principal product and accounts for 95-96% of the total MPTP metabolised by liver FMO. Limited studies with human liver whole homogenates suggest that *N*-oxygenation is also a major route for the metabolism of MPTP in man (Cashman and Ziegler, 1986). This reaction is catalysed exclusively by the FMOs. MPTP is also a substrate for P450s, producing nor-MPTP, however results suggest that P450s play a minor role in the metabolism of MPTP.

The only known physiological substrate for FMOs is cysteamine, which is converted to cystamine (Ziegler and Poulsen, 1977, Poulsen and Ziegler, 1977).

It is not clear why physiologically essential soft nucleophiles such as polyamines, amino acids and peptides, which are especially rich in cells, are also not oxidised by this enzyme. Although the 3-D structure of FMO is not

available, based on substrate structure-activity studies, it has been suggested that ionic groups on cellular nucleophiles are an important factor (Taylor and Ziegler, 1987). FMO readily catalyses the oxidation of monocationic amines or of anionic sulphur compounds where the charge is localised on sulphur e.g thioacetate, but the addition of a second charged group anywhere on the molecule generally blocks FMO activity. Except for cysteamine, all essential cellular nucleophiles are dications (polyamines), dipolar ions (amino acids and peptides) or have one or more anionic groups distal to the nucleophilic heteroatom (coenzyme A, biotin, thiamin pyrophosphate, etc). Therefore, this suggests that the position and number of ionic groups are the principal factors that enable the enzyme to discriminate between essential and xenobiotic soft nucleophiles. In addition to charge, steric features appear to exclude certain types of soft nucleophiles, e.g FMO from liver will not catalyse the oxidation of primary amines, although virtually all secondary or tertiary alkyamines free from other ionic groups are excellent substrates (Ziegler, 1990).

Of the broad range of FMO substrates mentioned above, those of particular importance to pharmacologists are those that contain nitrogen or sulphur. The reactions that some of these substrates undergo are described below.

1.3.1 Amines

N-Oxygenation of tertiary amines yields products referred to as amine oxides, which in an aqueous environment are protonated to form a quaternary derivative of hydroxylamine (fig 1.2). The amine oxides are stable and form crystalline *N, N, N* - trisubstituted hydroxylammonium salts with acids. The amine oxides are quite polar and those of low molecular weight are readily excreted.

N-oxides of many aliphatic and alicyclic tertiary amine drugs have been detected in urine of several species after administration of the parent compound (Jenner, 1971). Large species differences have been reported, and highest rates of *N*-oxidation are observed with hepatic tissues from pigs, dogs and guinea pigs. The *N*-oxygenation rate is also high in humans and is a major pathway for the metabolism and disposition of trimethylamine and a number of medicinal tertiary amines (Bickel, 1971). Lack of hepatic FMO-catalysed trimethylamine metabolism results in trimethylaminuria (fish odour syndrome) in man (described in section 1.5) (Al Waiz *et al.*, 1987a, Al Waiz *et al.*, 1987c).

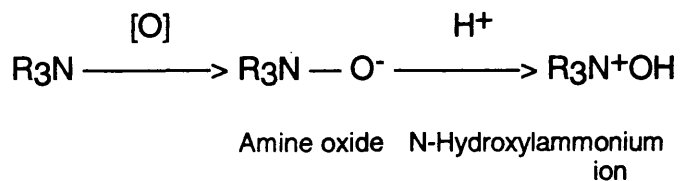
The *N*-oxygenation of secondary amines yields the corresponding hydroxylamine, which at physiological pH exists as neutral molecules. Hydroxylamines are fairly reactive compounds and are particularly susceptible to further oxidation to nitrones (fig 1.2). Coutts and Beckett (1977) have suggested that *N*-oxygenation may be a significant route for the metabolism of many medicinal secondary amines. However, tissue concentrations of secondary hydroxylamines are quite low, this is probably due to the presence of NADH-dependent hydroxylamine reductase in hepatic microsomes, which rapidly reduces primary and secondary hydroxylamines (Kadlubar *et al.*, 1973).

1.3.2 Organic sulphur compounds

Foreign compounds bearing nucleophilic divalent sulphur atoms fall into the following categories: sulphides, thiols, disulphides and thiones. Alkyl and aryl sulphides are readily oxygenated to sulphoxides and sulphones (fig 1.3).

Sulphoxides and sulphones are more polar than the parent sulphide and a number are excreted in the urine. Gillette and Kamin, (1960), have

Tertiary amines



Secondary amines

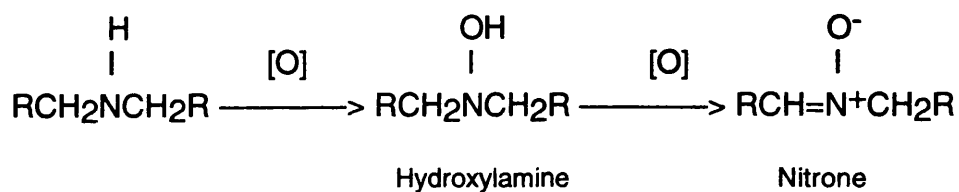
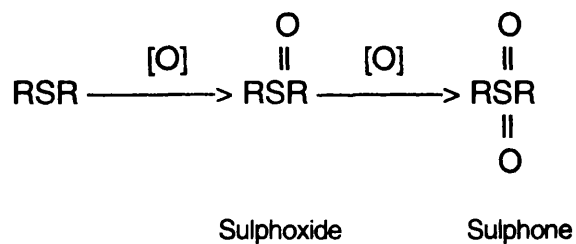


Fig 1.2 *N*-Oxygenated products of amines (from Ziegler,1980)

Sulphides



Thiols

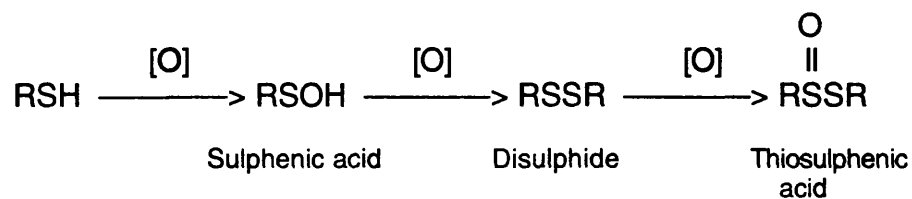


Fig 1.3 *S*-Oxygenated products of organic sulphur compounds (from Ziegler,1980).

shown that *S* -oxygenation of lipophilic sulphides is a common pathway for their metabolism and disposition and an important route for the detoxication of sulphides.

Oxidation of aryl or alkyl thiols yields extremely reactive sulphenic acids that react almost instantly with thiols yielding disulphides as the first stable oxidation product (fig 1.3). Further oxidation of disulphides can generate a host of intermediate products formed by sequential *S* -oxygenation or by *S* -oxygenations followed by hydrolytic cleavage of the sulphur-sulphur bond. *In vivo* the oxidation of foreign compounds beyond the stage of its disulphide would probably not occur. This is because alkyl or aryl sulphenic acids would preferentially react with glutathione (GSH) yielding mixed disulphides, the non-enzymatic reduction of which by GSH would regenerate the foreign thiol. This could lead to the depletion of GSH in tissues (Ziegler, 1980).

1.4 Nomenclature of FMOs (Lawton *et al.*, 1994)

FMO nomenclature is based on the comparisons of the percentage identities of the amino acid sequences of the mammalian FMOs. The identities between different forms are between 50 and 58% whereas that between apparent orthologues are 82% or greater.

The prefix, "FMO" is used to designate the gene family. The root symbol is followed by an Arabic numeral to distinguish each member of the family. The order of naming follows the chronology of publication of full-length sequences for each of the five forms. The symbols for the gene and cDNAs are italicized and symbols for the mRNAs and proteins are non-italicized. From the calculated rate of evolution of the FMOs, it appears that these enzymes arose 250-300 million years ago, about 200 million years prior to mammalian speciation (Dolphin *et al.*, 1991, Dolphin *et al.*, 1992).

1.4.1 FMO1

Human FMO1 is encoded by a single gene and the complete nucleotide sequence of the cDNA encoding FMO1 has been determined (Dolphin *et al.*, 1991). The deduced amino acid sequence shares 87% identity with the primary sequences of both the pig (Gasser *et al.*, 1990) and rabbit (Lawton *et al.*, 1990) hepatic forms of this FMO. FMO1 has been shown to be primarily a foetal form in human liver (Dolphin *et al.*, 1996), unlike its orthologue in pigs and rabbits where it constitutes the major form in this tissue. FMO1 mRNA is found in several foetal tissues including the liver, kidney and brain samples (Dolphin *et al.*, 1996). The significance of FMO1 in the developing human foetus is at present not known. In adult humans, FMO1 mRNA has been shown to be present in the kidney and in the skin (Dolphin *et al.*, 1996).

FMO1 is expressed in a gender specific manner in the livers of CD-1 mice (Falls *et al.*, 1995). The situation is similar with other mice strains (Swiss-Webster, C57BL/6 and DBA/2). These studies, based on the protein and mRNA levels, show that *FMO1* expression is 2-3 times higher in females than in males. Densitometric readings of western blot analysis of hepatic microsomes from male and female CD-1 mice, with anti-FMO1, showed that females exhibited two-three times more FMO1 than males. Hepatic RNA analysis of CD-1 mice, using northern blotting, showed a 2.4 kb transcript hybridized to FMO1 cDNA. The levels of this transcript in females was two times that found in males.

The expression of FMO1 in rabbit tissues has been investigated at the mRNA and protein levels in both male and female liver, lung, kidney, oesophagus, intestine, nasal mucosa (maxilloturbinates and ethmoturbinates) and gonadal tissue. Northern blot hybridization analysis performed with cDNA

probes for FMO1 showed marked differences in mRNA expression between tissues, with *FMO1* expression being highest in liver and intestine, followed by ethmoturbinates, maxilloturbinates and low, but detectable, levels in female kidney. Western blot analysis showed similar expression patterns of the FMO1 protein in these tissues (Shehin Johnson *et al.*, 1995)

The levels of FMO1 mRNA also appear to be increased during mid- and late-gestation in the liver of pregnant rabbits. *FMO1* in liver may also be regulated during gestation by progesterone or glucocorticoids as administration of these steroids enhance FMO1 mRNA levels 4-fold (Lee *et al.*, 1995). Therefore, it has been suggested that these steroids may play a role in the regulation of this FMO.

Recently, the expression of *FMO1* in sheep liver has been described (Longin Sauvageon *et al.*, 1998). This protein is a minor form expressed in the sheep liver, thus the profile of expression of FMOs in sheep liver is more like that found in humans and mice, rather than in animals such as the pig and rabbit.

Recent studies on *FMO1* have extended into the regulatory elements within the rabbit *FMO1* gene. This work has identified the presence of two promoters, a major upstream promoter, P₀, which initiates transcription from exon 0 and a second minor promoter, P₁, located approximately 200 bp downstream and initiating transcription from exon 1 (Luo and Hines, 1996). Transcription initiation from the major (P₀) promoter results in a mature mRNA in which exon 1 has been removed by alternative splicing. Thus, two mRNA species are possible, differing only in their 5' untranslated information. Deletion analysis and transient expression in HepG2 cells, has led to further definition of the major promoter and the identification of several positive and negative upstream regulatory domains (Luo and Hines, 1997). Upstream of P₀, three positive and two negative regulatory regions have been identified. Both P₀ and P₁ share the most proximal, positive regulatory domain but are

regulated differentially by more distal 5' sequences. Another potent negatively acting element has also been observed within intron 1.

1.4.2 FMO2

FMO2 was previously referred to as the "lung" form, due to its presence, in large amounts, in rabbit lung samples (Williams *et al.*, 1984, Tynes *et al.*, 1985). It was identified as being both immunochemically and enzymatically distinct from the form found in rabbit hepatic microsomes (Tynes *et al.*, 1986, Williams *et al.*, 1985, Tynes and Philpot, 1987).

Phillips *et al.*, (1995) have isolated a cDNA encoding human FMO2. RNase protection assays have demonstrated relatively high abundance of FMO2 mRNA in both adult and foetal human lung samples (Dolphin *et al.*, 1998 (submitted)). Williams *et al.*, (1990) found that FMO2 was undetectable by western blotting in all but one of 29 human lung samples, although it was abundant in the lung of rhesus macaque. An analysis of the cDNA nucleotide sequence of human FMO2 shows an in-frame translation termination codon, TAG, at codon 472. This codon is 64 codons upstream of a second in-frame termination signal corresponding exactly with the stop codon present in the cDNAs encoding FMO2 of rabbit (Lawton *et al.*, 1990), guinea pig (Nikbakht *et al.*, 1992) and rhesus macaque (Yueh *et al.*, 1997). Studies with a heterologously expressed human FMO2 lacking 64 amino acid residues from its C-terminus, showed that although this protein was targeted to the membrane of the endoplasmic reticulum, it was catalytically inactive. The lack of pulmonary expression of FMO2 in man may be due to the truncated polypeptide being unable to fold correctly and thus it is rapidly degraded.

The cDNA encoding rabbit FMO2 has been isolated and has 56% sequence similarity to that of a rabbit FMO1 cDNA (Lawton *et al.*, 1990). Northern blot analysis of rabbit lung total RNA show the presence of four

distinct transcripts ranging in size from 2.4, 2.6, 4.8 and 6.0 kb. It has been suggested that these bands represent FMO2 mRNA in differing stages of alternative splicing or variable 3' processing, the latter being consistent with the presence of multiple putative polyadenylation sites (Breitbart *et al.*, 1987).

Western blot analysis of tissues from guinea pigs, hamsters, rats, rabbits and mice have shown that FMO2 is expressed predominantly in the lung (Tynes and Philpot, 1987, Lawton *et al.*, 1990). The same studies showed that FMO2 was also detected in the kidney of rabbits, mice and hamster, but not in the kidney of guinea pig or rat. In the rabbit lung, FMO2 has been localised to the non-ciliated bronchiolar epithelial (Clara) cells by immunohistochemistry (Overby *et al.*, 1992). The FMO2 protein was also found in the ciliated, endothelial, type I and type II cells, and in the tracheal lining layer of rabbit lung.

FMO2 mRNA and protein is also present in the rabbit nasal mucosa, specifically the maxilloturbinates and ethmoturbinates areas and in the oesophagus (Shehin Johnson *et al.*, 1995). Sex-related differences in the expression of FMO2 were observed, with higher amounts of mRNA present in female rabbit oesophagus, nasal mucosa and kidney. Western blot analysis show a similar pattern of expression of the FMO2 protein in the same tissues. These workers suggest that the presence of high amounts of FMO2 in the olfactory tissues is probably due to their role in the removal of noxious odourants, detoxification of xenobiotics and perhaps odourant processing.

Recently, a cDNA clone with 85 and 84% sequence identity to the FMO2 cDNAs from rabbit and guinea pig respectively, has been isolated from the rhesus macaque (Yueh *et al.*, 1997). In this species also, the FMO2 protein was predominantly in the lung, with very little being expressed in the liver. FMO2 protein was also expressed in the nasal tissue but to levels that were lower than that found in the rabbit respiratory and olfactory tissues.

FMO2 shows catalytic characteristics that differ from the pig liver form (FMO1). FMO2 has a broader and higher pH optimum, it is not sensitive to inhibition by sodium cholate and is not as thermolabile as FMO1 (Williams *et al.*, 1985). Unlike FMO1, FMO2 has been shown to be inhibited by *n*-octylamine. FMO2 is inactive towards tricyclic antidepressants such as chlorpromazine and imipramine both of which are excellent substrates for FMO1 (Williams *et al.*, 1984).

FMO2 gene expression has been demonstrated to be regulated by sex hormones in experimental animals (Lee *et al.*, 1993, Lee *et al.*, 1995). During mid- and late-gestation, maternal rabbits have shown an increase in FMO2 protein in the lung. Studies on the rabbit *FMO2* gene (Wyatt *et al.*, 1996) have identified putative glucocorticoid responsive elements in the 5' flanking region. It has been suggested that hormonal levels regulate the induction of this FMO.

1.4.3 FMO3

A full length cDNA for FMO3 was isolated from an adult human liver cDNA library (Lomri *et al.*, 1992). A subsequent publication by Dolphin *et al.*, (1996) however showed a sequence which was variable to that obtained by Lomri *et al.* The latter sequence differs at seventeen residues when the two sequences are aligned. Further revisions of this sequence have been made and the most up to date information on the *FMO3* gene, cDNA sequence and predicted amino acid sequence have been recently published (Dolphin *et al.*, 1997b). The revised sequences show an amino acid sequence identity of 84% with that of the deduced rabbit FMO3 cDNA sequence (Burnett *et al.*, 1994).

Analysis of the tissue distribution of FMO3 mRNA shows that it is expressed primarily in the human liver (Dolphin *et al.*, 1996). The mRNA was

detected in lower abundance in adult kidney and lung. In human foetal samples, FMO3 mRNA was present at low concentrations in a single lung sample, in each of two liver samples, but was not detected in samples of kidney. In human liver, *FMO3* seems to be the most abundantly expressed *FMO*. Using monospecific antibodies and recombinant isoforms as standards, Overby *et al.*, (1997) showed that the amount of FMO3 was greater than that of FMO5 in all samples analysed. Recent studies on *FMO3* shows that mutations within the gene are responsible for the genetic disorder called 'fish-odour syndrome' (Dolphin *et al.*, 1997a) (section 1.5).

Variable species and tissue-specific differences in the expression of FMO3 mRNA have been observed in the distribution of FMO3 mRNA in the liver, lung and kidney of rabbit, rat, guinea pig, hamster and mouse (Burnett *et al.*, 1994). High amounts of FMO3 mRNA are expressed in the liver of rabbits, hamsters and mouse. The kidney of rat, guinea pig and mice also express high amounts of FMO3 mRNA. In mice, FMO3 mRNA is expressed in a gender specific manner, and is only expressed in the livers of females but not in males (Falls *et al.*, 1995). Recent studies by the same group have found that FMO3 mRNA was not expressed in mouse kidney of either gender (Falls *et al.*, 1997). These results were confirmed with western blot analysis which showed similar gender and tissue dependent expression of *FMO3* in mice.

Recent studies on the expression of FMOs in sheep liver, have shown that sheep predominantly express *FMO3* in their livers (Longin Sauvageon *et al.*, 1998). Thus, sheep show a profile of hepatic FMO expression that is similar to humans and female mice, but unlike that of other animals that predominantly express FMO1 as the major hepatic form.

The structural organization of the *FMO3* gene of human has been determined using a novel vectorette PCR based approach (Dolphin *et al.*, 1997). The *FMO3* gene contains 9 exons, the first of which is non-coding. The gene has a minimum size of 22.5 kb. The intron/exon structure described

by Dolphin *et al.*, (1997), is similar to that reported for rabbit *FMO1* (Wyatt *et al.*, 1996). The conservation of the number of exons suggests that the *FMO* gene family arose from a single ancestral gene.

1.4.4 FMO4

A full length cDNA encoding human FMO4 (previously known as FMO2) has been cloned and characterised (Dolphin *et al.*, 1992). The human FMO4 has a 55% sequence similarity with FMO1 of man (Dolphin *et al.*, 1991), pig (Gasser *et al.*, 1990) and rabbit (Lawton *et al.*, 1990). Northern blot hybridization has previously failed to detect the presence of this FMO in total RNA from human liver, lung or kidney. The use of a more sensitive and quantitative assay i.e RNase protection assay, revealed the presence of small amounts of FMO4 mRNA in several human adult and foetal tissues including the liver, lung and kidney (Dolphin *et al.*, 1996). This mRNA seems to be expressed constitutively in all tissues.

Northern blot analysis of RNA from liver, kidney and lung from rabbit, rat, guinea pig, hamsters and mice showed that FMO4 mRNA was expressed consistently in the tissues of all the species examined (Burnett *et al.*, 1994). FMO4 mRNA was found in greater amounts in the kidney than in the liver of all species examined but the amounts of the mRNA in the lung were below the level of detection.

FMO4 has not been well characterised in terms of its activity and characteristics. This has mainly been due to the inability to express FMO4 in heterologous systems. Attempts to express the protein in *E. coli*, insect cells, yeast and COS systems have failed due to the toxic nature of the protein. Recently however, a truncated form of FMO4 has been expressed successfully in *E. coli* (Itagaki *et al.*, 1996).

The widespread tissue distribution of FMO4 suggests that this protein may have some important house keeping function. To date, nothing is known of the *FMO4* gene.

1.4.5 FMO5

Full length cDNAs encoding FMO5 has been isolated from from rabbit (Atta Asafo Adjei *et al.*, 1993), human and guinea pig (Overby *et al.*, 1995). The human cDNA shares 87% sequence similarity to that of the guinea pig and 85% to the rabbit FMO5. Like all other forms of FMO, the identities with all known homologous forms are between 52 and 57%.

FMO5 mRNA analysis shows that this mRNA is expressed in adult and foetal human liver (Overby *et al.*, 1995). In the rabbit, FMO5 mRNA is expressed in the liver and kidney, but not in the lung (Atta Asafo Adjei *et al.*, 1993). The amount of FMO5 mRNA in rabbit liver is only about 25% that of FMO1. In mice, FMO5 demonstrates no gender specific expression at both the mRNA and protein level (Falls *et al.*, 1995). Anti-rabbit FMO5 antibodies have detected the presence of this isoform in the livers of adult humans, rabbits and guinea pigs and in human foetal liver. Using monospecific antibodies and recombinant isoforms as standards, Overby *et al.*, (1997) have shown that variable amounts of FMO5 are present in microsomal preparations from adult human male liver. The concentration of FMO3 was greater than that of FMO5 in all samples analysed and the ratio of FMO3 to that of FMO5 varied from 2:1 to 10:1.

Studies on rabbit, human and guinea pig FMO5, expressed in *E. coli*, have shown that methimazole is a poor substrate for this FMO. FMO5 in contrast to other FMOs has activity towards a few low-molecular weight primary amines such as *n*-octylamine (Atta Asafo Adjei *et al.*, 1993). Rabbit, human and guinea pig FMO5 have the same sensitivity to MgCl₂, sodium

cholate and elevated temperature. Although the kinetics associated with FMOs 1, 2 and 3 can vary significantly with some substrates (Lawton *et al.*, 1991, Overby *et al.*, 1995, Atta Asafo Adjei *et al.*, 1993), their specificities differ only slightly. FMO1 and FMO3 metabolise tricyclic antidepressants (Atta Asafo Adjei *et al.*, 1993, Williams *et al.*, 1985) and FMO2 metabolises short chain amines (Poulsen *et al.*, 1986, Tynes *et al.*, 1985). Other than this FMOs 1, 2 and 3 share the same list of substrates.

The FMO5 isoform can be considered the "black sheep" of the FMO gene family. It is the only FMO isoform expressed in both human adult and neonatal liver. These characteristics of FMO5 and its apparent lack of efficiency as a drug-metabolising enzyme suggests this isoform may have some physiological function. An involvement for FMO5 in the regulation of prenylated proteins has been suggested (Park *et al.*, 1994). Nothing is known to date about the *FMO5* gene.

1.5 Fish odour syndrome/Trimethylaminuria

Trimethylamine (TMA) is the highly volatile aliphatic amine responsible for the odour of rotting fish. TMA is released in the intestine by the action of bacteria on certain foodstuffs, such as lecithin, choline, carnitine, ergothioneine and betaine (present in egg yolk, liver, kidney, meats, beans and legumes and many other foods), containing the trimethylammonium $[(\text{CH}_3)_3\text{N}^+]$ group. TMA released within the intestinal tract is rapidly and efficiently absorbed. If unaltered, TMA would be excreted from the body via the sweat, breath and urine, resulting in individuals smelling strongly of its highly objectionable odour.

The reason this does not occur is that the normal (and only observed) metabolic pathway for TMA is its *N*-oxygenation to trimethylamine *N*-oxide (TMAO) (Al Waiz *et al.*, 1987b, Lintzel, 1934, de la Hueriga and Popper, 1951),

a reaction catalysed by FMO (Hlavica and Kehl, 1977). TMA has been demonstrated to be an excellent FMO substrate (Cholerton and Smith, 1991) and any TMAO generated is excreted mainly through the urine with no odorous consequences (Al-Waiz *et al.*, 1989).

There is, however, a well-documented clinical condition known as trimethylaminuria, or more colloquially 'fish-odour syndrome', that is characterised by an inability to *N*-oxygenate TMA to TMAO. Individuals having this condition excrete TMA in their breath, sweat and urine and so smell strongly of an odour resembling rotting fish (McKusick, 1983, Cholerton and Smith, 1991, Ayesh *et al.*, 1988, Chen and Aiello, 1993, Humbert *et al.*, 1970, Al-Waiz *et al.*, 1987, Ayesh *et al.*, 1993). Although the increased amounts of TMA itself does not appear deleterious to the individual, the resultant psycho-social impact can be devastating.

The metabolic disorder described here is inherited and referred to as 'primary trimethylaminuria', as opposed to 'secondary trimethylaminurias', which are non-genetic in origin and are secondary to other factors such as renal or hepatic disease or overload with TMA precursors.

The most direct molecular evidence for the cause of trimethylaminuria has come recently from and confirms that mutations in the *FMO3* gene are indeed responsible for this disorder (Dolphin *et al.*, 1997b, Dolphin *et al.*, 1997a). After establishing the internal organization of the human *FMO3* gene, each of its eight coding exons were amplified by PCR, both from normal individuals and from a family of children affected with trimethylaminuria. The amplified exons were sequenced and compared for differences. This identified some sequence differences, the most significant and interesting of which was a single base change, a C to T transition, within exon 4. As a result, a CCC triplet coding for proline-153 in the *FMO3* sequence from the normal individual becomes a CTC triplet coding for leucine in the individual with trimethylaminuria (for both alleles). The sequence of

exon 4 of the *FMO3* gene was then determined for the affected individuals' parents and two siblings. The parents were found to be heterozygous for this mutation, as would be expected if the mutation was causative of trimethylaminuria. Of the two other siblings examined, one was also trimethylaminuric and the other apparently unaffected. The former was found to be homozygous for the CTC mutation, whereas the latter was found heterozygous for the mutation. Four unrelated, non-trimethylaminuric individuals when examined were all found to be homozygous for the CCC triplet. Thus, it seemed a distinct possibility that in the case of one family at least, a single point mutation that inactivates or drastically lowers the catalytic activity of *FMO3*, results in trimethylaminuria. This was confirmed by heterologous expression of the mutant *FMO3* protein which had no catalytic activity (as measured by the *S*-oxidation of methimazole). Therefore, the Pro-153 to Leu-153 mutation is responsible for trimethylaminuria in the case of at least one family (Dolphin *et al.*, 1997a).

Eight different mutations have been found in the *FMO3* gene (Dolphin, personal communication). At present, work on the activities of their heterologously expressed forms is being carried out.

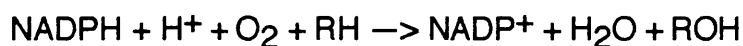
1.6 The Cytochrome P450-dependent monooxygenase system (CYP)

Several names exist for this system. These include, mixed function oxidase (MFO), CYP system and the cytochrome P450-dependent monooxygenase system. The term *monooxygenase* is derived from the fact that the enzyme catalyses the incorporation of one atom of oxygen into a substrate.

The CYP system is found in the microsomal membranes of many different cell types. Its major components are cytochrome P450, NADPH-

dependent cytochrome P450 reductase and lipid. Cytochrome b5 and cytochrome b5 reductase have also been proposed to form part of this system and are required for the metabolism of some compounds (Morgan and Coon, 1984). This system is central to the metabolism of many xenobiotics. Some of the reactions and substrates are shown in Table 1.2.

The reaction catalyzed by the CYPs has the following stoichiometry:



where RH represents the oxidisable substrate and ROH the hydroxylated metabolite. In addition to hydroxylation reactions, CYPs catalyse the *N*-, *O*- and *S*-dealkylation, oxidative and reductive dehalogenation and *N*-oxidation of many drugs, as outlined in Table 1.2.

1.7 CYP nomenclature and multiple forms

The Cytochrome P450 (CYP) superfamily is divided into families and subfamilies depending on their amino acid sequence similarities (reviewed in Nelson *et al.*, (1996), Nelson *et al.*, (1993) and Nebert *et al.*, (1989)).

As of 1998, 481 CYP genes and 22 pseudogenes had so far been described in 85 eukaryotes and 20 prokaryote species. Of the 74 gene families that exist, 14 are present in all mammals examined to date.

The derived amino acid sequence from one P450 gene family is usually defined as having less than 40% identity to an amino acid sequence from another P450 family. Mammalian P450 sequences within the same subfamily are always more than 55% similar.

Recommendations for naming a P450 gene include the italicized root symbol '*CYP*' (*cyp* for the mouse and *Drosophila*) denoting Cytochrome P450, an Arabic numeral designating the P450 family, a letter indicating the

Reaction	Example substrate
Aromatic hydroxylation	Lignocaine
Aliphatic hydroxylation	Pentobarbitone
Epoxidation	Benzo[a]pyrene
<i>N</i> -Dealkylation	Diazepam
<i>O</i> -Dealkylation	Codeine
<i>S</i> -Dealkylation	6-Methylthiopurine
Oxidative deamination	Amphetamine
<i>N</i> -Oxidation	3-Methylpyridine
	2-Acetylaminofluorene
<i>S</i> -Oxidation	Chlorpromazine
Phosphothionate oxidation	Parathion
Dehalogenation	Halothane
Alcohol oxidation	Ethanol

Table 1.2 Reactions catalysed by the CYP system (reproduced from Gibson & Skett, 1994)

subfamily, when two or more subfamilies are known to exist within that family, and an Arabic numeral representing the individual gene e.g *CYP1A1*. 'P' ('ps' in mouse and *Drosophila*) after the gene number denotes a pseudogene. The same numbers and letters are recommended for the corresponding gene products (mRNA, cDNA, enzyme), but non-italicized and in capital letters in all species e.g CYP1A1.

There are 36 known *CYP* genes and 10 pseudogenes in humans. Humans have 16 *CYP* families (Table 1.3), of which *CYPs* 1, 2, 3 and 4 seem to be those primarily associated with the metabolism of exogenous compounds, although they are able to metabolise some endogenous chemicals. Members of other *CYP* families, have been shown to possess specific metabolic functions, as shown in Table 1.3.

1.8 Importance of the CYPs

Some CYPs have the ability to activate certain chemicals to even more harmful products than the parent compounds themselves. This activation leads to cell toxicity and eventually to cell death. A study of these enzymes will help predict the potential for cancer induction by chemicals under development, such as pesticides, herbicides and food additives. The precise characterisation of the human forms will aid in studies determining individual risk-assessment from carcinogen exposure (Gonzalez and Gelboin, 1993).

It is important to study these enzymes in humans and in tissues of human origin because of the limitations in extrapolation, to humans, of studies carried out on laboratory animals. Some of these limitations include the gender differences in the expression of *CYPs* that exist in rodents. This situation seems irrelevant in humans because the differences between the sexes, with respect to *CYP* expression, are relatively small (Giudicelli and Tillement, 1977).

Family	Role
CYP1	drug metabolism
CYP2	drug and steroid metabolism
CYP3	drug metabolism
CYP4	arachidonic acid or fatty acid metabolism
CYP5	Thromboxane A2 synthase
CYP7A	bile acid biosynthesis (7-alpha hydroxylase of steroid nucleus)
CYP7B	brain specific form of 7-alpha hydroxylase
CYP8A	prostacyclin synthase
CYP8B	bile acid biosynthesis
CYP11	steroid biosynthesis
CYP17	steroid biosynthesis (17-alpha hydroxylase)
CYP19	steroid biosynthesis (aromatase, forms oestrogen)
CYP21	steroid biosynthesis
CYP24	vitamin D degradation
CYP26	retinoic acid hydroxylase (important in development)
CYP27	bile acid biosynthesis
CYP40	vitamin D3 1-alpha hydroxylase (activates vitamin D3)
CYP51	cholesterol biosynthesis lanosterol 14-alpha demethylase

Table 1.3 Summary of human CYP families and their roles

Species differences exist in the inducibility of CYPs and even within species, individual strains may vary in their inducibility (Nebert and Gielen, 1972). Orthologous P450s can differ in their catalytic specificity. For example, Human CYP2C10 although showing considerable sequence similarity to certain rat, rabbit and human proteins of the CYP2C subfamily, has a distinctly different catalytic activity, *S*-mephenytoin 4-hydroxylase (Umbenhauer *et al.*, 1987, Ged *et al.*, 1988).

In contrast to animal models, humans show large interindividual variations in CYP catalysed drug oxidation reactions. These variations sometimes lead to different susceptibilities in humans to pharmacological and toxicological actions of drugs, toxic chemicals and carcinogens.(Guengerich and Shimada, 1991).

Variation in human hepatic CYP amounts and activities are related to various factors. These include, genetic polymorphisms whereby heritable changes in the DNA lead to lack of production of the CYP, lack of inducibility or synthesis of a form of the CYP with an altered catalytic activity. (A polymorphism is usually defined as a genetically determined difference affecting $\geq 2\%$ of the population under consideration) (Ortiz de Montellano, 1995). Enzyme induction can also lead to variation in the hepatic expression of these enzymes because several CYPs are known to be induced by drugs and foodstuffs. Another factor involved is enzyme inhibition. The amount of a CYP may be decreased, or its catalytic activity may be lowered even in the absence of a decrease in the level of the protein. Some drugs and foodstuffs have been shown to act as inhibitors.

Human CYP subfamilies involved in foreign compound metabolism are summarised in Table1.4.

1.8.1 CYP1A subfamily

This subfamily has two members CYP1A1 and CYP1A2, which share a 68% amino acid sequence identity (Jaiswal *et al.*, 1985, Jaiswal *et al.*, 1986, Quattrochi *et al.*, 1985). CYP1A1 is similar to its orthologous counterpart in rats (Sogawa *et al.*, 1985) and mice (Gonzalez *et al.*, 1984) having 78% and 80% amino acid sequence similarity respectively

CYP1A1 is expressed at very low levels in human liver and is essentially an extrahepatic enzyme (Schweikl *et al.*, 1993). The same is true for experimental animals. However, upon treatment with polycyclic aromatic hydrocarbons e.g. 3-methylcholanthrene or benzo(a)pyrene, CYP1A1 levels are greatly induced (reviewed by Nebert and Jones, (1989)). The action of CYP1A1 on these compounds leads to their inactivation, and the production of mutagenic and carcinogenic metabolites. Aromatic hydrocarbon hydroxylase (AHH), 7-ethoxycoumarin-O-dealkylase (ECOD) and 7-ethoxyresorufin-O-dealkylase (EROD) activities are attributable to CYP1A1. Although well conserved in the animal kingdom, CYP1A1 is not known to have an endogenous substrate.

Human *CYP1A2*, is expressed essentially only in the liver (Schweikl *et al.*, 1993, Wrighton *et al.*, 1986). An enzyme activity associated with CYP1A2, although non-specific, is ECOD.

1.8.2 CYP1B subfamily

The human cDNA clone of CYP1B1 was isolated from a keratinocyte cell line (Sutter *et al.*, 1994). This CYP is induced in response to 2,3,7,8-tetrachlorodibenzo-p-dioxin (TCDD) and has been shown to play a major role in the metabolism of polycyclic aromatic hydrocarbons such as 7,12-

Families	CYP1	CYP2	CYP3
Subfamilies	1A1, 1A2 1B1	CYP2A6, CYP2A7, CYP2A13 2B6, 2B7 2C8, 2C9, 2C18, 2C19 2D6 2E1 2F1	3A3, 3A4, 3A5, 3A7

Table 1.4 Summary of human CYP families and subfamilies involved in foreign compound metabolism.

dimethylbenz(a)anthracene. Low amounts of CYP1B1 mRNA have been found to be constitutively expressed in several tissues such as the heart, brain, placenta, lung and liver (Hakkola *et al.*, 1997). The *CYP1B1* gene has recently been linked to primary congenital glaucoma (Stoilov *et al.*, 1998, Bejjani *et al.*, 1998, Sarforazi, 1997, Stoilov *et al.*, 1997).

1.8.3 CYP2A subfamily:

Three members of this subfamily exist in humans, *CYP2A6*, *CYP2A7* and *CYP2A13* (Yamano *et al.*, 1990, Fernandez Salguero and Gonzalez, 1995). *CYP2A6* is a minor form of CYP in the liver. The level of *CYP2A6* protein in liver is low (~ 4% of total hepatic P450 content) (Yun *et al.*, 1992). This CYP is primarily a hepatic enzyme being absent from extrahepatic tissues such as the adult human lung, colon, breast, kidney and placenta (Yun *et al.*, 1991, Miles *et al.*, 1990). *CYP2A6* actively catalyses the 7-hydroxylation of coumarin (Yamano *et al.*, 1990). This activity has been used as a marker for *CYP2A6*. Marked variability in the expression of this enzyme has been demonstrated in human liver microsomes, both at the protein and mRNA levels (Yamano *et al.*, 1990, Miles *et al.*, 1990). *CYP2A6* is known to contribute to the oxidation of tobacco-specific nitrosamines (Yamazaki *et al.*, 1992).

Genetic polymorphisms in the *CYP2A6* gene have recently been described (Fernandez Salguero and Gonzalez, 1995). These results show that individuals homozygous for the variant allele, *CYP2A6v1* are unable to 7-hydroxylate coumarin. Another variant, *CYP2A6v2*, was also found although its activity remains unknown.

CYP2A7, shares a 94% sequence identity to *CYP2A6* (Yamano *et al.*, 1990), however, *CYP2A7* encodes an inactive protein, with respect to coumarin metabolism (Ding *et al.*, 1995). Ding and his associates also found

an alternatively spliced version of CYP2A7 (CYP2A7AS). This mRNA species was found to be the major form in a skin fibroblast cell line. The basis for this variation is not known. Whether the protein product of this splice variant has a function is also unknown.

The *CYP2A13* gene has been identified by Fernandez-Salguero *et al.*, (1995). Computer analysis of the genomic clone has led to the prediction of a cDNA sequence for CYP2A13 having 95% sequence similarity with the cDNA of CYP2A6. No cDNA clone for CYP2A13 has been isolated to date.

1.8.4 CYP2B subfamily

This subfamily has been widely studied in rodents because its members are highly inducible by the anti-epileptic drug phenobarbital (PB).

A human cDNA for CYP2B6, which is 76% similar to the rat CYP2B1, has been characterised (Yamano *et al.*, 1989, Miles *et al.*, 1988). The amount of CYP2B6 in human liver is very low and the highest amount in 60 livers, examined by Mimura *et al.*, (1993), accounted for only 1% of the total hepatic CYP content. A large inter-individual variability has been reported for the hepatic levels of CYP2B6 mRNA (Yamano *et al.*, 1989) and protein (Mimura *et al.*, 1993, Shimada *et al.*, 1994). Recombinant CYP2B6 enzymes have been shown to catalyse the metabolism of nicotine (Flammang *et al.*, 1992). Little is known about the role of this CYP in drug metabolism, although cDNA-expressed CYP2B6 is an active catalyst of lidocaine *N*-deethylation (Imaoka *et al.*, 1996). Experiments with primary cultures of human hepatocytes have shown that expression of *CYP2B6* is inducible by treatment of the cells with phenobarbital, dexamethasone or rifampin (Chang *et al.*, 1997).

CYP2B7, (Yamano *et al.*, 1989) contains an internal in-frame stop-codon and is incapable of encoding a functional protein. Therefore, it is classified as a pseudogene (Nelson *et al.*, 1996).

CYP2C

The CYPs in this subfamily are involved in the oxidation of some important drugs such as Warfarin, Mephenytoin, Ibuprofen and Tamoxifen (reviewed in Miners and Birkett, 1998). Members of this subfamily constitute about 16% of the total hepatic CYP complement in man (Shimada *et al.*, 1994). CYP2C9 seems to have the highest catalytic activity in several reactions. Polymorphisms in the coding region of the CYP2C9 gene produce variants which have varying metabolic capacities for most CYP2C9 substrates (Yamazaki *et al.*, 1998).

CYP2D

The only human CYP2D enzyme expressed is CYP2D6. CYP2D7 and CYP2D8 are pseudogenes (Nelson *et al.*, 1996, Gonzalez *et al.*, 1988, Kimura *et al.*, 1989). The CYP2D6 polymorphism has been extensively characterised (reviewed in Yokoi and Kamataki, 1998). Poor metabolizers of debrisoquine represent about 10% of the Caucasian population. As the constitutive levels of CYP2D6 are low (1-2% of human hepatic P450) and the enzyme is non-inducible, any defect in CYP2D6-dependent metabolism may lead to the accumulation of the pharmaceutical reagent, leading to potential toxicity and possible adverse drug reactions (reviewed in Belpaire and Bogaert, 1996).

CYP2E

CYP2E1 is the only gene in this subfamily in most species. The enzyme has been of interest in human and experimental animal models because of the possible relevance to alcoholism, chemical carcinogenesis and diabetes (Guengerich and Shimada, 1991, Yang *et al.*, 1990 and Uematsu *et al.*, 1992). There is a polymorphism associated with this gene that is more common in Chinese people. The mutation correlates with a 2-fold increased risk of nasopharyngeal cancer linked to smoking (reviewed in Raunio, *et al.*, 1995 and Nebert *et al.*, 1996).

1.8.5 CYP3A subfamily

In humans, members of the *CYP3A* subfamily play an important role in the metabolism of foreign compounds. *CYP3A4* is the most abundant CYP and has a broad substrate specificity.

This subfamily consists of *CYP3A4*, *CYP3A5*, *CYP3A5P* and *CYP3A7*. The *CYP3A* enzymes account for an estimated 30% of total human CYP content in adult liver (Shimada *et al.*, 1997, Bork *et al.*, 1989), although large inter-individual differences exist in hepatic *CYP3A* content. The existence of another form, *CYP3A3*, is still in doubt (Nelson *et al.*, 1996). *CYP3A4* and *CYP3A5* are the main forms expressed in adult human liver, while *CYP3A7* is expressed in human foetal liver (Kitada and Kamataki, 1994, Kitada and Kamataki, 1979).

CYP3A4 is present in all adult human livers and is inducible by drugs such as rifampin (rifampicin) and dexamethasone (Pichard *et al.*, 1990, Schuetz *et al.*, 1993a, Chang *et al.*, 1997). In contrast, *CYP3A5* is expressed in only ~10-30% of liver samples (Wrighton *et al.*, 1989) and does not respond to typical *CYP3A* inducers. *CYP3A5* is 88% identical to *CYP3A4* and is polymorphically expressed (Wrighton *et al.*, 1989, Wrighton *et al.*, 1990). *CYP3A7*, was isolated from foetal liver (Kitada *et al.*, 1985, Kitada and Kamataki, 1979). Studies have also shown its presence in the adult endometrium and placenta (Schuetz *et al.*, 1993b).

Many commonly used drugs are substrates for *CYP3A4*, including erythromycin (Watkins *et al.*, 1987), nifedipine (Guengerich *et al.*, 1986) and midazolam (Gorski *et al.*, 1994).

Recent studies on rat *CYP3A23* have demonstrated that the glucocorticoid-inducible transcriptional activity of *CYP3A23* involves members of the nuclear receptor superfamily (Huss and Kasper, 1998). Furthermore, a glucocorticoid responsive element that mediates the induction of *CYP3A1* in rats has also been identified (Pereira *et al.*, 1998).

1.9 Metabolism of pesticides by FMOs and CYPs

Organophosphorus pesticides are metabolised extensively by mammals, insects and plants. The CYPs are primarily responsible for the oxidative reactions involved in the biotransformation of pesticides (Kulkarni and Hodgson, 1980). These biotransformations increase polarity and/or the ability of the pesticide to inhibit acetylcholinesterase.

Both the CYPs and FMOs are present in substantial amounts in hepatic microsomes, and are involved in a variety of pesticide oxidations including sulphoxidation (Tynes and Hodgson, 1985, Hajjar and Hodgson, 1982, Hajjar and Hodgson, 1980). Smyser and Hodgson (1985), have shown that organophosphates containing thioether e.g. disulphoton and phorate are rapidly oxidized by FMOs to yield an optically active sulphoxide as the only detectable metabolite. Levi and Hodgson (1988), found, using purified mouse liver FMO and CYPs, that although both these enzymes readily form the sulphoxide, FMO catalysed reactions yield the (-)-phorate sulphoxide and Cyp2b9 formed the (+)-phorate sulphoxide. Other CYPs generated racemic mixtures.

When phorate is incubated with FMO, phorate sulphoxide is the only metabolite formed (fig 1.4). This sulphoxide is not further oxidized. With the CYPs, although phorate sulphoxide is the principal product of CYP oxidation, the CYPs further utilise the phorate sulphoxide as a substrate to produce additional metabolites, the oxon sulphoxide, the sulphone and the oxon sulphone. Although both the (+) and (-) sulphoxide isomers are substrates for CYPs, incubation with the (+)-phorate sulphoxide favours formation of the oxon sulphoxide. The oxon sulphoxide is a more potent inhibitor of acetylcholinesterase.

Therefore, it can be seen that although both these enzymes metabolise the same substrate, different products are formed, and where the same

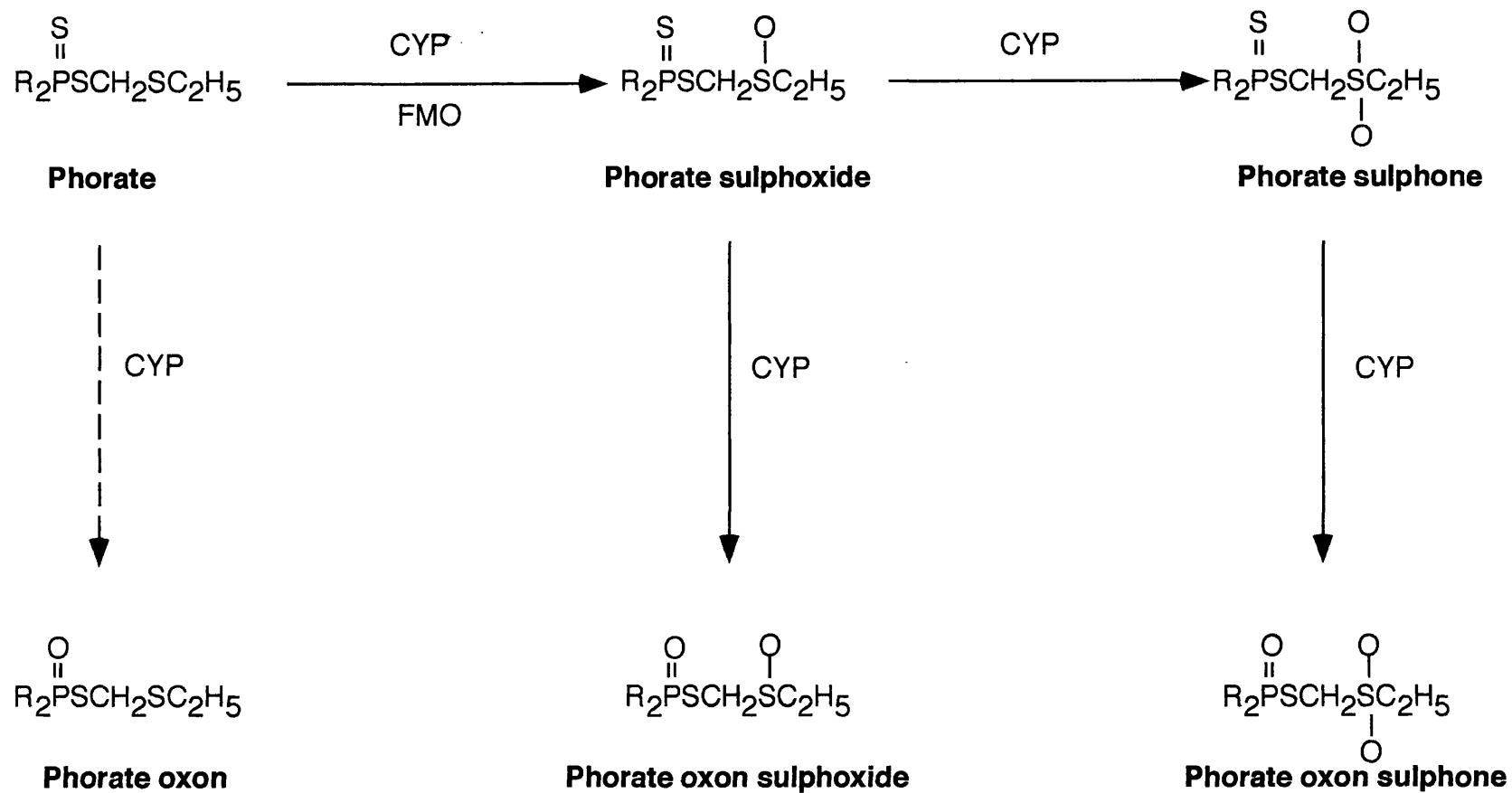


Fig 1.4 Summary of the oxidation products of phorate produced by CYPs and FMOs. (Reproduced from Levi and Hodgson, 1988). R=C₂H₅O

product is formed, they are optically different and have different properties. This is true for phorate and also 4-tolyl ethyl sulphide (Light *et al.*, 1982, Waxman *et al.*, 1982). Thus, knowledge of the drug metabolising enzymes and specific isoforms present, as well as their contribution to the metabolism of a particular compound can give an indication as to the products formed and the eventual effectiveness in detoxification or toxicity of the compound. Other agricultural chemicals that are substrates for the FMOs include carbamates, dithiocarbamates, thioureylenes, tertiary amines and organochlorines.

1.10 The skin

Much of this thesis is concerned with the expression of *FMOs* and *CYPs* in human skin.

The skin is one of the largest organs in the body. In man, it is estimated to represent approximately 10% of total body weight, with a surface area of 2m² (Rongone, 1983, Odland, 1983).

The skin forms an interface between the body and its external environment, forming an effective barrier against invasion of the body by microorganisms. It provides important thermoregulatory controls and maintains fluid balance by limiting the excessive loss of body water. Being the most external organ, the skin is constantly exposed to a variety of hazardous environmental agents and it is also a surface upon which drugs, cosmetics and miscellaneous chemicals are intentionally applied. Although an effective barrier, it is becoming apparent that it is not a complete barrier. In fact, the skin is now recognised as an important portal for the entry of chemicals into the systemic circulation. An important physiological function i.e thermoregulation, may modulate the systemic availability of chemicals absorbed through the skin, due to alterations in cutaneous blood flow.

It is now generally recognised that the skin is an organ capable of performing a variety of metabolic functions, including those involved in the metabolism of hormones, carcinogens, drugs and environmental chemicals reviewed in (Hotchkiss, 1992, Kao and Carver, 1990). Since skin contains enzymes capable of metabolising xenobiotics, any chemicals that are applied to the surface of the skin will, during the course of penetration through this organ, be exposed to available biotransformation systems that are present in the skin. The skin may therefore act as a route of systemic exposure to foreign chemicals, or it can be the target organ for local toxicity such as irritation, hypersensitivity, phototoxicity and skin cancer. Consequently, the ability of the skin to function as an organ of xenobiotic metabolism is of considerable interest.

1.10.1 The structure of the skin

The skin of mammals consists of 3 main layers, the epidermis, dermis and the subcutaneous layer (fig 1.5). The epidermis and dermis are separated from each other by a basement membrane. The mammalian epidermis is a renewing tissue which provides the outer surface coat of the body. Apart from representing a continuous supply of cells forming the external barrier (the stratum corneum), epidermal cells have been shown to possess a number of additional functional capabilities as listed in Table 1.6.

Main functions	Additional functions upon need
Cell division	Adhesion
Keratin synthesis	Migration
Synthesis of the basal lamina	Phagocytosis
Synthesis of glycocalyx	
Degranulation	

Table 1.6 Functional capacities of epidermal cells (reproduced from Christophers *et al.*, (1989)).

Phase I reactions	Phase II reactions
Oxidative reactions	Glucuronic acid conjugation
Alcohol oxidation	Sulfate conjugation
Hydroxylation	
Aliphatic	
Alicyclic	
Aromatic	
Deamination	Methylation
Dealkylation	
Reductive reactions	Glycine conjugation
Carbonyl reduction	
C=C reduction	
Hydrolytic reactions	Glutathione conjugation
Ester hydrolysis	
Epoxide hydrolysis	

Table 1.4 Examples of skin-mediated metabolic reactions (from Kao and Carver, 1990)

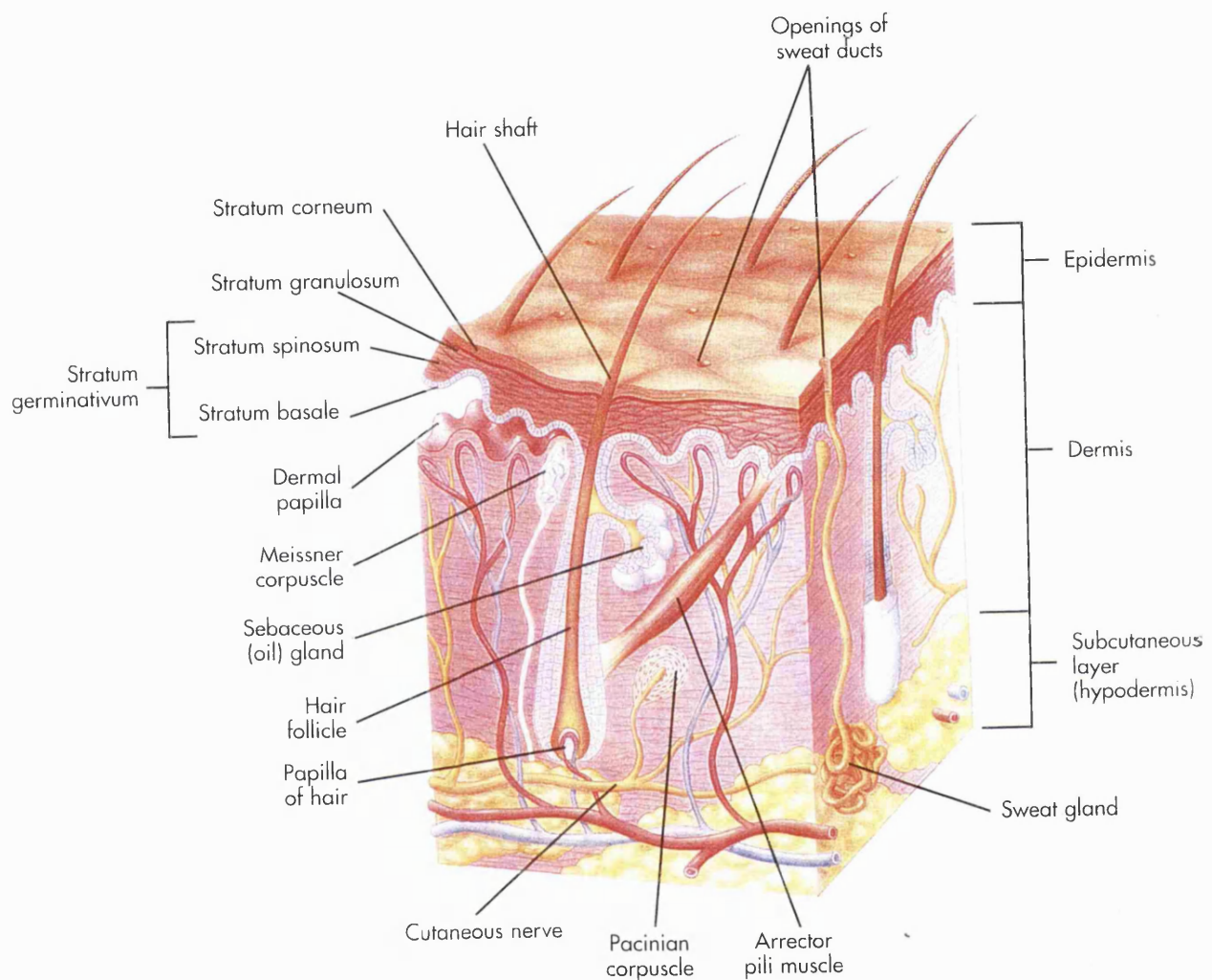


Fig 1.5 Microscopic diagram of the skin. The epidermis, shown in longitudinal section, is raised at one corner to reveal the ridges in the dermis (reproduced from Thibodeau and Patton. 1996).

1.10.1.1 The epidermis

This outer layer of stratified squamous keratinized epithelium is resistant to physical and chemical stresses. In areas such as the soles and palms, where friction and pressure is most intense, five distinct layers are present. In areas with less physical stresses (skin of chest, scalp etc), there are fewer than five layers. From the lower to the upper surface of the epidermis, the layers are designated as the *stratum germinativum* (made up of the stratum basale and stratum spinosum), *stratum granulosum* and *stratum corneum*.

The stratum germinativum consists of the lowermost layer of cells (stratum basale) and is regenerative. This layer lies on a thin basement membrane. As cells are produced by this layer, they migrate up through the overlying strata. During their migration they undergo morphological and physiological changes, becoming flattened, dead, dry keratinized flakes. As the dead cells are desquamated at the surface, they are replaced by later generations of keratinized cells. In addition to the generative cells found in this layer are the *melanocytes* or pigment producing cells. The melanocytes represent about 10-25% of the cells in this layer. The stratum spinosum is a relatively thick layer of slightly flattened cells and lies above the stratum basale. The cells have a spiny appearance, hence their name.

The stratum granulosum may have up to 5 layers, in thick skin (palms and soles), but in thin skin, (chest) these layers may be absent or poorly represented. The cytoplasm of these cells is filled with irregularly shaped, basophilic keratohyalin granules.

The stratum corneum is the outermost layer of the epidermis and is keratinized. The number of cell layers varies from a few in thin skin to many in thick skin. These tightly packed dead cells migrate to the surface where they are desquamated.

The epidermis separates the organism from a hostile environment and provides protection against physical, chemical and radiation injuries. It prevents penetration of harmful agents into the skin and the loss of body fluids into the environment.

1.10.1.2 The dermis

The dermis is a fibrous, elastic tissue lying below the epidermis and is continuous with the deeper subcutaneous layer. It varies between 0.3 and 4mm in thickness. The dermis imparts the characteristics of strength, durability, and pliability to the skin, and is normally thicker in areas receiving maximal mechanical stresses. Thus, it is thicker in the palms and soles than the skin of the back. The dermis is organised into an upper, moderately dense, *papillary layer*, which lies below the epidermis, and a lower, more dense *reticular layer*, which is continuous with the subcutaneous layer (hypodermis).

The papillary layer is the uppermost layer of the dermis, lying below a thin basement membrane. It is composed of a loose network of thin collagen, elastic and reticular fibres. The ground substance is moderately abundant, containing many fibroblasts, some macrophages, mast cells, melanocytes (not in palms and soles) and a few lymphocytes. In thick skin, the papillary layer may be organised into tall and sometimes branched dermal papillae. These papillae form a complex interlocking system with ridges and grooves of the epidermis. The papillae have an excellent vasculature and lymphatic supply and a few have sensory receptors for touch, *Meissner's corpuscles*.

The reticular layer, is the lower layer of the dermis and is composed of dense, irregular collagenous connective tissue. A network of elastic fibres is also present and interspersed with the collagen fiber bundles. The reticular layer has fewer cells than the papillary layer and the predominant cells are

macrophages and fibroblasts. Sweat glands, hair follicles and pressure receptors are present in this layer.

1.10.1.3 The subcutaneous layer

The subcutaneous layer is usually studied with the skin, but it is not part of it. It is composed of loose connective tissue, and is usually thicker than the dermis, and extends from the reticular layer of the dermis to the underlying muscles.

The stratum corneum exhibits reservoir characteristics although it serves as the main barrier to skin penetration. A topically applied compound may be absorbed into the skin via a variety of routes, these include, the partitioning into the lipophilic stratum corneum, diffusion across the stratum corneum, partitioning from the stratum corneum into the viable epidermis, diffusion across the epidermis and dermis and passage into dermal blood vessels (Guy *et al.*, 1987).

Differences exist between the skin of man and that of laboratory animals. For example the skin of man is less permeable than that of rodents and has fewer hair follicles. Permeability is greatest in the rabbit and decreases in the order rabbit, rat, guinea pig, pig, monkey, man (Bartek *et al.*, 1972). A variety of factors can affect absorption, these include, the nature of the chemical itself, the vehicle of absorption, the extent of hydration and temperature of the skin, anatomical site, skin appendages, the concentration of the chemical applied, occlusion of the site of application, skin damage and disease, dermal blood flow, and bacterial degradation on the skin surface.

1.10.2 Metabolism of foreign compounds in the skin

There have been numerous reports on the presence of xenobiotic metabolising enzymes in the skin. These include the CYPs, UDP glucuronyltransferases sulphotransferases and glutathione S - transferases. Studies on the presence of these enzymes have been carried out using classical techniques such as the use of skin homogenates, skin microsomes, and skin cell/organ cultures together with other methods specifically applicable to the skin e.g diffusion cells and culture of isolated hair follicles. The reactions involved are summarized in Table 1.5.

1.10.2.1 Localisation of xenobiotic metabolising enzymes within the skin

CYP activity towards ethoxycoumarin is similar in the dermis and epidermis of adult hairless mice, with higher total activity in the dermis due to its greater mass (Finnen *et al.*, 1985). The specific activities are greatest in sebaceous cells followed by differentiated keratinocytes and then basal keratinocytes. AHH specific activity is greater in the epidermis than the dermis with high activities in sebaceous cells and hair follicles (Mukhtar and Bickers, 1981, Akin and Norred, 1976, Thompson and Slaga, 1976).

1.10.3 FMOs in the skin

Until recently, studies on the role of FMOs and their involvement in xenobiotic metabolism in the skin had not been reported. One such study was carried out by Venkatesh *et al.*, (1992) to define the roles of FMOs and CYPs in xenobiotic metabolism in the skin.

In addition to enzymatic activities, antibodies to FMO from liver and lung were used in western blot analyses and immunohistochemical studies.

Venkatesh *et al.*, (1992) have shown FMO activity with both thiobenzamide and methimazole, both of which are good substrates for FMOs (i.e FMOs 1, 2 and 3, unknown for FMO4, and not good for FMO5). The FMO activity in the skin was 10 and 20% of liver microsomal activity with methimazole and thiobenzamide respectively.

Western blot analyses on mouse skin microsomes showed that antibodies developed to FMO purified from mouse liver cross-reacted with a protein in skin microsomes. Skin microsomes did not cross-react with antibodies developed to rabbit lung FMO (FMO2), indicating that FMO2 is not expressed in mouse skin.

Immunohistochemical studies using antibodies raised to mouse liver FMO were carried out to determine the localisation of the FMOs in mouse and pig skin. In nude mouse skin, all layers of the epidermis exhibited positive staining with the FMO antibody, when compared to the control. Fainter staining was present in sebaceous glands and in some cells of the hair follicle in CD-1 mice. In pig skin, the staining was confined primarily to the stratum granulosum and stratum spinosum layers of the epidermis.

Since both CYPs and FMOs are present in mouse skin, the relative contribution of these two systems in the oxidation of phorate was studied (Venkatesh *et al.*, 1992). They looked at the relative contribution of the CYP and FMO monooxygenase systems to the metabolism of phorate. This compound, which is an organophosphorus pesticide, is a substrate for both FMOs and CYPs (see section 1.9). Selective inhibitors for each enzyme system was used. These experiments showed that, in mouse skin, phorate sulfoxidation represented 3 to 4 % of the activity observed in liver microsomes. The selective inhibition studies showed that in mouse liver 68 to 84% of the phorate sulfoxidase activity was due to CYPs while FMO was

responsible for the remainder of the activity. In contrast, in mouse skin microsomes, FMO was responsible for 66 to 69% of phorate sulfoxidase activity whereas only 31 to 36% of the activity was due to CYPs. Therefore, although the total phorate sulfoxidase activity in skin microsomes represents a small percentage of that observed in the liver, in the skin, FMO appears to play a greater role than does CYP in the metabolism of phorate. The same occurs in the mouse kidney and lung (Kinsler *et al.*, 1988). This indicates the importance of FMO relative to CYPs in xenobiotic metabolism in extrahepatic tissues.

No studies on the expression of FMOs at the RNA level in the skin, both rodent and human, have been published to date. Although some results have been found in mouse skin, no studies on the presence of FMOs in human skin have been published. There has been a single mention of the presence of FMO1 in human skin by Dolphin *et al.*, (1996) who, using RNase protection assays, showed that <1 molecule of FMO1 mRNA/ cell was present in human skin.

1.10.4 CYPs in the skin

Progress towards the identification of the CYPs in extrahepatic tissues, such as the skin, has been limited by the difficulties encountered in using conventional methods which are often not applicable in tissues where CYP concentrations are too low. The skin is extremely resistant to homogenisation and the harsh techniques required to homogenise cutaneous tissue often results in the destruction of enzyme activities (Moloney *et al.*, 1982, Akin and Norred, 1976). Skin also contains relatively large amounts of metabolically inert material, (e.g collagen and keratin) and depending on the preparation procedures and the reference units used to express enzyme activity, variations in the amounts of these non-enzymic contaminants could greatly

influence the apparent specific activities measured in this tissue. Consequently, caution must be exercised when interpreting and comparing measurements of cutaneous drug-metabolising enzymes (Kao and Carver, 1990).

Through studies with cDNA-expressed proteins, many substances have been found that can be useful catalytic monitors for specific CYP enzymes or subfamilies. However, errors can sometimes be made when interpreting activity data derived from cDNA-expressed enzyme studies. The fact that a cDNA-expressed human CYP can catalyse a particular substrate oxidation reaction does not necessarily mean that in human tissues the corresponding enzyme will be an important catalyst in the same oxidation reaction. While certain compounds may be considered to be reasonably specific substrates for a particular CYP (or group of CYPs in the same subfamily), in the case of other CYP substrates, multiple enzymes may participate in their metabolism. Therefore studies with enzyme activities in isolation give little information on the exact isoform present in the tissue being investigated.

Despite these limitations, CYP activity in the skin of mouse and rat has been shown with a variety of substrates including benzo[a]pyrene, ethoxycoumarin, ethoxyresorufin and aldrin (Pohl *et al.*, 1976, Mukhtar and Bickers, 1981, Bickers *et al.*, 1982a, Rettie *et al.*, 1986). Induction of CYPs by PAHs such as 3-methylcholanthrene, aroclor 1254 (Bickers *et al.*, 1982b, Khan *et al.*, 1989a), crude coal tar (Bickers *et al.*, 1982b, Bickers and Kappas, 1978, Khan *et al.*, 1989b), and benzoflavone (Maloney *et al.*, 1982) has been shown to occur in the skin.

CYP1A1 is the most widely studied isoform in the skin. The amounts of this isoform are low, and can only be studied upon exposure of the skin to PAHs, β -naphthoflavone (BNF) and glucocorticoids (Mukhtar and Bickers,

1983, Merk *et al.*, 1987, Whitlock, 1986, Finnen *et al.*, 1984); reviewed in (Ahmad *et al.*, 1996).

Induction of *CYP1A1* by benz(a)anthracene and β NF at the mRNA level, using RT-PCR techniques, has been demonstrated in rat epidermis and in cultured human epidermal keratinocytes (Khan *et al.*, 1992). Treatment with these inducers results in a several fold increase in AHH activity in rat epidermis as well as in human keratinocytes (Khan *et al.*, 1992). Raza *et al.*, (1992) showed that topical application of β NF to rats caused a 2- to 6-fold elevation of *CYP1A1* mRNA and 3-14 times enhancement in monooxygenase activity in the epidermis. Two research groups have also shown that not the entire population of cells in the epidermis express *CYP1A1* at equivalent levels (Reiners *et al.*, 1992, Stauber *et al.*, 1995). These studies suggest there is differential expression of both basal and inducible xenobiotic metabolising enzymes in the epidermis, which is regulated as a function of the stage of epidermal differentiation e.g. superficial layers of the epidermis contained elevated β -NF induced *CYP1A1*.

Interestingly, the induction of *CYP1A1* mRNA and EROD has been shown to occur in the absence of xenobiotics (Sadek and Allen, 1994). Cultured human keratinocytes in suspension show an increase of both mRNA and enzyme activity. This increase has been shown to be independent of exogenous calcium concentrations and is thought to be cell type specific, because it does not occur in fibroblasts from the skin.

Other *CYP* isoforms have also been found to be expressed in the skin. Jugert *et al.*, (1994a) have shown the presence of multiple CYPs in mouse skin. Topical application of dexamethasone resulted in significant induction of *CYP1A1*, 2B1, 2E1 and 3A related enzyme activities (EROD, pentoxyresorufin *O* -deethylase (PROD), *p* -nitrophenol hydroxylase and erythromycin *N* -demethylase (EMDM) respectively). Immunoblot analysis carried out by the same group have shown that the protein amounts of these enzymes increase

2- to 10-fold upon topical application of dexamethasone. The mRNAs for CYP1A1 and CYP2E1 remain unchanged upon dexamethasone treatment. The effect of these compounds on the expression of *CYP2B1* and *CYP3A* were not reported.

Pyridine treatment of mouse skin has also been shown to lead to an increase in EROD, PROD and EMDM activities and in the protein amounts of CYP1A1, 2B1 and 3A which are responsible for these activities (Agarwal *et al.*, 1994). The mRNA for CYP1A increased in response to pyridine treatment.

The localisation of specific phase I and II enzymes in mouse, rat and human skin have been carried out using immunocytochemical techniques (Pendlington *et al.*, 1994, Murray *et al.*, 1988, Baron *et al.*, 1985, Baron *et al.*, 1986). In these studies, the presence of CYP1A1/2, CYP2B1/2 and CYP3A were investigated in the skin of the 3 different species. The pattern of staining was the same in each species studied and for each of the enzymes studied. Immunohistochemical techniques with antibodies to the rat proteins showed that the enzymes were located primarily in the epidermis and in the cells of the sebaceous glands. Using an antibody to the human CYP3A family, members of this family have been identified in the human skin, specifically the non-keratinized epidermis and the epithelium of the sebaceous gland, (Murray *et al.*, 1988). Members of both CYP2 and CYP3 have also been identified in the human epidermis, dermis and hair follicles (Van Pelt *et al.*, 1990). However, this group found a uniform distribution of members of the CYP3 family throughout the skin.

Northern blot analyses of RNA isolated from primary cultures of normal human keratinocytes show a 100-fold enhanced level of CYP1B1 mRNA after treatment with (TCDD) (Sutter *et al.*, 1994). Sutter and co-workers isolated the full-length 5.1 kb cDNA encoding CYP1B1 from human keratinocytes. This enzyme has been shown to play a major role in the metabolism of polycyclic aromatic hydrocarbons such as 7,12-dimethylbenz(a)anthracene, a

known skin carcinogen. Topical application of β NF or TCDD to SENCAR mice leads to the induction of CYP1B1 mRNA (Ahmad *et al.*, 1996).

Human keratinocyte cultures have been shown to have EMDM activity (thought to be attributable to CYP3A). Upon treatment of these cultures with dexamethasone and cyclosporin A, both of which are known inducers of CYP3A, this activity was induced. Western blot analysis have shown that the amount of CYP3A protein increased in response to these inducers (Jugert *et al.*, 1994b). There have been reports on the presence of CYP1A1, 2E1 and 3A mRNA in human keratinocyte cultures. The amounts of CYP2E1 and CYP3A mRNAs were found to be relatively higher than those of the other mRNAs present (Eichler *et al.*, 1996).

It is apparent that most of the studies on cutaneous foreign compound metabolising enzymes have been carried out using laboratory animals or cultures of human keratinocytes. Several species differences occur in the expression of these CYPs and as such, the extrapolation of this data to humans is under question. However, several models to study cutaneous xenobiotic metabolism are being developed. These include cultured epidermal keratinocytes (reviewed by Bouclier *et al.*, (1990), reconstructed human skin (Regnier *et al.*, 1990, Regnier and Darmon, 1989), cell lines (Rheinwald and Beckett, 1980, Allen Hoffmann and Rheinwald, 1984) and non-invasive methods such as hair follicle keratinocyte cultures (Lenoir *et al.*, 1993, Lenoir *et al.*, 1985) . Each of these methods have their disadvantages primarily due to the fact that the cultured cells do not retain the same *in vivo* drug metabolising capabilities and as such extrapolations from studies carried out on such systems are limited.

1.11 Scope of thesis

The aim of this thesis was to further characterise the *FMO* gene family of man. Our studies focused primarily on human skin, as little is known with regards to *FMO* gene expression in this tissue.

Southern blot hybridization analyses (**Chapter 3**) on human genomic DNA was carried out to determine the number of genes encoding each FMO. The field of FMOs is a relatively new one and there is still a sparsity of basic knowledge with regards to *FMO* genes and their expression.

We went on to investigate the expression of *FMOs 1, 2, 3, 4* and *5* in a variety of human tissue samples which included human liver, lung and kidney. These studies were extended to include primary cultures of human keratinocytes derived from whole skin and an immortalized human keratinocyte cell line (HaCaT). Investigations into the expression of the *FMO* genes were carried out at both the mRNA level and the protein level.

Northern blot hybridization analyses (**Chapter 4**) and RNase protection assays (**Chapter 5**) were used to investigate the tissue-specific expression of *FMOs 1, 2, 3, 4* and *5*, the latter method being more sensitive and quantitative than the former. In these studies comparisons between whole skin samples and keratinocyte cultures derived from the same skin samples were made. The expression of FMO1, 3, 4 and 5 mRNAs was then localised to particular regions of whole skin using *in situ* hybridization analysis (**Chapter 8**).

Protein expression studies were also undertaken, using western blot analyses (**Chapter 6**), enzyme activity assay studies (**Chapter 7**) and Immunohistochemistry. Western blot analyses were carried out using antibodies to rabbit FMOs1, 2, 3 and 5. Samples of whole skin homogenates, primary keratinocytes and HaCaT cells were used for western blot analyses, albeit unsuccessfully due to the cross-reactivity of the antibodies to keratins in

the skin, primary keratinocyte cultures and HaCaT cell samples. Enzyme activity assays were undertaken as a means of detecting FMO enzyme activity towards methimazole. These assays could be carried out only on whole skin microsomes and unfortunately the number of assays was limited by the scarcity of sample. The same antibodies that were used for western blot analyses were used in immunohistochemistry studies (**Chapter 8**). During these studies, it was hoped that we could localise FMOs to particular cell types in the skin that are devoid of keratins.

The CYPs have been an extensively studied family of enzymes, however few studies on their expression in human skin have been carried out. We examined the expression of *CYPs* in human skin, primary keratinocyte cultures derived from human skin and HaCaT cells, using the same techniques that were used for the *FMO* expression investigations (**Chapter 9**). Northern blot hybridization analyses, RNase protection assays and *in situ* hybridization were used to investigate the expression of three subfamilies, *CYP2A*, *2B* and *3A*. These experiments were followed by western blot analyses and immunohistochemical studies using antibodies to baboon *CYP2A*, rabbit *CYP2B* and rabbit *CYP3A*.

During the course of this study, comparisons between the expression of *FMOs 1, 2, 3, 4* and *5* and *CYPs 2A, 2B* and *3A* in whole skin samples to *in vitro* culture systems derived from whole skin, i.e primary cultures of human keratinocytes and HaCaT cells, were carried out (**Chapter 10**). This was to determine whether these culture systems would be suitable models for drug metabolism studies or for studies on the regulation of human *FMO* and *CYP* genes.

MATERIALS AND METHODS

2.1 Chemicals

All chemicals, except those used for tissue culture and unless otherwise specified, were analytical reagent grade and were purchased from BDH, UK. Chemicals used for tissue culture were of tissue culture grade. Dulbecco's Modified Eagle medium (DMEM), foetal calf serum, Penicillin and Streptomycin were purchased from Sigma Chemical Co., UK.

2.2 Cell culture conditions

2.2.1 HaCaT cells

Solutions

- Dulbecco's modified eagle medium (DMEM) containing 10% (v/v) foetal calf serum
- Penicillin (10mg/ml)
- Streptomycin (2.5 μ g/ml)

Fully supplemented medium contained penicillin at 0.1mg/ml and streptomycin at 0.025 μ g/ml.

- **Dulbecco's Phosphate Buffered Saline (PBS)**

Dulbecco's PBS was made from PBS tablets obtained from Sigma Chemical Co. One tablet was dissolved in 200 ml of water. The resultant solution is 0.01M phosphate buffer, 0.0027M potassium chloride and 0.137M sodium chloride and has a pH of 7.4.

The solution was autoclaved and stored at 2-8°C.

- 0.05% (w/v) diaminoethanetetra-acetic acid, disodium salt (EDTA) in PBS was prepared using tissue culture grade EDTA (Sigma Chemical Co. UK).

The appropriate amount of EDTA was added to PBS until dissolved. The resultant solution was autoclaved and stored at room temperature.

- 0.05% (w/v) trypsin/0.025% (w/v) EDTA in PBS was obtained commercially from Gibco BRL, UK.

The HaCaT cell line was a kind gift from Prof. Dr. Norbert E. Fusenig (German Cancer Research Foundation). HaCaT cells are a spontaneously transformed human epithelial cell line from adult skin which maintains full epidermal differentiation capacity (Boukamp *et al.*, 1988). "HaCaT" denotes their origin from human adult skin keratinocytes propagated under low Ca²⁺ conditions and elevated temperature.

The cells were shipped from Germany at ambient temperature. When the cells arrived, they were placed in an incubator without removing the medium. After 24 hours the medium was replaced with DMEM (fully supplemented) and the cells incubated for a further 24 hours. This was done as per instructions provided with the cells.

Cells were passaged at a maximal ratio of 1 to 10. To avoid rapid loss of differentiation, the cells were not passaged too often and the optimal time interval between passages was between 7-10 days. To harvest the cells or passage them, at confluence (or post confluence, optimum 3 to 4 days past confluence), the cultures were treated with 0.05% (w/v) EDTA to remove the desmosomes. The cells were incubated (up to 20 mins) until wide intercellular spaces were visible microscopically. The EDTA was then removed and a mixture of 0.05% (w/v) trypsin/0.025% (w/v) EDTA was added. The cells were incubated at 37°C until they detached from the tissue culture plastic (usually 2 to 5 mins). Cells were resuspended in complete culture medium and plated out.

2.2.2 Primary cultures of normal human epidermal keratinocytes

Two different types of primary human epidermal keratinocytes were used in these investigations. One was a commercially obtained culture of proliferating keratinocytes, the other was cultures of primary keratinocytes, established from full thickness skin after breast reduction surgery.

Solutions

- Dulbecco's PBS prepared as in 2.2.1
- Fully supplemented Leibovitz's L-15 medium (without glutamine) containing 10% foetal calf serum, penicillin (0.1mg/ml) and streptomycin (0.025µg/ml).
- Dispase (Gibco BRL). A 40 units/ml (10X stock solution) was made up in L-15 medium (containing antibiotics) but without foetal calf serum. Once dissolved the resultant solution was filter sterilized using a 0.22µm filter and stored at 4°C.

The stock solution was diluted, when required, in fully supplemented L-15 medium to make a 4 units/ml working solution .

- 0.02% (w/v) EDTA in PBS, was prepared as in 2.2.1.
- 0.1% (w/v) EDTA in PBS, prepared as in 2.2.1.
- Trypsin solution, 0.025% (w/v) trypsin/ 0.01% (w/v) EDTA in PBS obtained commercially from Clonetics Corporation, USA.
- Trypsin neutralising solution (TNS) (Clonetics Corporation, USA)
- Antibiotics for primary cultures established from breast skin were:
Kanamycin (Gibco BRL) was obtained as a stock solution of 10mg/ml (100X)
Gentamycin (Sigma Chemical Corporation) obtained as a stock solution of 10mg/ml (100X).

Ciproxin™ (Bayer, Germany) stock solution contains ciprofloxacin at 2mg/ml.

- Keratinocyte growth medium (KGM) (Clonetics Corporation, USA) was supplemented with:

Epidermal Growth Factor (EGF) (0.1ng/ml human recombinant)

Insulin (5mg/ml)

Hydrocortisone (0.5mg/ml)

Calcium (0.15mM)

Bovine Pituitary Extract (BPE) (0.03mg/ml)

Gentamycin (50mg/ml)

Amphotericin B (50ng/ml)

2.2.2.1 Commercially obtained culture of proliferating keratinocytes

Normal human epidermal keratinocytes were obtained as proliferating cultures from Clonetics Corporation, USA and grown under serum free conditions. The cells, which were 30-80% confluent upon arrival, were established from a single adult donor and arrived in a 25cm² flask. Upon arrival, the cells were incubated at 37°C, 5% CO₂ for 3-4 hours to equilibrate the temperature and CO₂ levels. The medium was then removed and replaced with fresh KGM (fully supplemented). The flask was then placed in a 37°C, 5% CO₂, humidified incubator for at least 24 hours.

When the cells reached 70-90% confluency, they were subcultured. For subculturing, the cells were first washed in PBS and then trypsinized using about 3 ml of Trypsin solution per 25cm² flask. The cells were monitored microscopically until approximately 50% of the cells had detached. At this stage to the culture was added 3 ml of warmed TNS. Cells were then quickly transferred to a sterile 15 ml centrifuge tube. The treated flask was examined under the microscope to ensure all the cells had been detached.

All skin samples were utilised with permission from the patients and as approved by the rules and regulations set out by the Ethics Committee of the local hospital.

The flask was rinsed with 2 ml of PBS to collect residual cells and the rinse solution added to the rest of the cells in the centrifuge tube. The harvested cells were centrifuged at 220g, at room temperature, for 5 mins and the supernatant removed. The cell pellet was resuspended in 2 ml of KGM and the cells then seeded onto new tissue culture plastic. After 24 hours, the cells were examined, the tissue culture medium changed and the cells incubated for an additional 24 hours after which the culture was reexamined. Thereafter, the medium was changed every other day until the culture was confluent, after which the cells were harvested for analysis.

2.2.2.2 Establishment of primary cultures of human keratinocytes derived from full thickness skin.

Skin samples from breast reduction mammoplasties were obtained from the Stephen Kirby Skin Bank, Queen Marys University Hospital, Roehampton. Skin was obtained only from females and did not come from individuals having mastectomies. Only the donors age was available, their medical history was unavailable.

A variety of safety precautions had to be taken because the samples provided were usually not screened for viral infection. All liquid debris from the sample, such as blood had to be placed in bleach for at least 24 hours before being discarded. Pieces of skin which had been processed were fixed in formalin before being incinerated. All procedures were carried out in a special containment facility.

The skin samples were placed epidermal side up, in a 10 cm Petri-dish. They were then spread out to flatten them. Samples were washed three times with PBS (with enough volume to cover the entire sample) to remove debris and blood from the skin surface. The PBS from the washes was discarded into bleach.

With a sterile scalpel, No. 20 (rounded blade) (Swann-Morton, UK), parallel cuts 2-3 mm deep and 2-3 mm apart were made into the tissue. Care was taken not to penetrate into the dermis. Cuts are made to allow the dispase access into the tissue.

L-15 medium, containing dispase at 4units/ml, was added (approximately 50-55 ml). The dispase containing media can be made separately or the dispase can be diluted by adding the stock solution to the media in the Petri-dish.

The following antibiotics were then added, Kanamycin at final concentration of 10 μ g/ml, Gentamycin at a final concentration of 10 μ g/ml , Ciproxin™, at a final concentration of ciprofloxacin of 0.01mg/ml. After the antibiotics were added, the tissue was left, dermal side upwards, at room temperature for 24 hours. The dispase digestion was found to work better if left for longer than the standard suggested overnight digestion. Even this was sometimes not long enough and the tissue had to be placed at 37°C for a futher 1-2 hours. This allowed for easier removal of epidermis from the dermis. It was found however, that dispase treatment at 37°C for 1-2 hours after the standard overnight digestion at room temperature led to low yield of cells during the trypsinization step.

On the next day, the tissue was turned over, epidermal side upwards, and the epidermis was stripped off from the dermis using fine watchmakers forceps. The epidermal strips were placed in a Petri-dish containing fully supplemented L-15 medium.

The epidermal pieces were then transfered to a Sterilin universal containing 10-15 ml of 0.02% EDTA (w/v) in PBS and washed three times with this solution. This solution washes off any foetal calf serum which inhibits the action of trypsin to be used in the next stage of the process.

5 ml of trypsin solution, previously warmed to 37°C, was added to the pieces of epidermis which were then placed at 37°C for 3 mins. Towards the

end of the 3 min trypsin digest, the bottle was shaken vigorously. At the end of 3 mins, 0.02% (w/v) EDTA in PBS (to make up to 20 ml) was added to stop the reaction. The mixture was shaken.

The resultant cell suspension was taken up with a pipette (care being taken not to take up large pieces of epidermis) and added to 5 ml of fully supplemented L-15 medium. The sample was centrifuged at 220g, at room temperature for 3 mins.

To the epidermal pieces that had not digested completely, more trypsin solution was added and digestion continued at 37°C for 3 mins. Trypsin digestion tends to liberate cells of the epidermis closest to the skin surface. After each digest, the samples being centrifuged contained liberated cells. A single 15 min digest in place of repeated 3 min digestions is not used because the outermost cells would die by the time the trypsin could act on the inner layers.

Trypsinization was usually carried out five times. In initial experiments, only three 5 min trypsinizations were carried out, however, it was observed that by the third trypsinization, the cells did not form a compact pellet, probably due to cell disintegration. Five, 3 min trypsinizations gave compact pellets up to the fifth trypsinization stage and thus helped in increasing the yield of cells obtained from a single sample.

The supernatant from each of the centrifugations was removed and the pellets resuspended in L-15 medium by tapping gently. The five resuspended pellets were pooled. The mixture was passed through a 40µm Cell Filter, (Falcon) into a Falcon Blue Max tube. The filtrate was placed in a Universal bottle (Bibby Sterilin) and recentrifuged. The supernatant was discarded and the pellet was resuspended as before, but this time in Clonetics KGM containing 10% foetal calf serum.

In initial experiments, the amount of foetal calf serum added was 2% (v/v), however, when the amount of serum added to the media was increased,

the number of keratinocytes attaching to the tissue culture plastic increased and thus the culture reached confluence in a shorter period of time. Therefore, 10% foetal calf serum was used for all cultures on which experimental analyses were carried out.

The resuspended mixture of cells was placed in a tissue culture flask and given a slight shake. Because the incubator that was used was not gassed the flask had to be gassed for a couple of minutes with a 5%CO₂/95% air mixture. The flask tops were screwed on tightly and the flasks placed in the 37°C incubator. After attachment of cells, the plating medium was replaced with serum free KGM.

Thereafter, the cells were fed once every 3 days at which time they were also regassed with 5% CO₂/ 95% air. When the keratinocytes had reached 90% confluency they were either harvested, or passaged.

Harvesting and passaging of keratinocytes

Plating efficiency of keratinocytes is not good and a lot of cells are lost at this stage. To harvest or passage the cells, the medium was first removed and replaced with 0.1% (w/v) EDTA in PBS (enough to cover the cells). After 10 mins the cells were monitored under a light microscope to ensure no detachment had occurred. Pre-warmed, trypsin solution (enough to cover cells) was added and cells incubated in a 37°C incubator for 1 min. This solution was poured off. Melanocytes are the first cells to detach, therefore this step is used to remove these cells. The remaining cells were incubated with trypsin solution for about 3-5 mins, monitored under a light microscope, and the flasks then tapped to detach cells. (Care needs to be taken so as not to over-trypsinize the cells as this leads to cell disintegration).

Once detached, the cells plus trypsin solution were poured into a universal containing approximately 10 ml of fully supplemented L-15 medium, to stop the reaction. The resultant cell suspension was centrifuged at 220g, at

room temperature, for 3 mins. If the cells were to be passaged, then the medium was removed and the cells were resuspended in approximately 10 ml (for 25cm² flasks) of L-15 medium and divided into two universals. Both samples were centrifuged, the supernatant removed and the cell pellets were resuspended in KGM containing 10% foetal calf serum. Cells were then plated out and gassed with 5% CO₂/ 95% air and placed in a 37°C incubator. After 3 days the medium was removed and replaced with serum free KGM.

Upon attachment of the passaged cells, the cells looked much larger. This implies that there is a strong possibility of the cells undergoing terminal differentiation. Proliferating cells are smaller than cells that are in the process of terminal differentiation. If terminal differentiation takes place, the cells do not divide and eventually die. As a result, the yield of cells after passaging is extremely low. It was decided not to passage primary keratinocytes and to use the initial cultures for all analyses.

If the cells were to be harvested then once trypsinized, they were added to L-15 medium, centrifuged and the pellet washed twice with PBS and frozen at -70°C until used for analyses.

2.3 Plasmid propagation and manipulation

2.3.1 Transformation of competent *E.coli* cells

Solutions

LB-Medium and LB-Agar

LB-Medium was prepared from capsules (Bio-Inc, USA). 5 capsules were placed in 200 ml of water. This was autoclaved. To prepare LB-Agar, 20 LB-Agar capsules were added to 500 ml of water and this was autoclaved. Ampicillin (50µg/ml) was added when the LB-Agar had cooled to ~50°C. The

agar was then poured onto sterile (Bibby-Sterilin, UK) plates and allowed to set at room temperature and then placed in a 37°C incubator to dry.

Transformation Buffer

10mM 2-(N-morpholino)ethanesulfonic acid (MES) pH 6.3

45mM MnCl₂.4H₂O

10mM CaCl₂.2H₂O

100mM KCl

3mM Hexaminecobalt chloride

SOB medium

SOB medium was prepared from capsules (BIO 101 INC, USA) as per manufacturers instructions. To 1 litre of water, 30 capsules were added and the resultant mixture autoclaved.

Method

A 10 ml culture of DH5α cells were grown overnight (no ampicillin added) in LB-medium. The next day, the OD of this culture was read at 550nm using LB-medium as a blank. An OD of 0.6-0.8 is required before the cells can be used for transformation. If the culture had an OD more than this, it was diluted, by adding 2 ml of culture medium to 9 ml of LB-medium and grown for an additional hour at 37°C, with vigorous shaking. The OD was then read again and when the required OD was obtained, the culture was incubated on ice for 10 mins (in Sterilin Universal bottles). Thereafter, the culture was centrifuged at 220g, at room temperature, for 10 mins and the supernatant discarded. The pellet was resuspended in 8 ml, ice-cold, transformation buffer. The culture was incubated on ice for a further 10 mins after which it was centrifuged at 220g, at room temperature, for 10 mins. The supernatant was removed and the bacterial pellet resuspended in 2 ml of

transformation buffer. 200 μ ls of the bacterial culture were then aliquoted out into 1.5 ml Eppendorf tubes. To each of the tubes except one, 2 μ g of DNA was added. A control tube was also set up into which no DNA was added. Samples were incubated on ice for half an hour and then at 42°C for 90 secs, after which they were put back on ice. SOB medium (1ml) was added to Falcon tubes (12 ml round bottom polypropylene tubes with caps) and the transformed bacteria added to this. The culture was incubated at 37°C, with vigorous shaking for 1 hour. For each sample, 200 μ l and 1 ml of the resultant culture was plated out onto LB-Agar plates, containing ampicillin (50 μ g/ml). Also plated out was the control bacteria, containing no DNA, on LB-Agar plates with and without ampicillin.

To see if the transformation was successful, a single colony was picked and used to inoculate LB-Medium with ampicillin (50 μ g/ml) and grown overnight at 37°C. A small scale plasmid preparation (see section 2.3.2) was carried out and the resultant DNA analysed.

If the small scale preparation and analyses proved that the bacteria had been transformed, a glycerol stock of the bacteria was made. Glycerol stocks were made in 2 ml 'Lock-Safe' Eppendorf tubes by adding 1 ml of the culture containing the transformed bacteria to 1 ml of a solution of 30% (v/v) glycerol in LB-medium, and snap freezing the mixture in liquid nitrogen. The stock was then stored at -70°C until further use.

2.3.2 Small scale plasmid preparation and analysis

Small scale DNA preparations were made using the alkaline lysis method (modified from Sambrook *et al.*, (1989)), to check various CYP and FMO subclones provided by Prof. Ian Phillips at Queen Mary and Westfield College, London.

Solutions:

Solution I

50mM glucose

25mM Tris-HCl pH 8.0

10mM EDTA, pH 8.0

Once prepared the solution was autoclaved and stored at 4°C

Solution II

0.2M NaOH

1% SDS

Solution II was always prepared fresh.

Solution III

5M potassium acetate	60ml
----------------------	------

glacial acetic acid	11.5ml
---------------------	--------

water	28.5ml
-------	--------

The resulting solution was 3M with respect to potassium and 5M with respect to acetate.

This solution was autoclaved and stored at 4°C.

TE buffer

10mM Tris-HCl, pH 8.0

1mM EDTA, pH 8.0

The solution was autoclaved and stored at room temperature.

10 X TBE

0.45M Tris-borate

0.01M EDTA

The solution was autoclaved and stored at room temperature.

Method:

The relevant glycerol stock was streaked onto LB-Agar plates containing Ampicillin (50 μ g/ml). The plates were incubated at 37 $^{\circ}$ C overnight. A single colony was picked and used to inoculate LB-medium also containing Ampicillin (50 μ g/ml). The culture was incubated overnight at 37 $^{\circ}$ C with vigorous shaking. 1.5 ml of the culture was placed in a 2 ml Eppendorf tube and centrifuged at 12000g, at room temperature, for 30 secs. The remaining culture was stored at 4 $^{\circ}$ C. The supernatant was removed, leaving the bacterial pellet as dry as possible. This pellet was resuspended in 100 μ l of ice-cold Solution I. 200 μ l of freshly prepared Solution II were added. The contents of the tube were mixed by inverting the tube rapidly five times and the tube was stored on ice for 5 mins. 150 μ l of ice-cold Solution III were then added and contents vortexed for 10 secs. The tube was stored on ice for 3-5 minutes, and then centrifuged at 12000g for 5 mins. The supernatant was transferred to a fresh tube and an equal volume of phenol (pH 8.0)/chloroform (1:1 (v/v)) added. The resultant mixture was vortexed and centrifuged at 12000g, at room temperature, for 2 mins. The aqueous phase was transferred to a fresh tube and the DNA precipitated using 2 volumes of ethanol at room temperature. The mixture was allowed to stand for 2 mins and then centrifuged at 12000g, at room temperature, for 5 mins. The supernatant was removed and the pellet was washed with 70% ethanol. The pellet was dissolved in 50 μ l of TE. The DNA was stored at -20 $^{\circ}$ C.

2.3.3 Restriction enzyme digestion

To analyse plasmid DNA, restriction enzyme digestion was carried out. The restriction enzyme used depended upon the site in the polylinker of the

vector that the fragment was cloned into. Generally, for restriction digests, 3-5 μ l of miniprep DNA was used. To this, an appropriate volume of 10X One-Phor-All Buffer (Pharmacia Biotech, Sweden) , 1 μ l (10mg/ml) of RNase A (Boehringer Mannheim, Germany), 5-10 units of the restriction enzyme (Pharmacia Biotech, Sweden) and water, to 20 μ l, was added . The digest was incubated at 37 $^{\circ}$ C for at least 2 hours. The fragments were visualized by electrophoresing the DNA in an agarose gel (% of which depended on the size of the fragment expected) containing ethidium bromide (0.5 μ g/ml), using 1XTBE as the running buffer and observing the gel under a UV transilluminator. The size of the fragment was determined by comparison to a molecular weight standard, 1kb ladder, (Gibco BRL, UK) which was also loaded on the gel.

2.3.4 Large scale (Maxi prep) of plasmid DNA

Large scale preparations of plasmid DNA were carried out using QIAGEN Plasmid kits (QIAGEN Inc, USA) and as per manufacturers instructions. A single bacterial colony was picked from the relevant plate, and inoculated into 200 ml of LB-medium containing ampicillin and allowed to grow overnight at 37 $^{\circ}$ C, with shaking. The bacterial cells were harvested by centrifugation at 6000g using a Sorvall GSA rotor, at 4 $^{\circ}$ C, for 15 mins. All traces of the supernatant were removed by inverting the open centrifuge tube, until all the medium was drained. The bacterial pellet was then resuspended in 10 ml of Buffer P1 (containing RNase A). The resultant mixture was then transferred to plastic tubes and thereafter, 10 ml of Buffer P2 were added. The mixture was gently mixed by inverting the tube 2-3 times and incubated at room temperature for 5 mins. 10 ml of chilled Buffer P3 was then added and the solution mixed immediately but gently by inverting the tube 5-6 times. The mixture was then incubated on ice for 20 mins. Buffers P1, P2 and P3 were all

provided with the kit. The solution was centrifuged at 20000g in a Sorvall SS-34 rotor at 4°C, for 30 mins . The supernatant was then removed promptly and it was recentrifuged under the same conditions for a further 15 mins. The supernatant was removed and passed through a nylon gauze into a Sterilin tube. While centrifugation took place, the QIAGEN-tip 500 was equilibrated by applying 10 ml of Buffer QBT to the tip and allowing the column to empty by gravity flow. The supernatant was applied to the tip and entered the resin by gravity flow. The QIAGEN tip was then washed twice with 30 ml of Buffer QC. The DNA was eluted with 15 ml of Buffer QF and collected in a 30 ml glass Corex tube. Thereafter, the DNA was precipitated using 0.7 volumes of isopropanol and centrifuged immediately at 15000g in a Sorvall SS-34 rotor, at 4°C, for 30 mins. The supernatant was carefully removed and the pellet washed briefly in 5 ml of 70% ethanol. The pellet was recentrifuged under the same conditions for 15 mins and the wash step repeated. After careful removal of the ethanol, the pellet was air-dried and resuspended in water. To determine the yield of DNA obtained, the DNA was diluted 1 in 100 and the OD read at 260 nm and its concentration determined using the equation below. The OD at 280 nm was also read to evaluate the protein:DNA ratio, which is usually around 1.8, for pure DNA.

$$\text{Concentration of DNA } (\mu\text{g/ml}) = A_{260} \times 50 \times \text{dilution factor.}$$

2.3.5 Retrieval of DNA from Low Melting Point agarose gels

Solutions:

50 X TAE

2M Tris-acetate

0.05M EDTA

The solution was autoclaved and stored at room temperature.

3M Sodium acetate pH 5.2

The solution was stored at room temperature.

Method:

Low melting point agarose gels (% depending on the size of the fragment being isolated) were prepared using Ultra pure Low melting point agarose (Gibco BRL, UK) and TAE to a working dilution of 1X. The DNA was prepared and electrophoresed. The fragments were observed under a UV light source and once the required fragment was identified, it was excised from the gel and the slice placed in a 1.5 ml Eppendorf tube. Two different methods of extraction were used depending on the amount of DNA in the slice (as estimated from the intensity of the band under UV light). The first method was employed when a substantial amount of DNA was present in the gel slice.

This method involved the addition of 5 volumes of 20mM Tris-HCl/1mM EDTA (pH 8.0) to the slice. The slice was then incubated at 65°C for 5 mins. The melted agarose was cooled to room temperature and an equal volume of phenol (pH 8.0) was added, and the solution vortexed for 20 secs. The samples were then centrifuged in a benchtop Eppendorf centrifuge, for 10 mins, to recover the aqueous phase. This process was repeated for the following extractions, phenol/chloroform (1:1 (v/v)) and chloroform. The final aqueous phase was transferred to a clean Eppendorf tube. 0.2 volumes of 10M ammonium acetate and 2 volumes of 100% ethanol (both at 4°C) were added. The tube was inverted several times and left at room temperature for 10 mins. The DNA was recovered by centrifuging the samples at 6000g, at 4°C, for 20 mins in a refrigerated Eppendorf centrifuge. If no pellet was observed, the samples were centrifuged in a bench top Eppendorf centrifuge for a further 15 mins at room temperature. The pellet was washed in 70% ethanol and recentrifuged at room temperature for 10 mins, the ethanol

removed and the pellet dried in a vacuum dessicator for 5-10 mins. The DNA was resuspended in a small volume (10 μ l) of sterile water.

The second method of DNA extraction involved the use of SPIN-X centrifuge filter units (Costar, USA). The gel slice was transferred to the top chamber of the unit and the tube then placed in liquid N₂ for 2-3 minutes after which it was centrifuged, in a bench top Eppendorf centrifuge, for 10 mins at room temperature. This process was repeated twice. 100 μ l of TE buffer were added to the top chamber. The tube was centrifuged as above for another 10 mins. The top chamber was removed and 0.2 volumes 3M Sodium acetate (pH 5.2) and 2 volumes of 100% ethanol were added. The DNA was precipitated overnight at -70°C. The pellet was obtained by centrifuging the samples for 15 mins after which the pellets were dried and resuspended in an appropriate volume (10 μ l) of water.

2.3.6 Preparation of radiolabelled probes for northern and Southern blot hybridization analysis

Radioactive probes for both northern and Southern blot hybridization analysis were prepared using the random priming method (Feinberg and Vogelstein, 1983)

Solutions:

10X Random primer buffer

600mM Tris-HCl, pH 7.8

100mM MgCl₂

100mM β -mercaptoethanol

5mM dNTP mix (dATP, dGTP and dTTP)

Obtained as stocks of 100mM solutions of the individual dNTPs (Pharmacia Biotech, Sweden). The appropriate amount of each dNTP was diluted in water to give a final concentration of 5mM of each dNTP in the mix.

20mM Dithiothreitol (DTT)

DTT was obtained from BDH, UK as a powder and dissolved in the appropriate amount of sterile water to give a 20mM solution. The solution was aliquoted and stored at -20°C until used.

Random primers

Random primers were purchased as a stock solution of 3.33mg/ml from Gibco BRL, UK and diluted in an appropriate volume of sterile water to give a final concentration of 75ng/ μ l. They were then aliquoted and stored at -20°C.

3^2P -[α] dCTP

The radioisotope with a specific activity of 3000 Ci/mmol, was obtained from NEN Dupont, Belgium.

Method:

The probe was prepared by combining the contents of Tube I and Tube II

Tube I contained:

20mM DTT	9 μ l
5mM dNTPs	2.4 μ l
10 X Random primer buffer	9 μ l
3^2P -[α] dCTP	6 μ l = 60 μ Ci

and

Tube II contained:

cDNA insert (in low melting point agarose)	100ng
Random primers	1.5 μ l
Water to make up to a total volume of 90 μ l after combining the contents of Tubes I and II.	

Tube II was boiled for 5 mins, briefly centrifuged, and its contents were added to Tube I. Thereafter, 1 μ l (6.435 units) of Klenow fragment (Pharmacia Biotech, UK) was added and the tube flicked, briefly centrifuged and placed at 37°C for at least 3 hours.

2.3.6.1 Measurement of the specific activity of the probe

To determine if the probe was satisfactory for use in hybridization analysis, its specific activity in cpm/ μ g was measured. This was done by spotting 1 μ l of probe on each of two pieces of DE81 paper (Whatmann, USA). One piece was marked (using a pencil) 'probe' whereas the other was marked 'control'. The filter marked 'probe' was washed 6 times, for 2 mins each, with 0.5M Na₂HPO₄, followed by 2 washes for 1 min each in water and finally a single wash in 95% ethanol. Both the 'control' and 'probe' filters were dried under an infra-red lamp for 1 min and placed in separate scintillation vials containing 1 ml of EcoScint™ scintillation fluid (National diagnostics, USA). The counts per minute (cpm) reading were obtained using a scintillation counter.

During random-primer labelling, there is net synthesis of DNA, while the initial DNA substrate remains unlabelled.

% incorporation was calculated using the following formula:

$$\frac{\text{cpm incorporated}}{\text{total cpm in sample}} \times 100$$

Probe yield = ng initial substrate DNA + ng DNA synthesised

As the average molecular weight of a nucleoside monophosphate in DNA is 350, for a labelled nucleotide with a specific activity of 3000 Ci/mmol:

$$\text{ng DNA synthesised} = \frac{\mu\text{Ci incorporated} \times 0.35 \times 4}{3}$$

The multiplication factor of 4 is included as there are four nucleotides, only one of which is labelled.

Once probe yield has been calculated, the specific activity can be determined:

$$\text{specific activity (dpm}/\mu\text{g)} = \frac{\text{total activity incorporated (dpm)}}{\text{probe yield } (\mu\text{g})}$$

where $1\mu\text{Ci} = 2.2 \times 10^6$ dpm.

Only probes having an activity of between 10^8 - 10^9 dpm/ μg were utilised for hybridization analyses.

Unincorporated nucleotides were removed by passing the probe through CHROMA SPIN columns (Clontech, USA). The probe was stored at -20°C until used.

Before use, the probe was boiled for 5 mins and then kept on ice until it was added to the hybridization solution (section 2.5.4).

2.4 Isolation of total RNA

Three different RNA isolation protocols were employed in the extraction of RNA from either tissues or cultured cells. These were as follows:

2.4.1 Guanidine thiocyanate/lithium chloride precipitation (Cathala *et al.*, 1983)

Solutions:

Lysis Buffer

5M guanidine monothiocyanate

10mM EDTA, pH 8.0

50mM Tris-HCl, pH 7.5

8% (v/v) β -mercaptoethanol

The guanidine monothiocyanate (29.54g) was dissolved in 10 ml of water at 50°C. 2.5 ml of 1M Tris-HCl was then added, followed by 1 ml of 0.5M EDTA, pH 8.0. The solution was made up to 50 ml with water and filter sterilised using a 0.22 μ m filter (Sartorius AG, Sweden). The β -mercaptoethanol was added in a fume hood, just before use, to give a final concentration of 8% (v/v).

3M and 4M Lithium chloride solutions

LiCl was obtained from Sigma Chemical Co. and was of molecular biology grade. Stock solutions of 3M and 4M LiCl were prepared with water and autoclaved. These solutions were stored at 4°C.

RNA solubilisation buffer

0.1% (w/v) SDS

1mM EDTA, pH 8.0

10mM Tris-HCl, pH 7.5

RNA solubilisation buffer was prepared by mixing 1 ml of 10% (w/v) SDS, 200 ml 0.5M EDTA, pH 8.0, 1 ml of 1M Tris-HCl, pH 7.5. The volume was made up to 100 ml using water. The solution was aliquoted, autoclaved and stored at room temperature.

Phenol, pH 6.0

Phenol (Fisons, UK) was thawed and aliquoted into "Blue Max" Falcon tubes. A buffering solution of 600 μ l of 0.5M EDTA, pH 8.0, 15 ml of 1M Tris-HCl, pH 7.5 and water to make 300mls, was prepared. An equal volume of this buffer was added to the phenol. The resultant solution was mixed thoroughly and left for phase separation. The aqueous phase was discarded. This procedure was repeated twice. The pH of the phenol phase was checked with indicator paper until it was 6.0. The final aqueous phase was then removed, the tubes covered in foil and stored at -20°C.

Chloroform:Isoamyl alcohol (IAA) 24:1 (v/v)

96 ml of chloroform was added to 4 ml of IAA. The tubes were covered in foil and stored at room temperature.

Saturated ammonium acetate solution

5g of ammonium acetate was dissolved in water. Additional salt was added until some remained undissolved. The resultant saturated solution was filter sterilised using 0.45 μ m filters (Sartorius AG, Sweden).

Method:

All the glassware used in the RNA preparations was cleaned thoroughly, siliconized and autoclaved. Siliconization of glassware such as Corex tubes was carried out by pouring a solution of dimethyldichlorosilane (BDH, UK) into the tubes and immediately pouring out. The tubes were then thoroughly rinsed with distilled water.

Total cellular RNA was isolated by homogenising the cells in 5M guanidine monothiocyanate followed by direct precipitation of the RNA by 4M LiCl. Cells were homogenised in lysis Buffer; 7 ml buffer/ml packed cells or per gram of tissue. Tissues were homogenised using a Polytron type PT10 OD homogeniser. The samples were placed in sterile Corex tubes and the RNA precipitated overnight at 4°C, by adding 4M LiCl (5 volumes:1 volume homogenate). The samples were centrifuged at 11000g at 4°C for 90 mins. Pellets were resuspended in 3M LiCl and centrifuged under the same conditions as above. To remove any excess proteins, the pellets were washed in 2M LiCl:4M Urea and centrifuged as above. The pellets from the second centrifugation were resuspended in 1-5 mls of solubilisation buffer by successive freezing and vortexing until they dissolved. The RNA was then extracted using phenol/chloroform (1:1), whereby, 1 volume of phenol, pH 6 was added the mixture, vortexed, and then 1 volume of chloroform/IAA added, the sample vortexed and centrifuged at 200g, at room temperature for 8 mins. If the interphase did not pack well the sample was frozen at -20°C and thawed. The sample was centrifuged under the same conditions. The phenol/chloroform extraction procedure was repeated. The aqueous phase was transferred to a clean tube and RNA precipitated using 0.05 volumes of ammonium acetate and 2 volumes of absolute ethanol at -20°C overnight or -70°C for 1 hour. The samples were centrifuged for 70 mins at 10000g, at -10°C and the pellets air-dried. The RNA pellets were dissolved in an appropriate volume of sterile water and the concentration determined

spectrophotometrically by measuring the absorbance at 260nm, using the formula:

$$\text{Concentration } (\mu\text{g/ml}) = A_{260} \times 40 \times \text{dilution factor}$$

The purity was determined by calculating the A_{260}/A_{280} (the ratio being between 1.8 and 2.0 for pure RNA samples). RNA integrity was checked by agarose/formaldehyde gel electrophoresis as described in section 2.5.1.

The above method was used to extract RNA from all tissue samples apart from whole skin. With whole skin, no RNA was obtained when this method was employed. Initially this method was used also for the extraction of RNA from cell pellets. Although RNA was obtained, the yield was very low. To maximise the yield from cell pellets the single tube Ultraspec™ (Biotex, USA) total RNA isolation kit was used.

2.4.2 Ultraspec™ RNA isolation kit

Where the amount of sample was limited, e.g primary keratinocyte cultures or when no RNA was obtained using the guanidine thiocyanate/LiCl method, the Ultraspec™ RNA isolation system (Biotecx laboratories Inc., USA) was used.

For whole skin, 1 ml of Ultraspec was used per 100 mg of tissue, and the sample homogenised using a Polytron PT10 OD homogeniser. When the tissue had been frozen, it was homogenised directly in the Ultraspec solution. Primary keratinocytes were lysed directly in the tissue culture flask by adding 1 ml of Ultraspec/35cm² culturing surface. The cell lysate was passed several times through a pipette and aliquoted immediately into microfuge tubes.

Following homogenisation, the homogenate was stored for 5 mins on ice to permit the complete dissociation of nucleoprotein complexes. 200µls of

chloroform per 1 ml of Ultraspec was added. The samples were covered and vortexed for 15 secs. and placed on ice for a further 5 mins. They were centrifuged at 12000g, at 4°C for 15 mins .

The aqueous phase was transferred to a fresh tube and an equal volume of isopropanol was added to each tube. The samples were placed on ice for 10 mins and centrifuged at 12000g at 4°C for 5 mins. The supernatant was removed and the RNA pellet was washed once in 75% ethanol and centrifuged at 7500g, at 4°C for 5 mins. The pellet was air-dried and dissolved in an appropriate amount of water at 4°C. The RNA was aliquoted and stored at -80°C. RNA concentrations were determined by measuring the absorbance at 260nm.

2.4.3 Guanidine thiocyanate/guanidine hydrochloride extraction procedure (Chirgwin *et al.*, 1979)

This method was used only for whole skin samples, the reasons for which are described in section 4.1.1.

Solutions

4M Guanidine monothiocyanate stock

This was prepared by mixing 50 g of guanidinium thiocyanate with 0.5 g of sodium N-lauroylsarcosine, 2.5 ml of 1M sodium citrate, pH 7.0, 0.7 ml of β -mercaptoethanol and 0.33 ml of 30% antifoam (BDH). Distilled water was added and the solution warmed and the pH adjusted to 7.0 with NaOH. The volume was made up to 100 ml at room temperature. The solution was made up in a fume cupboard and all equipment which came into contact with it was treated with dilute aqueous bleach.

7.5M Guanidine hydrochloride solution

A 7.5M solution was made up by mixing the appropriate amount of guanidine hydrochloride (Sigma biochemicals, UK) in water. The solution was neutralized to pH 7.0, buffered with 0.025vol of 1M sodium citrate, pH 7.0, made 5mM with respect to DTT and stored tightly closed at room temperature.

Method

Either fresh or frozen whole skin samples were used. 8mls of guanidine thiocyanate solution was used per 1 g of tissue. The tissue was homogenised using a Polytron PT10 OD homogeniser until no large lumps were observed. This process is very difficult as skin is an extremely fibrous tissue, and therefore, periods where the homogenate had to be cooled down were allowed before continuing with homogenisation. The homogenate was then centrifuged at 10000g, at 10°C for 10 mins.

To the supernatant, 0.025 volume (relative to the original volume) of 1M acetic acid and 0.75 volume of absolute ethanol were added. The resultant solution was vortexed and either stored overnight at -20°C or for an hour on dry-ice. The solution was then centrifuged at 8000g, at -10°C for 10 mins. The supernatant was discarded and the pellet redissolved in 0.5 volume (relative to the original volume of the homogenate) of 7.5M guanidine hydrochloride. The solution was then transferred to 15 ml Falcon tube, a final concentration of 1% (w/v) SDS was added and then vortexed to mix. One volume of phenol, pH 6, was added, the sample vortexed, then 1 volume of chloroform/IAA (24:1 (v/v)) was added. The solution was mixed by vortexing and either left overnight at -20°C or for 1 hour on dry ice. The samples were centrifuged, after thawing, for 10 mins and the aqueous layer carefully removed and transferred to another fresh tube. The aqueous layer was reextracted with phenol/chloroform (1:1). To the final aqueous layer, 2

volumes of ice-cold absolute ethanol were added in sterile Corex tubes and the RNA either precipitated overnight at -20°C or for 1 hour on dry ice.

The precipitate was centrifuged at 10000g, at 4°C for 15 mins. The ethanol was removed and the pellet washed in 1 ml of 80% ethanol. The RNA was centrifuged for 15 mins at 10000g at 4°C. The pellet was finally air-dried and resuspended in an appropriate volume of water. Another phenol extraction needed to be carried out for most of the whole skin samples. This consisted of first adding 1% (w/v) SDS (final concentration) followed by 1 volume phenol, pH 6.0 and 1 volume chloroform/IAA. The samples were centrifuged to separate the phases. The aqueous layer was removed to a clean tube and RNA precipitated with 1/10 volume saturated ammonium acetate and 2 volume ethanol. Thereafter, the samples were centrifuged and washed as previously described. The concentration of RNA was determined by measuring the absorbance at 260nm.

2.5 Northern blotting and hybridization analysis

Solutions:

10 X MOPS/EDTA

0.2M 3-(N-morpholino) propanesulfonic acid (MOPS)

50mM sodium acetate

10mM EDTA, pH 8.0

The pH of the solution was adjusted to 7.0 using NaOH after which it was covered in foil and autoclaved. The solution was stored at room temperature.

Stock electrophoresis sample buffer (ESB)

0.73 ml formaldehyde

2.25ml deionised formamide

0.3 ml glycerol

0.24 ml 10% (w/v) bromophenol blue

0.45 ml 10 X MOPS/EDTA

10 μ ls ethidium bromide solution (10mg/ml stock)

The sample buffer was filter sterilised through a 0.22 μ m filter, aliquoted and stored at -20°C. 25 μ ls of this buffer was added to 5 μ ls of each sample prior to electrophoresis.

20 X SSPE

3M NaCl

0.2M sodium phosphate pH 7.4

0.02M EDTA

The pH of the solution was adjusted to 7.4. It was autoclaved and stored at room temperature.

50 X Denhardt's solution (Denhardt, 1966)

1% (w/v) Ficoll (Type 400-DL)

1% (w/v) Polyvinylpyrrolidone

1% (w/v) BSA (Fraction V)

This solution was filter sterilised through a 0.22 μ m filter and stored at -20°C.

Salmon sperm DNA

Salmon sperm DNA, Sigma type III sodium salt (Sigma Chemical Co., USA) was denatured as described in Sambrook *et al.*, (1989). The DNA was dissolved in water to a final concentration of 10mg/ml and the solution stirred at room temperature to help the DNA to dissolve. The concentration of the NaCl was adjusted to 0.1M and the solution was extracted once with phenol and once with phenol/chloroform (1:1). The aqueous phase was recovered and the DNA sheared by passing it through a 17-gauge needle. The DNA

was precipitated by adding 2 volumes of ice-cold absolute ethanol. It was then centrifuged to recover the DNA and redissolved to a final concentration of 10mg/ml. The absorbance at 260nm, was read and the concentration of the DNA determined using the formula in section 2.3.4. The solution was boiled for 10 mins, aliquoted and stored at -20°C.

Just before use, the solution was boiled for 5 mins and then chilled on ice and was used at a concentration of 100µg/ml in prehybridization solutions and 200µg/ml in hybridization solutions (section 2.5.4).

Deionised formamide

5 g of a mixed bed ion-exchange resin AG501-X8 (Bio-Rad Laboratories, USA) was added to every 100 ml of formamide solution. The solution was stirred for 1 hour at room temperature. The solution was filtered twice through 3MM Whatman paper and once through a 0.45µm filter. It was aliquoted and stored at -20°C.

Method:

2.5.1 Gel preparation

The gel was prepared using the method of Fourny *et al.*, (1988). 1-1.5g of agarose, 10 ml of 10XMOPS/EDTA and 87 ml autoclaved water were mixed in an autoclaved conical flask. The agarose was dissolved by heating the solution in a microwave oven, then cooled to 55°C and 5.1 ml of 37% formaldehyde was added, in a fume cupboard. The gel was poured into a sterile gel tray and allowed to set for 1 hour. Prior to loading, the wells were flushed by pipetting electrophoresis buffer in and out of the wells.

2.5.2 Sample preparation and gel electrophoresis

RNA (10-30 μ g) (for northern blot hybridization experiments) or 1 μ g (when ascertaining RNA integrity), prepared using the methods described in section 2.4, was dissolved in a final concentration of 25mM EDTA and 0.1% (w/v) SDS, in a final volume of 5 μ l. Where samples were dilute, the sample was lyophilised and dissolved in 5 μ l of 25mM EDTA/ 0.1% (w/v) SDS. 25 μ l of ESB was added to each sample before heating at 65 $^{\circ}$ C for 15 mins. The samples were then loaded on a denaturing agarose gel.

The samples were electrophoresed at 30V (using 1 X MOPS as the electrophoresis buffer) for gels having samples that were to be subsequently blotted or at 100V for gels electrophoresed to check the integrity of the RNA samples. The gels were electrophoresed until the bromophenol blue migrated ~10 cm into the gel. RNA bands were visualised using a UV transilluminator and photographed using a Polaroid MP4 camera.

As molecular weight standards on gels to be used to prepare northern blots, 1 μ g of *E. Coli* total RNA was electrophoresed on the same gel. The *E.Coli* 23S and 16S rRNA served as molecular weight markers (2904bp and 1541bp respectively) together with the 28S and 18S rRNA present in eukaryotic cells i.e the samples (5.1kb and 1.9kb respectively).

2.5.3 Northern blotting

The electrophoresed RNA was transferred and capillary blotted onto optimised Nylon (BDH, UK) as per the instructions provided by the manufacturers.

Prior to blotting, the membrane was soaked in the transfer solution (10XSSPE). The gel was rinsed twice with distilled water. 3 pieces of 3MM Whatman paper was placed on a glass plate, these serve as a wick to allow

the transfer by capillary action. The gel was placed on top of the wick, RNA side upwards. The membrane was placed on top of the gel followed by 5 pieces of Whatman paper, cut to the size of the gel. Throughout the transfer, the paper on top of the gel was not allowed to come into contact with that below the gel. This was done by placing Saran Wrap around the sides of the gel. The glass plate, wick and gel assembly was placed in a trough containing transfer buffer. The wick of the filter paper dipped into the transfer buffer, this was done by raising the entire assembly on Petri-dishes. 6 sheets of Quick-Draw™ blotting paper (Sigma Chemical Co., USA) were placed upon the gel assembly, followed by another glass plate. A light weight was placed on top of the glass plate. The capillary action of the solution through the gel and up the Quick-Draw™ paper allows the solution to transfer the RNA molecules to the membrane. Transfer was allowed to occur between 3 hours to overnight. Following transfer, the well positions were marked on the filter, and the filter air-dried. The RNA was immobilized by baking the membrane at 80°C, followed by UV cross-linking using a UV-Stratalinker 1800 (Stratagene, USA). To ensure that all the RNA from the gel had been efficiently transferred, the gel was stained with 5µg/ml of ethidium bromide in 0.5M ammonium acetate and observed under a UV light source.

2.5.4 Prehybridization and hybridization of northern blots

Solutions:

Prehybridization solution

5 X SSPE

5 X Denhardt's reagent

100µg/ml Salmon sperm DNA

50% (v/v) Deionised formamide

2% (w/v) SDS

Prehybridization was carried out for at least 3-6 hours at 42°C

Hybridization solution

50% deionised formamide

5 X Denhardt's solution

5 X SSPE

200µg/ml Salmon sperm DNA

10% (w/v) dextran sulphate

2% (w/v) SDS

After boiling the probe for 5 mins, it was added to the hybridization solution and hybridization was allowed to occur overnight at 42°C

2.5.5 Washes

After hybridization, washes were carried out as follows:

- 2 X SSPE/ 1% (w/v) SDS at room temp for 15 mins once
- 1 X SSPE/ 1% (w/v) SDS at room temp for 15 mins twice
- 0.1 X SSPE/ 1% (w/v) SDS at room temp for 15 mins once
- 0.1 X SSPE/ 1% (w/v) SDS at between 55-65°C once or twice depending on the background non-specific hybridization.

The blot was covered in Saran wrap and autoradiographed for a minimum of 24 hours at -80°C with intensifying screens.

2.6 RNase protection assay (RPA)

Solutions:

RPA loading buffer

9.7 ml deionised formamide

0.1g Ficoll

5 mg bromophenol blue

5 mg xylene cyanol

0.3 ml H₂O

The loading buffer was filter sterilized using 0.22µm filters (Millipore, USA) aliquoted and stored at -20°C

Elution buffer

1.7 ml 7.5M ammonium acetate

0.5 ml 0.5M EDTA, pH 8.0

1.3 ml 10% (w/v) SDS

20.3 ml H₂O

The elution buffer was filter sterilized using 0.22µm filters (Millipore, USA) and stored at -20°C.

Hybridization buffer

80% deionised formamide

40mM PIPES (Piperazine-N,N'-bis[2-ethanesulfonic acid]), pH 6.5

0.4M NaCl

0.1mM EDTA

The hybridization buffer was filter sterilized using a 0.22µm filter (Millipore, USA) and stored at -20°C.

RNase solution

10mM Tris-HCl, pH 7.5

1mM EDTA, pH 8.0

0.2M NaCl

0.1M LiCl

The Ambion RNase cocktail (consisting of RNase A and T1 mix, 500U/ml and 20,000U/ml respectively) was added at a dilution of 1 in 625. This solution was made up on the day of use.

³⁵S labelled 1kb ladder

1kb ladder was obtained from Gibco BRL and was labelled using a fill-in reaction and [$\alpha^{35}\text{S}$]-dATP (ICN Pharmaceuticals, USA). The reaction tube contained:

1 μg 1Kb ladder

1X One-Phor-All buffer (Pharmacia)

1 μl Klenow fragment (6.435units)

30 μCi [$\alpha^{35}\text{S}$]-dATP specific activity of 1000Ci/mmol

0.4mM of each dGTP, dCTP and dTTP

The reaction mixture was incubated at 37°C for 30 mins thereafter 1 μl 0.5M EDTA was added and the tube heated to 65°C for 10 mins.

0.5 μl of this reaction was used and made up to 4 μl with RPA loading buffer.

5 X rNTP mix

20 μl rATP final concentration 2mM

20 μl rUTP final concentration 2mM

20 μl rGTP final concentration 2mM

1 μl rCTP final concentration 0.1mM

The mix was made up to 100 μl with H₂O

8M Urea/6% Polyacrylamide gel

All gels for RPAs were cast using the Mighty Small apparatus (Hoeffer Scientific, USA). Either 0.5mm thick or 1.5mm thick gels were cast depending on whether they were to be used to purify the probe or to separate protected fragments.

Gels were prepared using the Sequagel™ Sequencing System (National Diagnostics, Atlanta USA). This consists of Sequagel Concentrate, Sequagel Diluent and Sequagel Buffer.

The following formula (as provided by the manufacturer) was used to calculate the volume of individual SequaGel components needed. All gels contained a final concentration of 8.3M urea and 1XTBE.

$$V_c = \frac{(V_t)(X)}{25}$$

$$V_b = 0.1 (V_t)$$

$$V_d = V_t - (V_c + V_b)$$

where:

V_c = volume of Sequagel Concentrate to be used (ml)

V_b = volume of Sequagel Buffer to be used (ml)

V_d = volume of Sequagel Diluent to be used (ml)

V_t = Total volume of gel casting solution desired (ml)

X = % gel desired.

800 μ l of 10% (w/v) ammonium persulfate and 40 μ l of N, N, N', N'-Tetramethylethylenediamine (TEMED) (Bio-Rad Laboratories, UK) was added for every 100 ml of gel casting solution.

2.6.1 RNA transcription and transcript purification

The following constructs were used as RNase Protection probes for the CYPs. All listed CYP constructs were made previously by Dr C. Palmer in the laboratory of Prof. Ian Phillips.

- 1) pBS2A6(288) 288bp BamHI/Pst1 fragment cloned into pBluescript
- 2) pBS2B6(450) 150bp HindIII subfragment cloned into pBluescript
- 3) pBS3A4(240) 240bp HindIII/SacI fragment cloned into pBluescript

FMO constructs for RPA analysis were prepared by Dr. C. Dolphin in the laboratory of Prof Ian Phillips. They were as follows:

- 1) p8A1-6 FMO1
- 2) pFMO2/2/15 FMO2
- 3) pBS form II FMO3
- 4) 2A1L-2 FMO4
- 5) p1C1/1b/C FMO5

Antisense transcripts were transcribed from each construct using the promoter that lies at the 3' end of the cDNA (either T7 or T3) depending on the orientation of the insert in pBluescript.

Each construct was linearised by digestion with a restriction enzyme that digests the plasmid at the opposite end of the promoter being used to transcribe the probe.

2.6.1.1 *In vitro* transcription

The following were added to a RNase free 1.5 ml Eppendorf.

5 μ l 5 X Transcription buffer (Stratagene *in vitro* transcription kit)
(Stratagene, USA)

0.1 μ l 0.75mM DTT (Stratagene *in vitro* transcription kit)

5 μ l 5 X NTP mix

2.5 μ l [α -³²P] CTP (Amersham , UK) = 50 μ Ci specific activity of 800Ci/mmol

0.5 μ g linearised DNA

1 μ l RNAsin (Promega)

1 μ l RNA polymerase (T3 or T7) = 10 units

H₂O to make the reaction volume up to 25 μ l.

The reaction mix was incubated at 37°C for 30 mins.

The percentage of radioactive CTP incorporated into the probe was measured by spotting 0.5 μ l of the reaction mixture onto DE81 paper (Whatman, USA) and washing it with 0.5M Na₂HPO₄ to remove unincorporated nucleotides. The percentage incorporation was calculated as detailed in section 2.3.6.1.

2.6.1.2 DNase digestion

After transcription, 10 units of RNase-free DNase I (Stratagene) were added to the transcription reaction and the resultant mixture was incubated at 37°C for 30 mins.

The RNA transcript was precipitated by adding 0.1 volume 3M Sodium acetate and 3 volumes of absolute ethanol and placing on dry ice for 30 mins.

The precipitated probe was centrifuged for 5 mins, the supernatant removed and the pellet resuspended in 4 μ l of RPA loading buffer.

The sample was heated at 80°C for 3 mins and thereafter loaded onto a pre-run, 0.5mm thick 8M Urea/6% polyacrylamide gel (Mighty small, Hoeffer USA). The sample was electrophoresed at 6W, until the bromophenol blue was 1 cm from the bottom of the gel.

The gel was exposed for 20 secs to an X-Ray film (Kodak X-OMAT, Eastman Kodak, USA) and the film developed immediately. The resultant band on the film, corresponding to the radiolabelled probe, was cut from the film, and the film used as a stencil to cut out the band from the gel. The gel fragment was placed into 1 ml of RNA elution buffer. The radiolabelled probe was eluted at 37°C for 2 hours.

After elution, the elution buffer containing the RNA probe was divided into 2 aliquots of 500 μ ls each. RNA was precipitated with 2 volumes absolute ethanol, 20 μ g tRNA and 0.2M NaCl, on dry ice for at least 30 mins. The sample was then centrifuged for 15 mins, the supernatant discarded and pellet resuspended in 200 μ ls of Hybridization buffer.

The probe was counted once again by placing 2 μ l into scintillation fluid and the cpm/ μ l calculated. The probe was then diluted to 1 X 10⁴cpm/ μ l with Hybridization buffer to prevent radiolysis and stored in aliquots at -20°C.

2.6.1.3 Hybridization

All hybridizations were performed in a reaction volume of 30 μ l. Two point assays were carried out for each RNA sample e.g 5 μ g and 10 μ g. To each sample tube, between 4X10⁴ - 1X10⁵ cpm of probe were added. Also added was tRNA to make up a final total RNA concentration of 1 μ g/ μ l. A negative control hybridization containing only tRNA was also included. The

hybridization mixtures were heated at 80°C for 10 mins before incubating them overnight at 45°C.

2.6.1.4 RNase digestion

350µl of RNase solution was added to each tube. The tubes were incubated at 30°C for 30 mins. The RNase digestion was stopped by adding 10µl of 10% (w/v) SDS and 10µl of proteinase K (20mg/ml, Ambion USA). The tubes were incubated for 20 mins at 37°C.

2.6.1.5 Analysis of protected fragments

The digested samples were extracted once with phenol:chloroform (1:1; v/v) and RNA was precipitated with 3 volumes of absolute ethanol on dry ice for 30 mins. The samples were centrifuged at 10000g, at room temperature, for 10 mins, the ethanol discarded and pellets allowed to air dry.

Each sample was resuspended in 4µl of RPA loading buffer, heated at 80°C for 3 mins and loaded onto a pre-run 1.5mm thick 8M Urea/6% polyacrylamide gel. Samples were electrophoresed at 6W per gel (when the mighty small apparatus was used) or 140V (when larger 10cm X 13cm Hoeffer apparatus was used), until the xylene cyanol was 1cm from the bottom of the gel.

The gel was fixed in 10%(v/v) methanol, 10%(v/v) acetic acid for 30 mins, rinsed in water and dried at 80°C under vacuum. The dried gel was exposed to autoradiographic film (Eastman Kodak, USA) ranging from overnight to 3 days depending on the signal intensity.

2.6.1.6 Standard curve

To quantitatively determine the amount of a specific mRNA present in the samples, a standard curve was prepared on the same day as the samples. The standard curve consisted of various probe dilutions and was electrophoresed in an identical manner to the digested samples.

The standard curve was exposed to the same X-ray film as were the samples and for an equivalent amount of time. Multiple exposures were made of both samples and standard curve to avoid errors caused by saturation of the film.

The resultant exposures were then analysed using an Imaging Densitometer (Bio-Rad, Model GS-670). The signal obtained from the standard curve was plotted graphically and the values obtained from the samples interpolated against this curve.

2.6.1.7 Calculation of specific radioactivity of probe

The specific radioactivity of the riboprobe is determined by the concentration of CTP and radionuclide in the transcription reaction mixture described in section 2.6.1.1.

1 μ l of the reaction mix contains 2.5 pmoles of radioactive CTP and 20 pmoles of non-radioactive CTP. Therefore, the total amount of CTP in 1 μ l of reaction mixture is 22.5 pmoles.

1 μ Ci is equivalent to 2.2×10^6 dpm, therefore, 50 μ Ci is equivalent to 1.1×10^8 dpm and 1 μ l of reaction mix is equivalent to 4.4×10^6 dpm.

Therefore, 22.5 pmoles of CTP = 4.4×10^6 dpm.

1 mole of CTP = 6.023×10^{23} molecules (Avogadro's number).

Therefore, 22.5 pmoles of CTP has 1.36×10^{13} molecules of CTP. Thus, 1 μ l of probe contains 1.36×10^{13} molecules of CTP.

The minimum limit of detection using RPAs was found to be 0.05 molecules of mRNA/cell.

On average, 25% of every probe has C residues, for example, an antisense probe of 169 nucleotides contains 42 C residues. Using this example,

1 molecule of probe = 42 C residues

So, every 1 μ l of reaction mix contains $1.36 \times 10^{13}/42$ molecules of probe = 3.23×10^{11} molecules of probe.

As mentioned before 1 μ l = 4.4×10^6 dpm

therefore 3.23×10^{11} molecules of probe = 4.4×10^6 dpm.

This specific activity can be used to calculate the number of probe molecules protected in a RNase protection assay.

For example:

If a protected signal of 500cpm was obtained in an RNase protection assay utilising 40 μ g of total RNA prepared from human liver. If the probe used was that above i.e 169 nucleotides long.

Then the number of molecules protected can be calculated:

$(500 \times 3.23 \times 10^{11}) / 4.4 \times 10^6 = 3.67 \times 10^7$ molecules protected

This value may be related to the amount of tissue used in the assay by assuming a 5pg yield of RNA from each hepatocyte. Since 40 μ g of RNA was used for the assay, this corresponds to 8×10^6 cells.

Therefore the amount of protected molecules/cell = 4.6 molecules/cell.

2.7 *In situ* hybridization (Angerer *et al.*, 1987)

Solutions

Proteinase K solution

Proteinase K (Ambion, USA) obtained as a solution of 20mg/ml was diluted to the required concentration in 0.1M Tris-HCl, 50mM EDTA, pH 8.0.

0.1M Triethanolamine

Triethanolamine (BDH, UK) was obtained as a 7.5M solution, and diluted to 0.1M with water.

The pH of this solution was adjusted to 8.0 with HCl.

Acetic anhydride

Acetic anhydride (Fisons, UK) was supplied as a 100% solution. It was used at a final concentration of 0.25% (v/v) in 0.1M triethanolamine buffer.

20 X SSC

2M Sodium chloride

0.3M Trisodium citrate

The pH of this solution was adjusted to 7.0 with HCl. Thereafter, it was autoclaved and stored at room temperature.

1 X STE

100mM NaCl

20mM Tris-HCl, pH 7.5

10mM EDTA, pH 8.0

The solution was filter sterilised through a 0.22 μ m filter and stored at room temperature.

***In situ* hybridization mix**

(final concentrations given)

1.2M NaCl

20mM Tris-HCl, pH 7.5

4mM EDTA, pH 8.0

2 X Denhardt's solution

2mg/ml tRNA

Final hybridization solution

2 volumes hybridization mix

2 volumes deionised formamide

1 volume 50% (w/v) dextran sulfate

1 X 10⁷cpm/ml probe

Method

2.7.1 Specimen preparation

All specimens were processed by the Histopathology Department, UCL, London. Tissue samples were fixed in formal saline solution for at least 24 hours. The entire specimen processing was mechanised, taking approximately 14 hours, during which the tissues were dehydrated by increasing concentrations of alcohol (ethanol), infiltrated with xylene (a linking agent between the alcohol and the wax) and finally impregnated with wax. The tissues were embedded into metal moulds so that a cold wax block could be made. After the blocks cooled, they were taken out of their moulds and were ready to be cut.

2.7.2 Slide preparation, sectioning and mounting

All excess wax was removed with a blunt knife and the blocks placed in the chuck holder of the microtome. The surface of the tissue was revealed by "trimming in" the block on the blade of the microtome. After the block had been trimmed in, it was left to cool on an ice tray for 20-30 minutes before the 5 μ m section cutting was carried out. After sections were cut, they were floated onto a 40°C waterbath before being picked up onto a glass slide. All glass

slides used were coated with Vectabond™ (Vector Laboratories). The slides were drained and then placed in a 60°C oven for 30 mins. The slides were then used for the various procedures described below.

2.7.3 Prehybridization treatments

All the following steps were carried out in standard glass slide carriers.

- The sections were deparaffinized by immersion in HistoClear (National Diagnostics, USA) twice for 5 mins each.
- Hydration of the sections by passing them through a graded series of ethanol concentrations (99, 99, 95, 80, 60, and 30%), 3 mins each, followed by rinsing them with distilled water twice.

Proteinase K digestion was carried out to maximize accessibility of the radiolabelled riboprobe to the target sequences within the tissues without causing loss of RNA from sections or deteriorating the morphology of the tissue. Proteinase K (20mg/ml) (Ambion Inc., USA) was diluted to various concentrations (1-200µg/ml) depending on the tissue and/or duration of fixation.

- In trial experiments, concentrations of 50 and 200µg/ml proteinase K were used in order to optimise the conditions. Before the digestion, the slides were incubated in Proteinase K buffer (0.1M Tris-HCl, 50mM EDTA, pH 8.0), at 37°C for 15 mins. Thereafter, Proteinase K digestion was carried out at 37°C for 30 mins.
- Following Proteinase K treatment, the slides were rinsed in water two times and then 0.1M triethanolamine, pH 8.0, for 5 mins each. The slide carrier was blotted onto paper towels to remove excess buffer. Undiluted acetic anhydride was added to an empty, dry staining dish into which the slide carrier was placed. Sufficient 0.1M triethanolamine was then added

to give a final acetic anhydride concentration of 0.25% (v/v). The slides were incubated at room temperature for 10 mins in this solution. The purpose of this step is to neutralise positive charges on the sections and slides and thus reduce electrostatic binding of the probe.

- The slides were then rinsed briefly with 2 X SSC.
- The sections were dehydrated through increasing concentrations of ethanol i.e the same series as before only in reverse order, for 2 mins each.

The slides were allowed to air-dry for 10-15mins, after which hybridization with the probe was carried out.

2.7.4 Probe preparation

Antisense RNA transcripts were prepared using the same method as that used to prepare RNase protection riboprobes (section 2.6.1.1).

5 μ l 5X Transcription Buffer (Stratagene *in vitro* transcription kit)

0.1 μ l 0.75mM DTT

5 μ l 5X NTP mix*

1 μ l RNAsin (Promega)

0.5 μ g linearised template DNA

78 μ Ci [α -³⁵S] UTP (NEN Dupont) specific activity 1250Ci/mmol

1 μ l T3 or T7 RNA polymerase (10 units)

Water to make up to 25 μ l

*** 5X NTP mix**

2mM ATP

0.1mM UTP

2mM GTP

2mM CTP

The reaction mixture was incubated at 37°C for 30 mins.

0.5µl was spotted, washed and read to calculate the amount of incorporation of the probe (see section 2.3.6.1). The remaining mixture was incubated with 1µl (10 units) of RNase free DNase for 30 mins.

The labelled riboprobe was precipitated with 0.1 volumes of 3M sodium acetate and 3 volumes of absolute ethanol on dry ice for 10 mins, followed by centrifugation at 12000g, at room temperature for 10 mins. The supernatant was discarded and pellet washed with 80% ethanol and centrifuged for a further 5 mins. The supernatant was discarded and the pellet dried.

The pellet was resuspended in 1 X STE (100µls) and stored at -20°C. Usually, the probe was used on the same day it was prepared or on the next day.

2.7.5 Hybridization

Before hybridization, the total amount of hybridization solution (for both sense and antisense probes) to be used was calculated.

Slide number X 200µls = total amount of hybridization solution required

The total amount of hybridization solution was then divided into two and the appropriate amount of each probe solution (sense or antisense) added to give a final concentration of probe to be 1×10^4 cpm/µl. The solution containing the probes was heated at 80°C, for 30 secs and then kept at 55°C. DTT was added to the heated probe mixtures to give a final concentration of 50mM.

200µls of probe mixture was pipetted onto each slide and covered with Nesco[®] film. The slides were transferred to a moist chamber and hybridized overnight at 55°C.

2.7.6 Post-hybridization washes

Solutions

RNA wash solution I (800 ml)

400 ml Formamide

40 ml 2 0 X SSC

800 μ ls β -mercaptoethanol

Water to make up 800 ml

The solution was warmed and kept at 55°C

RNA wash solution II (400 ml)

2 ml 20 X SSC

400 μ ls β -mercaptoethanol

Water to make up 400 ml

The solution was warmed and kept at 55°C.

RNase solution (200 ml)

20 ml 5M NaCl

2 ml 1M Tris-HCl, pH 8.0

320 μ ls RNase cocktail (Ambion Inc., USA)

Water to make up 200 ml

The solution was warmed and kept at 37°C

0.6M NaCl/30% (v/v) ethanol (200 ml)

7.01g NaCl

200 ml 30% (v/v) ethanol

0.6M NaCl/60% (v/v) ethanol (200 ml)

7.01g NaCl

200 ml 60% (v/v) ethanol

After hybridization, the slides were rinsed with 2XSSC, at room temperature. The slides were transferred to slide holders and rinsed with fresh 2 X SSC, at room temperature for 15 mins.

- The slides were washed twice with RNA wash solution I at 55°C for 15 mins each.
- Thereafter, the slides were incubated with RNase solution at 37°C for 30 mins.
- After RNase digestion, the sections were washed twice with RNA wash solution I at 55°C, for 15 mins each.
- This wash was followed by two washes with RNA wash solution II at 55°C, for 15 mins each.
- The slides were dehydrated for 2 mins each in the following sequence of graded alcohols:

0.6M NaCl/30% ethanol

0.6M NaCl/60% ethanol

80% ethanol

95% ethanol

100% ethanol

The slides were air-dried for approximately 1 hour before being coated with emulsion.

2.7.7 Autoradiography

The NTB-2 emulsion (Eastman KODAK, USA) is insensitive to standard darkroom lighting, such as a safelight equipped with a Wratten red No.1 filter. However, whenever possible, procedures, such as drying, were carried out in absolute darkness.

When emulsion was received, it was melted in a 45°C water bath, and mixed, 1:1, with prewarmed 0.6M ammonium acetate.

It was stored in 10-20ml aliquots at 4°C, under light-tight conditions.

When ready to dip slides, an aliquot of emulsion was removed and warmed to 45°C for 30-40mins in a water bath set up in the darkroom. The emulsion was carefully poured into a dipping chamber and the slides slowly and evenly immersed 1-2 times in the emulsion.

The slides were blotted onto paper towels to remove excess emulsion and allowed to dry for 45 mins while standing on their ends. The slides were then transferred to light-tight slide boxes along with desiccant wrapped in tissue paper, placed into another box and stored at 4°C for 1-4 weeks.

2.7.8 Development

The box containing the slides was removed from the refrigerator and allowed to come to room temperature (~30-45 mins).

The slides were transferred to a glass slide holder in the darkroom and developed for 2 mins in KODAK Dektol developer stock solution made into a working solution by diluting 1:1 with water. The reaction was stopped with distilled water for 30 secs and the slides fixed with KODAK Fixer, used at full strength for 5 mins. The slides were then rinsed in water for 5 mins.

From here on, the slides could be handled in the light.

Slides were counterstained with hematoxylin for 5 mins and rinsed well with tap water. The slides were then dipped into 'blueing solution' (1% (v/v) acetic acid) for 10 secs after which they were washed under tap water for 5 mins. To stain the cytosol, the slides were stained with eosin for 5 mins. After staining with eosin, the slides were rinsed thoroughly with tap water, dehydrated in a graded series of ethanol (30%, 60%, 70%, 90% and 100%) and cleared two times in HistoClear for 3 mins each. The slides were then mounted using Histomount™ (National Diagnostics), covered with a coverslip and viewed under a light microscope.

2.8 Isolation of proteins from cell pellets derived from HaCaT cell cultures and primary keratinocyte cultures

Various different methods were used to isolate proteins from the cell pellets. The final method used was one that gave maximal yield of protein. The details of the different isolation methods used are detailed below.

In initial experiments, whole cell homogenates were obtained by homogenising a cell pellet in an equal volume of homogenisation buffer (10mM sodium phosphate buffer, pH 7.25, 1mM EDTA, and 20% (v/v) glycerol). Phenylmethylsulfonyl fluoride (PMSF) was added to this buffer to give a final concentration of 4mM. Cells were homogenized using a glass-glass homogenizer.

The main drawback of this method was that upon addition of the SDS-PAGE loading buffer, nuclei were broken open and the DNA within them liberated leading to the sample becoming highly viscous. To reduce viscosity, the sample was passed a few times through a 19 gauge syringe needle. This however resulted in considerable loss of sample.

A second method was then tried so as to eliminate the DNA from the sample (Demlehner *et al.*, 1995). This entailed the use of a cell lysis buffer

consisting of 15mM Tris-HCl, pH 7.5, 2% (w/v) SDS, 8M Urea, 10mg/ml leupeptin, 10mg/ml aprotinin and 1mM PMSF. The cell pellet was homogenised in an equal volume of buffer, using a glass-glass homogenizer. The homogenate was then diluted five times with 15mM Tris-HCl, pH 7.5 and cleared of DNA by methanol/chloroform/water extraction (Wessel and Flugge, 1984). The extraction was carried out by adding 400 μ ls of methanol to 100 μ l of protein sample. The samples were centrifuged at 9000g at room temperature for 10 secs. 100 μ ls of chloroform was added and the samples vortexed and recentrifuged under the same conditions. For phase separation, 300 μ ls of water was added and the samples vortexed and centrifuged at 9000g, at room temperature for 1 min. The upper phase was removed and discarded. A further 300 μ ls of methanol was added to the rest of the lower chloroform phase and the interphase consisting of the precipitated protein. The samples were mixed and centrifuged at 9000g, at room temperature for 2 mins, to pellet the protein. The supernatant was removed and the protein pellet dried. The pellets of protein were resuspended in 2% (w/v) SDS. This method was also found to be unsatisfactory because resuspension of the pellet was extremely difficult and when frozen the previously resuspended protein became insoluble upon thawing.

The third method tried used the principle of trying to break open as many of the cells as possible and the elimination of DNA from the resultant extract. To do this two different methods of cell lysis were used after the cells had been resuspended in an equal volume of homogenisation buffer (10mM sodium phosphate buffer, pH 7.25, 1mM EDTA, and 20% (v/v) Glycerol). PMSF was added to this buffer to give a final concentration of 4mM)

- i) sonication: This was done in bursts of 4 secs, 4 times at an amplitude of 6 with a rest period of between 10-20 seconds between each burst. Sonication was carried out on ice.

ii) glass beads: 2 volumes of glass beads were added to the resuspended cells and the tube vortexed for a few seconds.

To eliminate DNA, samples from each of the above two methods was taken and a solution of 10% (w/v) Protamine sulfate (Sigma Aldrich, UK), dissolved in water, was added to give a final concentration of 2.5% (w/v). The samples were then stirred at 4°C for 30 minutes followed by centrifugation in a bench-top Eppendorf centrifuge at room temperature for 10 mins.

To compare if the addition of protamine sulfate made any difference to the proteins obtained, samples from both the sonication and glass beads lysis methods were also analysed.

2.8.1 Preparation of microsomes from whole skin samples

Solutions

Sucrose Buffer (pH 6.8)

85.57g/l Sucrose

1.8g/l Tris

37.2g/l EDTA

The pH was adjusted to 6.8 with glacial acetic acid and the solution stored at 4°C.

Microsomal resuspension buffer

0.154M Potassium chloride

10mM N-2-hydroxyethylpiperazine-N-2-ethane sulphonic acid (HEPES), pH 7.5

1mM EDTA

20% (v/v) glycerol

Method

Whole skin samples were obtained from the Stephen Kirby Skin Bank, Queen Marys University Hospital, Roehampton. The skin provided was usually from breast reduction surgery and occasionally from abdominoplasties. For microsome preparation, full thickness skin was used. If the skin had been frozen, it was thawed out by defrosting it in sucrose buffer, at 37°C.

The skin was thoroughly rid of all subcutaneous fat and blood before being minced. This removal of fat was essential to obtain a maximal yield of microsomes as well as providing ease in homogenisation. Larger pieces of skin were chopped into smaller pieces on a Petri-dish containing ice to ensure that the sample remained cold. The pieces were finely cut and transferred into 5 ml of sucrose buffer for homogenisation.

The sample was homogenised, in 20 sec bursts and periodically placed on ice. The homogenisation was carried out at least 6-7 times. The sample was then put through a nylon mesh and all the liquid was squeezed out into a beaker. The unhomogenized and coarse bits of remaining tissue were discarded into formalin for disposal. The sample was centrifuged at 10000g in a Sorval SS-34 rotor at 4°C, for 20 mins. The mitochondrial pellet obtained after the first spin was discarded and the supernatant transferred to 26.3 ml polycarbonate Beckman centrifuge bottles (with screw caps). Care was taken not to disturb the floating fat during the transfer of the supernatant. The supernatant was centrifuged in a Beckmann ultracentrifuge L7 at 100000g in a 70Ti rotor at 4°C for 90 mins.

After centrifugation, the supernatant (cytosol) was removed and the pellet (microsomes) washed with sucrose buffer. The pellet was scraped off the tube and placed in a glass-glass homogenizer and an appropriate amount of microsomal resuspension buffer added. Once resuspended, the microsomes were aliquoted and stored at -70°C until used for enzyme activity

assays or for western blotting. The cytosol was also aliquoted and kept at -70°C for use in the above mentioned assays.

2.9 Determination of protein content

Protein content was determined by the method of Lowry *et al.*, (1951).

Reagent A

- (i) 2% (w/v) potassium sodium tartrate
- (ii) 1% (w/v) copper sulphate
- (iii) 2% (w/v) sodium carbonate in 0.1M NaOH (prepared fresh)

Reagents (i) and (ii) were mixed first and then reagent (iii) added in a ratio of 1:1:100 (v/v/v) respectively.

Reagent B

Folin Ciocalteu reagent was diluted 1:1.5 (v/v) with water.

To every 0.2 ml of sample, 1 ml of reagent A was added. The samples vortexed and after 20 mins, 0.1ml of reagent B added. The tubes were mixed immediately and left for 45 mins in the dark. The absorbance of each sample was read at 700nm.

Standard protein dilutions were prepared from a stock solution of Bovine Serum Albumin (BSA).

2.10 Western Blotting

Solutions:

2 X Protein loading buffer

1% (w/v) SDS

10mM EDTA

† 10mM Sodium phosphate buffer, pH 7.25

1% (v/v) β -mercaptoethanol

15% (v/v) glycerol

0.01% (w/v) bromophenol blue

4mM PMSF

The buffer was filter sterilized using 0.22 μ m filter, aliquoted and stored at -20°C.

† Sodium phosphate buffer was made up by mixing 1M Na_2HPO_4 with 1M NaH_2PO_4 until the required pH was obtained. This gave a 1M solution of the buffer. This was diluted to the required working concentration.

4 X Buffer pH 8.8

1.5M Tris

0.4% (w/v) SDS

The solution was made up to a pH of 8.8 with HCl, autoclaved and stored at room temperature.

4 X Buffer pH 6.8

0.5M Tris

0.4% (w/v) SDS

The buffer was made up to a pH of 6.8 with HCl, autoclaved and stored at room temperature.

SDS-PAGE gel running buffer

0.025M Tris

0.192M Glycine

0.1% (w/v) SDS

The running buffer was prepared just before use.

Transfer/Blotting buffer

0.025M Tris

0.192M Glycine

20% (v/v) methanol

The transfer/blotting buffer was prepared fresh.

Coomassie brilliant blue stain

0.2% (w/v) Brilliant blue 6

10% (v/v) glacial acetic acid

45% (v/v) methanol

45% (v/v) water

The solution was filtered through 3MM Whatmann paper and stored at room temperature.

Destaining solution

10% (v/v) glacial acetic acid

45% (v/v) methanol

45% (v/v) water

The solution was stored at room temperature.

Method:

2.10.1 SDS-Polyacrylamide gel preparation

Varying volumes of Protogel (37.5:1, acrylamide to bisacrylamide stabilised solution, National Diagnostics, USA) and water were mixed to obtain a gel having the required percentage of acrylamide. Generally the volume of Protogel required for gel casting solutions of any volume and acrylamide concentration was calculated using the formula below:

$$V_p = \frac{(X)(V_t)}{30}$$

30

where, V_p = Volume of Protogel to be used (ml)

X = % acrylamide desired in gel

V_t = Total volume of gel casting solution desired (ml).

1 ml of 10% (w/v) ammonium persulfate and 0.1 ml of TEMED was added for every 100 ml of gel casting solution.

Separating gels of 7, 10 and 13% acrylamide concentrations were used depending on the protein to be analysed, whereas stacking gels were always at 3% acrylamide concentration. The gels were set in a Bio-Rad Protean II gel casting apparatus. Either 1.5 mm or 0.75 mm combs and spacers were used, however, the 0.75 mm combs and spacers when used resulted in the detection of stronger bands when the western blot was probed with the relevant antibody. These bands tended to be blurred. The separating gels were set first and overlaid with 0.1% (w/v) SDS and allowed to set for at least 3 hours. The overlay was poured off and the stacking gel poured and allowed to set for at least 3 hours.

Prior to electrophoresis, the wells were flushed with running buffer to wash off any unpolymerized acrylamide.

2.10.2 Sample preparation and gel electrophoresis

Samples were prepared by adding an equal volume of 2 X protein loading buffer and boiling the resultant mixture for 3 minutes. β -mercaptoethanol was then introduced ($1\mu\text{l}$ for every $10\mu\text{l}$ of sample containing protein loading buffer). The samples were centrifuged for 3 mins to remove any undissolved material prior to loading them on the gel.

The gel was electrophoresed at 25 mA/gel to stack the proteins and the current increased to 35 mA/gel to separate them. The proteins were electrophoresed until the blue dye was 1cm from the bottom of the gel.

2.10.3 Visualisation of proteins

To visualise the integrity of the proteins extracted, the gel was stained for at least 30 mins and not more than 3 hours, using Coomassie brilliant blue stain, following which it was destained until the blue background faded completely.

2.10.4 Antigen detection

Solutions:

10 X TBS

200mM Tris

5M NaCl

The pH of this solution was adjusted to 7.5 with HCl,. The solution was autoclaved and stored at room temperature.

1 X TTBS

1 X TBS

0.1% (v/v) Tween 20

100 μ l of Tween 20 were used for every 100 ml of 1 X TBS

This solution was prepared on the day of use.

Blocking solutions

3% (w/v) gelatin in 1 X TBS

The gelatin was dissolved in 1 X TBS by heating. The resultant solution was cooled to 37°C before use.

OR

0.2% (w/v) I - Block (TROPIX Inc, USA) in 1 X TBS

The I - Block was heated until dissolved. The solution was cooled to room temperature after which 0.1% (v/v) Tween 20 was added.

Method:

2.10.4.1 Transfer of Proteins

Proteins from SDS-PAGE gels were transferred onto supported nitrocellulose filters (BDH, UK). The gel apparatus was dismantled and the gel placed on the filter. Any bubbles between the gel and filter were removed by running a pipette gently over the gel. The gel and filter were then sandwiched between 3MM Whatman paper and blotting pads (all previously soaked in transfer buffer). This sandwich was placed in a blotting cassette which in turn was placed in a blotting tank (Bio-Rad, UK), with the filter facing the anode and the gel facing the cathode. Transfer was allowed to take place overnight at a constant current of 100mA. Thereafter, the current was turned up to 200mA for 1 hour to immobilize the proteins onto the filter.

2.10.4.2 Antigen detection

Antigen detection was performed using two different detection systems:

a) Colour development

b) Chemiluminescence

The Bio-Rad alkaline phosphatase (AP) or horseradish peroxidase (HRP) colour development kits were used depending on the nature of the secondary antibody. Certain secondary antibodies were only available as conjugates of alkaline phosphatase. The AP colour development kit is also known to be more sensitive in terms of visualisation of the antigen antibody complex.

Chemiluminescence was used when a higher degree of sensitivity was required, such as the detection of very low amounts of CYPs in the HaCaT cells or primary human keratinocytes. This method of detection was carried out using either the HRP luminescent visualisation system (National Diagnostics, USA) or the *Western-Star*[™] chemiluminescent detection system (TROPIX Inc., USA). The latter system was used with AP conjugated secondary antibodies. Both methods were carried out according to the manufacturers' instructions and are very similar apart from the actual visualisation step. Briefly, the filter was immersed in blocking solution and allowed to incubate for at least 1 hour. The filter was washed in 1XTTBS for 10 mins, followed by incubation at room temperature (with shaking), for 2 hours with the primary antibody. The primary antibody solution was removed and the filter washed twice for 10 mins with 1XTTBS. Thereafter, the secondary antibody having the AP conjugate (or HRP conjugate), which was diluted according to the manufacturers instructions in blocking buffer, was added and the filter allowed to incubate with the conjugate for 1 hour. The conjugate solution was removed and the filter washed twice with 1XTTBS for 10 mins each, followed by a 5 mins wash with 1 X TBS.

Colour development was carried out using chromogenic solutions provided in the kit i.e for the AP, 5-bromo-4-chloro-3-indoyl phosphate (BCIP) and nitroblue 1-naphthol (NBT). For the HRP, 4-chloro-1-naphthol and

hydrogen peroxide were used as per the manufacturers instructions. The colour development was stopped by immersing the filter in distilled water.

Chemiluminescent visualisation of antigens was also carried out as per the manufacturers instructions and the proteins visualised using X-ray film. The substrate for the HRP chemiluminescent reaction is luminol. HRP in the presence of hydrogen peroxide converts luminol to a product which emits light. The substrate for the Western-Star™ Chemiluminescent Detection System is CDP-Star™, which is a chemiluminescent substrate for alkaline phosphatase.

Those blots that were probed and detected using the chemiluminescent substrates could be stripped and reprobed with another antibody.

Stripping solution:

62.5mM Tris-HCl, pH 6.8

2% (w/v) SDS

100mM β- mercaptoethanol

The blot was incubated for 30 mins at 70°C in the stripping buffer. It was washed three times with 1XTTBS for 5 mins each. To verify the removal of the previous antibodies, the detection protocol was repeated, but this time omitting the primary antibody incubation. Complete removal of antibodies was confirmed by the absence of an image on the film.

2.11 Immunohistochemistry (IHC)

IHC was carried out on both formaldehyde fixed sections of human tissues and primary keratinocytes cultured on glass coverslips.

2.11.1 IHC background and procedure

IHC was carried out using the VECTASTAIN *Elite* ABC Kit (Vector Laboratories, USA). This method relies on the high affinity with which avidin binds four molecules of biotin. Activated esters of biotin will react with primary amines (lysine residues) to form stable amide bonds and can therefore be used to biotinylate lysine-containing antibody molecules. Biotinylation of primary antibodies can reduce antigen-binding capacity. This problem is circumvented by biotinylating a secondary antibody specific for the primary. The avidin-biotin complex or ABC method requires the use of 3 reagents, unlabelled primary antibody, biotinylated secondary antibody specific for the primary and a preformed complex of peroxidase-conjugated biotin and avidin (ABC). The ABC reagent is prepared fresh and allowed to form at room temperature before being applied to the tissue sections containing unlabeled primary and biotinylated secondary antibodies. The great sensitivity of this detection method relies on the formation of the macromolecular ABC complex, which contains multiple biotinylated enzyme molecules per avidin molecule. This preformed complex then reacts with free biotin residues on the secondary antibody, thereby introducing multiple enzyme molecules per primary antibody.

Human tissue sections were prepared as described in section 2.7.1 and 2.7.2. Cells were cultured on coverslips using the same media as described in section 2.2.2. The only difference being the treatment of the coverslips with 70% ethanol before plating the cells out. The coverslips were placed in 24 well tissue culture plastic plates (NUNC, USA). Until attachment of cells took place, the cells were cultured in KGM containing 10% foetal calf serum, thereafter they were cultured in serum free KGM. The medium was

changed after every 3 days. IHC was carried out when the cells were about 70-80% confluent.

2.11.2 IHC on cultured cells

Cells were washed three times with phosphate buffered saline (PBS) and then fixed. Two different methods for fixation were used to ascertain the most effective method for the keratinocytes. Cells were fixed with either ice-cold methanol or with an ice-cold mixture of chloroform/acetone (1:1; v/v). Methanol fixation was done for 3 mins, whereas the chloroform/acetone fixation was carried out for 5 mins. When the latter method was used, the coverslips had to be removed from the multiwell plates to be fixed. Upon fixation, the cells were washed thoroughly with PBS and in the case of the chloroform/acetone fixation method the coverslips could then be placed back into the multiwell plates. Endogenous peroxidase activity was quenched by incubating the cells with 0.3% (v/v) H₂O₂ in water, for 30 mins. The cells were then washed with PBS for 5 mins followed by incubation with diluted normal blocking serum (180µls in 12 ml of PBS) for 20 mins. Blocking serum was prepared from the species in which the secondary antibody was made. The samples were then washed once with PBS and incubated with the relevant primary antibody for 30 mins. The samples were washed once with PBS for 5 mins and incubated with the appropriate biotinylated secondary antibody solution (30µls of biotinylated secondary antibody from kit in 6 ml of PBS). The sections were washed once with PBS for 5 mins and incubated with VECTASTAIN *Elite* ABC reagent. The VECTASTAIN *Elite* ABC reagent was prepared half an hour before use by adding 2 drops of Reagent A to 5mls of PBS, mixing the resultant solution, then adding 2 drops of Reagent B and mixing again. Reagents A and B are provided with the kit. The samples were washed once again for 5 mins with PBS and then incubated for 2-10 mins in

peroxidase substrate solution. 2 different types of substrates were used. These were Diaminobenzidine (DAB) substrate (part of the DAB substrate kit for peroxidase) and VECTOR[®] VIP substrate (part of the VECTOR[®] VIP substrate kit for peroxidase). The substrates were prepared as follows:

DAB substrate:

DAB is a chromogen. In IHC reactions, the HRP forms a complex with its substrate H₂O₂, which oxidizes DAB to produce the end product of the reaction, a coloured molecule and water. DAB yields a reddish brown stain.

The substrate was prepared by adding 2 drops of Buffer Stock Solution (provided in kit) to 5 ml of distilled water and the solution mixed well. 4 drops of DAB Stock Solution were added and the solution mixed again. Thereafter, 2 drops of Hydrogen Peroxide Solution were added and the solution mixed. The samples were incubated with this solution until suitable staining developed, monitored by observing the colour reaction under a light microscope. The reaction was stopped by washing the sections or cells with distilled water for 5 mins.

VECTOR[®] VIP substrate:

The VECTOR[®] VIP substrate produces a purple reaction product. The substrate was prepared by adding 3 drops of Reagent 1 to 5 ml of PBS and the solution mixed. 3 drops each of Reagents 2 and 3 were added, with mixing in between each addition. Lastly, 3 drops of hydrogen peroxide were added and the final solution mixed.

The samples were incubated with this substrate until a suitable level of staining was achieved (generally 2-15 minutes). The colour development was stopped by washing the samples with distilled water for 5 mins. After incubation with substrate, the coverslips were mounted onto glass slides

using HISTOMOUNT (National Diagnostics, USA). The slides were then observed under the microscope and photographed.

2.11.3 IHC on paraformaldehyde fixed tissue sections

The method employed is a modified version of that recommended by the manufacturer (Vector Laboratories, USA). For sections of human skin tissue, the procedure was essentially identical except for the treatment before the incubation with the hydrogen peroxide. The sections were first dewaxed using HistoClear (National Diagnostics, USA). This was carried out two times for 5 mins each. Thereafter the sections were rehydrated, twice with 100% ethanol, for 3 mins each, twice with 95% ethanol for 3 mins each and finally rinsed in water.

2.11.3.1 Antigen unmasking

Two different methods were used for the retrieval of antigens in paraformaldehyde fixed sections.

- Epitopes were unmasked by incubating with trypsin (0.1% (w/v) trypsin, 0.1% (w/v) calcium chloride and 20mM Tris-HCl, pH 7.8) at room temperature for between 2-20 mins. The unmasking reaction was stopped by placing the slides in cold water.
- The other method involved the use of a microwave oven to unblock the chemical cross-linking. This was carried out by placing the deparaffinized tissue sections into a Coplin jar filled with enough 10mM citrate buffer, pH 6.0 to immerse the slides completely. The citrate buffer is bought as a solution called 'Antigen unmasking solution' from Vector Laboratories, USA. The slides were microwaved for two 5 min cycles with the power setting adjusted so that the buffer boiled for at least 3 mins in each cycle.

Between each cycle, the buffer was changed. The tissue sections were cooled at room temperature in buffer for 20 mins before the IHC procedure was carried out.

2.11.3.2 Antigen detection using IHC

- After antigen retrieval, the tissue sections were immersed in PBS for 5 mins.
- Endogenous peroxidase activity was quenched by immersing the slides in a bath of 3% (v/v) H₂O₂ in water or 0.3% (v/v) H₂O₂ in methanol. The sections were then washed thrice in a PBS bath.
- The slides were blocked using the appropriate non-immune serum (same animal as the secondary antibody is raised in), diluted as described for the cultured cells (section 2.11.2), for 30 mins.
- The primary antibody was applied and the sections incubated with this antibody for 30 mins in a humidified chamber. After incubation, excess primary antibody was blotted and the sections were rinsed once, and then washed three times in a buffer bath.
- The biotinylated secondary antibody was applied and the sections incubated for a further 30 mins. The excess antibody was blotted and the sections washed three times in the buffer bath. During secondary antibody incubation. The ABC reagent was prepared as described in section 2.11.2.
- The sections were incubated for between 45-60mins with the ABC reagent, after which they were washed in a buffer bath three times.
- DAB solution was prepared as described in section 2.11.2, and this was applied to the tissue sections for between 8-10 mins. The sections were washed and the staining intensified with one drop of NiCl₂ (provided in the substrate kit).

For each type of tissue and antibody, negative controls were also carried out. This is so that specific staining can be evaluated relative to the background. Negative controls included the use of pre-immune serum derived from the same species.

2.12 Methimazole assay (Dixit and Roche, 1984)

Solutions

Assay buffer

0.1M Tris-HCl

1mM EDTA

The pH of the buffer was adjusted to 8.4 with HCl and the solution autoclaved and stored at room temperature.

DTT

A 4mM working stock of DTT was prepared fresh by adding the appropriate amount of DTT to the assay buffer.

5,5'-Dithio-bis(2-nitrobenzoic acid) (DTNB)

A 12mM working stock solution of DTNB (Sigma Aldrich Co, UK) was prepared by dissolving the appropriate amount of solid DTNB in ethanol. This amount usually gave a concentration of 5mg/ml.

β -Nicotinamide adenine dinucleotide phosphate, reduced form (NADPH)

NADPH, tetrasodium salt, (Sigma Aldrich Co, UK) was used at a stock concentration of 20mM in assay buffer. This was prepared fresh before the assay was carried out.

2-Mercapto-1-methylimidazole (Methimazole)

Methimazole (Sigma Aldrich Co, UK) was made up in assay buffer to give a stock concentration of 200nM.

The final concentration of DTT, NADPH and DTNB in a total volume of 2 ml was 0.02mM, 0.1mM and 0.06 μ M respectively. The final concentration of methimazole was 2mM. Samples were assayed as follows. To 1.9 μ ls of assay buffer (aerated and placed in a 37 $^{\circ}$ C water bath), 100 μ ls (equivalent to not more than 2 mg of protein) of microsomes were added. To this mixture, DTT (10 μ ls of 4mM stock), DTNB (10 μ ls of 12mM stock) and NADPH (10 μ ls of 20mM stock) were added. The solution was divided into two cuvettes (1 ml each). Methimazole (10 μ ls) was added to only the sample cuvette whereas the other cuvette served as a "blank". The course of the reaction i.e the disappearance of the yellow colour due to the conversion of nitro-5-thiobenzoate (TNB) (yellow) to DTNB (colourless) was followed by measuring the optical density of the sample at 412nm and 37 $^{\circ}$ C, using a Cary 3, split beam spectrophotometer. The extinction coefficient of 14,100 M⁻¹cm⁻¹ for methimazole (Riddles *et al.*, 1983) was used.

- To ascertain the effects of Emulgen 911 on the activity, Emulgen 911 (Kao Corporation, Tokyo, Japan) (0.2%; v/v) was added to the assay buffer and the experiment carried out as above.
- *n*-octylamine, a positive effector of FMO activity and a CYP inhibitor, was used to determine whether the activity was attributable to FMO or to CYP, *n*-octylamine was used at a concentration of 2.4mM.
- Microsomal membranes from insect cells expressing FMOs 1, 3 and 5 were used as controls.

The methimazole assay is only linear up to a total protein concentration of 1mg/ml, above which the oxidation of TNB becomes non-linear.

- The assay was also carried out in the absence of proteins, but in the presence of detergent and *n*-octylamine to determine if these compounds carried out any non-enzymatic reduction of TNB to DTNB.

2.13 Determination of P450 reductase activity

P450 reductase activity was determined using the artificial electron acceptor cytochrome c as described by Vermilion and Coon, (1974). This assay was carried out to determine the integrity of the skin microsomes.

The reaction mixture contained, in a final volume of 1 ml, 300 μ mol of potassium phosphate, pH 7.7/0.001 μ mol EDTA/0.1 μ mol NADPH and 0.04 μ mol cytochrome c. Assays of skin microsomes and rat liver microsomes (used as a positive control) also contained 0.6 μ mol of KCN. The reaction was started by the addition of NADPH. The rate of reduction of cytochrome c was determined spectrophotometrically by measuring the increase in absorbance at 550nm and using the extinction coefficient of 21mM⁻¹cm⁻¹ for reduced cytochrome c (Williams and Kamin, 1962).

RESULTS AND DISCUSSION

DNA ANALYSIS

3.1 Southern blot hybridization analyses

To elucidate the number of genes encoding each FMO and their complexity, Southern blot hybridization analyses were carried out on human genomic DNA digested with three different restriction enzymes (*Eco* RI, *Hind* III, *Bam* HI). Genomic DNA extraction, digestion and Southern blotting of digested DNA was carried out by Dr. Colin Dolphin (Queen Mary and Westfield College, London). The blots were then processed in the course of this investigation.

Each blot was hybridized to radiolabelled cDNA probes encoding either FMO2, 3, 4 or 5. Hybridization and washing conditions were such that only strictly homologous sequences would hybridise to one another.

3.1.1 FMO2

Eco RI digests the *FMO2* gene to produce 5 distinct bands (fig 3.1). The size of the fragments are given in Table 3.1. The intensity of the hybridizing band varies depending on the length of the radiolabelled probe hybridizing to the fragment and also due to the possibility of partially digested DNA fragments.

Five *Eco* RI fragments of total size approximately 25 kb hybridized to the *FMO2* cDNA. Three *Hind* III fragments of total size approximately 24 kb hybridized to the cDNA. The *Bam* HI fragments were very faint, but at least 2 distinct bands hybridized to the *FMO2* cDNA. The sum total of the size of these fragments was approximately 19 kb.

The *FMO2* gene therefore has a minimum size of 19.2 kb, which corresponds well with that of the human *FMO3* gene whose minimum size has been estimated to be approximately 22.5 kb (Dolphin *et al.*, 1997b). The small size of the gene suggests that FMO2 is encoded by a single gene.

Enzyme	<i>Eco</i> RI	<i>Hind</i> III	<i>Bam</i> HI
	7.2	9.2	10
	6.4	7.4	9.2
	4.7	7.1	
	3.8		
	3.1		
Total length (kb)	25.2	23.7	19.2

Table 3.1 Lengths of fragments observed when human genomic DNA was digested with *Eco* RI, *Hind* III and *Bam* HI and hybridized to the cDNA encoding FMO2. Length of fragments is given in kilobases.

3.1.2 FMO3

Southern blot hybridization analyses was carried out on genomic DNA digested with *Bam* HI, *Hind* III or *Eco* RI (fig 3.1). The blot was hybridized with the cDNA encoding FMO3. Autoradiography revealed the size of the hybridizing fragments which are given in Table 3.2

Eco RI digests *FMO3* to yield 10 fragments of total size 47.6 kb. However, the presence of some faintly hybridizing bands suggests that a number of these are due to partial digestion of the genomic DNA. These include, the 4.7 kb fragment (made up of the 2.5 kb and 2.3 kb) or the 3.2 kb fragment (partial digest of the 2.3 kb and 0.9 kb fragments). Another possibility for the large size observed with the *Eco* RI digest, may be the presence of a very long 3' or 5' flanking sequence. *Hind* III yields 3 bands, of a total size approximately 21.6 kb, with the 8.0 and 7.4 kb bands being the most intensely hybridizing. *Bam* HI digested DNA hybridized to 5 fragments of which the 9.0 and 8.0 kb bands were the most intense. The total size of the *Bam* HI fragments is approximately 25.7 kb.

Enzyme	<i>Eco</i> RI	<i>Hind</i> III	<i>Bam</i> HI
	10.2	8.0	9.0
	9.0	7.4	8.0
	7.4	6.2	4.1
	5.9		2.6
	4.7		2.0
	3.2		
	2.5		
	2.3		
	1.5		
	0.9		
Total length (kb)	47.6	21.6	25.7

Table 3.2 Summary of hybridizing bands observed when human genomic DNA digested with *Eco* RI, *Hind* III and *Bam* HI was probed with the *FMO3* cDNA.

The above results show that the minimal size of the *FMO3* gene is 21.6 kb. These results are very close to those obtained by Dolphin *et al.*, (1997b), who have determined the structural organization of the human *FMO3* gene. They have shown the gene size to be at least 22.5 kb.

3.1.3 *FMO4*

The Southern blot used for the analyses of *FMO2* was stripped and then reprobbed with the cDNA encoding *FMO4* and the results visualised by autoradiography (fig 3.1).

Nine *Eco* RI fragments hybridized to the probe. The two most intensely hybridizing fragments were 1.5 kb and 3.8 kb in size. *Hind* III digested the *FMO4* gene to yield 3 fragments, 2 of which were strongly hybridizing (11.1 and 7.4 kb). Although the DNA in the *Bam* HI digest track is smeared, 4

fragments could be distinguished. The size of the hybridizing fragments is summarized in Table 3.3.

Enzyme	<i>Eco</i> RI	<i>Hind</i> III	<i>Bam</i> HI
	9.0	11.1	9.0
	8.3	7.4	7.1
	7.6	5.0	6.4
	6.6		2.1
	5.8		
	4.7		
	3.8		
	2.0		
	1.5		
Total length (kb)	49.3	23.5	24.6

Table 3.3 Summary of fragment sizes obtained after hybridization of *FMO4* cDNA to human genomic DNA digested with the restriction enzymes, *Eco* RI, *Hind* III and *Bam* HI.

The *Eco* RI fragments give a total size of 49.3 kb. This is probably due to partial digestion of genomic DNA with this enzyme. Partial digests include the 5.8 kb (3.8 kb and 2.0 kb) and the 6.6 kb (2.0 kb and 4.7 kb) fragments. The above results indicate the minimum size of the *FMO4* gene is approximately 26 kb. This corresponds to the size of the genes encoding *FMOs* 2 and 3 (above) as well as that found by Dolphin *et al.*, (1997b).

3.1.4 *FMO5*

The Southern blot used for the analyses of *FMO3* was stripped and then reused for the analysis of *FMO5*. The full length *FMO5* cDNA was hybridized to digested genomic DNA fragments. The blot was washed under

high stringency conditions and the pattern of bands observed on the autoradiograph is shown in fig 3.1. Table 3.4 summarizes the sizes of the hybridizing fragments.

Enzyme	<i>Eco</i> RI	<i>Hind</i> III	<i>Bam</i> HI
	7.4	7.1	9.2
	6.6	6.6	8.3
	6.3	6.3	5.8
	4.9	5.9	3.0
	4.0	1.6	
	3.1		
	2.1		
	1.7		
Total length (kb)	36.1	27.5	26.3

Table 3.4 Summary of fragment sizes obtained when human genomic DNA was digested with *Eco* RI, *Hind* III and *Bam* HI. The full length cDNA encoding FMO5 was used for the hybridization analyses.

Eco RI digests the *FMO5* gene to produce 8 distinct fragments having a total size of approximately 36.1 kb. Five *Hind* III fragments of total size 27.5 hybridized to the *FMO5* cDNA. *Bam* HI digests the gene to yield 4 fragments of total size 26.3 kb.

The large total size observed with the *Eco* RI digest is again probably the result of partial digestion by this restriction enzyme. Thus, the 6.6 kb fragment is probably the partial digest which upon complete digestion would yield the 4 kb and 1.7 kb fragments. The large size could also be due to the presence of long 3' and 5' flanking sequences on either side of the *FMO5* gene.

3.2 Discussion

Southern blot hybridization analyses of restriction endonuclease digested human genomic DNA yields information of the basic gene structure. This includes studying the number of genes that may encode a particular protein.

Southern blot hybridization analysis of the *FMO1* gene was not carried out in this investigation because this has previously been done (Dolphin *et al.*, 1991). The hybridization of the *FMO1* cDNA to human genomic DNA digested with *Eco* RI, *Hind* III or *Pst* I, showed a relatively simple pattern of hybridization, suggesting that *FMO1* is encoded by a single gene.

When full length cDNA clones encoding the various FMOs were used to probe human genomic DNA digested with either *Bam* HI, *Hind* III or *Eco* RI, a relatively simple banding pattern was observed as indicated in fig 3.1 and tables 3.1, 3.2, 3.3 and 3.4. This suggests that as is the case for *FMO1*, FMOs 2, 3, 4 and 5 are also encoded by single genes. No evidence exists for more than one member of an FMO family.

The presence of only a single gene in each FMO family can only be substantiated by carrying out Southern blot analyses with exon specific radiolabelled probes for each of the four cDNAs. If a single strongly hybridizing band is observed, then it can be concluded that a single gene exists for that particular FMO. Both human *FMO1*, and *FMO4* have been confirmed in this way to be encoded by single genes (Dolphin *et al.*, 1992). Human genomic DNA was hybridized to a probe complementary to a sequence located within either the 3' non-coding region of the cDNA encoding human *FMO1* or *FMO4* separately. The probes used correspond to sequences contained within single exons of the corresponding genes. Single

hybridizing fragments were detected in genomic DNA digested by *Eco* RI, *Bam* HI or *Pst* I.

Southern blot hybridization analyses can also give an idea of the size of the gene. However only an approximation of the size can be made because when using a full length cDNA as the hybridization probe, flanking regions of the gene will also be included if the restriction enzyme digests the genes to give a fragment that includes flanking regions together with the exons to which the cDNA will hybridize. This may be the reason that the total length of the *FMOs* 2, 3, 4 and 5 hybridizing fragments vary between approximately 40 kb and 20 kb.

To date, only the gene structure of human *FMO3* (Dolphin *et al.*, 1997b) and rabbit *FMO1* are known (Wyatt *et al.*, 1996). Human *FMO3* contains nine exons, the first of which is entirely noncoding. There are eight intervening introns that range in size from >6 kb for intron 2 to 241 bp for intron 4, indicating a minimum size of 22.5 kb for the *FMO3* gene (fig 3.2). The sizes of *FMOs* 2, 3, 4 and 5 determined in the present study are very similar to that obtained by Dolphin *et al.* (1997b) for *FMO3*. The results suggest that members of the *FMO* gene family are each encoded by single genes of approximately 23 kb.

The structure of the rabbit *FMO1* has been elucidated and this gene was found to contain 8 introns, ranging in size from 1.4 to 10 kb and nine exons ranging in size from 73 to 747 bases (Wyatt *et al.*, 1996). Further studies on the rabbit *FMO1* gene have shown the presence of two promoters. Three positive regulatory elements and two negative regulatory elements have also been observed in this gene (Luo and Hines, 1997).

On the assumption that the structure of all the human *FMO* genes is similar, it is probable that the large bands observed in the Southern blot hybridizations with *Eco* RI digest of *FMO3*, *FMO4* and *FMO5*, are due to the presence in these hybridizing fragments of flanking sequences or the partial

digestion of DNA. The location of the restriction enzyme sites within the introns and the identification of exactly which exons the cDNAs hybridize to, cannot be determined from Southern blot hybridization analyses carried out in my studies. This is because, the sequences of the introns are not known to date, and, although the gene structure may be similar, in terms of numbers of exons and introns, the sizes of the introns between the different *FMO* genes may vary.

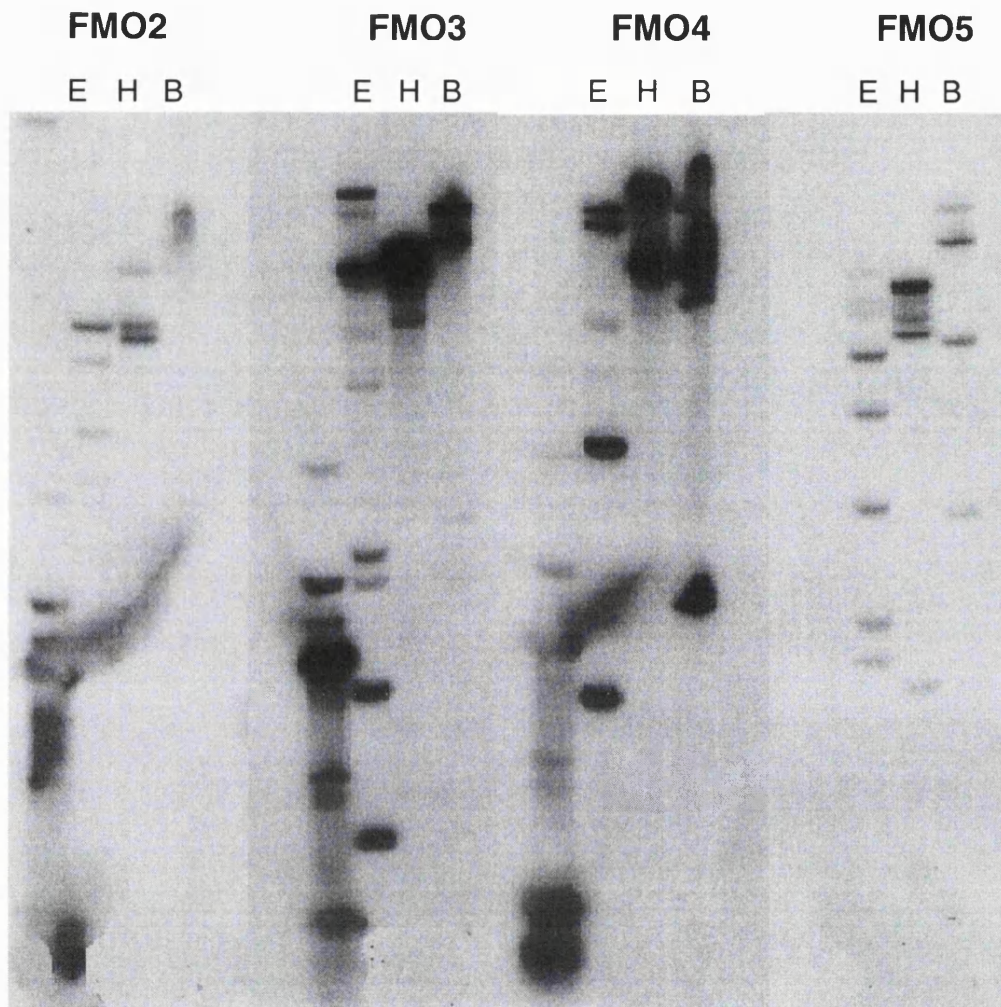


Fig 3.1 Human genomic DNA samples (10 μ g) were digested with *Eco* RI (tracks E), *Hind* III (tracks H) and *Bam* HI (tracks B) and hybridized with the full length cDNAs encoding FMO2, FMO3, FMO4 or FMO5.

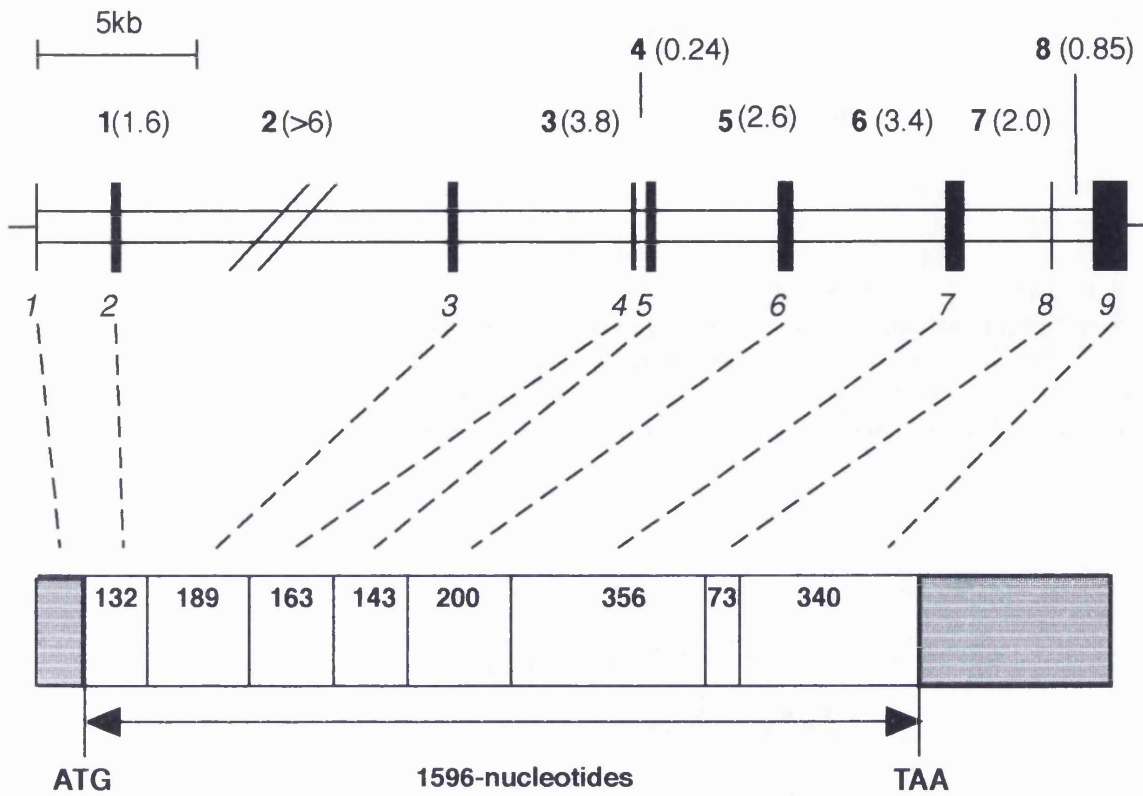


Fig 3.2 Structural organization of the human *FMO3* gene. Introns (horizontal open boxes) are numbered in boldface type and their approximate sizes (in kilobases) are shown in parentheses. Exons (solid vertical boxes) are numbered in italics and are linked by dashed lines to the equivalent regions within the mRNA (open boxes) that contain the exon length (in nucleotides) or in the case of exons 2 and 9, the length of the protein coding regions within the exon. Shaded regions represent the 5' and 3' untranslated regions within the mRNA. Reproduced from Dolphin *et al.*, 1997b.

RNA ANALYSES

Human tissues (except for skin) were a gift and obtained from the MRC human genetics unit, Galton laboratories, U.C.L.

4.1 Detection of FMO mRNA using northern blot hybridization analyses

Northern blot hybridization analyses were carried out on various mammalian tissues and cultured cells to determine the expression of FMO mRNAs in these samples. The tissues analysed included human liver, lung, kidney and skin, a primary culture of human epidermal keratinocytes, HaCaT cells, cynamologous monkey lung, marmoset liver, rabbit liver and lung.

4.1.1 Extraction and integrity of RNA from varlous tissue and cell samples

Total RNA was extracted from various samples. A guanidine thiocyanate/lithium chloride extraction procedure was used for all tissues except human skin (see section 2.4.1). For this a guanidine hydrochloride/guanidine thiocyanate extraction procedure was used (section 2.4.3). RNA was extracted from cultured cells using the Ultraspec™ total RNA extraction system (section 2.4.2). RNA samples were electrophoresed on a denaturing formaldehyde gel to ascertain their integrity. Using the optimised RNA extraction protocol for the different sample types, the 28S and 18S bands were clearly visible and there was no smearing of bands, showing that the RNA was undegraded (fig 4.1.1, lanes 2, 4, 6, 8, 11 and 12). Therefore these samples could be used for northern blot hybridization analyses and RNase protection assays.

Three different methods were used for the extraction of total RNA. For tissues such as liver, lung and kidney the guanidine thiocyanate/lithium chloride extraction procedure was employed and intact RNA was obtained. Neither the guanidine thiocyanate/lithium chloride nor the Ultraspec™ RNA isolation method could be used for whole skin samples because the RNA was

lost/degraded during these procedures (see fig 4.1.1, lanes 1, 3, 5, 7, 9 and 10 and fig 4.1.2A, lane 3).

For whole skin samples, the guanidine hydrochloride/guanidine thiocyanate method was used. This produced intact RNA (fig 4.1.2B, lanes 2, 3 and 4). The reasons for the success of this method for isolating intact RNA from human skin are not known. This method is usually used for tissues with high RNase content. Reasons for the success of this method could be the efficiency of homogenisation of the tissue in guanidine thiocyanate and sodium N-lauroylsarcosine or the addition of SDS to 1% before the phenol extraction procedure (see section 2.4.3). Even so, analysis of skin RNA by agarose gel electrophoresis showed that the 28S and 18S bands were smeary. To obtain clear, sharp 28S and 18S RNA bands, it was necessary to re-extract all skin RNA samples with phenol in the presence of 1% SDS (fig 4.1.2B, lane 1 as compared to lanes 2, 3 and 4). For cultured cells, the Ultraspec™ RNA isolation system was used as it is a one step process maximizing the yield of RNA extracted from the few cells obtained after culture (fig 4.1.1, lanes 2, 4, 6, 8, 11 and 12).

4.2 Northern blot hybridization anaiyses

FMOs are responsible for the metabolism of a variety of pharmaceuticals and pesticides, yet few studies on the expression of FMOs, at the RNA level, in human tissues such as the liver, lung and kidney have been published. The skin is one of the major portals of entry to pesticides and environmental chemicals into the human body. The expression and distribution of FMOs in this organ and cells derived from it is unknown. The expression of FMO mRNAs in a primary culture of human epidermal keratinocytes and an immortalized human keratinocyte (HaCaT) cell line was investigated. Only limited studies were carried out on whole human skin due

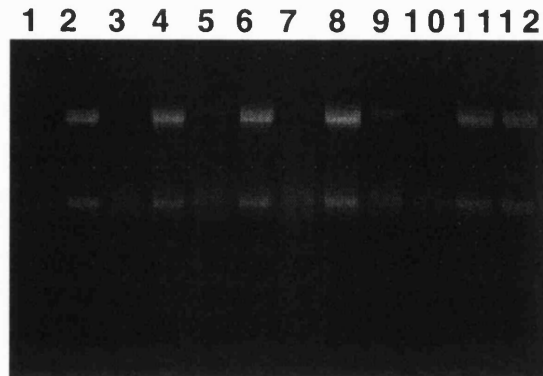


Fig 4.1.1 RNA samples (2 μ g) were electrophoresed through a 1% denaturing formaldehyde gel as described in section 2.5. Lanes 1, 3, 5, 7, 9 and 10 show RNA extracted from whole skin samples. Lanes 2, 4, 6, 8, 11 and 12 are RNA samples extracted from primary human keratinocyte cultures obtained from their corresponding whole skin samples. RNA in was extracted using the UltraspecTM RNA isolation system.

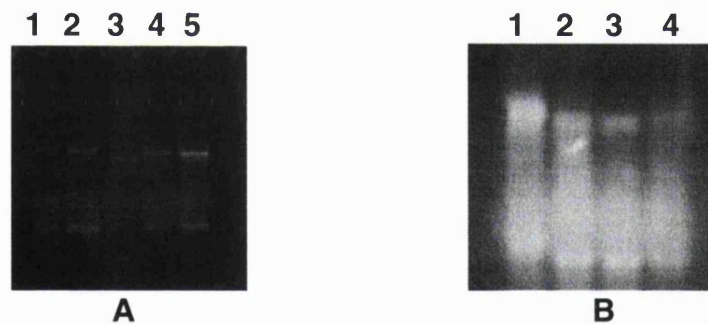


Fig 4.1.2 RNA samples (1 μ g) were electrophoresed through a 1% denaturing formaldehyde gel as described in section 2.5. Fig (A) shows samples of RNA extracted using the guanidine thiocyanate/lithium chloride extraction procedure as detailed in section 2.4.1. Lane 1, human liver, lane 2, human lung, lane 3, human whole skin, lane 4, human kidney, lane 5, rabbit liver. Fig (B), samples of RNA extracted from whole skin using the guanidine thiocyanate/guanidine hydrochloride extraction procedure as outlined in section 2.4.3. Lane 1, whole skin sample in which the final SDS, phenol/chloroform stage was omitted, lanes 2, 3 and 4, all steps were carried out as detailed in section 2.4.3.

to the unavailability of tissue. Studies on the HaCaT cells were also undertaken due to the limited availability and expense of human tissues and primary cultures derived from them. These cells could offer an alternative system for biotransformation studies. However, this is possible only if HaCaT cells express a similar range of FMOs as do human tissues such as the skin or primary keratinocytes derived from human skin.

4.2.1 Expression of FMO1 mRNA

A full length cDNA clone encoding FMO1 (previously isolated in our laboratories) (Dolphin *et al.*, 1991) was used to probe a northern blot containing RNA from adult human liver, lung, kidney and skin, rabbit liver and lung, cynamologous monkey lung, marmoset liver, a primary culture of human epidermal keratinocytes and HaCaT cells. The results obtained are shown in fig 4.2.1 and 4.2.2. FMO1 mRNA was detected in both human skin samples analysed (fig 4.2.1, lanes 2 and 3). This 2 kb band was faint and barely visible. No bands were observed in the human liver samples electrophoresed concurrently on the gel or in the RNA extracted from the primary culture of human keratinocytes and the HaCaT cells. The marmoset liver RNA sample showed 3 bands that hybridized to the human cDNA probe encoding FMO1 (fig 4.2.1, lane 7 and fig 4.2.2, lane 15). These bands were approximately 4.2 kb, 2.3 kb and 1.6 kb in size, with the 2.3 kb band being the most intense. When rabbit liver RNA was probed with the same human cDNA, a transcript of approximately 2.2 kb was observed (fig 4.2.2, lane 10). The lengths of the transcripts correlate to those obtained by Dolphin *et al* (1991) who found that the cDNA encoding FMO1 hybridized to an mRNA that was approximately 2.3 kb in human foetal liver. Furthermore, the presence of FMO1 mRNA in human skin confirms the results obtained by Dolphin *et al.*, (1996). These results also confirm the presence of a single FMO1 mRNA in

rabbit liver, a result obtained previously by Lawton *et al.*, (1990) who detected a 2.6 kb band in hepatic RNA samples obtained from rabbit when hybridized to a cDNA encoding the hepatic FMO1 from rabbit. The lack of FMO1 mRNA in primary cultures of human keratinocytes may be due to *FMO1* not being expressed in this particular layer, i.e. the epidermis of skin, or that culture conditions have suppressed the expression of *FMO1*. The absence of FMO1 mRNA in the HaCaT cells, may be due either to culture conditions, or to the numerous passages these cells have undergone. The presence of FMO1 mRNA in marmoset liver has not been previously reported. It is interesting to note that adult human liver does not express FMO1, but FMO1 is expressed in the liver of other adult animals such as pig, rabbit and marmoset. The evolutionary implications of this finding suggest that the switch in the expression of *FMO1* in the liver occurred fairly recently in the evolutionary chain.

4.2.2 Expression of FMO2 mRNA

A full length cDNA encoding human FMO2 has been previously isolated and cloned in our laboratories (Phillips *et al.*, 1995). This cDNA was radiolabelled using the random priming method and used to analyse various tissue and culture samples using northern blot hybridization analysis, as described in section 2.5. A very strong signal was obtained with three of the four human, the cynomolgous monkey and rabbit, lung RNA samples (fig 4.3). No hybridization was observed with human, rabbit and monkey, liver RNA samples or with the HaCaT and a primary culture of human epidermal keratinocyte RNA samples. In all four human lung samples, cynomolgous monkey and rabbit lung RNA samples, the most intense hybridizing band was approximately 5.8 kb in size. In three out of the four human lung samples, (fig 4.3, lanes 3, 4 and 5), a hybridizing band was also observed, at about 7.4 kb.

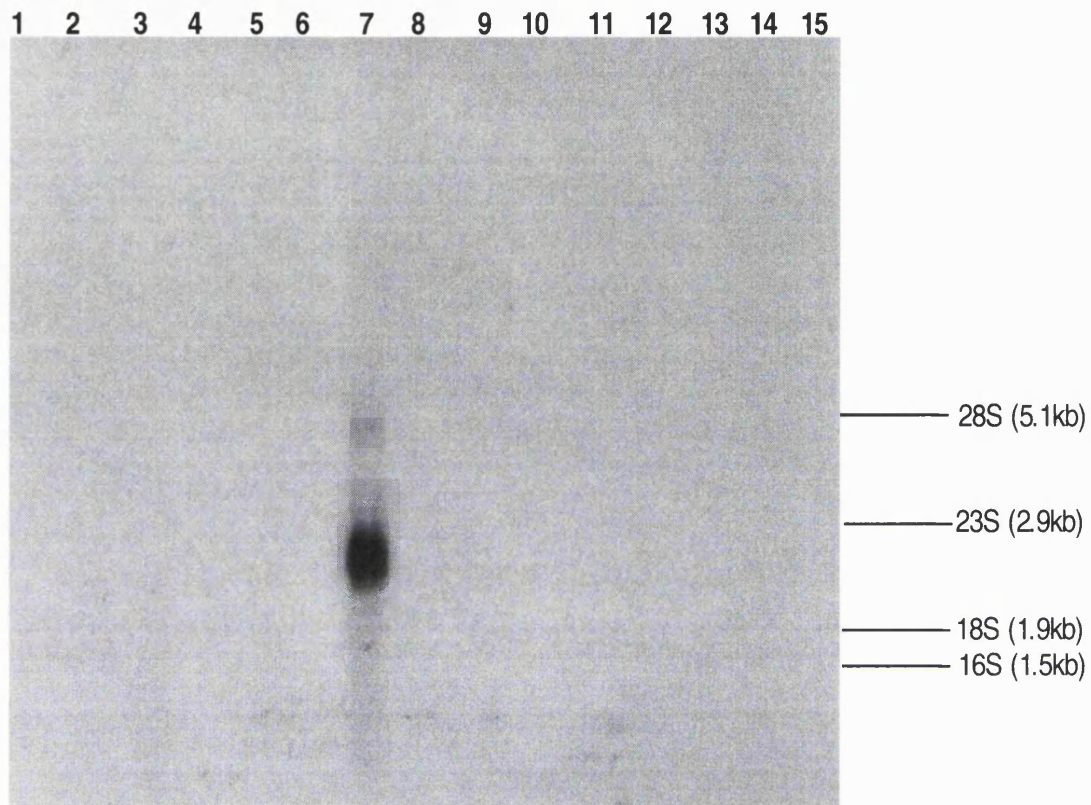


Fig 4.2.1 RNA samples (15 μ g) were electrophoresed on a 1% denaturing formaldehyde agarose gel as detailed in section 2.5. RNA was from human whole skin (lanes 2 and 3), adult human liver (lane 5), adult marmoset liver (lane 7), HaCaT cells (lanes 9-12) and a primary culture of human epidermal keratinocytes (lane 14). Lane 1 and 13, *E. coli* total RNA (1 μ g) was electrophoresed to serve as size markers together with the 28S and 18S rRNA in the samples and used for the subsequent estimation of the transcript size. The northern blot was hybridized with a full length cDNA encoding FMO1. Autoradiography was carried out for 3 weeks.

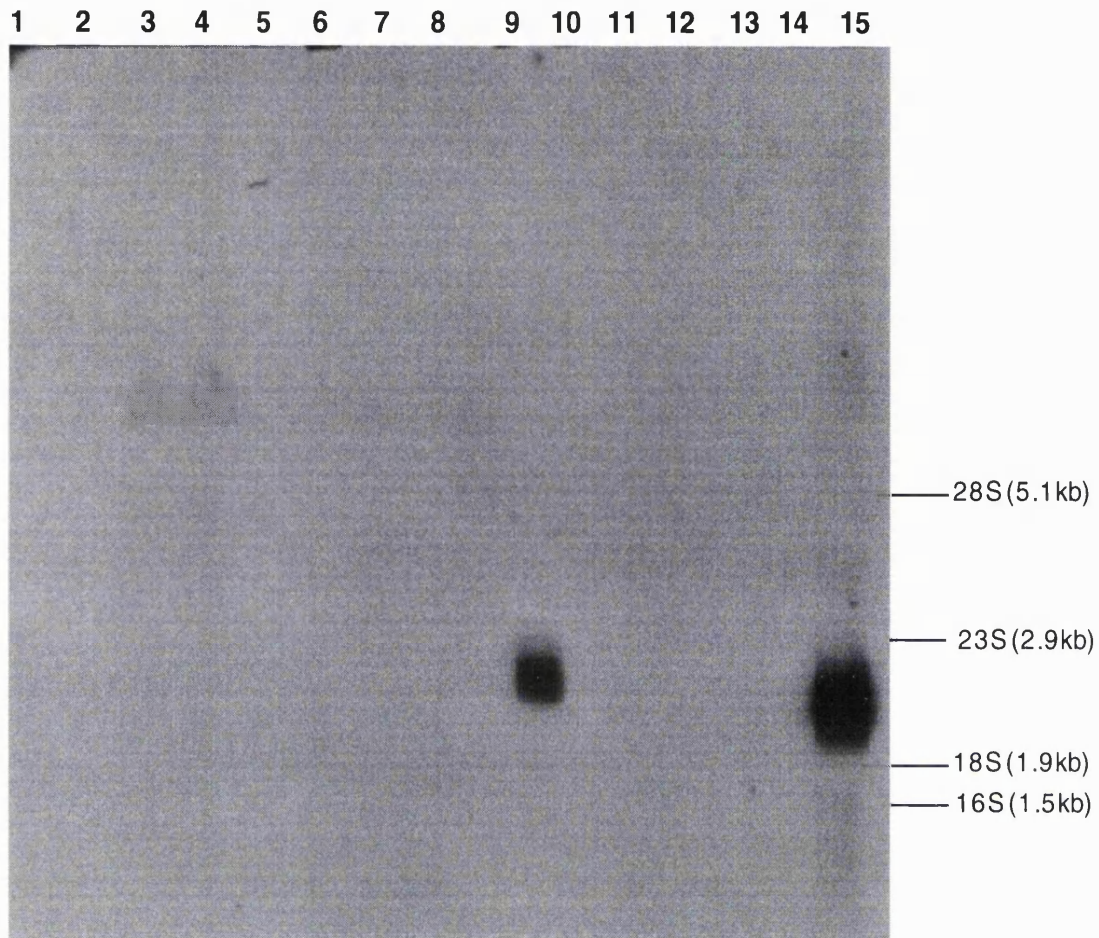


Fig 4.2.2. RNA samples (15 μ g) were electrophoresed on a 1% denaturing formaldehyde agarose gel as described in section 2.5. RNA was from human lung (lanes 2-5), cynamologous monkey lung (lane 6), rabbit lung (lane 7), human liver (lanes 8 and 9), rabbit liver (lane 10), HaCaT cells (lane 13), a primary culture of human epidermal keratinocytes (lane 14) and marmoset liver (lane 15). Total *E. coli* RNA (1 μ g) was electrophoresed concurrently (lanes 1 and 12). These served as size markers together with the 28S and 18S rRNA in the samples and were used to determine transcript size. The blot was hybridized with a radiolabelled cDNA encoding FMO1. Autoradiography was carried out for 1 week.

The human lung samples in lanes 3 and 5 also showed a lower transcript of 4.6 kb.

FMO2 cDNA hybridized to 5 different transcripts in the cynomolgous monkey lung RNA, ranging in size from 10.5, 7.4, 5.8, 4.6 and 2.8 kb. Other transcripts were present, but could not be accurately sized. The most predominant transcript in the monkey lung was 5.8 kb. In the rabbit lung RNA sample, only 2 transcripts of 5.8 kb and 6.9 kb were observed, the smaller transcript being the most predominant.

This result contrasts with those of Lawton *et al.*, (1990) who observed four distinct FMO2 transcripts of 2.4, 2.6, 4.8 and 6.0 kb in rabbit lung samples, the intensity of each transcript being very similar. No data on the expression of *FMO2* in human lung, or in cynomolgous monkey lung has been published. FMO2 mRNA transcripts in the cynomolgous monkey lung are similar to those obtained in the rhesus macaque lung where multiple transcripts of different sizes were obtained when rhesus lung RNA was hybridized to a cDNA encoding the rhesus lung FMO form. The major FMO2 transcript observed in the Rhesus macaque is approximately 5 kb in size (Yueh *et al.*, 1997).

4.2.3 Expression of FMO3 mRNA

A full length cDNA encoding human FMO3 cloned in our laboratories was used to investigate the tissue-specific expression of FMO3 mRNA (Dolphin *et al.*, 1996). Northern blot analysis of human lung and liver, rabbit lung and liver, cynomolgous monkey lung, marmoset liver, HaCaT and a primary culture of human epidermal keratinocyte RNA is shown in fig 4.4. Intense hybridizing bands were observed in all liver RNA samples, (lanes 8, 9 and 10). The probe hybridized, albeit weakly, to three of the four human lung samples (lanes 3, 4 and 5). No FMO3 transcripts were observed in either the

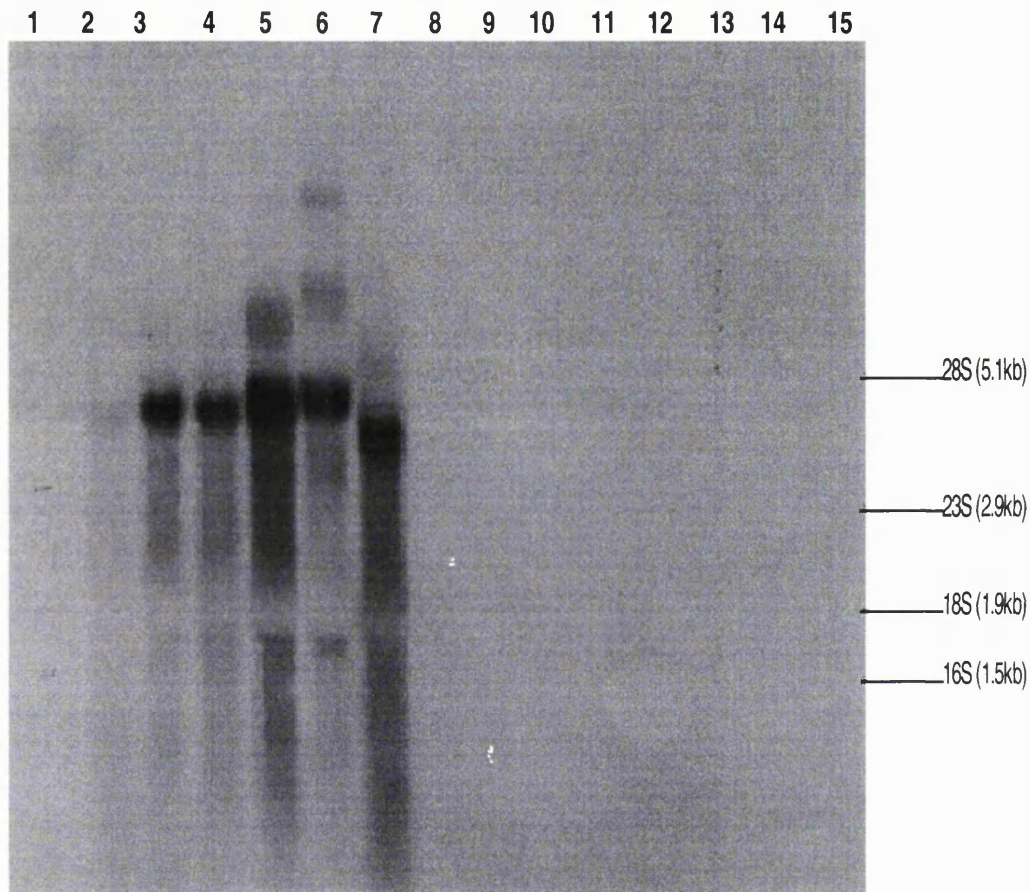


Fig 4.3 RNA samples (15 μ g) were electrophoresed on a 1% denaturing formaldehyde agarose gel as described in section 2.5. Samples were from human lung (lanes 2-5), cynamologous monkey lung (lane 6), rabbit lung (lane 7), human liver (lanes 8 and 9), rabbit liver (lane 10), HaCaT cells (lane 13) and a primary culture of human epidermal keratinocytes (lane 14). Total *E. coli* RNA (1 μ g) was also electrophoresed (lanes 1 and 13) and used as size markers together with the 28S and 18S rRNA in the samples. The northern blot was hybridized with a full length cDNA encoding human FMO2. Autoradiography was carried out for 48 hours.

cynomolgous monkey lung or in rabbit lung RNA samples (lanes 6 and 7 respectively).

The major species of mRNA encoding FMO3 in all the human samples, liver and lung, was approximately 2.4 kb. In the human liver tracks, a certain degree of smearing was observed below the main band. This is probably due to mRNA degradation. The size of the predominant FMO3 transcript is similar to that obtained by Lomri *et al.*, (1992) who detected a single FMO3 transcript, 2.3 kb in size, in human liver RNA.

In rabbit liver RNA, two hybridizing bands were observed at 3.2 kb and 2.4 kb. The former being the more abundant FMO3 mRNA form in rabbit liver. Burnett *et al.*, (1994) detected only one hybridizing band in rabbit liver mRNA when they used a 720 bp fragment of the rabbit FMO3 cDNA as a hybridization probe. They did not report the size of the FMO3 transcript observed.

Marmoset liver RNA showed an intensely hybridizing band at 4.1 kb with several fainter bands of lower molecular weight.

No FMO3 transcripts were observed in either the HaCaT or the primary culture of human epidermal keratinocyte RNA samples.

4.2.4 Expression of FMO4 mRNA

A full length cDNA encoding FMO4 has been previously isolated and cloned in our laboratories (Dolphin *et al.*, 1992). The cDNA was hybridized to a northern blot containing RNA from human lung and liver, cynomolgous monkey lung, rabbit lung and liver, HaCaT cells and a culture of primary human epidermal keratinocytes (fig 4.5).

Hybridizing bands were observed in all liver and lung samples. In the human liver samples, a single transcript of 4 kb was observed. Two transcripts of 5.5 kb and 3.5 kb, were present in the human lung RNA

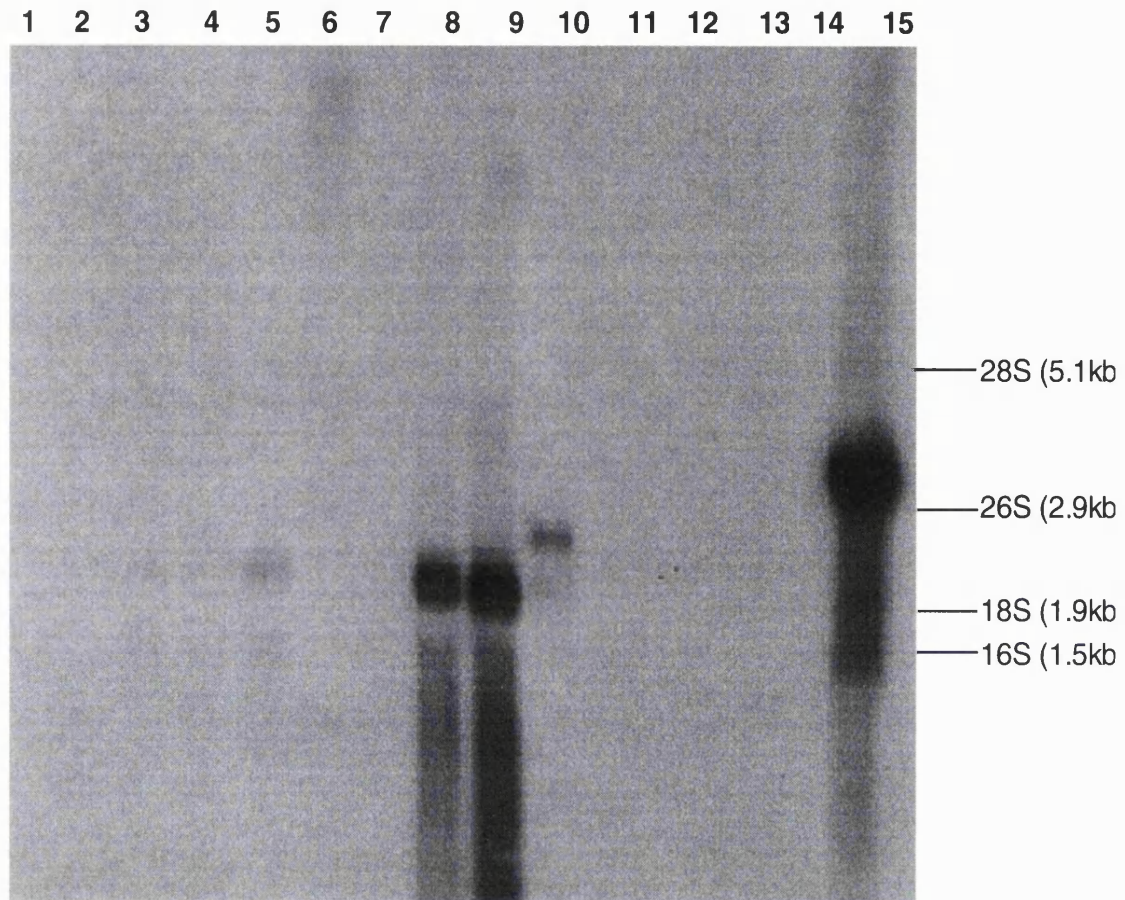


Fig 4.4 RNA samples (15 μ g) were electrophoresed on a 1% denaturing formaldehyde agarose gel as detailed in section 2.5. RNA was from human lung (lanes 2-5), cynamologous monkey lung (lane 6), rabbit lung (lane 7), human liver (lanes 8 and 9), rabbit liver (lane 10), HaCaT cells (lane 13), a culture of primary human epidermal keratinocytes (lane 14) and marmoset liver (lane 15). Total *E. coli* RNA (1 μ g) was electrophoresed concurrently with the samples (lanes 1 and 12). These served as size markers together with the 28S and 18S bands in the samples. The northern blot was hybridized with a radiolabelled cDNA encoding FMO3. Autoradiography was carried out for 24 hours.

samples. The 3.5 kb transcript was the more predominant (fig 4.5, lanes 2-5). A single hybridizing band of 3.6 kb was observed in the cynamologous monkey lung RNA sample (lane 6). The rabbit lung sample showed three weakly hybridizing bands of 5.5 kb, 4.7 kb and 4 kb (lane 7). In the rabbit liver, two transcripts of 4.7 and 4 kb were observed (lane 10). The lower transcript was the more abundant form in this tissue. This result is similar to those obtained by Burnett *et al.*, (1994) who also observed two FMO4 transcripts in rabbit liver.

No bands were detected in the RNA from a primary culture of human epidermal keratinocytes. Two transcripts of 3.6 kb and 2.5 kb were observed in the HaCaT cells, the larger transcript being the more predominant.

4.2.5 Expression of FMO5 mRNA

A full length cDNA clone encoding FMO5 has been previously isolated in our laboratories (Phillips *et al.*, 1995). This cDNA was used in northern blot analysis of RNA from human liver and lung, cynamologous monkey liver, rabbit liver and lung, and from cultures of HaCaT cells and a culture of primary human epidermal keratinocytes (fig 4.6). Bands were observed in all samples, except rabbit lung RNA, HaCaT and the primary culture of human epidermal keratinocytes. Both the human liver RNA samples showed four FMO5 transcripts (lanes 8 and 9). Due to the smearing of the samples, it was not possible to identify the total number of hybridizing bands in the human liver samples. The two predominant transcripts were 5 kb and 2.8 kb in size. Two transcripts, 5 kb and 2.7 kb in size, were observed in all four of the human lung RNA samples, (lanes 2-5). The larger transcript was more predominant.

The FMO5 cDNA hybridized to two transcripts of 6 kb and 2.8 kb in cynamologous monkey lung RNA (lane 6). The 2.8 kb transcript was the more predominant form.

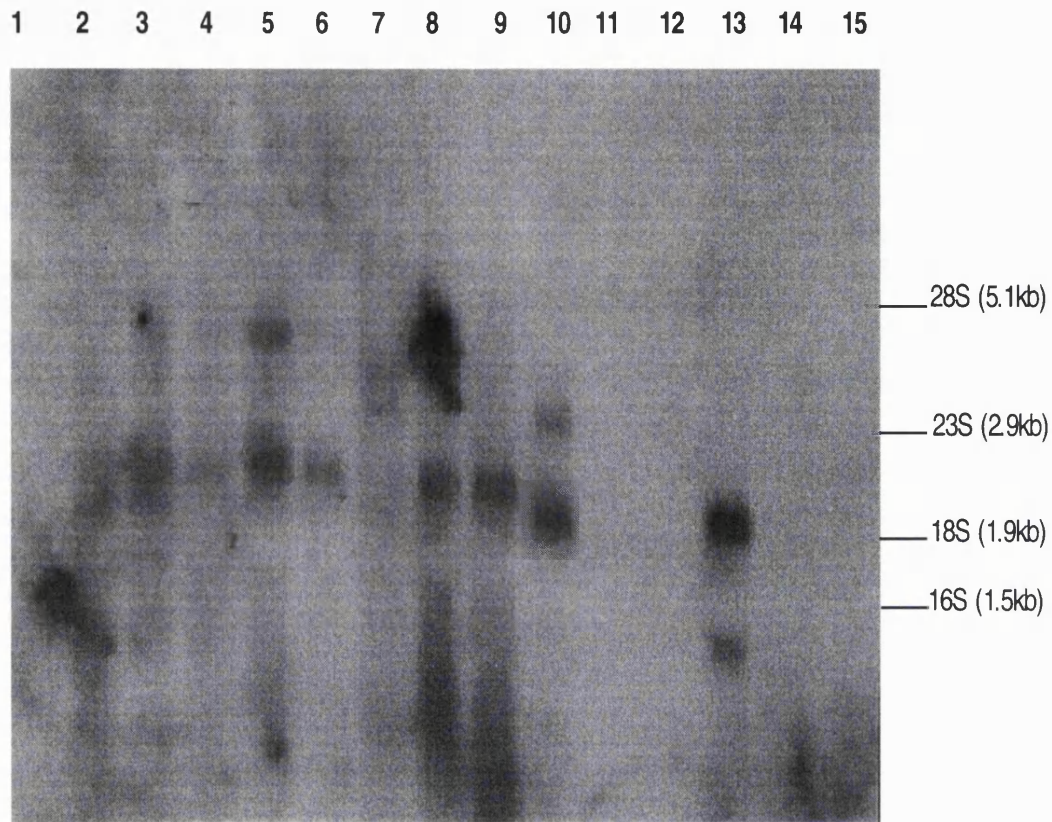


Fig 4.5 RNA samples (15 μ g) were electrophoresed on a 1% denaturing formaldehyde agarose gel as described in section 2.5. Samples were from human lung (lanes 2-5), cynomolgous monkey lung (lane 6), rabbit lung (lane 7), human liver (lanes 8 and 9), rabbit liver (lane 10), HaCaT cells (lane 13) and a primary culture of human epidermal keratinocytes (lane 14). Total *E.coli* RNA (1 μ g) was also electrophoresed (lanes 1 and 13) and used as size markers together with the 28S and 18S rRNA in the samples. The northern blot was hybridized to a full length cDNA encoding human FMO4. Autoradiography was carried out for 6 days.

Four FMO5 transcripts were observed in the rabbit liver RNA sample. These ranged in size from 10, 7.7, 4.5, and 2.5 kb. The more strongly hybridizing transcripts were the 7.7 kb and 2.5 kb. These results are similar to those of Atta Asafo Adjei *et al.*, (1993), who showed that a full length cDNA encoding the rabbit FMO5 hybridizes to two rabbit liver species of mRNA, of 2.6 kb and 5.4 kb.

In marmoset liver RNA, one major FMO5 transcript of 2.5 kb was observed.

4.3 Summary of FMO mRNA expression

The results obtained using northern blot hybridization analyses with cDNAs encoding FMOs 1, 2, 3, 4 and 5 are summarized in Table 4.1.

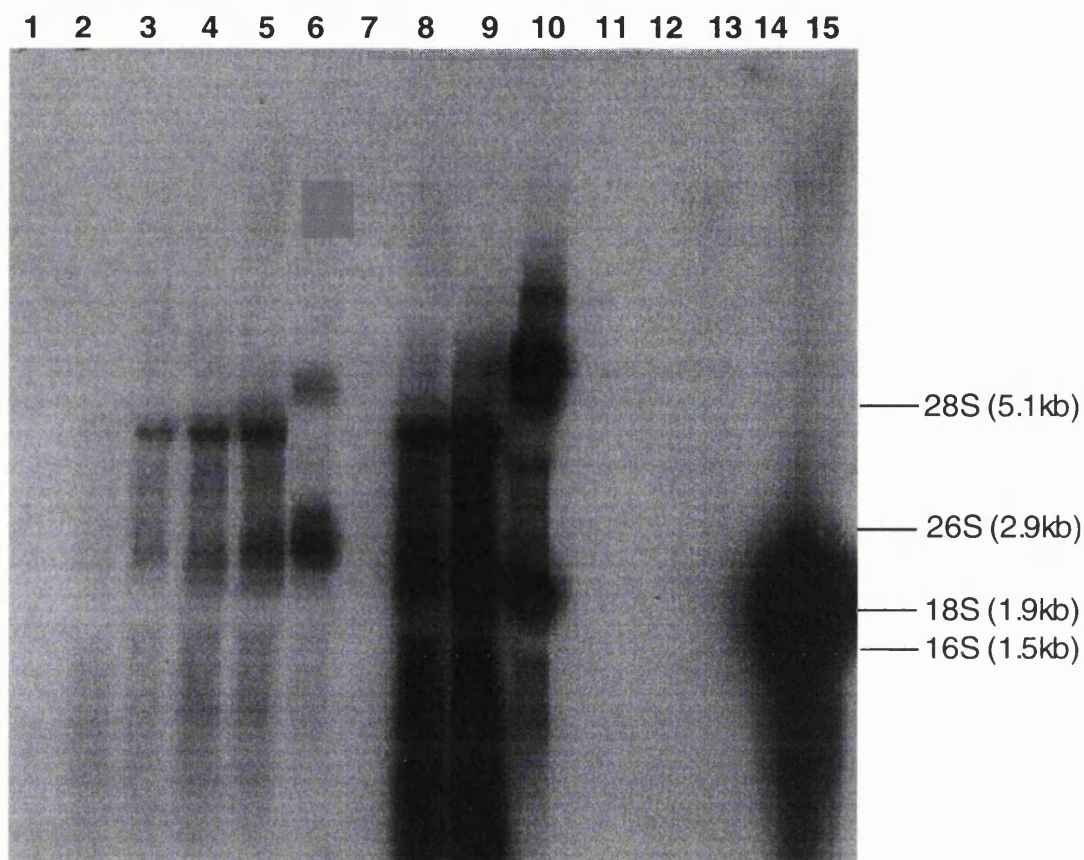


Fig 4.6 RNA samples (15 μ g) were electrophoresed on a 1% denaturing formaldehyde agarose gel as described in section 2.5. RNA was from human lung (lanes 2-5), cynamologous monkey lung (lane 6), rabbit lung (lane 7), human liver (lanes 8 and 9), rabbit liver (lane 10), HaCaT cells (lane 13), a primary culture of human epidermal keratinocytes (lane 14) and marmoset liver (lane 15). Total *E. coli* RNA (1 μ g) was electrophoresed concurrently (lanes 1 and 12). These served as size markers together with the 28S and 18S rRNA in the samples and were used to detemine transcript size. The blot was hybridized with a radiolabelled cDNA encoding FMO5. Autoradiography was carried out for 1 week.

RNA samples	FMO1	FMO2	FMO3	FMO4	FMO5
Human liver	-	-	++++	+	++++
Human lung	-	++++	+	+	+++
Rabbit liver	++	-	++	+	++++
Rabbit lung	-	++++	-	+	-
Cynomolgous monkey lung	-	++++	-	+	++++
Marmoset liver	+++	-	++++	ND	++++
HaCaT cells	-	-	-	++	-
Primary human epidermal keratinocytes	-	-	-	-	-
Human skin	+	ND	ND	ND	ND

Table 4.1 Summary of results obtained from northern blot hybridization analyses using full length cDNA clones from FMOs 1, 2, 3, 4 and 5. (ND = not determined)

5.1 Detection of FMO mRNAs using RNase Protection Assays (RPAs)

When northern blot hybridization analysis was used, long autoradiographic exposure times were required to detect the small amounts of FMO mRNAs present in skin and cultured cell samples. It was therefore decided to use RNase Protection Assays (RPAs) to detect the presence of FMO mRNAs in these samples. RPA is a method that is more quantitative and offers greater specificity and sensitivity than northern blot hybridization analysis. A direct comparison between different RNA samples can be made, with respect to the amounts of a particular mRNA species present.

Studies were extended to include a comparative analysis of FMO mRNAs in whole skin and in cultures of keratinocytes derived from these tissue samples. Samples of human liver, lung and kidney total RNA were used as either positive or negative controls depending on the FMO mRNA under investigation.

cDNA fragments of FMO 1, 2, 3, 4 or 5 had been previously cloned into the plasmid pBluescript KS plus by Dr. Colin Dolphin (Queen Mary and Westfield College, London). The cDNA subclone constructs are shown in figs 5.1.1, 5.1.2, 5.1.3, 5.1.4 and 5.1.5. pBluescript contains the promoter sequences of the bacteriophages T3 and T7. Therefore, using the appropriate RNA polymerase (T3 or T7) it is possible to synthesize either an antisense or sense mRNA.

5.2 Detection and quantification of FMO1 mRNA

An *Eco* RI-*Sac* I fragment that spans the nucleotides 798-962 of the coding region of *FMO1* was cloned into pBluescript (fig 5.1.1). This plasmid was named p8A1-6. *In vitro* transcription from the T7 promoter of p8A1-6

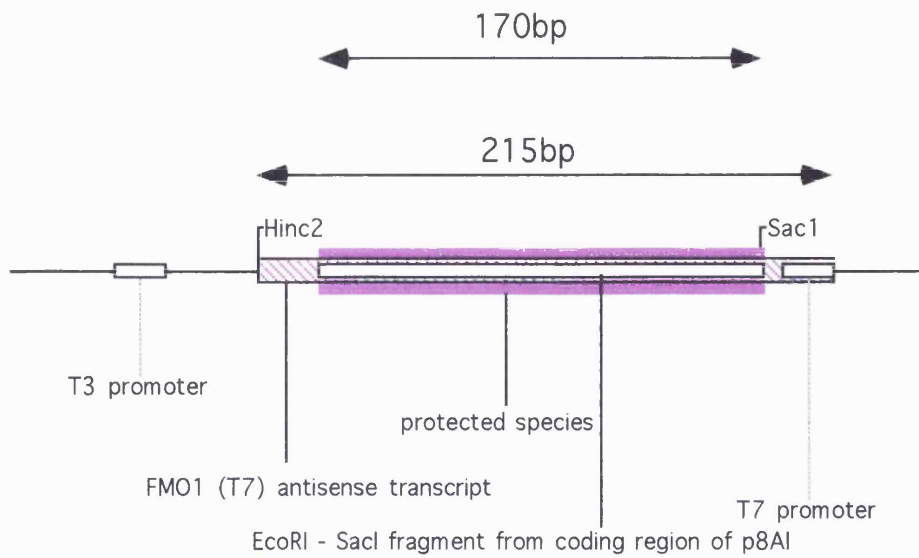


Fig 5.1.1 p8A1-6; *Eco* RI-*Sac* I fragment spanning nucleotides 798 to 962 of the coding region of *FMO1* (Dolphin *et al.*, 1991) cloned into pBluescript.

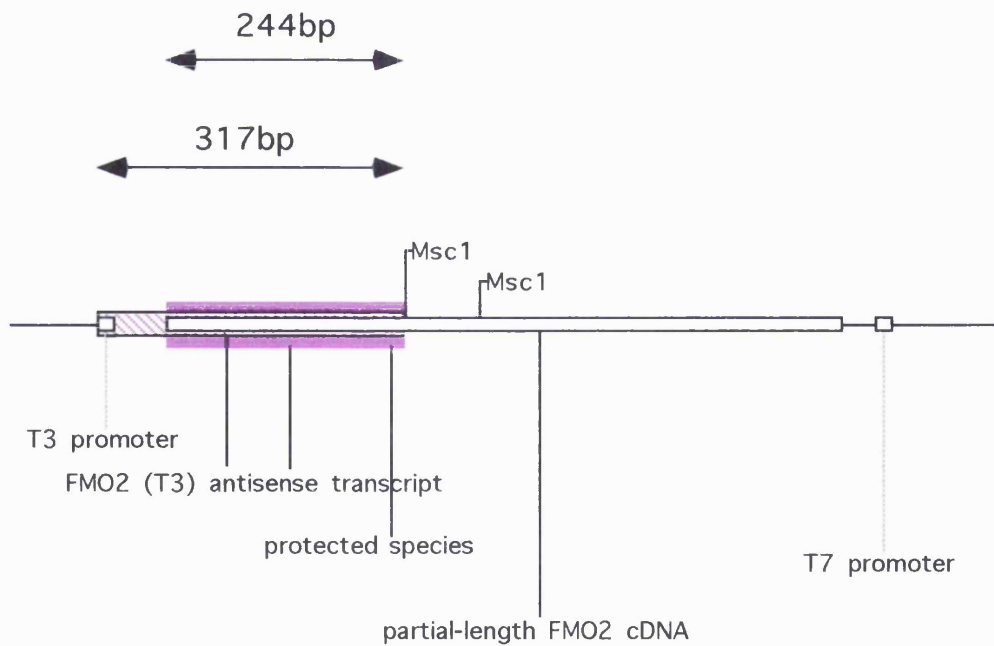


Fig 5.1.2 pFMO2/2/15; a fragment comprising nucleotides 50 to 749 of the *FMO2* gene (Phillips *et al.*, 1995) cloned into pBluescript.

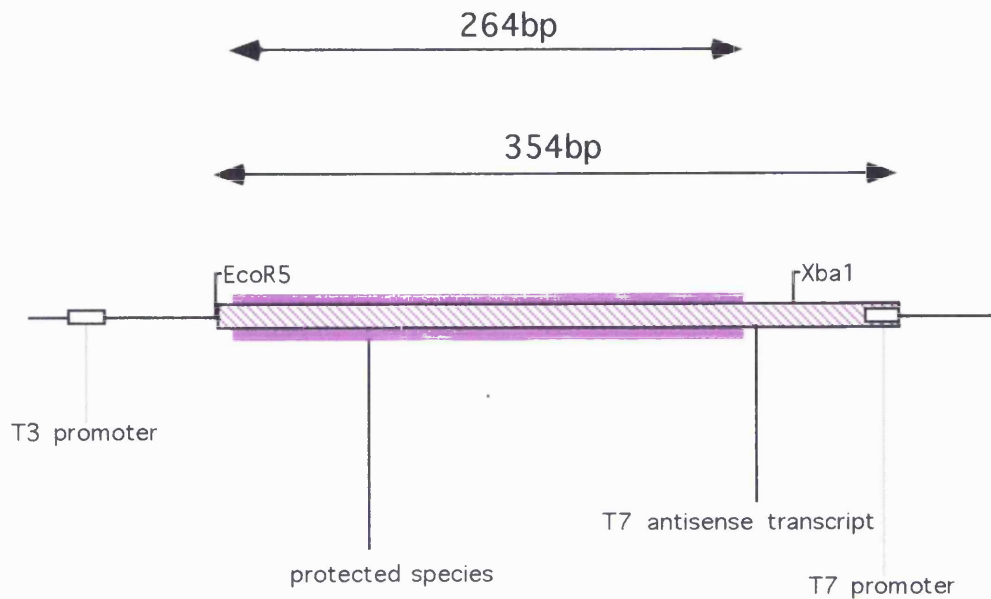


Fig 5.1.3 pBSformII; constructed by RT-PCR amplification of a 264 bp sequence containing the last 40 bases of the coding region and the first 224 bases of the 3' untranslated region of the FMO3 mRNA.

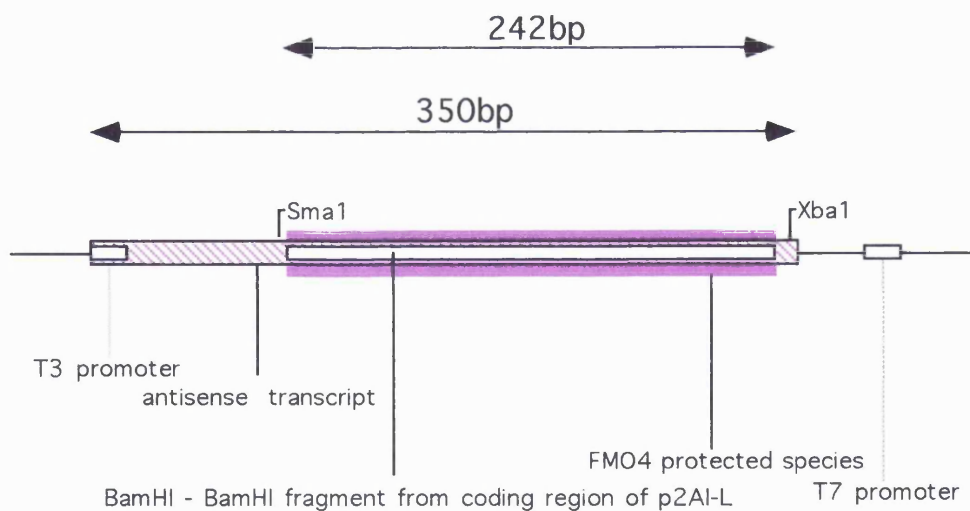


Fig 5.1.4 2A1L-2; constructed from the digestion of the clone 2A1L (Dolphin *et al.*, 1992) by *Bam* HI, encompassing the nucleotides 1340 to 1576 of the coding region of the FMO4 cDNA.

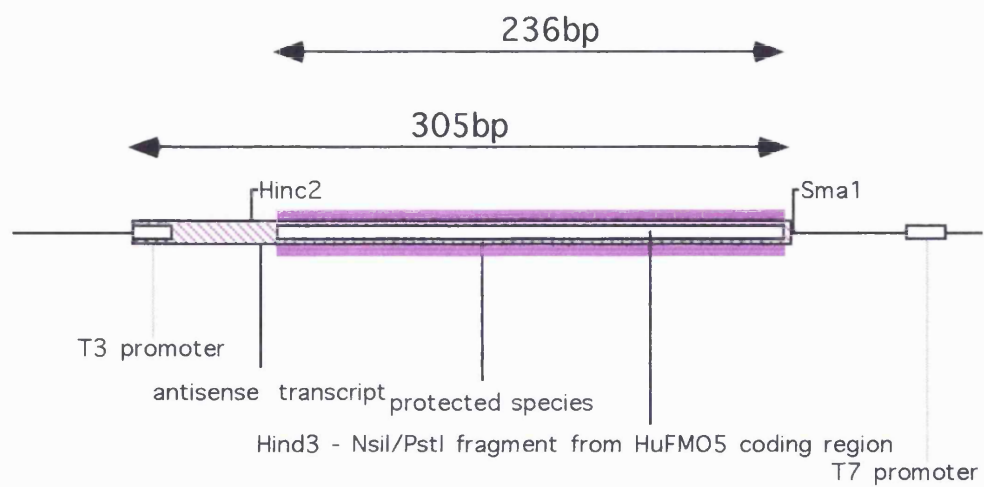


Fig 5.1.5 pIC1/1B/C; A *Hind* III- *Pst* I fragment spanning 332 to 558 bp of the coding region of the human FMO5 cDNA (Phillips *et al.*, 1995) cloned into pBluescript.

produced a radiolabelled antisense riboprobe, 215 bases long. This probe was hybridized overnight, at 45°C, to total RNA samples isolated from skin, primary cultures of human epidermal keratinocytes and HaCaT cells (as detailed in section 2.6.1.2). Human kidney and marmoset liver RNA samples were used as the positive controls (Dolphin *et al.*, 1996), whereas human liver and lung RNA were used as the negative controls.

Following digestion of hybrids with RNaseA/T1, a protected fragment of 170 bp was detected in the positive controls, human kidney and marmoset liver RNA samples. Fig 5.2.1 and 5.2.2 shows the protection pattern obtained in this assay. Of a total of nine whole skin samples analysed, six were found to express FMO1 mRNA. Of the five primary cultures of human epidermal keratinocyte samples analysed only one sample expressed FMO1 mRNA. FMO1 mRNA was also detected in HaCaT cells. The negative controls of human liver and lung RNA were both negative.

The amount of FMO1 mRNA present in the above samples was determined from a standard curve of known amounts of FMO1 antisense RNA as described in section 2.6.1.6. The standard curve was prepared at the same time as the test samples and both sets of samples were exposed concurrently to the same sheet of X-ray film. The quantitative results are summarized in fig 5.2.3 and Table 5. 1.

The amount of FMO1 mRNA expressed in human skin samples shows slight variation between individuals with a range between 1.3×10^5 to 2.4×10^5 molecules of FMO1 mRNA per μg of total RNA or between 0-1.2 molecules of FMO1 mRNA/cell. It is usual to express RNase protection results as the number of molecules of a specific mRNA per cell. In the case of the skin, I have assumed that the average amount of mRNA per skin cell is approximately 5pg (Little and Jackson, 1987).

Four of the whole skin samples contained <1 molecule of FMO1 mRNA/cell and two had just a little more than 1 molecule of FMO1 mRNA/cell.

These results are comparable to those obtained by Dolphin *et al.*, (1996) who also found < 1 molecule of FMO1 mRNA per cell in the single human skin sample analysed.

A comparison between the amount of FMO1 mRNA present in the human kidney and skin showed that in a kidney cell, FMO1 mRNA comprises approximately 1.35×10^{-4} % of the total mRNA, whereas in a skin cell FMO1 mRNA constitutes 1.5×10^{-5} % of the total mRNA in the cell. On average, a single cell of the kidney contains 10 times the amount of FMO1 mRNA than a single cell of the skin does.

The protection of a 170 bp fragment in marmoset liver RNA shows that the marmoset FMO1 mRNA is very similar in sequence to the human FMO1 mRNA. The two sequences must be at least 98% similar, with a few point mutations, otherwise bands smaller than 170 bp would have been observed when the marmoset sample was electrophoresed. This RNase protection assay confirms the results obtained from the northern blot hybridization analyses, (see fig 4.2.1 and 4.2.2). The expression of FMO1 mRNA in the liver of a lower primate is interesting because it indicates that the lack of expression of *FMO1* in adult human liver is a relatively late evolutionary event. All other adult mammals express FMO1 mRNA in their liver, but in man FMO1 mRNA is expressed only in foetal liver. This FMO is therefore subject to developmental regulation in man.

5.3 Detection and quantification of FMO2 mRNA

A region comprising nucleotides 50 to 749 of the FMO2 cDNA was subcloned into the plasmid pBluescript KS plus (fig 5.1.2). The plasmid was named pFMO2/2/15. Linearization of pFMO2/2/15 was carried out using *Msc I* and using T3 RNA polymerase, a 317 nucleotide long antisense transcript was synthesised. The antisense probe was hybridized to human liver, lung

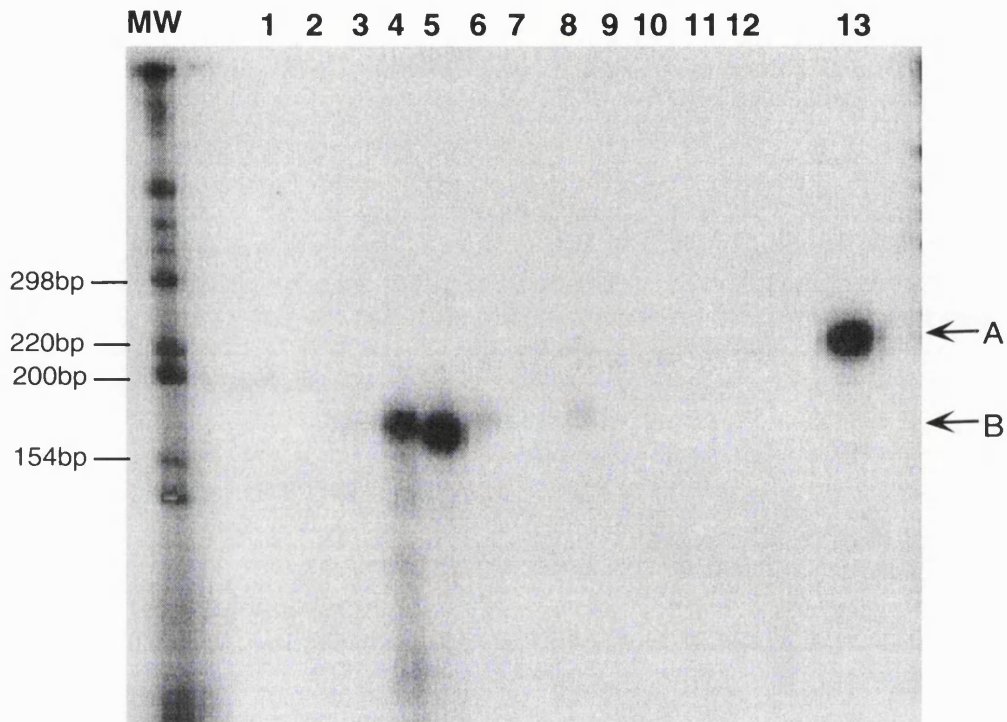


Fig 5.2.1 Analysis of FMO1 mRNA by RNase protection. 30 μ g of total RNA was hybridized to antisense FMO1 mRNA (transcribed from pBSFMO1). Each reaction contained 1 X 10⁵cpm of riboprobe. All assays were performed as described in section 2.6 RNA from human liver (5 μ g) (track2), human lung, (10 μ g), (track 3), human kidney (10 μ g) (track 4), marmoset liver (10 μ g) (track 5) were used as controls. RNA was from human skin (tracks 6, 8 and 10), primary cultures of human epidermal keratinocytes (tracks 7, 9 and 11) and HaCaT cells (track 12). Track 13 contains undigested antisense transcript. Track 1 contains a control for digestion of the transcripts, by RNase A/T1, in the presence of 30 μ g of tRNA. Molecular weight standards (MW) were ³⁵S-labelled fragments derived from the 1kb ladder set from Gibco BRL (section 2.6). The arrows indicate the position of the undigested transcript (A, 215bp) and protected hybrid (B, 170bp). Autoradiography was carried out for 18 days.

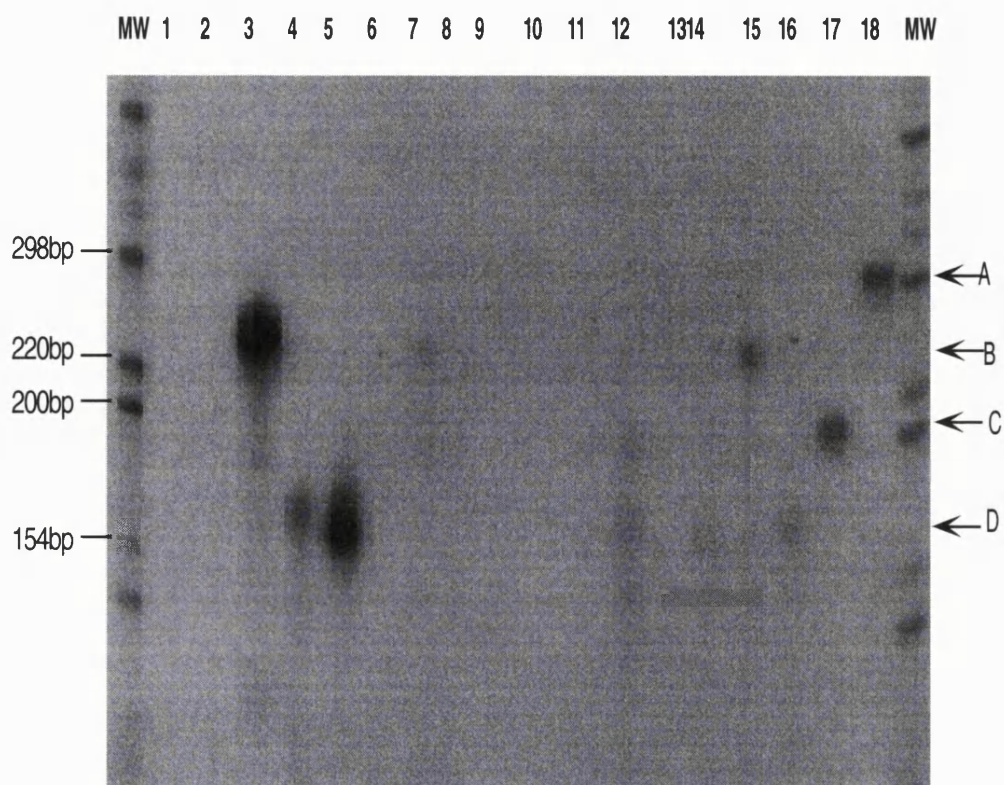


Fig 5.2.2 Analysis of FMO1 and FMO2 mRNA by RNase protection. 30 μ g of total RNA was hybridized to antisense FMO1 and FMO2 mRNAs. Each reaction contained 1 X 10⁵cpm of each riboprobe. All assays were performed as described in section 2.6. RNA from human liver (5 μ g) (track 2), human lung (10 μ g) (track 3), human kidney (10 μ g) (track 4), marmoset liver (10 μ g) (track 5) were used as controls. RNA was from human skin (tracks 6, 8, 10, 12, 14 and 16), primary cultures of human epidermal keratinocytes (tracks 7, 9, 11, 13 and 15). Track 1 contains a control for digestion of the transcripts, by RNase A/T1, in the presence of 30 μ g of tRNA. Tracks 17 and 18 contain undigested antisense transcript of FMO1 and FMO2 respectively. Molecular weight standards (MW) were ³⁵S-labelled fragments derived from the 1kb ladder set from Gibco BRL (section 2.6). The arrows indicate the positions of the undigested FMO1 transcript (C, 215bp), protected hybrid (D, 170bp), undigested FMO2 transcript (A, 317bp) and protected FMO2 hybrid (B, 244bp). Autoradiography was carried out for 6 days.

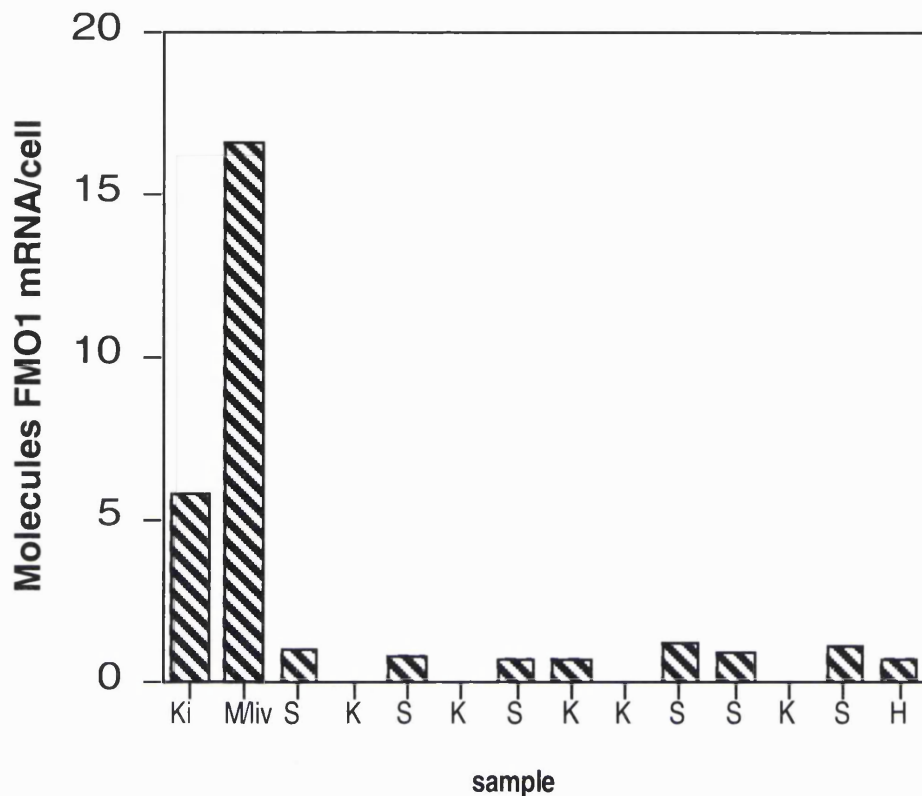


Fig 5.2.3 FMO1 mRNA concentrations in human kidney (Ki), marmoset liver (M/liv), human skin (S), primary human epidermal keratinocyte (K) and HaCaT (H) cell samples. Samples were analysed as described in section 2.6. The FMO1 antisense transcript was hybridized to human kidney, marmoset liver, human skin, primary cultures of human epidermal keratinocyte and HaCaT cell RNA and digested with a mixture of RNase A/T1. The digested RNA was electrophoresed and autoradiographed. The resulting signals were compared to a standard curve of undigested probe and the concentrations of the mRNA in the samples calculated as described in section 2.6.1.6.

and skin RNA samples as well as to RNA from primary cultures of human epidermal keratinocytes derived from the corresponding skin samples and to HaCaT cellular RNA.

The protection pattern obtained in this assay is shown in figs 5.2.2, 5.3.1 and 5.3.2. A band of 244 bp, corresponding to the protected fragment, was observed in the human lung sample. None of the skin samples analysed showed the presence of FMO2 mRNA. Of the eight primary cultures of human epidermal keratinocyte RNA samples analysed, four showed the presence of the FMO2 mRNA. No expression of *FMO2* was detected in the HaCaT cells.

FMO2 was not detected in the human liver and kidney samples. In a separate experiment however, after prolonged exposure, of the gel, to the X-ray film, FMO2 mRNA was detected in the kidney sample analysed, but none was found in the liver sample (fig 5.3.2).

The expression of FMO2 mRNA in the lung (11.19 molecules of FMO2 mRNA/cell) was approximately 15 times that detected in the primary cultures expressing FMO2 mRNA (0.68 molecules FMO2 mRNA/cell). The expression of *FMO2* in the primary cultures did not correspond to the age of the individual from whom the original skin was derived. These results are shown in fig 5.3.3.

The results obtained for the expression of FMO2 mRNA in the human liver, lung and kidney are similar to those obtained by Dolphin *et al.*, (1998, submitted) who has detected the expression of the FMO2 mRNA in high abundance (13 molecules/cell) in the human lung, but in lower amounts (3 molecules/cell) in the human kidney. FMO2 mRNA has also been found to be present in the foetal lung samples, but not in foetal liver or kidney.

FMO2 gene expression has been demonstrated to be regulated by sex hormones in experimental animals (Lee *et al.*, 1993, Lee *et al.*, 1995) and putative glucocorticoid responsive elements have been identified in the 5' flanking region of the rabbit *FMO2* gene (Wyatt *et al.*, 1996). It is possible that

the primary cultures express FMO2 mRNA because hormones such as insulin and hydrocortisone were added to the culture medium. The reason as to why only some of the primary cultures expressed FMO2 mRNA whereas the other primary cultures did not, is not known.

5.3B Detection and quantification of FMO3 mRNA

The plasmid (pBSformII) used for the FMO3 RNase protection experiments was constructed by RT-PCR amplification of a 264 bp sequence that contained the last 40 bases of the coding region and the first 224 bases of the 3' untranslated region of the FMO3 mRNA (fig 5.1.3). Linearization of pBSformII with *Eco* R5 followed by *in vitro* transcription using T7 RNA polymerase produced a 354 base antisense transcript.

Total RNA derived from human liver, lung, kidney, skin, primary cultures of human epidermal keratinocytes and HaCaT samples were isolated as described in section 2.4. After digestion of the hybrid, with RNase A/ T1, a protected fragment of 264 bp was observed in those samples containing FMO3 mRNA. The protection pattern obtained is shown in figs 5.3.1, 5.3.2 and 5.4.1. In some samples, a doublet was observed probably indicating the presence of an allelic variant of *FMO3*. Studies in our laboratory have detected several polymorphisms within the *FMO3* gene.

FMO3 mRNA was detected in human liver, lung and kidney. The liver contains the greatest amount of FMO3 mRNA (11.39 molecules/cell), whereas the lung (0.41 molecules/cell) and the kidney (0.33 molecules/cell) contain only small amounts. Six skin samples were analysed for the presence of FMO3 mRNA, five expressed *FMO3*. The amounts of this mRNA did not vary greatly between skin samples, ranging from 3×10^4 - 8×10^4 molecules of FMO3 per microgram of total RNA or 0.13-0.45 molecules/cell. Of the seven primary cultures of human epidermal keratinocytes analysed, three contained

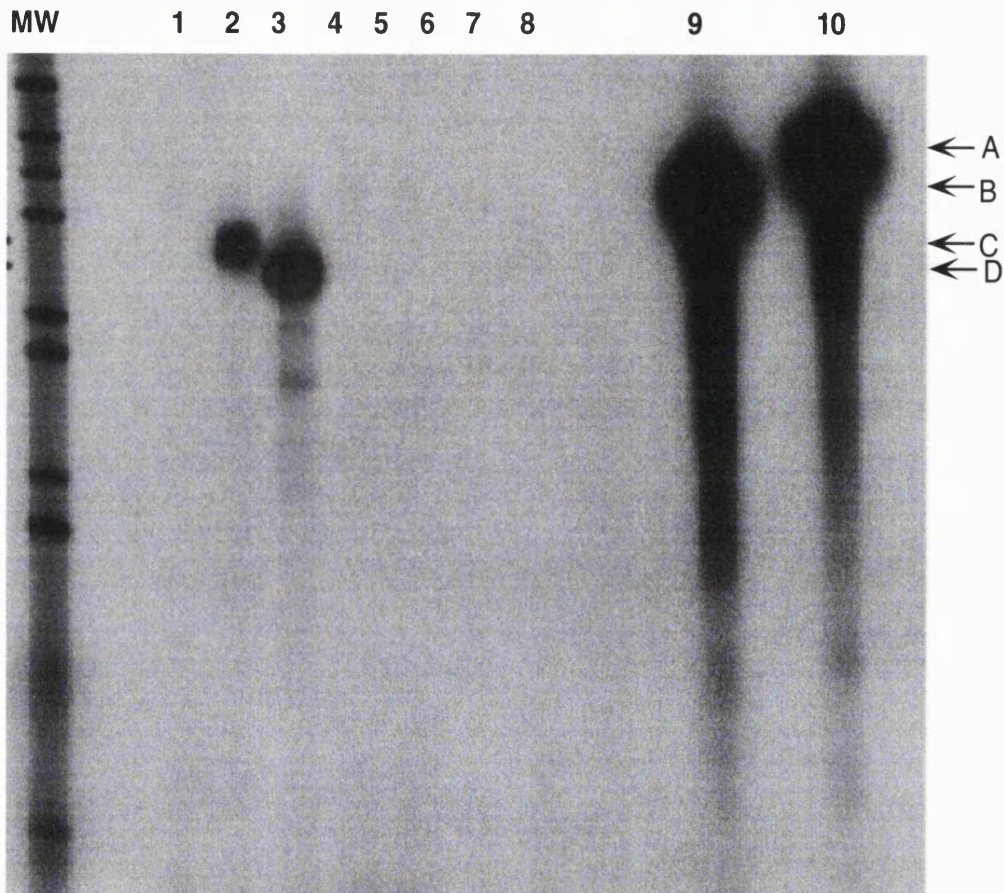


Fig 5.3.1 Analysis of FMO2 and FMO3 mRNAs by RNase protection. 10 μ g of total RNA was hybridized to antisense FMO2 and FMO3 mRNAs. Each reaction contained 1 X 10⁵cpm of each riboprobe. All assays were performed as described in section 2.6. RNA from human liver (5 μ g) (track 2) and human lung (10 μ g) (track 3) were used as controls. RNA was from human skin (track 6), primary cultures of human epidermal keratinocytes (tracks 4, 5 and 7) and HaCaT cells (track 8). Track 1 contains a control for digestion of the transcript, by RNase A/T1, in presence of 10 μ g of tRNA. Tracks 9 and 10 contain undigested FMO2 and FMO3 antisense transcripts respectively. Molecular weight standards (MW) were ³⁵S-labelled fragments derived from the 1kb ladder set from Gibco BRL (section 2.6). The arrows indicate the length of undigested FMO2 transcript (B, 317bp), protected FMO2 hybrid (D, 244bp), undigested FMO3 transcript (A, 354bp) and protected FMO3 hybrid (C, 264bp). Autoradiography was carried out for 1 week.

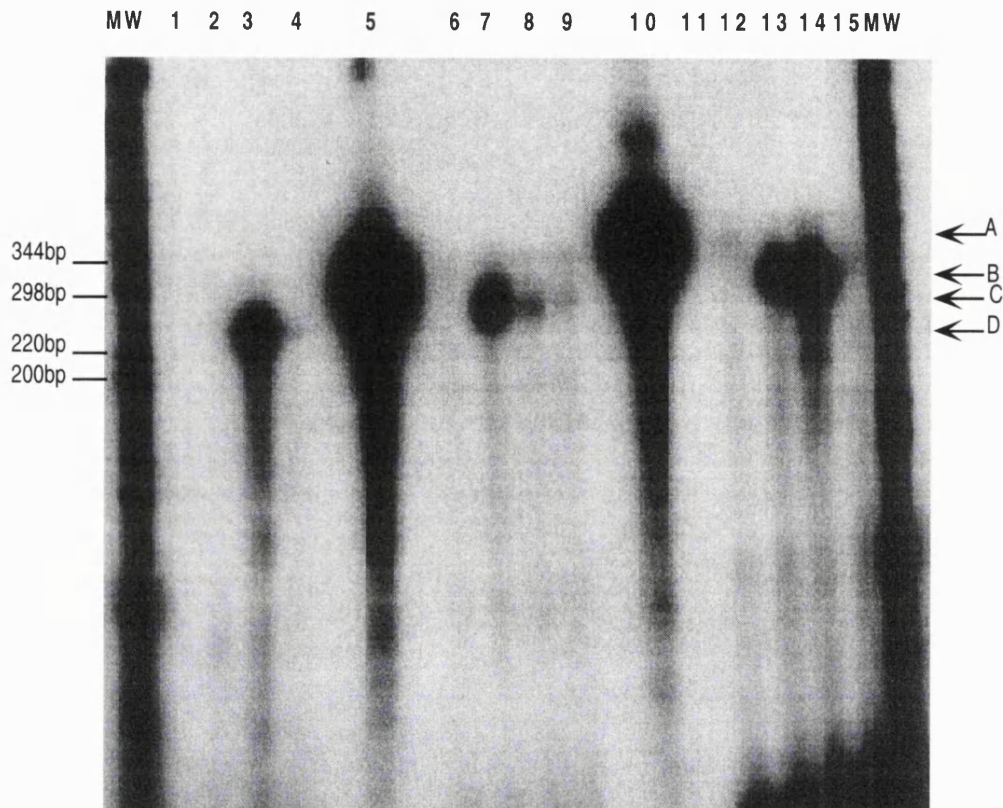


Fig 5.3.2 Analysis of FMO2 and 3 mRNAs by RNase protection. 30 μ g of total RNA was hybridized to FMO1 and FMO2 mRNAs. Each reaction contained 1 X 10⁵cpm of each riboprobe. All assays were performed as described in section 2.6. RNA was from adult human liver (5 μ g), human lung (10 μ g) and human kidney (10 μ g). Human liver (tracks 2, 7 and 13), human lung (tracks 3, 8 and 14) and human kidney (tracks 4, 9 and 15). Tracks 1, 6 and 12 contain a control for digestion, by RNase A/T1, in the presence of 10 μ g of tRNA. Track 5 contains undigested FMO2 transcript and track 10 contains undigested FMO3 transcript. Tracks 1-4 contain samples hybridized with FMO2 antisense transcript, tracks 6-9 samples hybridized with FMO3 antisense transcript and tracks 12-15 samples hybridized with both FMO2 and FMO3 antisense transcripts together. The arrows indicate the length of the undigested FMO2 transcript (B, 317bp), protected FMO2 hybrid (D, 244bp), undigested FMO3 transcript (A, 354bp) and protected FMO3 transcript (C, 264bp). Molecular weight standards (MW) were ³⁵S-labelled fragments derived from the 1kb ladder set from Gibco BRL (section 2.6). Autoradiography was carried out for 4 weeks.

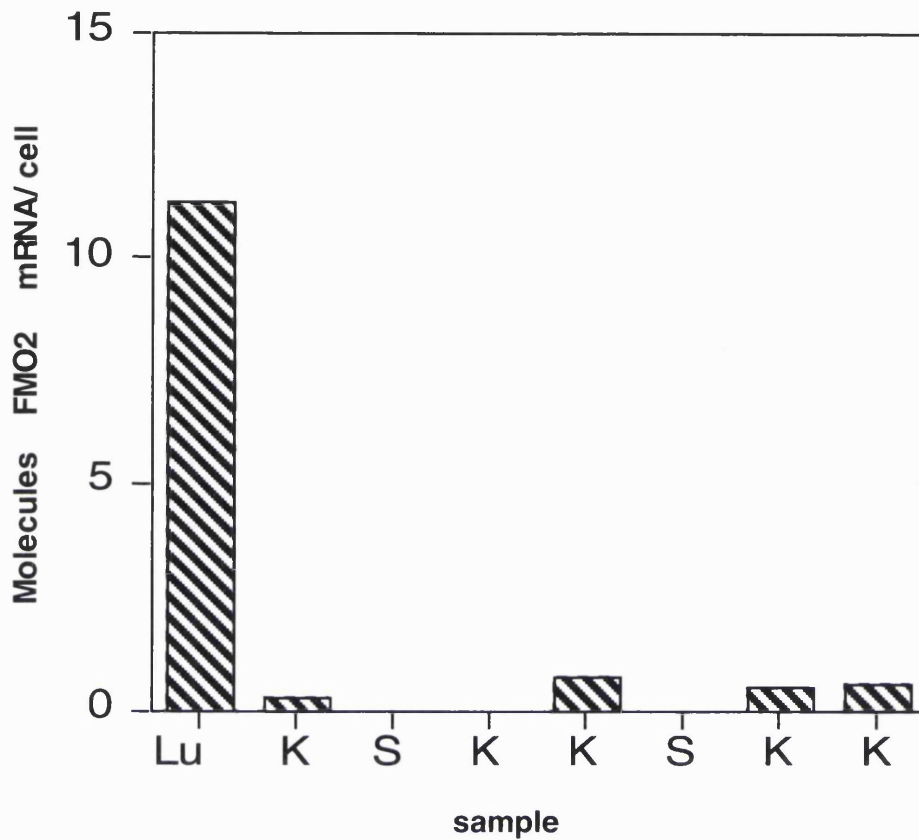


Fig 5.3.3 FMO2 mRNA concentrations in human lung (Lu), human skin (S) and primary human epidermal keratinocyte samples (K). Samples were analysed as described in section 2.6. The FMO2 antisense transcript was hybridized to human lung, human skin and primary cultures of human epidermal keratinocyte RNA and digested with a mixture of RNase A/T1. The digested RNA was electrophoresed and autoradiographed. The resulting signals were compared to a standard curve of undigested probe and the concentrations of the mRNA in the samples calculated as described in section 2.6.1.6.

FMO3 mRNA. The amounts of this mRNA varied from between 3×10^4 - 4×10^4 molecules of FMO3 per microgram of total RNA or 0.14-0.21 molecules/cell (fig 5.4.2). Therefore, it appears that *FMO3* expression does not drop significantly in culture. No correlation between the ages of the individuals from which the skin was obtained and expression of FMO3 mRNA in culture or in whole tissue was seen. No FMO3 mRNA expression was detected in the HaCaT cells.

The presence of FMO3 mRNA in the human liver is well documented and has been observed using northern blot analyses (see section 4.2.3). The presence of FMO3 in the human lung has been reported by Dolphin *et al.*, (1996), who also showed the expression of low amounts of FMO3 mRNA in human kidney samples.

5.4 Detection and quantification of FMO4 mRNA

The RNase protection plasmid for analysis of FMO4 mRNA was constructed by digestion of the clone 2A1L (Dolphin *et al.*, 1992) by *BamH* I to produce a 236 bp fragment from the coding region (1340-1576bp) of the FMO4 cDNA (Dolphin *et al.*, 1996). This fragment was cloned into the plasmid pBluescript KS plus to produce the plasmid 2A1L-2 (fig 5.1.4). This plasmid was linearized using *Xba* I and the antisense riboprobe transcribed using T3 RNA polymerase. The radiolabelled riboprobe was hybridized to human liver, lung, kidney and skin total RNA. Human skin samples were analysed together along side their corresponding primary cultures and RNA extracted from HaCaT cells. A 242 bp protected fragment was observed, after RNase A/T1 digestion, in all positive samples (fig 5.5.1 and 5.5.2).

FMO4 mRNA was detected in the human liver, lung, kidney and in two of the three skin samples analysed. The amount of FMO4 mRNA in the liver, lung and kidney samples differed, with kidney having the highest amount

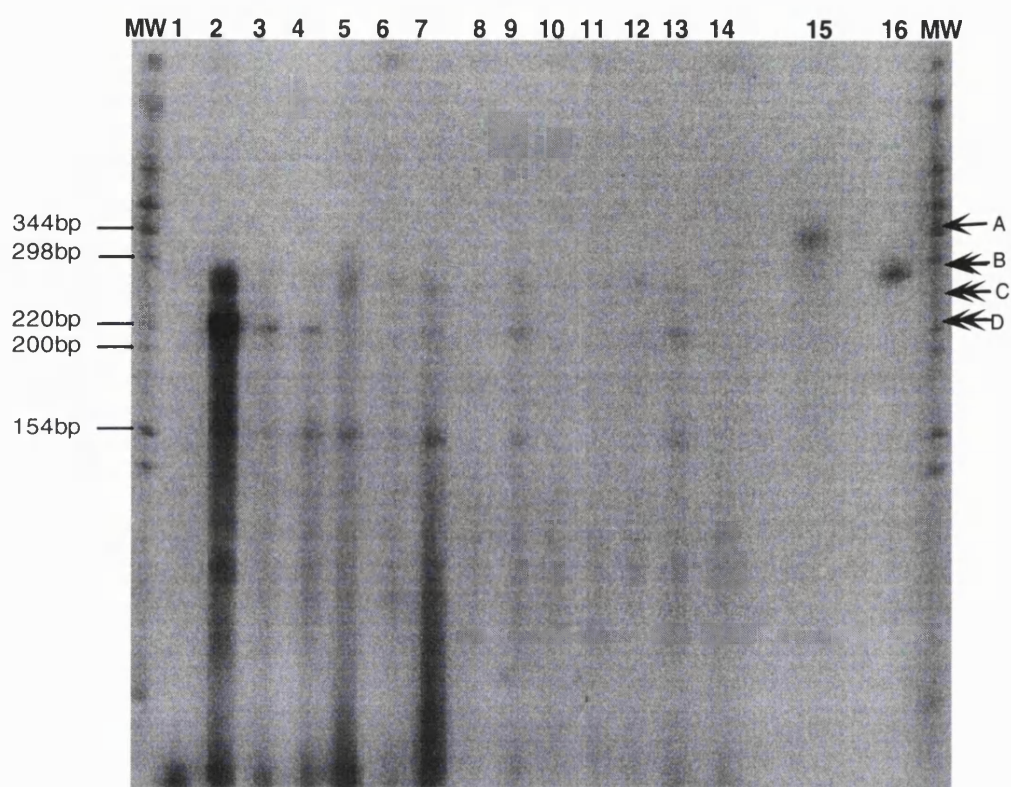


Fig 5.4.1 Analysis of FMO3 and FMO5 mRNAs by RNase protection. 30 μ g of total RNA was hybridized to antisense FMO3 and FMO5 mRNA. Each reaction contained 1 X 10⁵cpm of each riboprobe. All assays were performed as described in section 2.6. RNA from human liver (5 μ g) (track 2), human lung (10 μ g) (track 3) and human kidney (10 μ g) (track 4) were used as controls. RNA was from human skin (tracks 5, 7, 9, 11 and 13), primary cultures of human epidermal keratinocytes (tracks 6, 8, 10 and 12) and HaCaT cells (track 14). Track 1 contains a control for digestion, by RNase A/T1, of the transcript in presence of 30 μ g of tRNA. Tracks 15 and 16 contain undigested antisense transcript for FMO3 and FMO5 respectively. Molecular weight standards (MW) were ³⁵S-labelled fragments derived from the 1kb ladder set from Gibco BRL (section 2.6). The arrows indicated the length of undigested FMO3 transcript (A, 354bp), protected FMO3 hybrid (C, 264bp), undigested FMO5 transcript (B, 305bp) and protected FMO5 hybrid (D, 242bp). Autoradiography was carried out for 8 days.

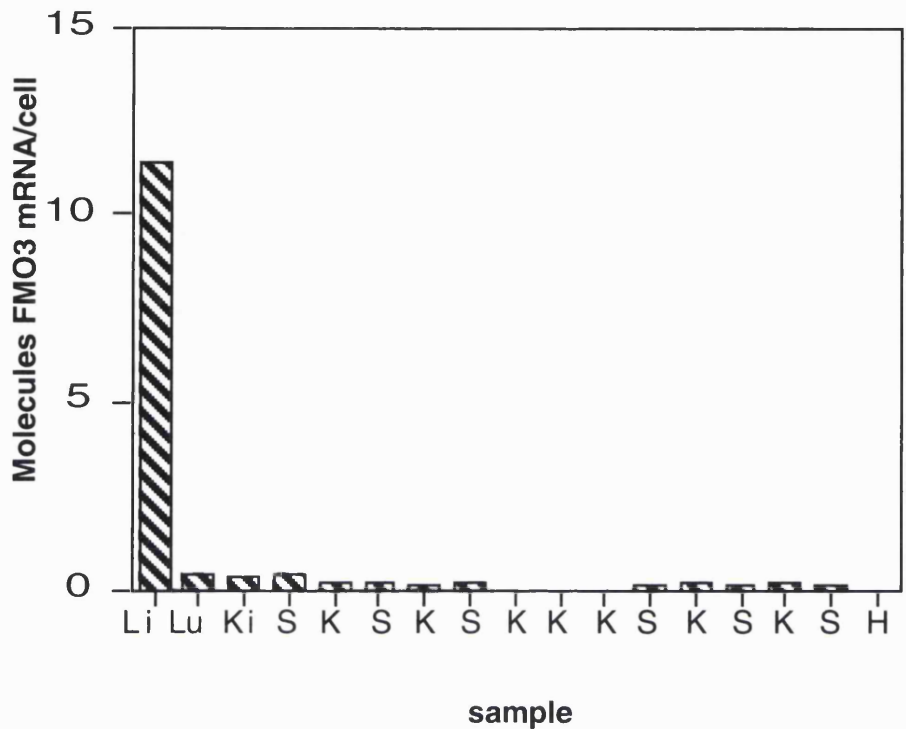


Fig 5.4.2 FMO3 mRNA concentrations in human liver (Li), human lung (Lu), human kidney (Ki), human skin (S), primary human epidermal keratinocytes (K) and HaCaT (H) cell samples. Samples were analysed as described in section 2.6. The FMO3 antisense transcript was hybridized to human liver, lung, kidney, primary cultures of epidermal keratinocytes and HaCaT RNA and digested with a mixture of RNase A/T1. The digested RNA was electrophoresed and autoradiographed. The resulting signals were compared to a standard curve of undigested probe and the concentrations of the mRNA in the samples calculated as described in section 2.6.1.6.

(4×10^4 molecules/ μg of total RNA or 0.23 molecules/cell) and the lung the lowest (9×10^3 molecules/ μg of total RNA or 0.05 molecules/cell) (fig 5.5.3). The amount of FMO4 mRNA in the liver sample was approximately 0.15 FMO4 mRNA molecules/cell.

The amount of expression in both the positive skin samples was low (0.01 molecule/cell). FMO4 RNA was present in high amounts in the HaCaT cells (3×10^4 molecules per μg total RNA or 0.16 molecules/cell) (fig 5.5.3). This confirmed the results obtained previously in the northern blot hybridization analyses. No FMO4 mRNA was detected in any of the primary cultures of human epidermal keratinocytes studied.

The results obtained for the human liver and kidney are similar to those obtained by Dolphin *et al.*, (1996) who detected the presence of FMO4 mRNA in all these tissues from adult humans, although in low abundance. These workers however did not detect FMO4 mRNA in adult human lung.

5.5 Detection and quantification of FMO5 mRNA

A *Hind* III-*Pst* I fragment spanning 332-558 bp of the coding region of the human FMO5 cDNA was subcloned into the plasmid pBluescript KS plus (fig 5.1.5). This plasmid (p1C1/1B/C) was used as the template for the synthesis of an antisense FMO5 riboprobe. The plasmid was linearised with *Sma* I and the antisense transcript was synthesised using T3 RNA polymerase. The radiolabelled riboprobe was hybridized to human liver, lung and kidney RNA samples. These studies were extended to HaCaT cells and human skin and primary cultures of human epidermal keratinocytes derived from the skin samples.

A 236 bp protected fragment indicating the presence of FMO5 mRNA was detected in the human liver, lung and kidney samples (fig 5.5.1 and 5.5.2). The amount of FMO5 mRNA in these three tissues differed, the liver

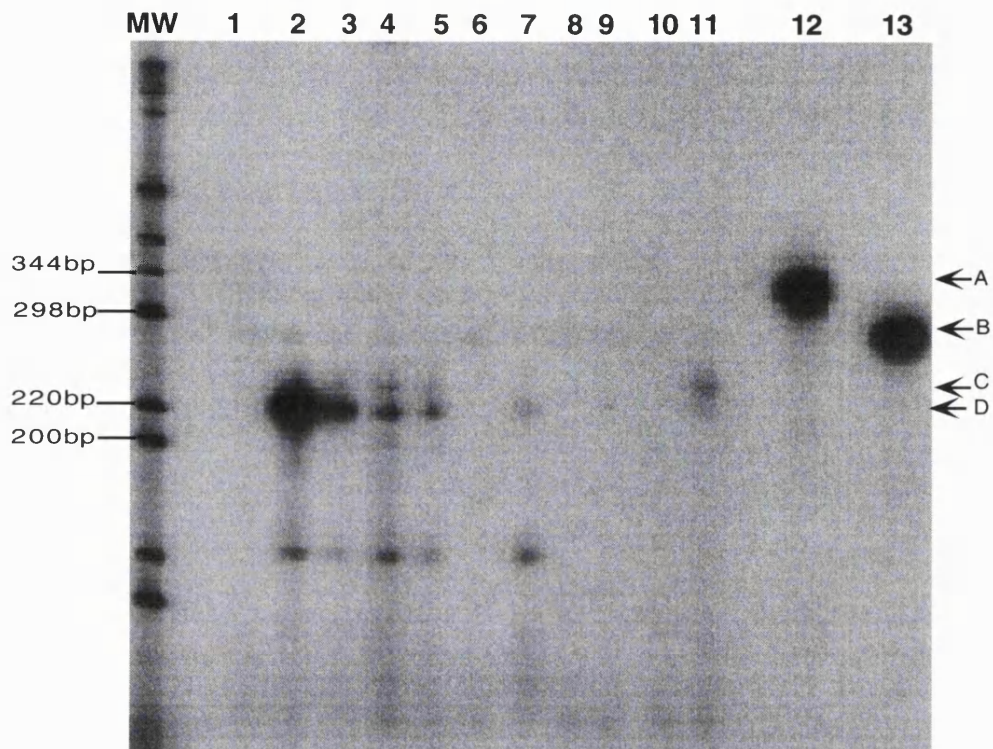


Fig 5.5.1 Analysis of FMO4 and FMO5 mRNAs by RNase protection. 30 μ g of total RNA was hybridized to antisense FMO4 and FMO5 mRNA. Each reaction contained 1×10^5 cpm of each riboprobe. All assays were performed as described in section 2.6. RNA from human liver (5 μ g) (track 2), human lung (10 μ g) (track 3) and human kidney (10 μ g) (track 4) were used as controls. RNA was from human skin (tracks 5, 7 and 9), primary cultures of human epidermal keratinocytes (tracks 6, 8 and 10) and HaCaT cells (track 11). Track 1 contains a control for digestion of the transcripts, by RNase A/T1, in the presence of 30 μ g of tRNA. Tracks 12 and 13 contain undigested FMO4 and FMO5 antisense transcripts respectively. Molecular weight standards (MW) were 35 S-labelled fragments derived from the 1kb ladder set from Gibco BRL (section 2.6). The arrows indicate the positions of the undigested FMO4 transcript (A, 350bp), protected FMO4 hybrid (C, 242bp), undigested FMO5 transcript (B, 305bp) and protected FMO5 hybrid (D, 236bp). Autoradiography was for 2 weeks.

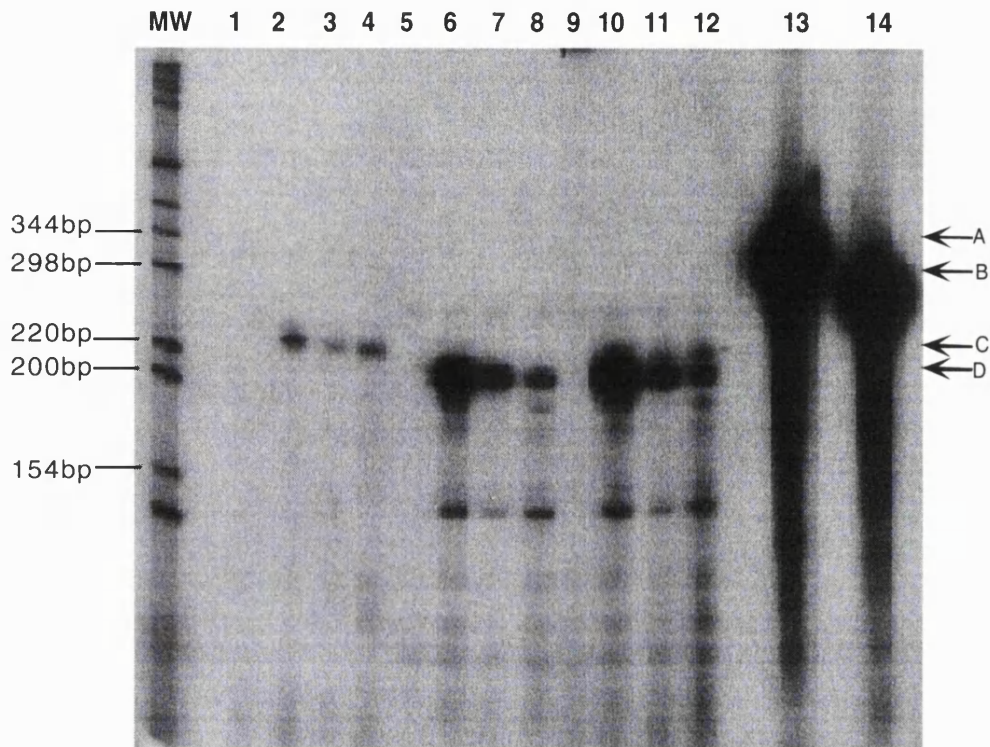


Fig 5.5.2 Analysis of FMO4 and FMO5 mRNAs by RNase protection. 10 μ g of total RNA was hybridized to FMO4 and FMO5 mRNAs. Each reaction contained 1 X 10⁵cpm of each riboprobe. RNA was from human liver (5 μ g), human lung (10 μ g) and human kidney (10 μ g). All assays were performed as described in section 2.6. Human liver (tracks 2, 6 and 10), human lung (tracks 3, 7 and 11) and human kidney (tracks 4, 8 and 12). Tracks 1, 5 and 9 contain a control for digestion, by RNase A/T1, in the presence of 10 μ g of tRNA. Tracks 1-4 are samples hybridized with the FMO4 antisense transcript, tracks 5-8 are samples hybridized with the FMO5 antisense transcript and tracks 9-12 are samples hybridized with both FMO4 and FMO5 antisense transcripts together. Track 13 contains undigested FMO4 antisense transcript and track 14 contains undigested FMO5 antisense transcript. Molecular weight standards (MW) were ³⁵S-labelled fragments derived from the 1kb ladder set from Gibco BRL (section 2.6). The arrows indicate the positions of the FMO4 antisense transcript (A, 350bp), protected FMO4 hybrid (C, 242bp), FMO5 antisense transcript (B, 305bp) and protected FMO5 hybrid (D, 236bp). Autoradiography was carried out for 16 days.

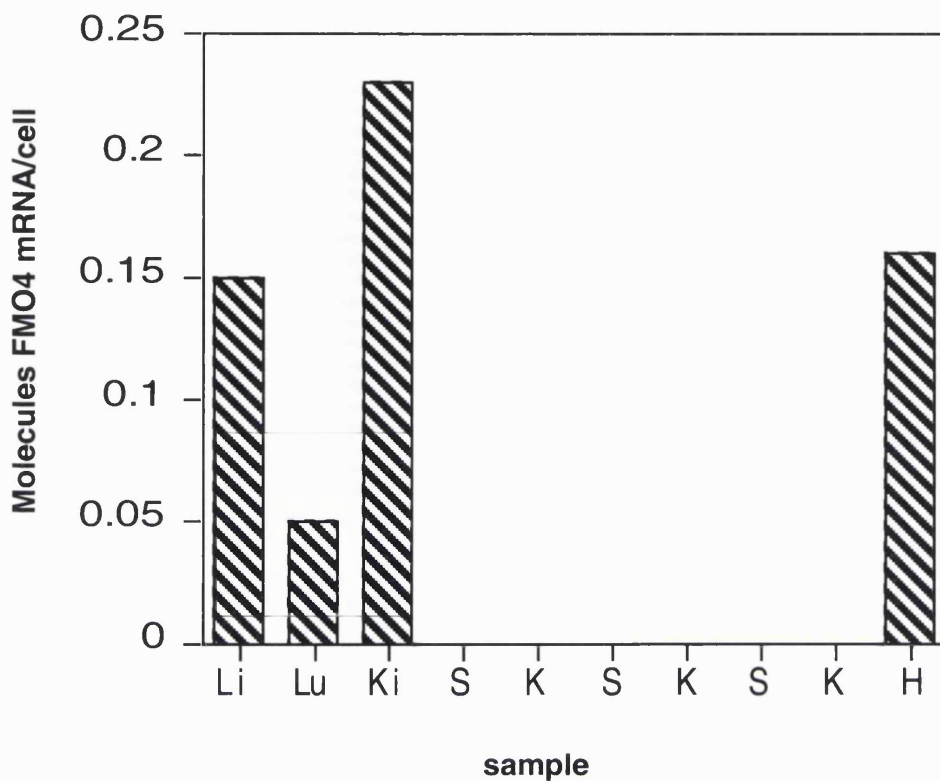


Fig 5.5.3 FMO4 mRNA concentrations in human liver (Li), human lung (Lu), human kidney (Ki), human skin (S), primary human epidermal keratinocytes (K) and HaCaT (H) cell samples. Samples were analysed as described in section 2.6. The FMO4 antisense transcript was hybridized to human liver, lung, kidney, primary cultures of human epidermal keratinocyte and HaCaT RNA and digested with a mixture of RNase A/T1. The digested RNA was electrophoresed and autoradiographed. The resulting signals were compared to a standard curve of undigested probe and the concentrations of the mRNA in the samples calculated as described in section 2.6.1.6.

having the highest (8×10^6 molecules FMO5/ μg total RNA or 26.92 molecules/cell) and the kidney the lowest (1.5×10^5 molecules FMO5/ μg total RNA or 1.02 molecules/cell). The amount of FMO5 mRNA in the lung was approximately 1.61 molecules/cell.

FMO5 mRNA was detected in five of the eight skin samples analysed. The amount varied considerably, from between 2×10^4 - 1×10^5 molecules FMO5/ μg total RNA or 0.1-0.48 molecules/cell (fig 5.6). FMO5 was not detected in any of the primary cultures derived from these samples. The HaCaT cells expressed relatively high amounts of FMO5 mRNA (5×10^4 molecules/ μg total RNA or 0.23 molecules/cell).

To date, no quantitative studies on the expression of *FMO5* in human tissues have been published and therefore no comparisons between the results obtained here and those obtained by others can be made.

5.6 Summary of results

No previous studies on the range of FMOs present in the human skin have been published. The studies above show both the spectrum of FMOs present and the amounts of each of the mRNAs in human skin. A summary of these results are shown in Table 5.1. Although studies on the presence of FMOs have been conducted on the skin, these have been primarily on mouse skin and restricted to the expression of *FMOs* at the protein level (Venkatesh *et al.*, 1992).

The extension of our studies to primary cultures of human keratinocytes derived from the whole skin samples analysed were carried out to investigate whether the same range of FMOs were present in the cultured cells as were in the whole tissues from which they were derived. Also analysed was an immortalised culture of human epidermal keratinocytes (HaCaT).

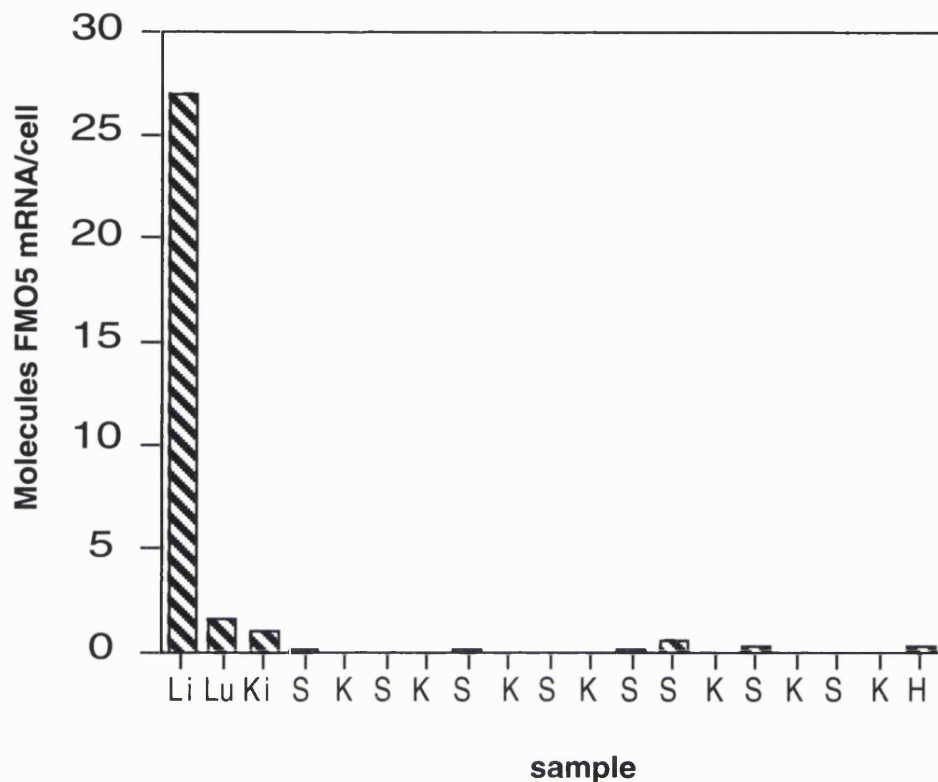


Fig 5.6 FMO5 mRNA concentrations in human liver (Li), human lung (Lu), human kidney (Ki), human skin (S), primary cultures of human epidermal keratinocytes (K) and HaCaT (H) cell samples. Samples were analysed as described in section 2.6. The FMO5 antisense transcript was hybridized to human liver, lung, kidney, primary cultures of human epidermal keratinocyte and HaCaT RNA and digested with a mixture of RNase A/T1. The digested RNA was electrophoresed and autoradiographed. The resulting signals were compared to a standard curve of undigested probe and the concentrations of the mRNA in the samples calculated as described in section 2.6.1.6.

The results show that *FMOs 1, 3 and 5* are expressed in different skin samples, although at varying levels. None of the whole skin samples analysed contained *FMO2* mRNA. *FMO1* mRNA is present in the greatest abundance in most of the skin samples analysed. *FMO3* and *5* mRNAs were present in similar amounts. The primary cultures of human epidermal keratinocytes expressed *FMOs 1, 2 and 3*, although at varying levels in different cultures. There was no correlation between the age status of the individuals from which these samples were derived and the presence of the *FMO* mRNAs.

The HaCaT cells express *FMOs 1, 4 and 5*. The relatively high expression of *FMO4* in these cells (0.16 molecules/cell) compared to the liver and lung (0.15 and 0.05 molecules/cell respectively) would make this system a useful tool in the further characterization of the factors that regulate the *FMO4* gene.

It is apparent from the above results that the human skin expresses a variety of *FMOs*, although the levels of their expression is low. However, the expression of these *FMOs* in locations where they would come in direct contact with their substrates would mean that they could play an important role in detoxification of foreign compounds in the skin.

In situ hybridization analysis on sections of whole skin was subsequently carried out to determine the cellular localisation of the *FMO* mRNAs (Chapter 8).

Samples	FMO1	FMO2	FMO3	FMO4	FMO5
Human liver	0	0	11	0.15	27
Human lung	0	11	0.41	0.05	1.6
Human kidney	5.8	ND	0.33	0.23	1.0
whole skin 46yrs	0.99	ND	ND	0.01	0
primary cells 46yrs	0	ND	ND	0	0
whole skin 28yrs	0.77	0	ND	0.01	0.26
primary cells 28yrs	0	0.68	0	0	0
whole skin 58yrs	0.67	ND	ND	0	0
primary cells 58yrs	0.69	0.56	0	0	0
whole skin 31yrs	1.2	0	0.45	ND	0.1
primary cells 31yrs	ND	ND	0.21	ND	0
whole skin 28yrs	0.85	ND	ND	ND	ND
primary cells 28yrs	0	0.51	ND	ND	ND
whole skin 24yrs	ND	ND	0.19	ND	0.12
primary cells 24yrs	ND	ND	0	ND	0
whole skin 502	ND	ND	0.2	ND	0
primary cells 502	ND	ND	0.14	ND	0
whole skin ?yrs	ND	ND	0.13	ND	0
primary cells ?yrs	ND	ND	0.17	ND	0
whole skin 24yrs	1.1	0	0.15	ND	0.1
primary cells 47yrs	0	0.23	ND	ND	ND
HaCaT cells	0.68	0	0	0.16	0.23

Table 5.1 Amounts of FMO1, 2, 3, 4 or 5 mRNAs expressed in molecules of FMO mRNA/cell. (ND= Not determined)

PROTEIN ANALYSES

6.1 Western blot analyses of cultured cells, microsomes and whole tissue proteins

Western blot analyses were carried out on proteins extracted from HaCaT cells, commercially available primary cultures of human epidermal keratinocytes, keratinocytes established from breast reduction full thickness skin, microsomes from whole skin and homogenates of various tissues.

Anti-baboon CYP2A, anti-rabbit CYP2B and anti-rabbit CYP3A were a kind gift from Dr. Patrick Maurel (INSERM, Montpellier, France). All the above CYP antibodies have been reported to cross-react with the human isoforms belonging to the same subfamily. Initial investigations on the FMOs were carried out using a general antibody raised to the pig hepatic FMO, i.e FMO1. This antibody was a gift from Dr. Daniel M. Ziegler (Clayton Foundation Biochemical Institute, University of Texas, USA). Subsequent western blot analyses were carried out using antibodies raised to specific FMOs. Antibodies to FMO1, 3 and 5 were raised in goat using the rabbit liver FMOs as antigens. Antibodies to FMO2 were raised in goat using rabbit lung FMO2 as the antigen. These FMO antibodies were a kind gift from Dr Richard M. Philpot (NIEHS, North Carolina, USA). The FMO3 antibody was reported to cross-react with all five FMO isoforms (Philpot, personal communication).

To ascertain whether we could use western blotting analyses to detect these proteins, initial experiments were carried out on HaCaT cells and primary cultures of human epidermal keratinocytes. The HaCaT cells were chosen due to their unlimited availability, as compared to primary cultures of keratinocytes. Also, these cells are derived from a single donor and therefore interindividual variation, as is seen in the expression of various *CYPs* could be eliminated.

A number of problems were encountered when the HaCaT cells and primary human epidermal keratinocytes were used to test protein extraction

and detection protocols. Table 6.1 summarises the problems encountered and the strategies employed in solving these problems.

6.1.1 Extraction of proteins

The use of the standard protein extraction procedures, employed in our laboratory to lyse cells from primary and immortalized cultures, namely glass-glass homogenisation of the cells, proved to be ineffective in lysing HaCaT cells. When the homogenised cells were stained with trypan blue, the nuclei of the cells were not stained and about 90% of the cells remained intact. To ensure a substantial yield of protein from cultures of the HaCaT cells, alternative procedures were used to lyse the cells. These were, the use of either, glass-beads or sonication of samples. Of these two methods, sonication proved to be the more successful for extracting protein. This was because when glass-beads were used to shear the cells, a large amount of the protein extracted was lost during the recovery and removal of the sample from the glass beads.

Similar problems were not encountered in lysing cells from primary cultures of human keratinocytes. However, to standardise extraction procedures, these cells were also sonicated to extract cellular protein.

6.1.2 Sample viscosity

The problem of sample viscosity has been encountered by others working with keratinocyte cultures or with cells having more than their normal complement of DNA. The latter is the case with the HaCaT cells, which are aneuploid and have 78-88 chromosomes, rather than the normal complement of 46 (Boukamp *et al.*, 1988).

Problem	Strategy	Result
Difficulty in extracting proteins	a)homogenization using glass-glass homogeniser b)extraction via sonication c)extraction with glass-beads	see section 6.1.1
Viscosity of sample	a)passing the protein sample through a 19 gauge syringe needle several times b)addition of protamine sulfate to extracted protein followed by centrifugation. c)Centrifugation, no addition of protamine sulfate.	see section 6.1.2
Antigen detection (lack of it)	a)Increasing the protein concentration loaded onto gel. b)Varying antibody (both primary and secondary) concentrations used in antigen detection. c)Incubating HaCaT cells with known inducers of CYPs, e.g Phenobarbital, Dexamethasone and Pyridine. All of which have been reported to increase CYP related enzyme activities in the skin. d)Increasing the sensitivity of detection by using chemiluminescent substrates.	see section 6.1.3
Cross-reactivity	a)optimization of antigen detection by using different blocking solutions. b)Determining the source of cross-reactivity. c) Using a monoclonal antibody (CYP2E1)	see section 6.1.4

Table 6.1 Summary of problems encountered during western blot hybridization analyses proteins derived from human skin and cultured cells

Viscosity problems only arose when SDS-PAGE loading buffer was added to an aliquot of cell homogenate. This was probably due to the SDS content of the loading buffer, which solubilized the nuclear membrane leading to the release of genomic DNA.

Several methods were employed in an attempt to reduce the viscosity of the samples. After addition of the SDS-PAGE loading buffer, the sample was repeatedly passed through a 19 gauge syringe needle to shear the DNA and thereby reduce viscosity. This method however, resulted in sample loss.

Clearing the homogenate of DNA using chloroform/methanol/water (section 2.8) has been used previously to eliminate DNA from HaCaT whole cell homogenates. However, the protein pellet obtained by this procedure was very difficult to solubilize. In cases where the protein appeared to become soluble, once frozen, it precipitated out of solution. This method was therefore abandoned.

Protamine sulphate is a polycationic macromolecule which binds with DNA precipitating it. Protamine sulphate (2.5%; w/v) was added to cell lysates after sonication and glass bead extraction in an attempt to precipitate any DNA liberated during cell lysis. When such samples were analysed by SDS-PAGE gel electrophoresis, it was apparent that a population of the proteins within the samples had been removed by the protamine sulphate. It has been shown that protamine sulfate adsorbs certain proteins in its precipitate and indeed protamine precipitate adsorption has been used as a step in enzyme purification (Welch and Scopes, 1981). In case the precipitated proteins were the ones of interest to us, the use of protamine sulfate to eliminate DNA from the samples was abandoned.

The method that proved to be the most effective in eliminating sample viscosity was simply to centrifuge the sonicated samples at 4°C. This step removed the nuclei and left only soluble proteins in the supernatant. This

procedure was therefore used in the extraction of proteins from all samples of cultured cells.

6.1.3 Antigen detection

Once the problems with the extraction of the proteins were solved, the samples were electrophoresed on SDS-PAGE gels and blotted onto supported nitrocellulose. The immobilised proteins were then analysed with the various antibodies mentioned in section 6.1.

Initial results showed no cross-reacting bands with the various antibodies, and therefore, the amount of protein loaded onto the gel for electrophoresis was increased from 20 μ g to 80 μ g. Increasing the total amount of protein loaded led to further problems. The probability during antigen detection of the antibodies (polyclonal) cross-reacting with non-specific proteins is much higher. As the total amount of protein electrophoresed was increased, a number of non-specific background bands appeared. These non-specific cross-reacting bands always electrophoresed either faster or slower than the positive control samples loaded in adjacent tracks. Varying the dilution of both secondary and primary antibodies used for detection, in an attempt to eliminate non-specific bands, was also tried. However, this resulted in either no bands being observed or only non-specific background bands.

There was a distinct possibility that the amounts of both CYPs and FMOs in the HaCaT cells are simply too low to detect. Therefore, two methods were used to try and improve the detection of low amounts of these proteins. The first was to treat the cells with compounds that have been previously shown, by others, to increase the enzyme activity of the particular CYPs in the skin. The second method was to use the more sensitive detection system of chemiluminescence. Previously, antigen detection was

accomplished using an alkaline phosphatase colour development procedure, which though more sensitive than a horseradish peroxidase colour development system, is not as sensitive as the alkaline phosphatase chemiluminescent system.

Induction of CYP proteins and related enzyme activity by phenobarbital (Pham *et al.*, 1989, Vizethum *et al.*, 1980, Pannatier *et al.*, 1982, Damen and Mier, 1982), pyridine (Agarwal *et al.*, 1994) and dexamethasone (Jugert *et al.*, 1994) has been reported to occur in rodent skin. HaCaT cells were incubated **separately with various doses of each of these compounds**. No induction of members of the CYP2A, CYP2B and CYP3A families was observed when either the colour or chemiluminescent development methods were employed. It was unfortunate that most of the non-specific bands detected using the chemiluminescence method tended to be of similar molecular weight as the proteins being investigated and therefore, even if we were detecting the CYPs or FMOs, these proteins would have been masked by cross-reacting bands. These non-specific bands were probably keratins which have an approximate molecular weight of between 40000 and 70000 depending on the electrophoretic technique being used (Baden, 1980, Steinert and Idler, 1975, Skerrow, 1974).

It proved impossible to extract microsomes from HaCaT cells even when large quantities of cells were used. The reason for this is unknown.

6.1.4 Cross reactivity of antibodies to HaCaT and keratinocyte proteins

A similar pattern of cross-reacting bands was seen with all antibodies used. Attempts were made to eliminate this cross-reactivity by optimising the blocking conditions. I-Block (Tropix Inc, USA) was substituted for gelatin. Although the I-Block proved to be a more efficient blocking solution than

gelatin in that it reduced the intensity of the cross-reacting bands, it did not eliminate them.

To try to pin-point the source of cross reactivity, blots with immobilised protein were incubated with either primary antibody only, or secondary antibody only or pre-immune serum only. Pre-immune serum recognised the same non-specific bands as the primary antibody used. The secondary antibody also cross-reacted with the same proteins.

During the course of this work, a report was published showing that polyclonal antibodies cross-react with keratins in skin and skin derived cells (Vecchini *et al.*, 1995). Monoclonal antibodies on the other hand do not. To test if this was indeed the case, western blots were incubated with a monoclonal antibody to rat CYP2E1. This was the only monoclonal antibody available to us at that time. The background banding pattern with this antibody was negligible and when HaCaT cells were treated with a high concentration (2mg/ml) of pyridine, a specific band corresponding exactly to that in the positive control of CYP2E1 was observed.

Due to the lack of success in detecting any significant amounts of either CYPs or FMOs in the HaCaT cells and primary keratinocyte cultures, using western blot analyses, this approach was abandoned.

6.2 Western blot analyses on skin microsomes

Microsomal membranes were prepared from human skin to eliminate the keratin population and enrich the total CYP and FMO content in the sample to be analysed. Western blot analyses on human skin microsomes were subsequently carried out. Because the yield of microsomes from whole skin is very low, analyses were only carried out using antibodies to the various FMO proteins.

Microsomes and cytosol prepared from human skin were electrophoresed and blotted onto nitrocellulose. Blots of these samples were incubated separately with anti-FMO1, 3 and 5. Samples of heterologously expressed FMOs were used as positive controls (fig 6.1). In both the microsomes and cytosol a band that electrophoresed faster than the positive control was observed. The identity of this band is unknown, but it is probably the same cross-reacting band detected in previous experiments with the HaCaT cells. On the same gel whole tissue homogenates of adult human liver and kidney were also loaded . This was carried out to establish that in whole tissues the bands observed were the same size as those expressed in insect cells.

When the blot was probed with an anti-FMO1 antibody (Fig 6.1, panel A), a faint band of the same molecular weight as the lower band observed, in both whole skin microsomes and cytosol, (lanes 1 and 2) was present in the kidney (lane 3). A higher molecular weight band that was the same size as that observed for heterologously expressed FMO1 (lane 4) was also observed in the human kidney sample.

The anti-FMO3 antibody gave similar results (fig 6.1, panel B), but in this instance the tissue that served as a positive control was human liver. A faint lower molecular weight band corresponding to that observed in the human skin microsomes and cytosol (lanes 1 and 2) was present in this sample (lane 3), together with another faint but higher molecular weight band that corresponded in size to the heterologously expressed human FMO3 (lane 4).

The anti-FMO5 antibody did not detect bands corresponding to the positive control in either the human liver or human kidney samples (fig 6.1, panel C, lanes 3 and 4). This antibody however cross-reacted strongly to a band in both the human skin microsomes and cytosol (lanes 1 and 2). This

band was the same molecular weight as that detected by the anti-FMO1 (panel A) and anti-FMO3 (panel B) antibodies.

Unfortunately, due to the unavailability of sufficient quantities of human tissues such as the liver and kidney, microsomes from these samples could not be prepared. As a result the bands observed, in the tissue homogenates, are faint and barely detectable (not clearly visible in fig 6.1).

The most likely explanation for the cross-reacting bands, in human skin microsomes and cytosol, is contamination by keratins. However, to determine if the lower molecular weight band detected by different antibodies was an FMO, an antibody reported to cross-react with all FMOs (anti-FMO3) was used to probe a western blot containing FMO1, 2, 3 and 5 expressed in *E. Coli* (provided as positive controls by Dr. R. Philpot) and various test samples. Only FMO5 and FMO3 were detected by this antibody. The specificity of the antibody for FMO5 was so low that the band (fig 6.2 lanes 7 and 8) is barely detectable. Neither FMO1 nor FMO2 were detected. This showed that the anti-FMO3 did not have the ability to detect FMOs 1 and 2. In a mixture of FMO3 and FMO5, the antibody has a higher specificity for FMO3 than it does for FMO5 (lane 9). Because FMO3 and FMO5 have different electrophoretic mobilities they can be differentiated on a western blot. However, the use of the FMO3 antibody to differentiate the two forms cannot be carried out, due to the high specificity for the antibody for FMO3 as compared to FMO5. As to whether the FMO3 antibody can detect FMO4, for which no antibody is yet available, is unknown.

It is possible that the reason no corresponding band is observed in human skin microsomes with any of the FMO antibodies is because the amount of this protein is too low to be detected or because the isoform present in the human skin could be FMO4. The expressed FMO4 protein was not available to us. This is because until recently FMO4 has not been expressed in a heterologous system. However with the recent expression of

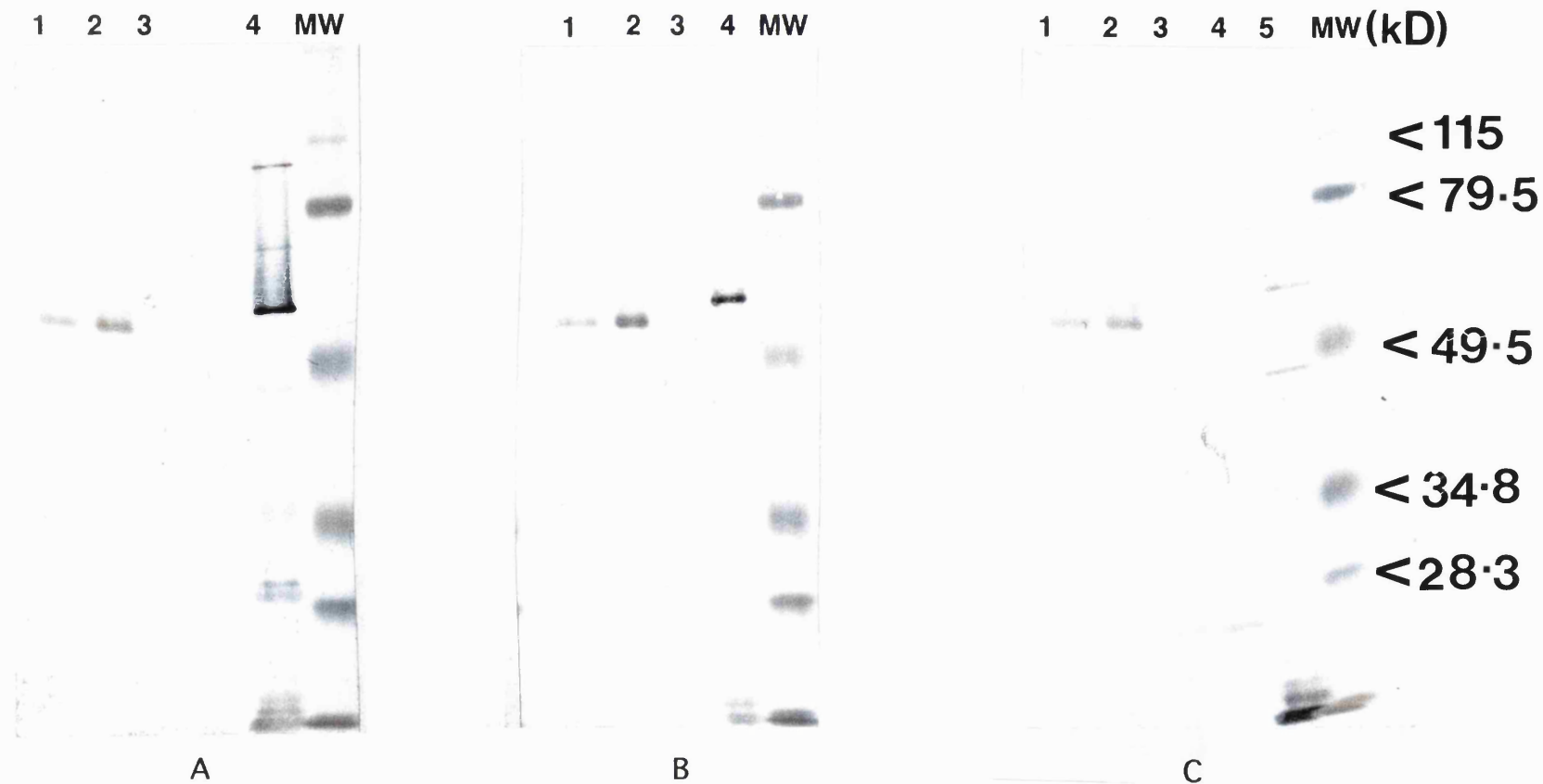


Fig 6.1. Western blot analyses with anti-FMO1 (panel A), anti-FMO3 (panel B) and anti-FMO5 (panel C). Whole skin microsomal membranes (40 μ g) (lane 1, panels A, B and C) and cytosol (40 μ g) (lane 2, panels A, B and C), liver homogenate (40 μ g) (lane 3, panels B and C) and human kidney homogenate (40 μ g) (lane 3, panel A and lane 4, panel C). 1 pmol of each heterologously expressed FMO1 (panel A, lane 4), FMO3 (panel B, lane 4) and FMO5 (panel C, lane 5) was electrophoresed concurrently to serve as positive controls. A prestained molecular weight marker (MW) from Bio-Rad, was also electrophoresed to estimate the relative sizes of the bands observed.



Fig 6.2 Western blot analysis of heterologously expressed FMOs1, 3 and 5 using an anti-FMO3 antibody reported to cross-react with all FMO isoforms. 1pmol and 2 pmol FMO1 (lanes 1 and 2 respectively), FMO2, 1pmol and 2 pmol (lanes 3 and 4 respectively), FMO3, 1pmol and 2 pmol (lanes 5 and 6 respectively), FMO5, 1pmol and 2pmol (lanes 7 and 8 respectively) and a mixture of FMO3 (1pmol) and FMO5 (2pmol), lane 9. Whole skin microsomes (40 μ g), lane 10 and skin cytosol (40 μ g), lane 11 were electrophoresed concurrently with 40 μ g each of human liver (lane 12), human lung (lane 13) and human kidney (lane 14) homogenates. Molecular weight standards (MW) from Bio-Rad were also electrophoresed for the subsequent estimation of the size of the band obtained.

Molecular weight standards are the same as indicated in fig 6.1.

a truncated form of this protein (Itagaki, 1996), an antibody to FMO4 should soon be available. With the availability of such an antibody, studies on the expression of FMO4 in the human skin and other human tissues will be possible.

Because of the problems encountered with the western blot analyses, two different strategies were employed to investigate if any FMOs were expressed at the protein level in human skin, enzyme activity assays (Chapter 7) and immunohistochemistry (Chapter 9).

7.1 Spectrophotometric assay of the Flavin containing monooxygenase

Enzyme activity studies on human skin microsomes, using methimazole (MI) as a substrate, were carried out because it was not possible to detect the FMOs using western blot analyses (chapter 6). The limited availability of primary cultures of human epidermal keratinocytes and the difficulty in extraction of protein and microsomes from the HaCaT cells, prohibited the same assays being carried out on these cultured cells.

MI (*N*-methyl-2-mercaptoimidazole) has been shown to be a highly specific substrate for the FMOs 1, 2, 3 and 4 (Ziegler, 1980, Poulsen *et al.*, 1974). FMOs catalyse the *S*-oxygenation of MI to the imidazole-sulphenic acid and glutathione (GSH) immediately reduces this intermediate, regenerating the parent substrate (fig 7.1). Only reaction 'a' in fig 7.1 is enzyme catalysed. At GSH concentrations above 1 mM the nonenzymatic reduction of the sulphenic acid (reactions 'b' and 'c') is much faster than the enzyme catalysed step, 'a'. Oxygen uptake in the presence of MI, NADPH and GSH was initially devised as an assay to measure the activity of FMO1 in whole homogenates and cell subfractions (Ziegler, 1980).

A more sensitive spectral assay to measure FMO activity is based on the conversion of nitro-5-thiobenzoate (TNB) to 5,5'-dithiobis(2-nitrobenzoate) (DTNB) (Dixit and Roche, 1984). The conjugate disulfide of MI can oxidise TNB to DTNB. TNB is yellow in colour but DTNB is colourless. The reaction is followed by measuring, at 412nm, the disappearance of the coloured product. The measured reaction results in the oxidation of two molecules of TNB per catalytic cycle. The oxidation of MI and subsequent reduction of TNB to DTNB is shown in fig 7.2.

This assay was used to measure FMO activity in human skin microsomes.

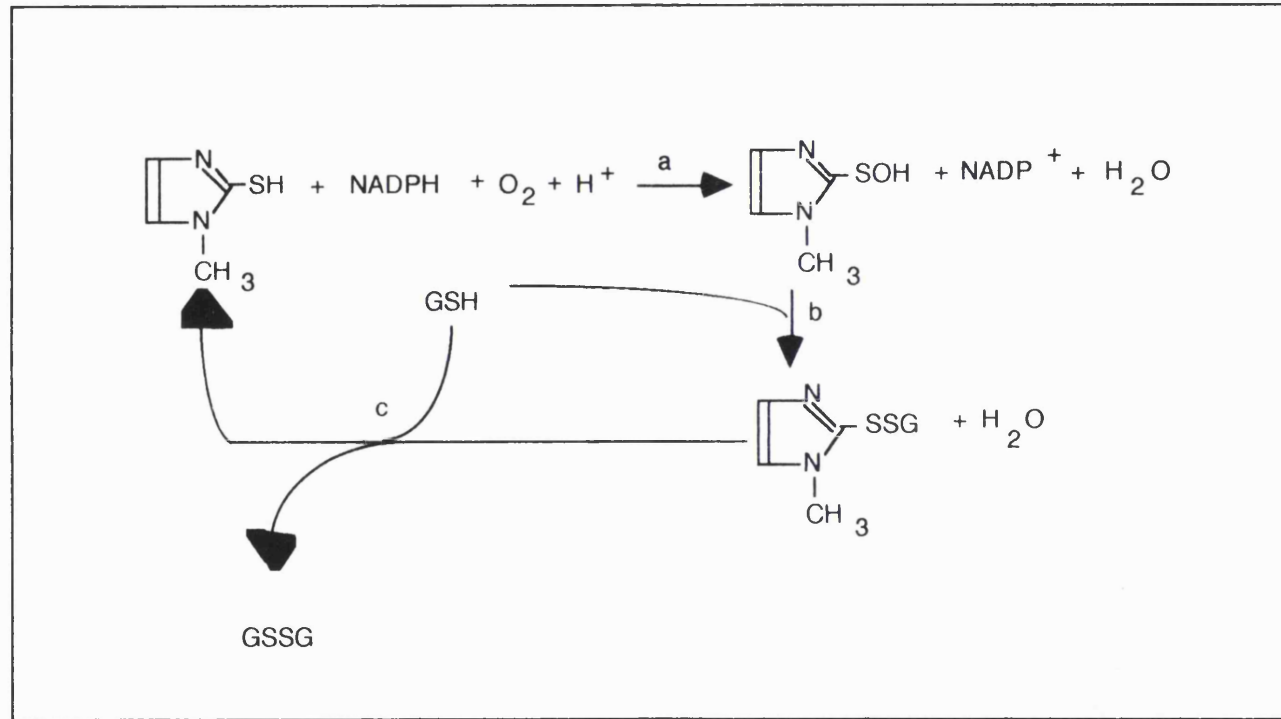


Fig 7.1 Oxygenation of methimazole by FMO and the reduction of the oxygenated product by glutathione (GSH) (reproduced from Ziegler, 1980).

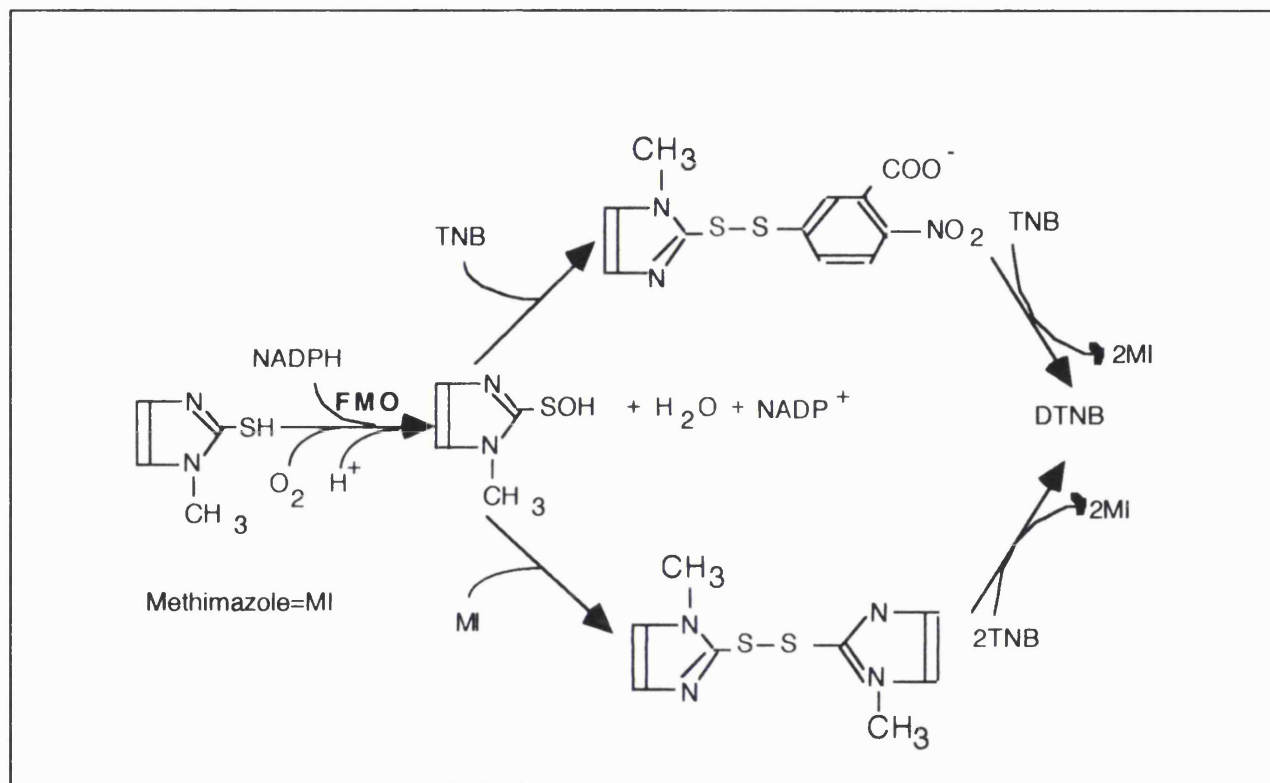


Fig 7.2 Oxidation of methimazole (MI) by the flavin containing monooxygenase, and reaction of the oxidised product with either MI or TNB to generate the conjugate disulphide of MI, which then reduces TNB to DTNB (reproduced from Dixit *et al*, 1984).

7.2 Results and discussion

Whole skin microsomal membranes were prepared as described in Section 2.8.1. It was necessary to pool the microsomal membranes from five different individuals to provide sufficient material for enzyme activity studies.

Control assays were performed using heterologously expressed FMO 1, 3 and 5 protein.

7.2.1 Activity of heterologously expressed FMOs 1, 3 and 5

To ensure that the assay was working, FMOs 1, 3 and 5 expressed in a baculovirus/insect cell system were used as controls. Insect cell microsomal membranes were prepared and provided by Dr. Colin Dolphin (Queen Mary and Westfield College, London). The amount of FMO per mg of microsomal protein in each of these control samples was determined by carrying out quantitative western blot analyses (described in section 2.10). Using known amounts of the respective FMOs, (provided by Dr. R. Philpott), standard curves were generated for each of the FMOs following densitometric analyses of the western blots. The amount of FMO in the insect microsomal membranes was approximately 0.055 pmol FMO/ μ g total protein for each FMO1, FMO3 and FMO5 samples. No FMO was detected in the microsomes from uninfected cells or insect cells infected with the wild type virus.

The microsomes from uninfected insect cells, and microsomes from insect cells infected with the wild type virus were used in the activity studies. Neither of these samples had activity towards MI. FMO1 has the highest activity towards MI (0.38nmoles MI min⁻¹pmol⁻¹), followed by FMO3 (0.04nmoles MI min⁻¹pmol⁻¹). FMO5 has no detectable activity towards MI. The activity of FMO5 towards methimazole is the same as that of the control

samples, *T.ni* cells and *T.ni* cells infected with wild type virus. These results are shown in Table 7.1 and fig 7.3.

Under conditions in which the substrate is in excess, the k_{cat} values for FMOs 1 and 3 can be calculated.

$$k_{cat} = \frac{V_{max}}{[E]_0}$$

where V_{max} is the limiting value of the rate of reaction under saturating substrate concentrations and $[E]_0$ is the concentration of the enzyme.

From the above equation, the k_{cat} for FMO1 would be 380 min^{-1} , while that for FMO3 would be 40 min^{-1} (Table 7.1 and fig 7.4). The k_{cat} for FMO5 could not be determined.

Overby *et al.*, (1997) found that human FMO3 and 5 expressed in *E. coli* have a K_m of 0.035 and 6 mM respectively. They concluded that FMO5 has a general lack of activity towards MI. Expressed FMO5 from guinea pig and rabbit also have little activity towards MI (Overby *et al.*, 1995), with an exceptionally high k_m for MI of 3 and 10 mM respectively.

The k_{cat} obtained for the heterologously expressed FMO3 (40 min^{-1}) is similar to that obtained by (Dolphin *et al.*, 1997) who found a k_{cat} of 36 min^{-1} in a separate batch of human FMO3, expressed in a baculovirus/insect cell system. Rabbit FMO3 expressed in *E.coli* has a k_m for MI of $\sim 30 \mu\text{M}$ (Burnett *et al.*, 1994). FMO1 expressed in COS-1 cells has a k_m of $2.8 \mu\text{M}$ towards MI (Lawton *et al.*, 1991). Although the heterologous expression systems were different in these two reports it shows that FMO1 has a higher affinity for methimazole than does FMO3. These results concur with those obtained above which show that MI is metabolized more efficiently by FMO1 than it is by FMO3. The k_{cat} for FMO1 being 380 min^{-1} , whereas that for FMO3 being 40 min^{-1} . To investigate the effect of Emulgen 911 and *n*-octylamine on FMO1, 0.2% (v/v) Emulgen 911 and 2.4mM *n*-octylamine was added to the assay

FMO form	$-\Delta \text{ Abs}$ 412nm/min	Specific activity (nmoles MI min ⁻¹ 1mg ⁻¹)	Specific activity (nmoles MI min ⁻¹ pmol ⁻¹)	$k_{\text{cat}} = \frac{V_{\text{max}}}{[E]_0}$ (min ⁻¹)
1	0.028	20.86	0.38	380
3	0.028	2.16	0.04	40
5	0	0	0	ND

Table 7.1 Specific activities of FMO1, 3 or 5 expressed in insect cells with 2mM MI as substrate. The amount of FMO in each of the expressed FMO1, FMO3 and FMO5 samples was 0.055pmol FMO/ μg total microsomal protein. The FMO catalysed oxidation of methimazole leads to 2 molecules of TNB being oxidized per catalytic turnover, giving a molar absorbance coefficient at pH 8.4 of 14,100 M⁻¹cm⁻¹. (ND= Not determined).

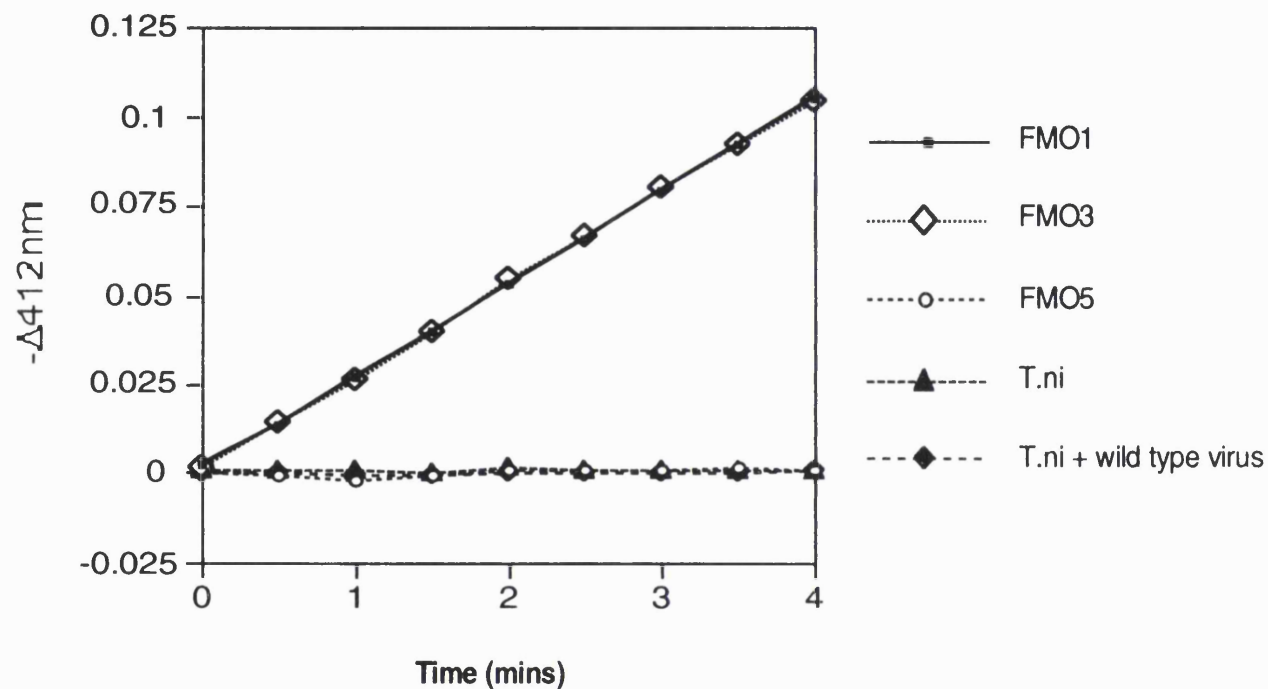


Fig 7.3 Activity of heterologously expressed FMO1, FMO3 and FMO5 towards methimazole. The concentrations of the microsomal membrane samples were as follows, *T.ni* (6.3mg/ml), *T.ni* + wild type virus (5.6mg/ml), FMO1 (9.52mg/ml), FMO3 (9.2mg/ml) and FMO5 (5mg/ml). The concentration of FMO in each of the expressed samples was 0.055 $\mu\text{mol}/\mu\text{g}$ of total microsomal protein. Microsomes from uninfected insect cells and from insect cells infected with the wild type virus were used as negative controls. The rate of disappearance of the coloured product (DTNB) was measured at 412nm. Note: The amount of FMO1 used for the assay was 1/10 of the amount of FMO3 or FMO5.

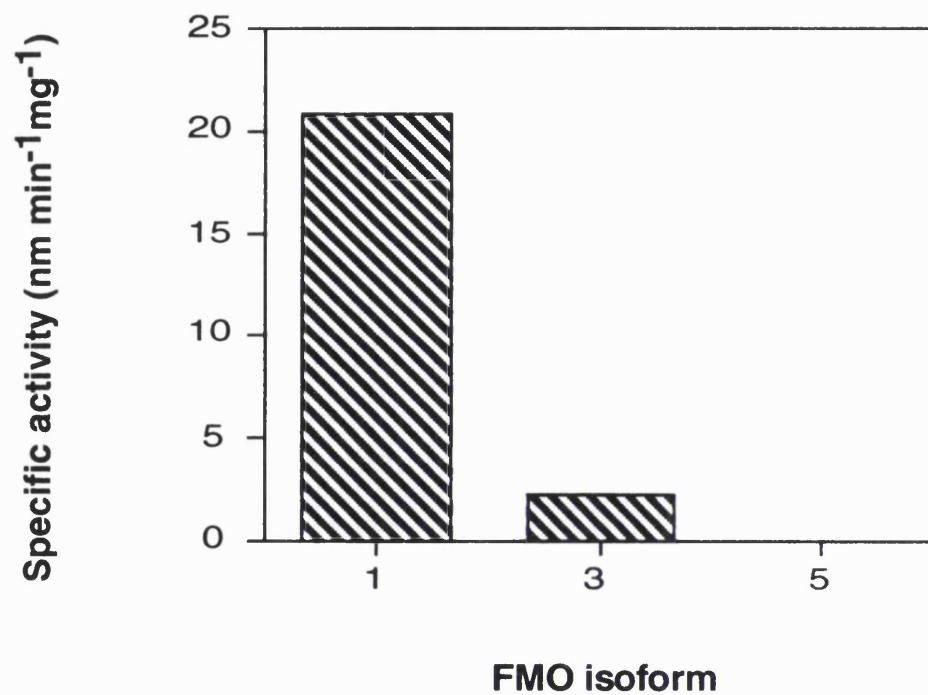


Fig 7.4 Summary of the activity of FMOs 1, 3 and 5 with methimazole as substrate. Activities are calculated as nmol min⁻¹mg⁻¹ using the total microsomal protein concentration.

mixture, both separately and together, and the rate of TNB oxidation measured. Negative controls comprising all the assay constituents without microsomes were also carried out to determine if any enzyme independent oxidation of TNB occurred in the presence of detergent, *n*-octylamine or both. The results obtained are shown in Table 7.2 and figs 7.5 and 7.6 .

Both *n*-octylamine and Emulgen 911 enhanced FMO activity towards MI. The highest activity (25.72 nmoles MI mg⁻¹min⁻¹) was obtained in the presence of 2.4mM *n*-octylamine, followed by that in the presence of both Emulgen 911 and *n*-octylamine (24.21nmoles MI mg⁻¹min⁻¹). The latter value does not differ from that in the presence of only *n*-octylamine. Therefore the addition of Emulgen 911 by itself has an enhancing effect on FMO1 activity, but Emulgen 911 in the presence of *n*-octylamine provides no additional enhancement of activity (fig 7.6)

The data obtained shows that a small amount of enzyme independent oxidation of TNB occurs in the presence of Emulgen 911 and absence of FMO1. Venkatesh *et al.*, (1992) have reported that Emulgen 911 could not be used with the methimazole/DTNB assay as it was found to interfere with the assay. The reasons for this interference was not given. *n*-octylamine by itself does not cause any such oxidation. The above results show that both Emulgen 911 and *n*-octylamine have the ability to increase the activity of FMO1. It was expected that activity in the skin microsomes would be low and for any activity to be observed, it might be necessary to add the above compounds to the assay mixture.

The solubilisation of mouse and rabbit microsomes with 1% (v/v) Emulgen 911, apparently increases FMO activity (Tynes and Hodgson, 1985). This is thought to be due to increased cofactor or substrate accessibility to the enzyme. However, Emulgen 911 also appears to decrease the effective active site concentrations of lipophilic substrates, presumably due to ligand partitioning into detergent micelles, resulting in a lower concentration of free

Assay	Specific activity (nmole min⁻¹mg⁻¹)
FMO1	19.67
FMO1 + emulgen	23.46
FMO1 + N-octylamine	25.72
FMO1 + emulgen + N-octylamine	24.21

Table 7.2 Specific activity in nmole min⁻¹mg⁻¹ of FMO1 in the presence of 0.2% (v/v) Emulgen 911 and *n*-octylamine. These were added separately or together to ascertain their effects on the activity of FMO1 towards methimazole.

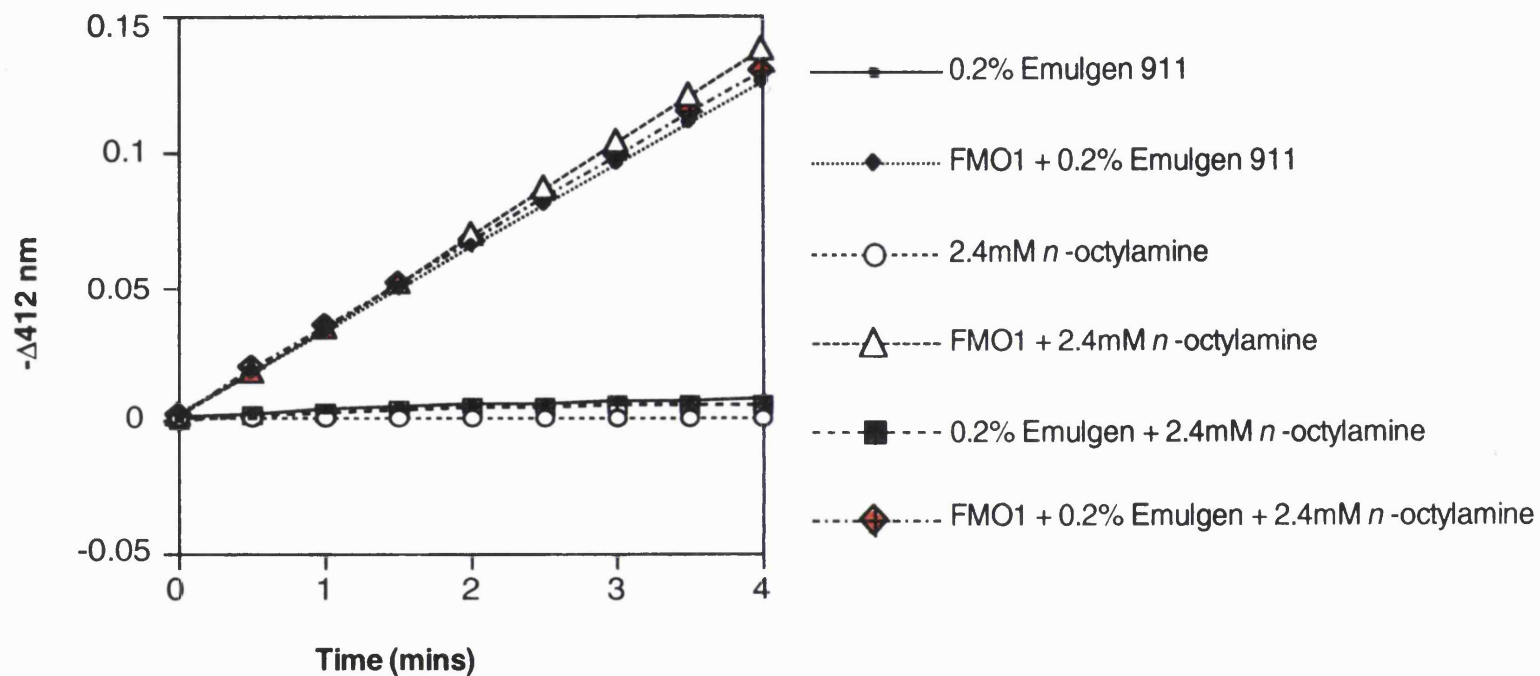


Fig 7.5 Activity of FMO1 in the presence of *n*-octylamine and/or Emulgen 911. The activity of FMO1 with enhancers such as *n*-octylamine (2.4mM) or Emulgen 911 (0.2% v/v) or both were followed over a time course of 4 mins. Controls for each reaction contained the appropriate components but no microsomes. The rate of disappearance of the coloured product (DTNB) was measured at 412nm.

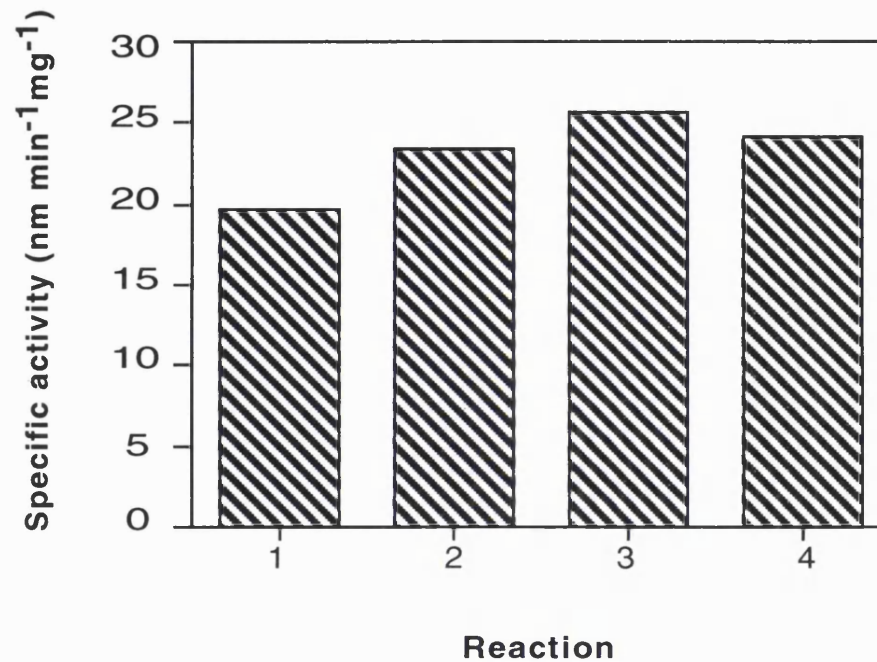


Fig 7.6 Summary of the effects of *n*-octylamine and Emulgen 911 on the activity of FMO1. Reaction 1 (FMO1), reaction 2 (FMO1 + 0.2% (v/v) Emulgen 911), reaction 3 (FMO1 + 2.4 mM *n*-octylamine) and reaction 4 (FMO1 + 0.2% (v/v) Emulgen 911 + 2.4 mM *n*-octylamine). Activities are calculated as nmol min⁻¹ mg⁻¹ using the total microsomal protein concentration of FMO1 (9.53mg/ml).

substrate. A number of substrates therefore tend to be metabolised poorly by microsomes solubilised with Emulgen 911, e.g *N, N*-dimethylaniline.

Primary amines e.g *n*-octylamine activate pig liver FMO to produce 1.5-2.5 fold increases in V_{max} by binding at an effector site(s) distinct from the catalytic site (Ziegler and Mitchell, 1972, Ziegler *et al.*, 1973). In addition *n*-octylamine has been shown to cause about a 2 - fold increase in the activity of FMO1 expressed in *E. coli* (Burnett *et al.*, 1994). Dixit *et al.*, (1984) have shown that concentrations of 2.4mM *n*-octylamine causes an activation of FMO activity in rat liver microsomes.

Emulgen 911 and *n*-octylamine are also inhibitors of CYPs and in tissue microsomes, there is the possibility of oxidation occurring due to the presence of these enzymes, these compounds would therefore negate any effects of P450 dependent oxidation of TNB.

7.3 Measurement of FMO activity in whole skin microsomes

Human skin microsomal membranes from five different individuals were pooled in order to obtain enough sample to carry out the assay. Quantification of the amount of FMO in the skin microsomal samples was not possible because of the problems described in section 6.1. Unfortunately, due to the unavailability of human skin microsomes, detailed kinetic analyses on FMO activity could not be carried out.

Activity measurements on skin microsomes in the absence of detergent and enhancers, in the presence of detergent and in the presence of both detergent and enhancers were carried out in order to maximise any FMO activity that might be present. The results obtained are shown in Fig 7.7.

The graphs show the non linearity of the reaction associated with these microsomes. The addition of detergent to the assay mixture led to an increase in the rate of oxidation of TNB in the sample containing skin

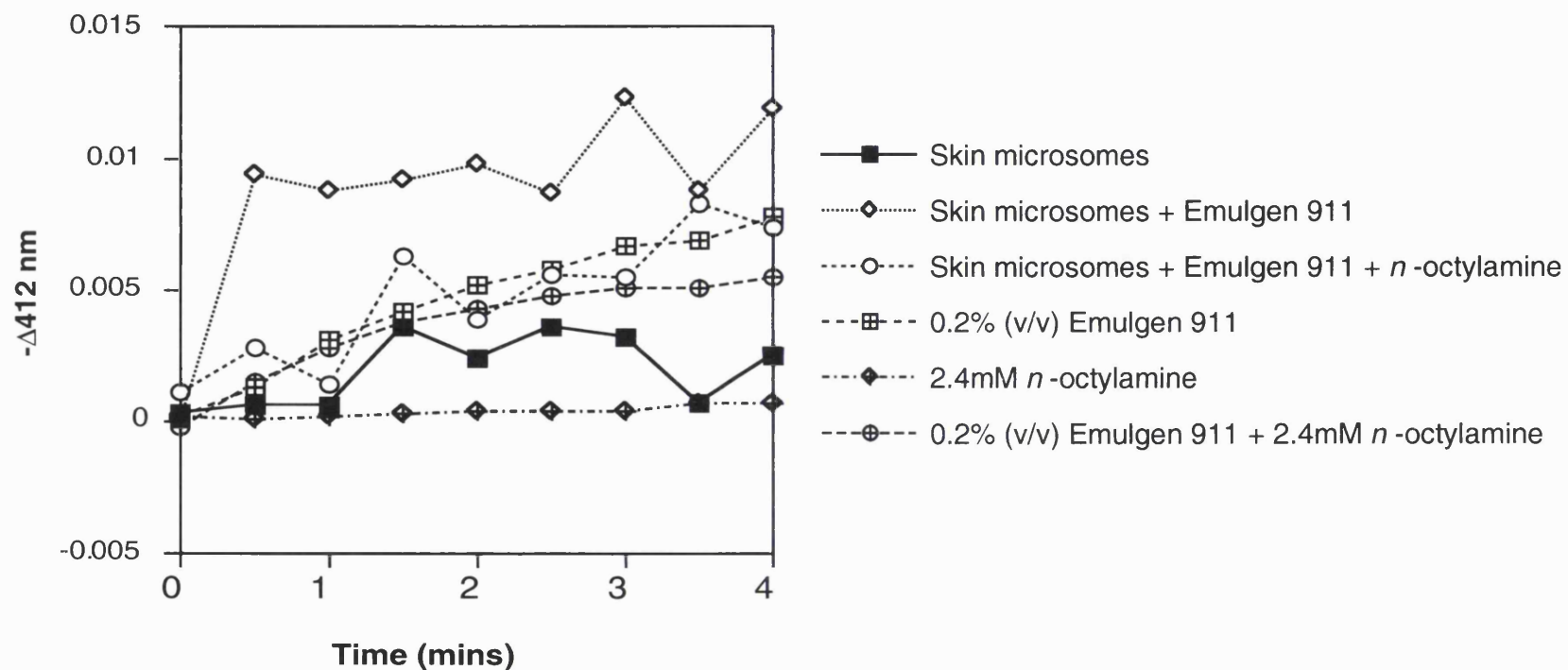


Fig 7.7 Activity of human skin microsomal membranes, in the presence and absence of enhancers, with methimazole as a substrate. Human skin microsomes were prepared as described in section 2.8.1. 600 μg of microsomes were used for each assay and the rate of reaction measured at 412nm. The effects of enhancers such as Emulgen 911 (0.2% v/v) and *n*-octylamine (2.4mM) was also assessed. Negative controls for the reaction included reaction mixtures made up of all the constituents except for microsomes. Note expanded scale as compared to figs 7.3 and 7.5.

microsomes. A comparison of this with a control containing Emulgen 911 (and no microsomes) shows that the increase in activity is not sufficient to confirm the presence of FMO activity in these microsomes. The presence of both *n*-octylamine and Emulgen 911 in the reaction mixtures had little or no effect on the activity as compared to that observed with skin microsomes in the absence of both these substances. The activity was no different to the basal activities observed with 0.2% Emulgen 911 alone, or with 0.2% Emulgen 911 and 2.4mM *n*-octylamine. The presence of Emulgen 911 in the assay mixture seems to lead to the increase in the oxidation of TNB irrespective of the presence or absence of microsomes, i.e enzyme independent TNB oxidation.

There could be several reasons for the non-linearity observed, including the presence of contaminating proteins present in the skin microsomes. When the methimazole assay has been used on rat liver homogenate, the plot of total FMO activity was found to be non-linear and could not be reproduced (Coecke *et al.*, 1992) . It was concluded that this was because of interference due to the formation of precipitates after the addition of DTNB. Coecke *et al.*, attributed this to contaminating proteins which are either soluble or loosely bound to the membrane. Contaminating cytosolic proteins were present in the skin microsomal fractions as was observed during western blot analysis (section 6.1). This suggests that these contaminants could be a factor in the non-linearity observed when MI activity in the skin microsomes was assayed. Non-linear kinetics have also been observed for oxidations catalysed by mouse (Tynes and Hodgson, 1985) and rat (Cashman and Hanzlik, 1981) hepatic microsomal FMOs. It has been suggested that this may be due to the presence of two or more FMO enzymes in the preparations examined.

Another factor that could have led to the inconclusive results obtained with the skin microsomes is the loss of FMO activity during preparation of

microsomes. Ziegler, (1980) reports that in studies on pig liver FMO (FMO1), in the absence of NADPH, the activity of the FMO is sensitive to thermal inactivation at temperatures above 30°C and that half of the activity is destroyed by thermal equilibration at 37°C for as little as 6 mins. Thermal instability is a characteristic of the microsomal FMOs in all tissues and seems to be an intrinsic property of the enzyme. It is possible that the reason for the lack of detection of this enzyme in the skin microsomes could be either total lack of activity in the microsomes or the extreme thermal lability of the enzyme.

To determine the integrity of the skin microsomes, an additional assay determining P450-reductase activity was also carried out. This assay is based on the spectral measurement of the rate of reduction of cytochrome c in the presence of NADPH and cytochrome P450-reductase which is known to be present in all microsomes (section 2.13).

Hepatic microsomes from phenobarbital treated rats were used as a positive control for this assay. These microsomes have been shown previously to contain P450 reductase activity. The results obtained with rat liver microsomes is shown in fig 7.8, and that with the skin microsomes is shown in fig 7.9.

Unfortunately due to the scarcity of sample, neither the substrate concentrations nor the protein (enzyme concentrations) could be varied and thus kinetic studies were not possible. However, from the limited results obtained, the specific activity could be calculated per milligram of microsomal protein. These results are summarized in Table 7.3

The results in Table 7.3 show that the skin has P450 reductase activity albeit in much lower amounts than rat liver microsomes. However, considering that western blot analyses showed that there was contamination of the microsomes with cytosolic proteins, this is not the true value of activity per milligram microsomal protein for the skin microsomes. It serves the

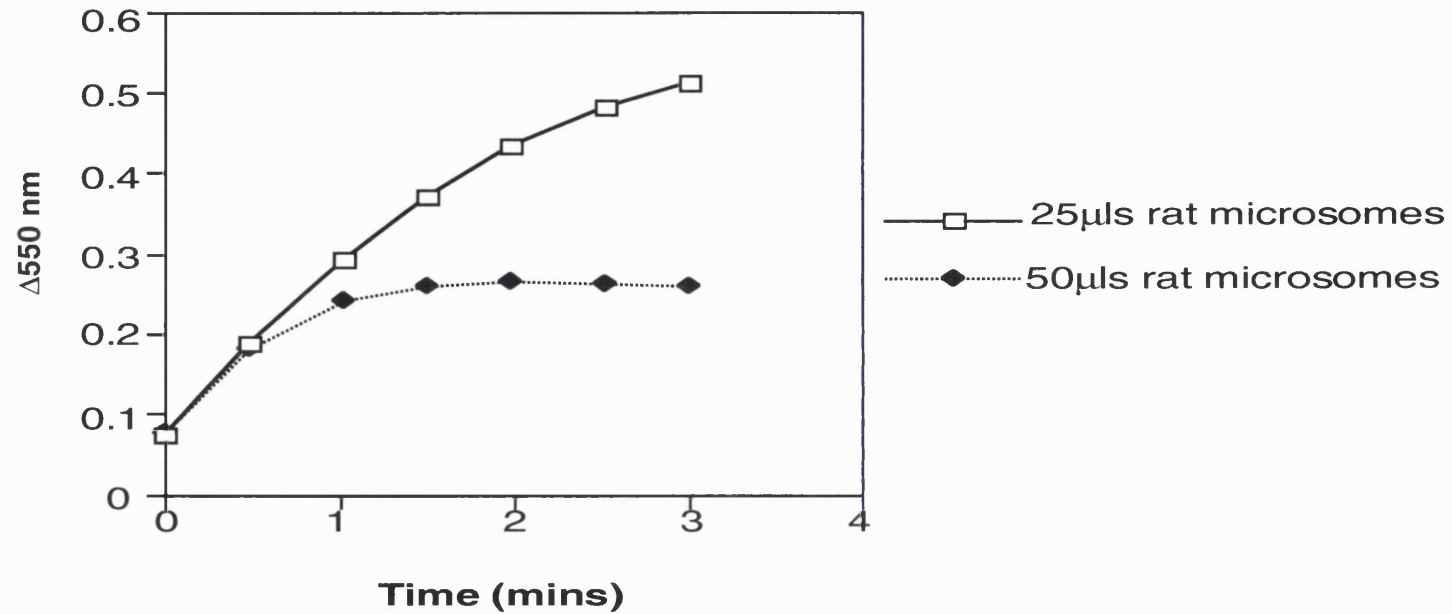


Fig 7.8 Activity of P450-reductase in rat liver microsomes. Two different amounts of rat liver microsomes were used for the assay. The concentration of the rat microsomes was $16.34 \mu\text{g}/\mu\text{l}$. 50 μls showed saturation after less than 1 min. The rate of the reaction was measured at 550 nm using 25 μls of microsomes.

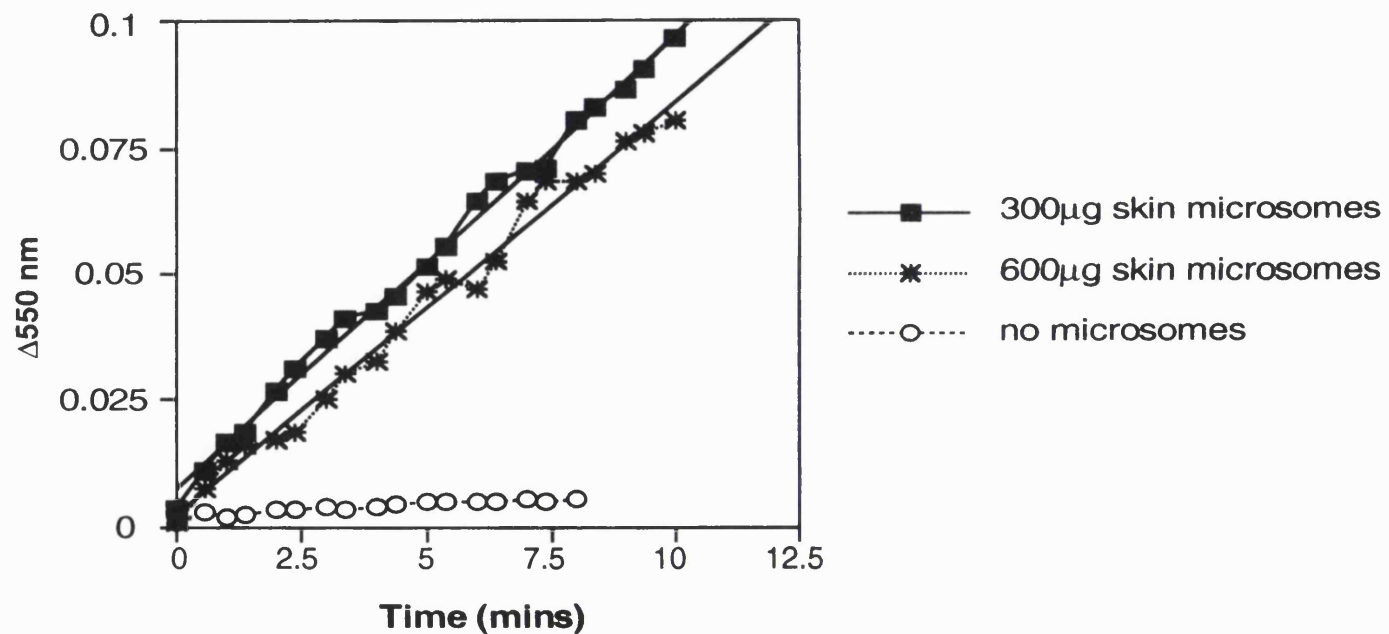


Fig 7.9 P450-reductase activity in human skin microsomes. 300 μg and 600 μg per reaction mixture of skin microsomes were used to assay the activity of P450-reductase. A reaction excluding microsomes was used as the negative control. The change in absorbance was measured at 550nm.

Sample	Specific activity (nmole min ⁻¹ mg ⁻¹)
Whole skin microsomes	1.11
Rat liver microsomes	362.4

The extinction coefficient for reduced cytochrome c is 21mM⁻¹cm⁻¹ (Williams and Kamin, 1964).

Table 7.3 Summary of the specific activity of P450-reductase (in nmole min⁻¹mg⁻¹) in whole skin microsomes and rat liver microsomes.

purpose however, of confirming that the microsomes had retained some enzyme activity through the extraction process. This result varies considerably from that obtained by Pohl *et al.*, (1983), who found an activity of 8 nmoles product $\text{min}^{-1}\text{mg}^{-1}$ when mouse skin microsomes were assayed for P450 reductase. This value could be higher than that obtained by us for a number of reasons, including the fact that species differences in the expression of P450 reductase exist. It is possible however that some activity may have been lost during the extraction procedure and hence the low activity observed.

CELLULAR LOCALISATION

8.1 Cell-type specific expression of FMOs in the human skin

Two different methods were used to investigate the cell-type specific expression of *FMOs* in human skin, namely immunohistochemistry (IHC) and *in situ* hybridization analyses. Both these studies were carried out on paraformaldehyde fixed sections of whole human skin. The sections used for these studies were obtained from a single individual.

8.2 Immunohistochemical localisation of FMOs in human skin

As described in Chapter 7, western blot analyses of whole skin microsomes and cytosol showed non-specific cross-reacting bands with all the FMO antibodies available to us (anti-FMO1, FMO3 and FMO5). The goal of all immunohistochemical procedures is the identification of specific antigens *in situ* by antibodies that are visualised via the use of reporter molecules such as enzymes or fluorochromes. IHC enables the localisation of proteins within a tissue. Proteins not present in large quantities in tissues, but localised to particular areas or cells of the tissues can be observed. Cells containing the protein being investigated are stained more intensely than are the controls. Successful IHC requires that the antigenic epitope recognised by the primary antibody is preserved through tissue fixation, embedding, sectioning, and staining procedures.

The procedure described in section 2.11.3, was used on paraformaldehyde fixed sections embedded in wax. Anti-FMO1, FMO3 and FMO5 antibodies were used separately to detect their respective antigens in this tissue. Paraformaldehyde fixation is known to dramatically reduce the antigenicity of tissue either as a result of epitope masking (cross-linking) or the destruction of protein conformation (denaturation). Techniques such as proteolytic digestion (described in section 2.11.3.1) can be used to unmask

the epitopes blocked by chemical cross-linking, however, they do not restore antigenicity lost by denaturation. Two methods were used to unmask antigens. Proteolytic digestion with trypsin was carried out as described in section 2.11.3.1. No difference was observed between tissue sections on which this procedure was carried out and those tissue sections which had not been treated.

A second method of unmasking the cross-linked antigens involved the use of high temperatures, as described in section 2.11.3.1. The latter method showed clear and localised staining in some of the tissues known to express the proteins being investigated e.g. human kidney. We decided to use high temperature antigen unmasking for all further IHC experiments.

IHC was carried out using antibodies to FMO1, 3 and 5. Tissues known to express these proteins in relatively high quantities were used as positive controls. These were sections of the human kidney for FMO1 and human liver for both FMO3 and FMO5. Unfortunately, sections of human liver did not give any reactivity with any of the FMO antibodies used. The probable reason for this is the fact that the human liver sections obtained by us were from postmortems. The time between the excision of the samples and fixation was not known. A further problem with the liver sections is that none of the sections were from normal, control livers. In most of the sections, the tissues were necrotic and liver structure could not be discerned.

Only the skin and kidney were known to have been flash frozen as soon as they were obtained and thereafter fixed in paraformaldehyde. All the skin samples and the kidney sample were from normal individuals.

8.2.1 FMO1 localisation

Anti-rabbit FMO1 was used for IHC studies on sections of the human skin and kidney. This is the only antibody for which a 'positive' control was

available. The negative control was carried out by incubating the section with non-immune goat serum, all the other incubations were the same as for the samples being tested.

Fig 8.1 shows the results obtained on a sample of human kidney. The proximal and distal tubules in the cortex of the kidney show distinct staining, but the staining is greater in the proximal tubules than it is in the distal tubules, indicating the presence of higher amounts of the FMO1 protein (fig 8.1B). Higher magnification of the proximal tubule (fig 8.1C), shows that FMO1 protein is located primarily towards the luminal side of the cells. No staining was observed in the glomerulus. The negative control, fig 8.1A, shows only faint background staining.

Sections of the human skin showed only background staining and no localisation of the protein with the anti-FMO1 antibody. No observable differences between the negative control and sections being tested were seen. One of the reasons for this could be that the amount of FMO1 expressed in the skin may be very low, such that the antibody that was being used could not detect this low amount.

The antibody could detect the FMO1 in the kidney because the amounts of the protein in this tissue are relatively high and could also be observed in the western blot analyses (fig 6.1, panel A). Western blot analyses did not detect the presence of FMO1 in the skin microsomes. Thus, it would seem that an antibody with a higher titre will be required to detect the low amounts of this protein in the human skin if it is present.

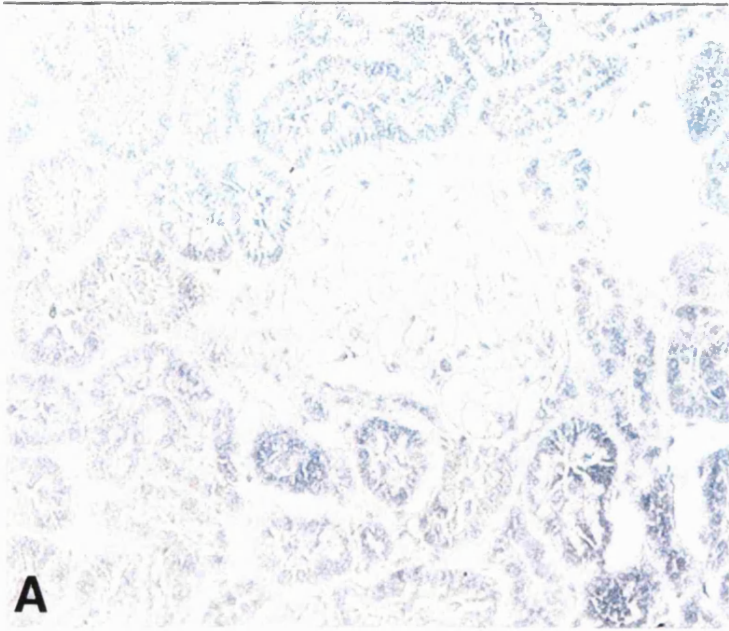
8.2.2 FMO3 and 5 localisation

No positive controls were available for the detection of these proteins. When sections of human skin were incubated with either the anti-rabbit FMO3 or the anti-human FMO5 antibodies, background staining was observed with

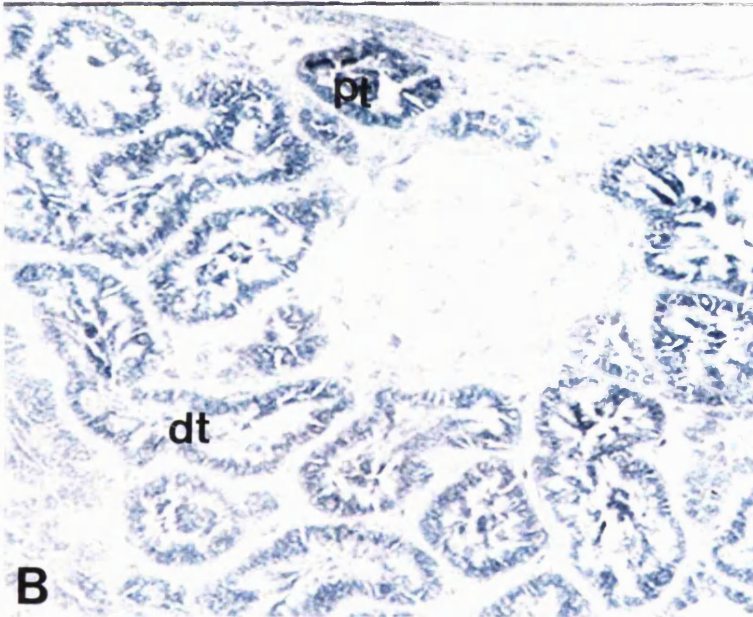
Fig 8.1 Localisation of FMO1 to the proximal and distal tubules in the human kidney cortex.

Sections of human kidney were incubated with an anti-rabbit FMO1 antibody, raised in goat (B and C) or with goat pre-immune serum (A). FMO1 was detected in the proximal (pt) and distal tubules (dt), with the proximal tubules staining more intensely. Higher magnification (C) shows more intense staining towards the luminal side of the cells lining the proximal tubules.

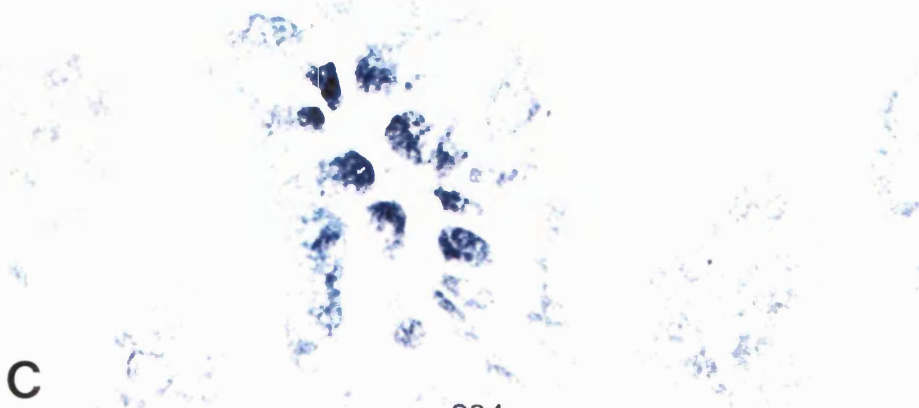
Magnification X110



A



B



C

no areas of localised staining. There was no difference in staining between the negative controls and samples being tested.

Once again, the probable reason for this is the low antibody titres of the particular antibodies that we were using. The same antibodies did not detect FMO3 or FMO5 when western blot analyses were carried out on whole skin microsomes (fig 6.1, panel B and C).

8.3 *In situ* hybridization analyses

In situ hybridization analyses were carried out on fixed sections of human skin. The RNase protection assays using whole skin RNA showed the presence of a variety of FMOs in whole human skin. Depending on the individuals from whom the skin was obtained, FMOs 1, 3 and 5 were expressed, albeit at low concentrations (<1 molecule/cell). RNA from the skin of the individual used for *in situ* hybridization analyses, had been previously extracted and RNase protection assay analyses for the presence of the various FMO mRNAs had confirmed the expression of FMO1, 3 and 5 mRNAs (chapter 4). Because of the absence of expression of FMO2 mRNA in this sample of skin and also of the other skin samples previously analysed, no *in situ* hybridization analyses using the FMO2 antisense or sense RNA probes were carried out.

In situ hybridization analyses with radiolabelled antisense probes encoding FMOs 1, 3, 4 or 5 were carried out separately. FMO4 mRNA expression was investigated, despite not being detected using RPAs, because this FMO has been reported to be constitutively expressed in virtually all human tissues (Dolphin *et al.*, 1996). As negative controls, the corresponding sense probes were hybridized to separate skin sections. The constructs used for these analyses were the same as those for the RNase

protection assay (chapter 4). The only difference being the type of radioactivity (^{35}S -UTP) used to synthesise the sense and antisense probes.

Many different protocols have been developed for the detection of mRNA by *in situ* hybridization. The method used by us is a modification of that developed by Angerer *et al.*, (1987). With paraformaldehyde fixed sections, it is important to enable the probe to penetrate the tissue. To do this, various concentrations of proteinase K have to be used to determine the best conditions. Of the two different concentrations used, $50\mu\text{g/ml}$ and $200\mu\text{g/ml}$, the latter proved the most effective in enabling probe penetration.

8.3.1 Localisation of FMO mRNAs in human skin

The expression of FMO1, 3, 4 and 5 mRNAs was investigated in sections of the same human skin. These were all analysed as described in section 2.7. FMO1 (fig 8.2 and 8.3), FMO3 (fig 8.4 and 8.5), FMO4 (fig 8.6 and 8.7) and FMO5 (fig 8.8, 8.9 and 8.10) mRNAs were detected in the skin samples analysed.

The resulting microautoradiograms demonstrated a strong and specific hybridization of the FMO1 and 5 antisense probe to the epidermis and sebaceous glands of the skin. The amount of FMOs 3 and 4 in the skin sample analysed were much lower, however, the riboprobes hybridized to the same regions as the other FMOs. Other regions within the section such as the Meissner's corpuscle were negative, indicating that the signal was specific to the above regions of the skin. The signals were significantly above those obtained with the sense probe.

Of the four FMOs tested, FMO5 was the most highly expressed in both the epidermis and the sebaceous glands. The next highly expressed FMO was FMO1, followed by FMO3 and finally FMO4. These results are different to those obtained with the RNase protection assays. The RNase protection

analyses showed the presence in this particular sample of approximately 1.1 molecules/cell of FMO1, 0.15 molecules/cell of FMO3 and 0.1 molecules/cell of FMO5. The reason for this discrepancy is probably due to the assumption of an average value which takes into account all the cells from which the RNA has been extracted. *In situ* hybridization analyses takes into account the localisation of the RNA within particular cells.

The localisation of the FMOs in the epidermis is uniform and not restricted to particular areas of the epidermis i.e the stratum spinosum, the stratum granulosum or the stratum germinativum. In the sebaceous glands all the FMOs are expressed in the sweat producing cells of the sebaceous glands.

A structure which is possibly a hair follicle was present in some of the sections analysed. FMOs 1, 3 and 5 were highly expressed in sections where this structure was found. It is possible that upon an even longer exposure of the sections probed with the FMO4 riboprobe the same strong signal would also be observed.

8.4 Discussion

In the IHC procedures carried out, polyclonal antibodies to the various FMOs were used. Monoclonal antibodies are preferable to polyclonal antibodies in this procedure because they have a high affinity and are specific. But, the use of a monoclonal antibody in tissues that have been chemically fixed, i.e with paraformaldehyde, has a disadvantage in that if the single epitope recognised by the antibody is irretrievably lost, a false-negative result will be obtained.

The use of polyclonal antibodies in the experiments performed had a major drawback. When the various tissue samples, especially sections of whole skin were probed with these antibodies, a high degree of background

Fig 8.2 Localisation of FMO1 mRNA to the epidermis of human skin.

Sections of human skin were incubated with ³⁵S-labelled antisense FMO1 RNA (A) or ³⁵S-labelled sense FMO1 RNA (B). The antisense probe hybridized to cells within the epidermis. Autoradiography was for 4 weeks. Magnification = X 110

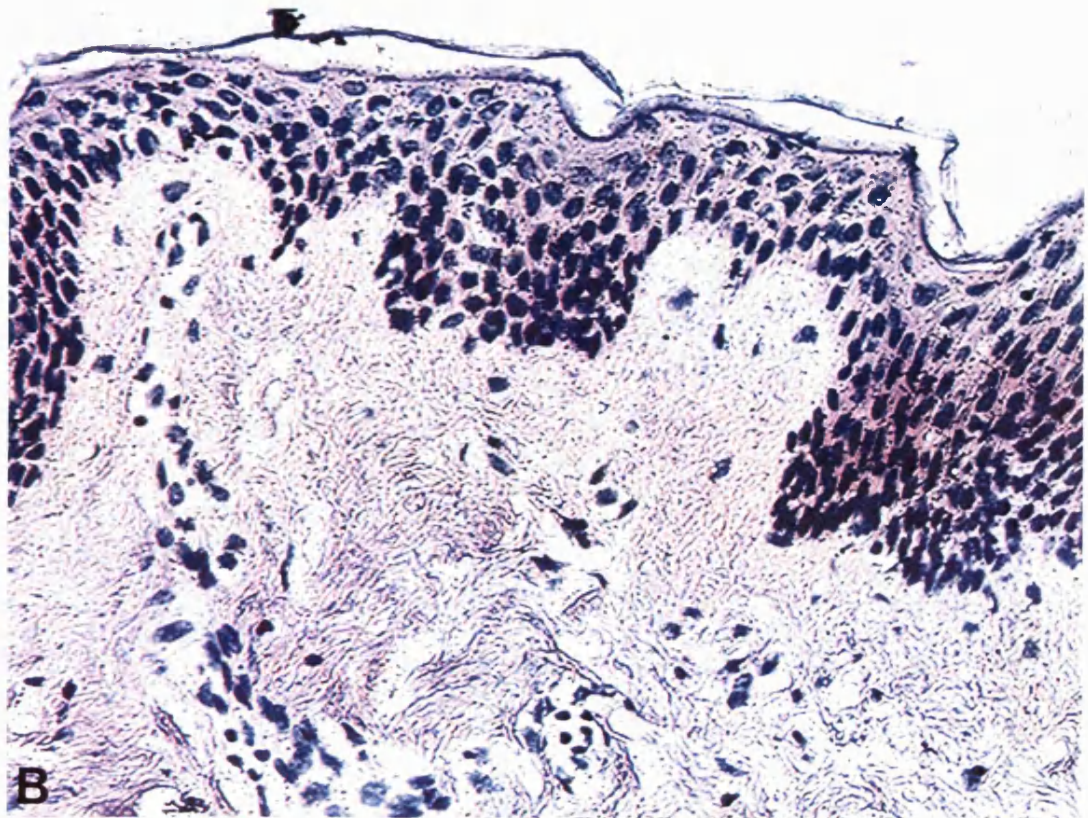
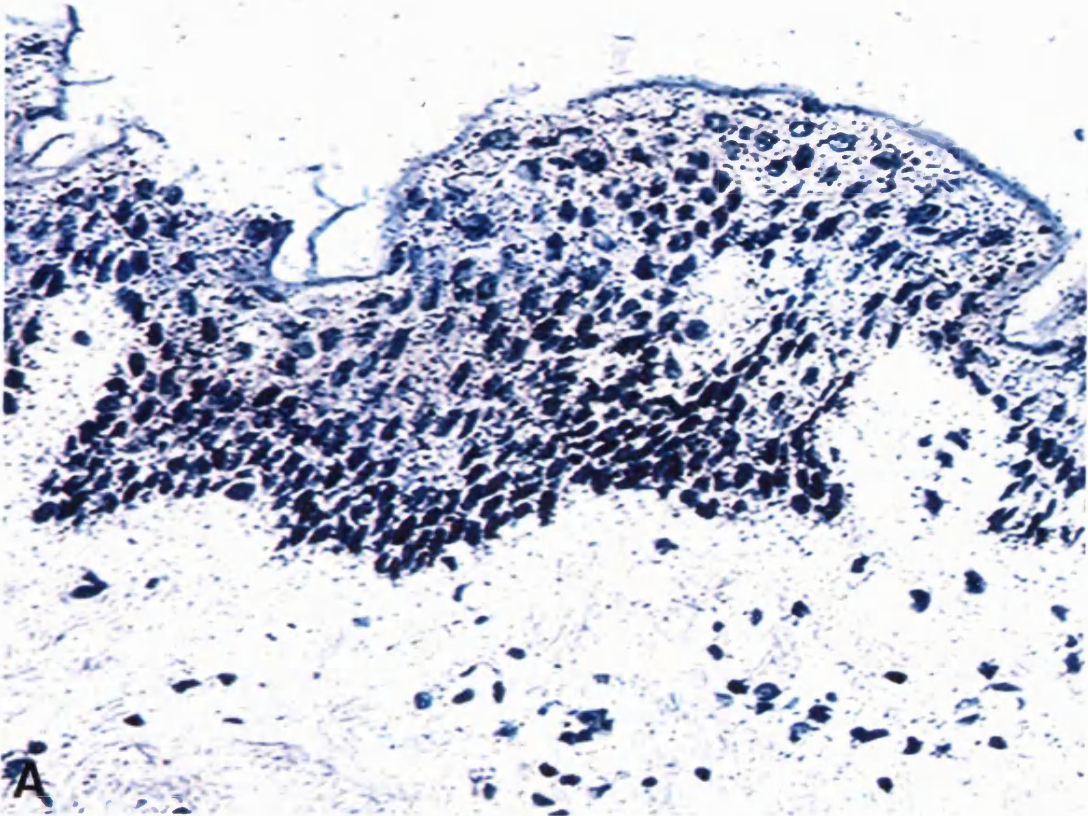


Fig 8.3 Localisation of FMO1 mRNA to the sebaceous gland in human skin.

Sections of human skin were incubated with ^{35}S -labelled antisense FMO1 RNA (A) or ^{35}S -labelled sense FMO1 RNA (B). The antisense probe hybridized to the sweat producing cells of the sebaceous gland. Autoradiography was for 4 weeks. Magnification = X110

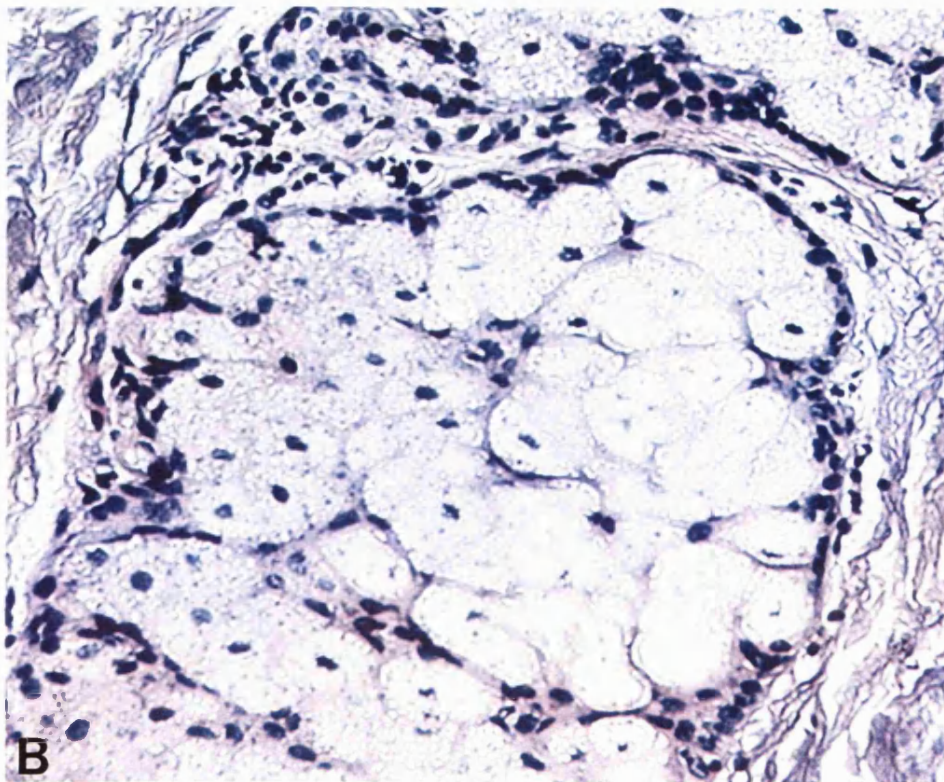
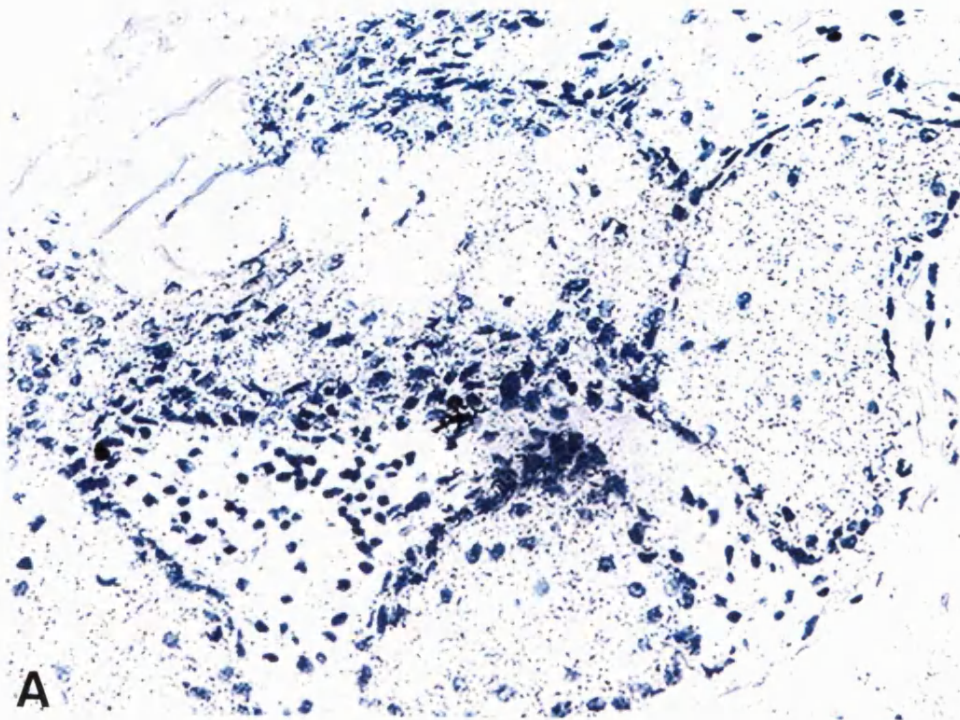


Fig 8.4 Localisation of FMO3 mRNA to the epidermis of human skin.

Sections of human skin were incubated with ^{35}S -labelled antisense FMO3 RNA (A) or ^{35}S -labelled sense FMO3 RNA (B). The antisense probe hybridized to cells within the epidermis. Autoradiography was for 4 weeks.

Magnification = X110

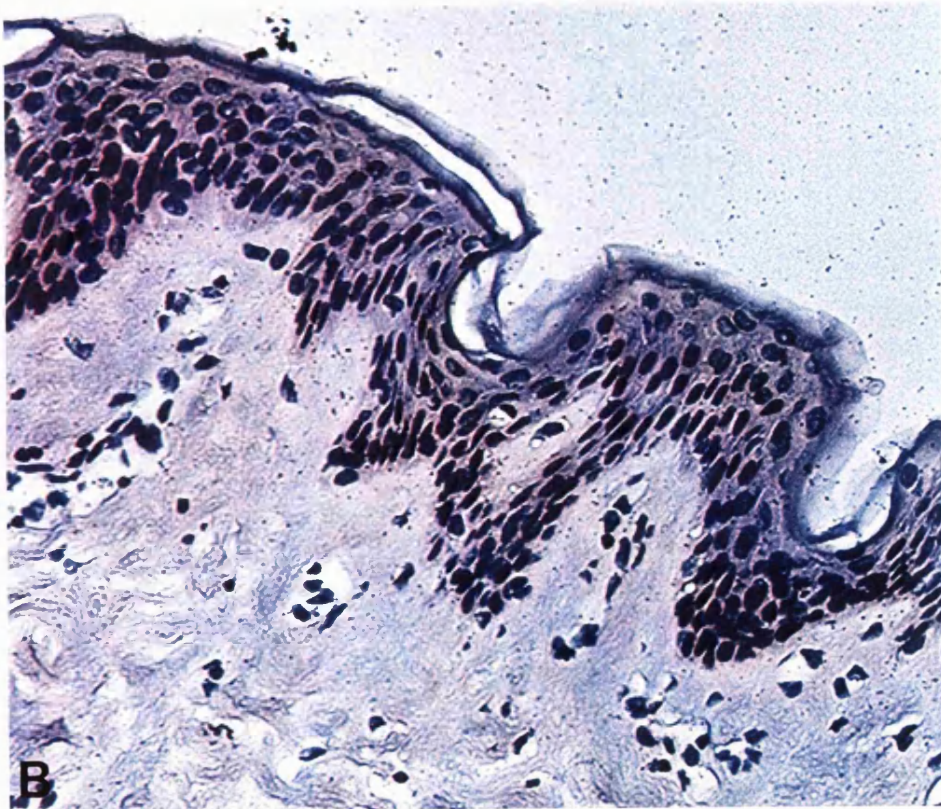
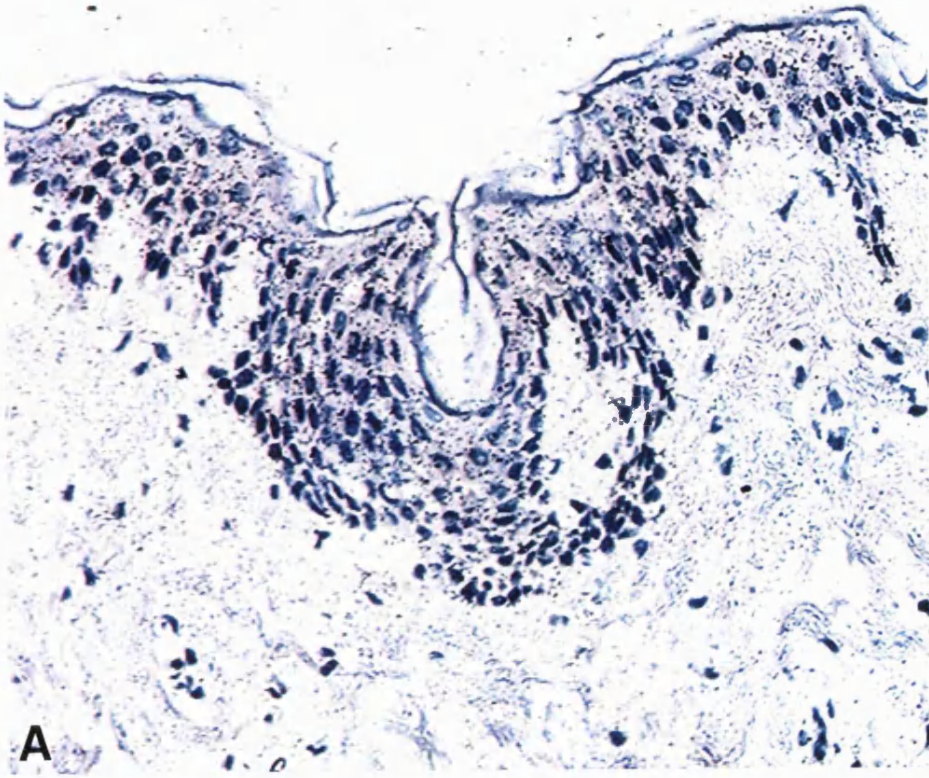


Fig 8.5 Localisation of FMO3 mRNA to the sebaceous gland of human skin

Sections of human skin were incubated with ³⁵S-labelled FMO3 RNA (A) or ³⁵S-labelled sense FMO3 RNA (B). The antisense probe hybridized weakly to the cells of the sebaceous glands.. Autoradiography was for 4 weeks.
Magnification = X110

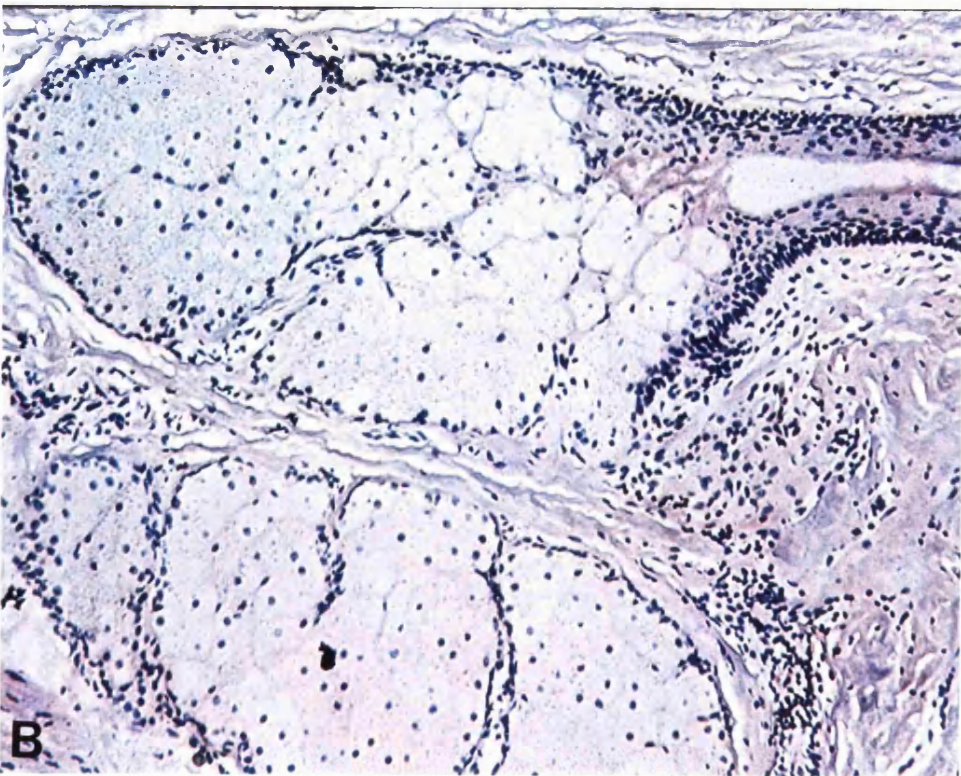
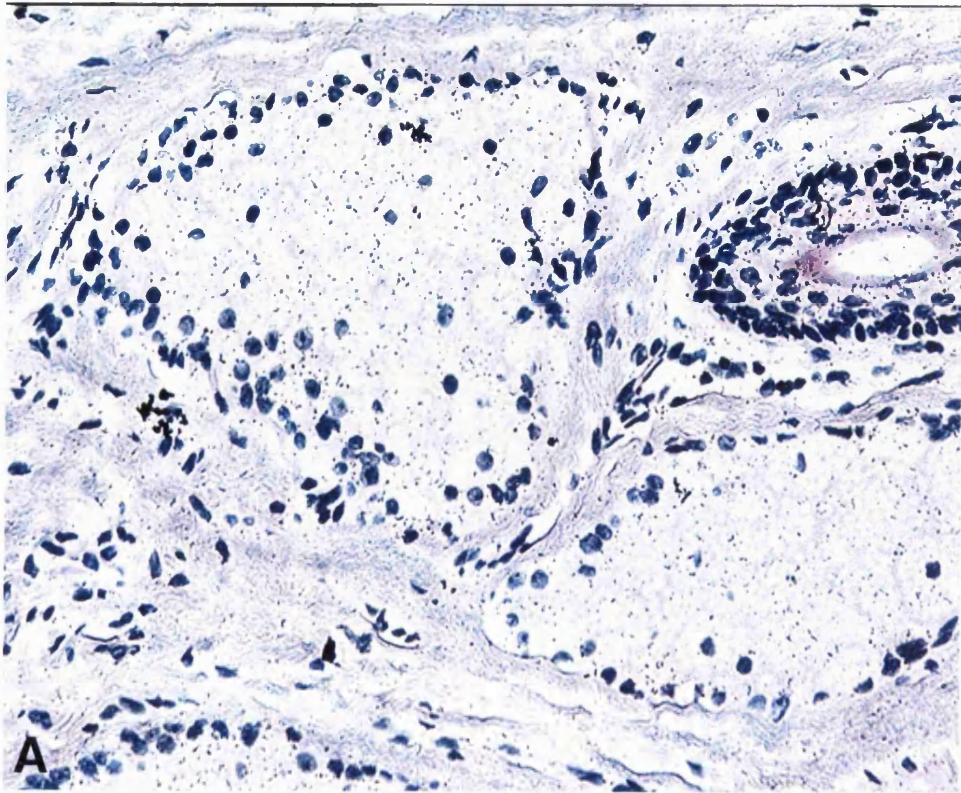


Fig 8.6 Localisation of FMO4 mRNA to the epidermis human skin.

Sections of human skin were incubated with ^{35}S -labelled antisense FMO4 RNA (A) or ^{35}S -labelled sense FMO4 RNA (B). The antisense probe hybridized weakly to cells within the epidermis. Autoradiography was for 4 weeks. Magnification = X110

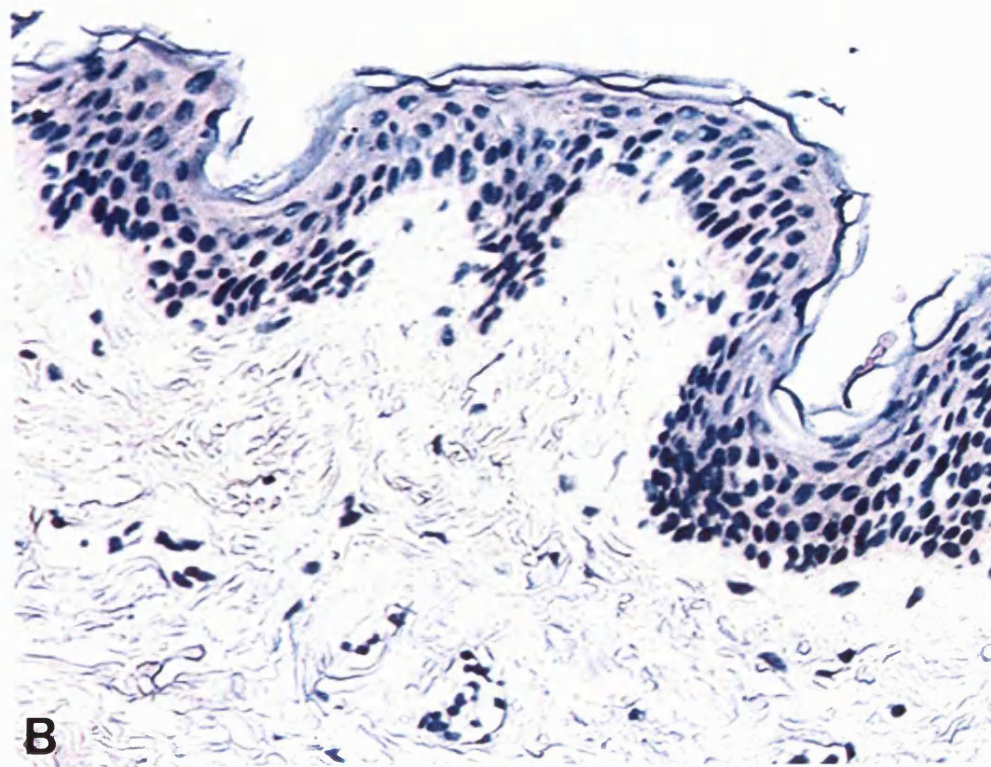
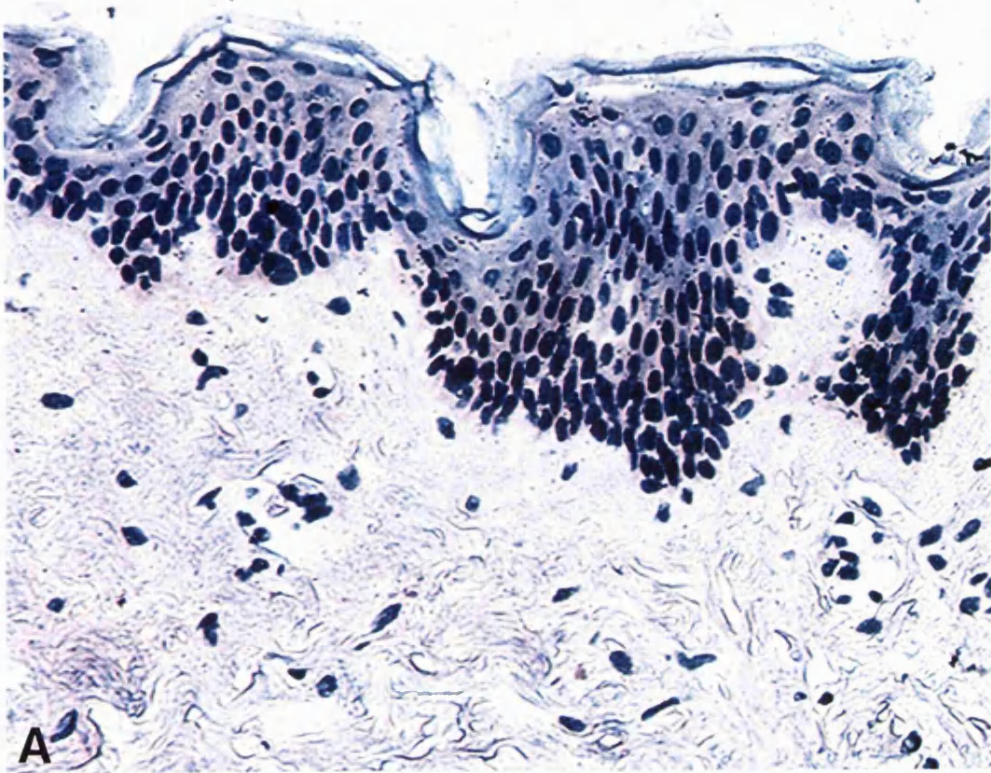


Fig 8.7 Localisation of FMO4 mRNA to the sebaceous gland in human skin.

Sections of human skin were incubated with ^{35}S -labelled antisense FMO4 RNA (A) or ^{35}S -labelled sense FMO4 RNA (Bi and Bii). The antisense probe hybridized weakly to cells within the sebaceous gland. Autoradiography was for 4 weeks. Magnification (A) = X50 and (B) = X110

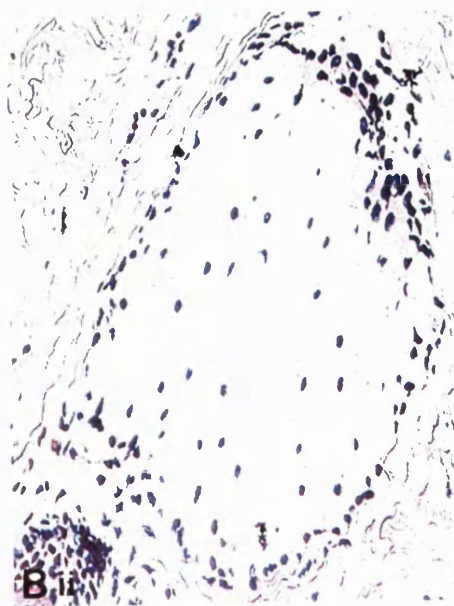


Fig 8.8 Localisation of FMO5 mRNA to the epidermis of human skin.

Sections of human skin were incubated with ^{35}S -labelled antisense FMO5 RNA (A) or ^{35}S -labelled sense FMO5 RNA (B). The antisense probe hybridized strongly to cells within the epidermis. Autoradiography was for 4 weeks. Magnification = X110

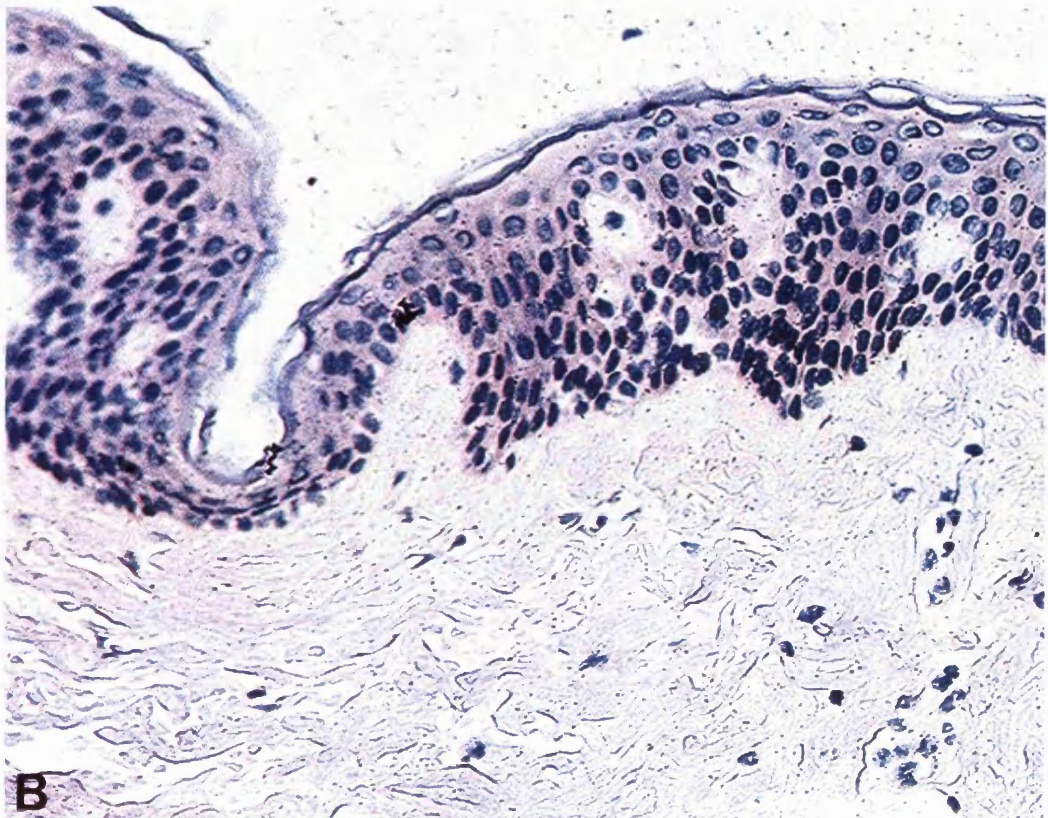
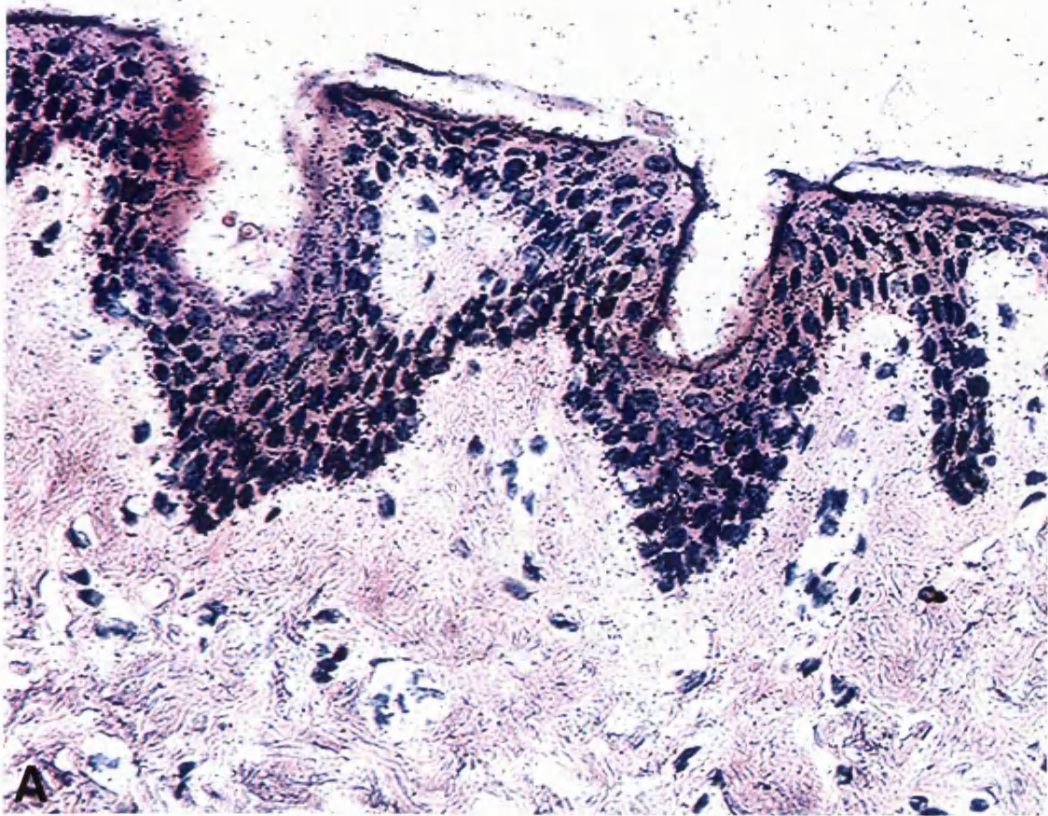


Fig 8.9 Localisation of FMO5 mRNA to the sebaceous glands of human skin.

Sections of human skin were incubated with ^{35}S -labelled antisense FMO5 RNA (A) or ^{35}S -labelled sense FMO5 RNA (B). The antisense probe hybridized strongly to the sweat producing cells of the sebaceous gland and to a structure that could possibly be the hair follicle. Autoradiography was for 4 weeks. Magnification = X50

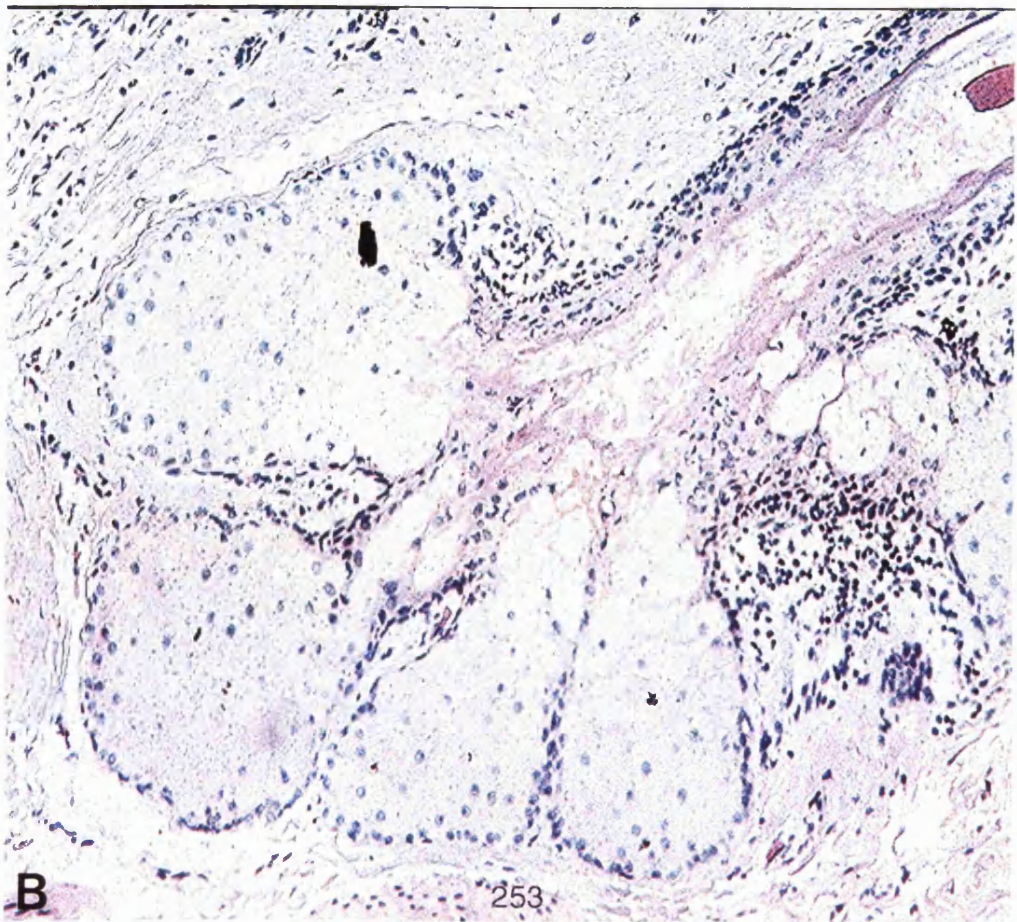
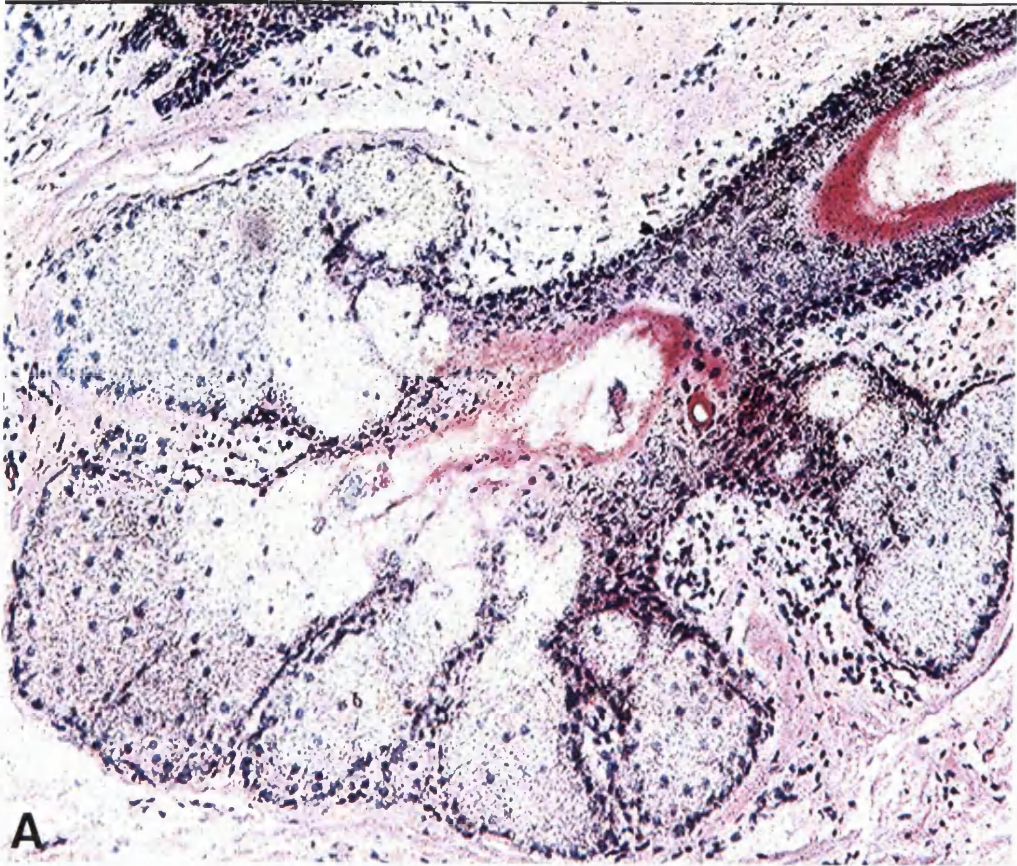
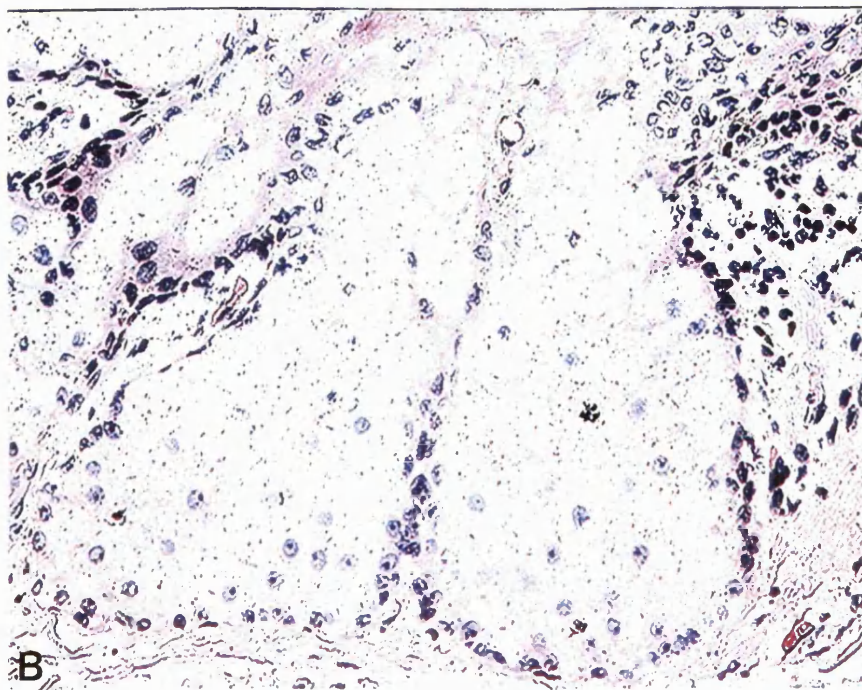
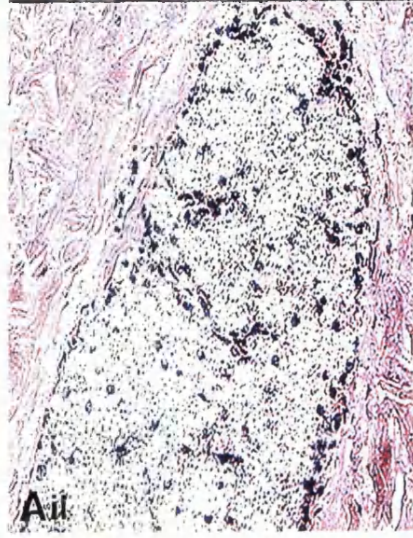
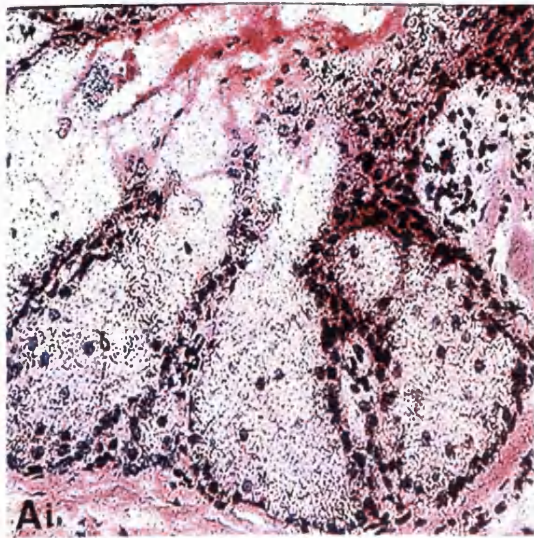


Fig 8.10 Localisation of FMO5 mRNA to the sebaceous glands of human skin.

Sections of human skin were incubated with ^{35}S -labelled antisense FMO5 RNA (Ai and Aii) or ^{35}S -labelled sense FMO5 RNA (B). The antisense probe hybridized strongly to the sweat producing cells of the sebaceous gland. Autoradiography was for 4 weeks. Magnification = X110



staining was observed. This is probably due to the fact that the antibodies available to us were not affinity purified resulting in epitope cross-reactivity. This was particularly important in tissues such as the skin, where due to high background staining, it was difficult to determine if any of the relevant enzymes were present. In particular was the strong background staining observed in the epidermis in the pre-immune serum negative control. This background staining was present predominantly in the epidermis, probably due to cross-reactivity with the keratins present in this layer, as was the case when western blot analyses were carried out.

The results for the IHC using the human kidney sections and the anti-FMO1 antibody were the most conclusive. The kidneys are the primary route for the excretion of xenobiotic compounds from the body. It is well documented that the kidney contains drug metabolising enzymes and that all compounds that are excreted in the urine either pass through or are concentrated in the kidney.

It has been shown that FMO1 mRNA is expressed in adult human kidney where it is the predominant FMO present (Dolphin *et al.*, 1996). FMO1 mRNA is also expressed in human foetal tissues such as the liver, kidney, lung and brain (Dolphin *et al.*, 1996). In laboratory animals, apart from the mouse, FMO1 constitutes the major FMO in the adult liver (Gasser *et al.*, 1990, Lawton *et al.*, 1990). Bhamre *et al.*, (1993) have localised the kidney FMO in rats to the proximal and distal tubules of the nephron and the collecting ducts. They, however, give no clear indication as to which FMO isoform they are detecting. The results obtained by us with the human kidney, show similarity to those obtained by Bhamre *et al.*, (1993) in terms of the localiation of FMO, except that we found no distinct staining of the collecting tubules.

The results that we obtained with the human kidney seem to indicate that the kidney may serve as an important extrahepatic organ of detoxification. 99% of the water in the renal glomerular filtrate is reabsorbed as it traverses

through the tubules (Thibodeau and Patton, 1996). This facilitates the reabsorption and reentry of some of the xenobiotics into the circulation. The presence of these enzymes in this particular location within the kidney is a probable defense mechanism that the body has developed. The enzymes may take part in local degradation of the metabolites. It is interesting that in man, *FMO1* is expressed only in the adult kidney and in the skin, the regulatory mechanisms involved in this tissue specific expression are not known.

To date no comprehensive studies have been published on the expression and localisation of the FMOs in the human skin. The results obtained using *in situ* hybridization analyses with FMOs 1, 3, 4 and 5 shows the presence of mRNAs of these FMOs in the epidermis and sebaceous glands. The significance of the presence of FMOs 1, 3, 4 and 5 in these particular locations within the human skin is not known, however it is quite possible that the enzymes are present in these particular areas because, as mentioned earlier, the epidermis is the area of the skin that comes into direct contact with the external environment. The sebaceous glands have openings onto the surface of the skin and therefore can also serve as entry portals to exogenous chemicals. The presence of the FMOs within these structures could possibly be a defensive mechanism developed by the body to prevent the effects of harmful chemicals.

Studies carried out on mouse skin have been restricted to the localisation of the protein (Venkatesh *et al.*, 1992). This group showed the presence of FMO protein in the epidermis of both mouse and pig skin. They used an antibody raised to mouse liver FMO for this study. However, it was not stated whether the protein had been raised from male or female mice. FMO1, 3 and 5 are present in female mouse livers and FMOs 1 and 5 in male mouse livers. Thus, the use of antibodies to study localisation of FMOs in this study is problematic, in that it is not known to which FMOs the antibody was

raised. Thus, any work done on localisation with such antibodies must be correlated to studies showing the co-localisation of their corresponding mRNA.

Unfortunately it was not possible to correlate the results we obtained in the *in situ* hybridization analyses with immunohistochemical analyses. The availability of antibodies having higher titres than those used by us or highly specific monoclonal antibodies will allow the elucidation of whether the proteins corresponding to FMOs 1, 3, 4 and 5 mRNAs are expressed in human skin.

CYTOCHROMES P450 IN SKIN

9.1 Detection of CYPs in human skin and keratinocyte culture samples

There have been numerous reports on the presence of CYP mRNAs and proteins in the skin of rodents, yet few studies on their expression in human skin have been published. The most widely studied isoform in human skin has been CYP1A1, however, no reports on the complete range of CYPs in the human skin have been published. During the course of this investigation, we carried out studies to ascertain the range of CYPs in the human skin and to determine their cellular localisation in this tissue.

As with the FMOs, to detect the presence of CYP mRNA, northern blot hybridization analyses and RNase protection assays were carried out. To localise the mRNA to specific cell types within the skin, *in situ* hybridization analyses were performed. Western blot analyses were used to determine the expression of CYP protein in human skin microsomes. IHC was used to determine the localisation of the protein. No enzyme activity assays could be carried out with microsomes derived from whole skin because of the unavailability of sample.

9.2 CYP mRNAs

The presence of members of the human CYP2A, CYP2B and CYP3A subfamilies in the human skin was investigated by carrying out northern blot hybridization analyses of RNA from whole skin, a primary culture of human epidermal keratinocytes and HaCaT cells. RNase protection assays were carried out on RNA derived from whole skin samples and their corresponding keratinocyte cultures as well as from HaCaT cells.

9.2.1 Detection of CYP2A

9.2.1.1 Northern blot hybridization analyses

A cDNA clone encoding CYP2A6, pH6, had been previously isolated in our laboratories (Phillips *et al.*, 1985a). The full length insert (1.2kb) was used as a hybridization probe for northern blots of RNA from human liver and lung, cynomolgous monkey lung, rabbit liver and lung, marmoset liver and from cultures of HaCaT cells and a primary culture of human epidermal keratinocytes.

A strong signal was obtained in one of the human liver samples (fig 9.1.1, lane 9), rabbit liver (lane 10) and marmoset liver (lane 14). The band observed in the human liver and rabbit lung samples was approximately 2 kb in length, whereas in the marmoset liver it was approximately 1.8 kb in length. A weakly hybridizing band at 4 kb was detected in the human liver sample. No bands were observed in RNA from the HaCaT cells or the primary culture of human epidermal keratinocytes. The second human liver sample showed no hybridizing bands with the probe.

9.2.1.2 RNase protection assays

An antisense riboprobe transcribed from pBS2A(288), a 288bp 5' *Bam* HI/*Pst* I subfragment of pH6 subcloned into pBluescript (fig 9.1.2), was used to quantify CYP2A6 mRNA in samples of RNA from human skin, primary cultures of human epidermal keratinocytes and HaCaT cells. The antisense probe was transcribed from the T7 promoter, using T7 RNA polymerase. Human liver RNA which had shown the presence of CYP2A mRNA during northern blot analyses was used as a positive control.

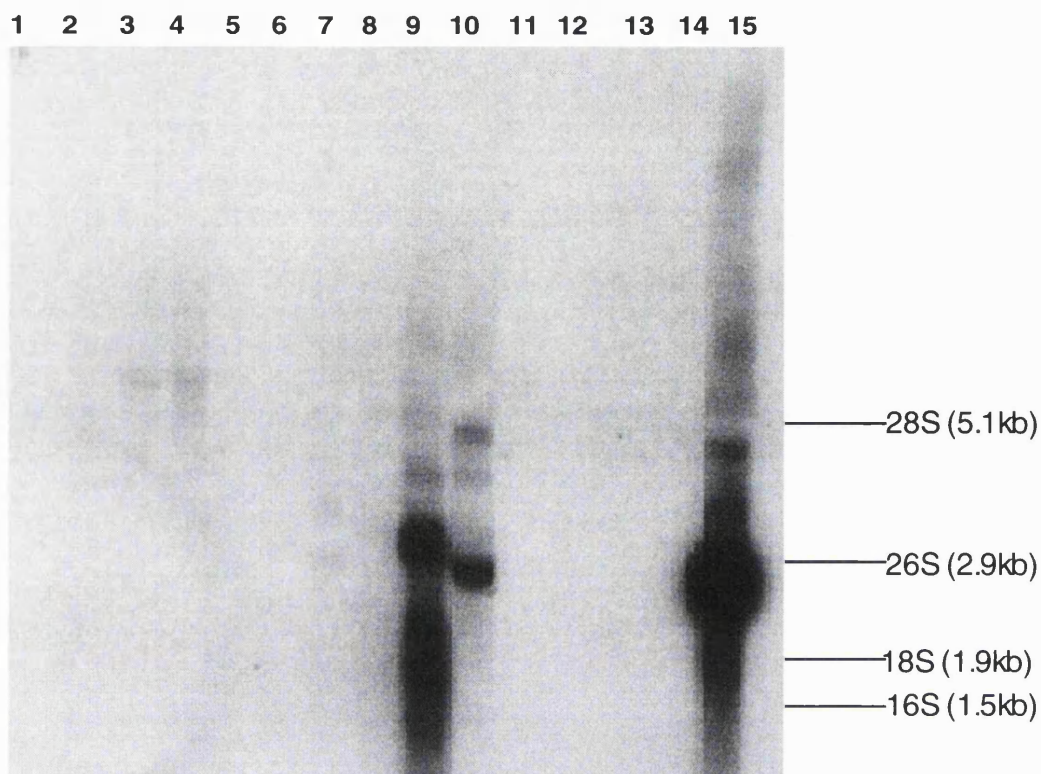


Fig 9.1.1 RNA samples (15 μ g) were electrophoresed on a denaturing agarose gel. Samples were from human lung (lanes 2-5), cynamologous monkey lung (lane 6), rabbit lung (lane 7), human liver (lanes 8 and 9), rabbit liver (lane 10), HaCaT cells (lane 13), a primary culture of human epidermal keratinocytes (lane14) and marmoset liver RNA (lane 15). Total *E. Coli* RNA (1 μ g) electrophoresed concurrently with the samples (lanes 1 and 12) served as size markers with the 28S and 18S rRNA in the samples. The blot was hybridized with a radiolabelled full length cDNA encoding CYP2A6. Autoradiography was carried out for 1 week.

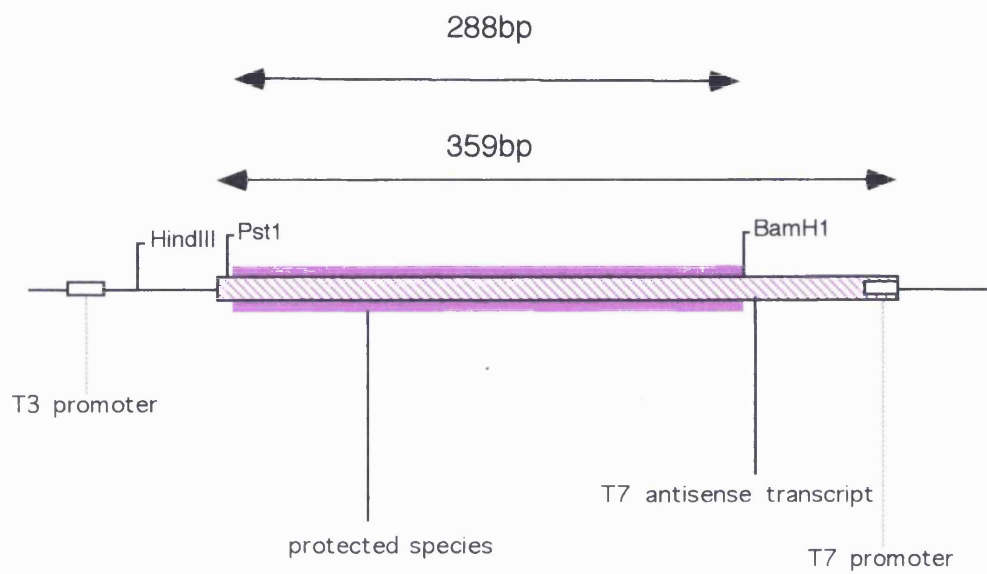


Fig 9.1.2 pBS2A(288); a 288bp 5' *BamH I/Pst I* subfragment of pH6 cloned into pBluescript.

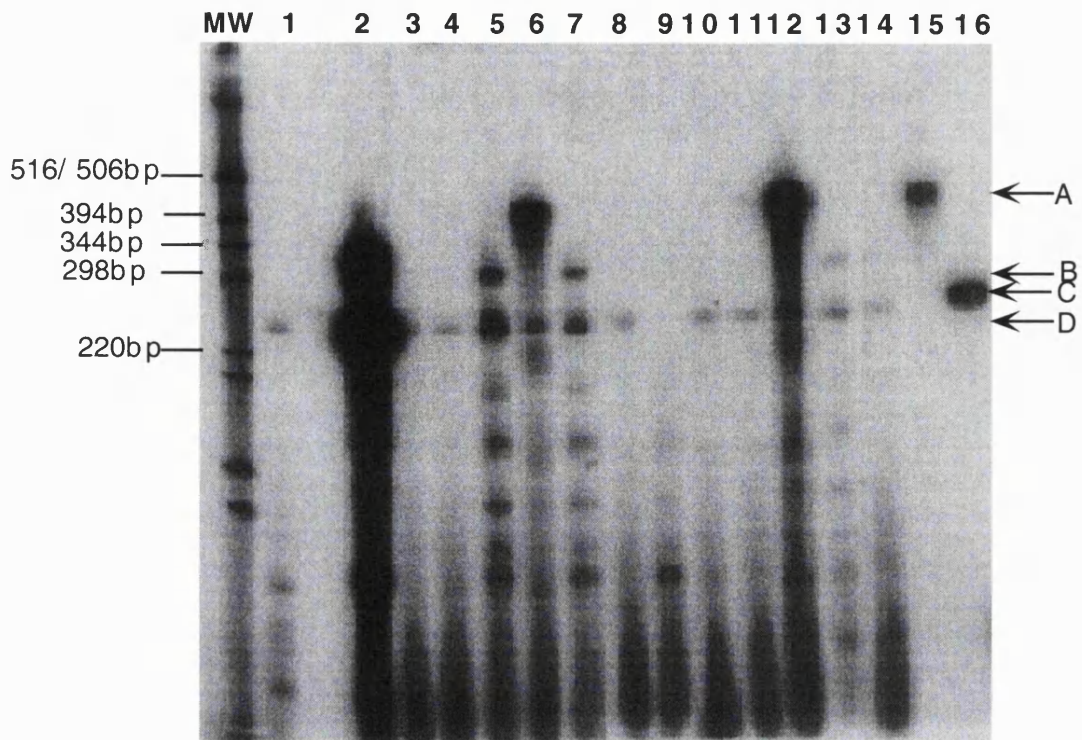


Fig 9.1.3 Analysis of CYP2A6 and CYP3A4 mRNAs by RNase protection. 30 μ g of total RNA was hybridized to antisense CYP2A6 and CYP3A4 mRNAs. Each reaction contained 1 X 10⁵cpm of riboprobe. All assays were performed as described in section 2.6. RNA from human liver (5 μ g) (track 2) was used as the positive control. RNA was from human skin (tracks 3, 5, 7, 9 and 13), primary cultures of human epidermal keratinocytes (tracks 4, 6, 8, 10, 11 and 12) and HaCaT cells (track 14). Track 1 contains a control for digestion of the transcripts, by RNase A/T1, in the presence of 30 μ g of tRNA. Tracks 15 and 16 contain undigested CYP2A6 and CYP3A4 antisense transcripts respectively. Molecular weight standards (MW) were ³⁵S-labelled fragments derived from the 1kb ladder set from Gibco BRL (section 2.6). The arrows indicate the length of the CYP2A6 undigested transcript (A, 359 bp), CYP2A6 protected hybrid (B, 288bp), CYP3A4 undigested transcript (C, 250bp) and CYP3A4 protected hybrid (D, 240bp). Autoradiography was carried out for 2 weeks.

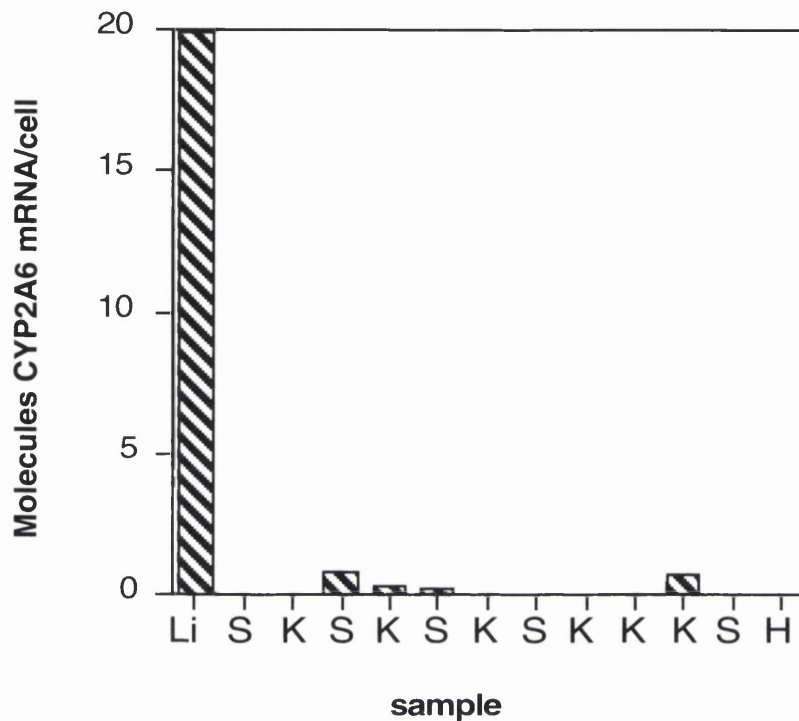


Fig 9.1.4 CYP2A6 mRNA concentrations in human liver (Li), human skin (S), primary cultures of human epidermal keratinocytes (K) and HaCaT cells (H). Samples were analysed as described in section 2.6. The CYP2A6 antisense transcript was hybridized to human liver, human skin, primary cultures of human epidermal keratinocytes and HaCaT RNA and digested with a mixture of RNase A/T1. The digested RNA was electrophoresed and autoradiographed. The resulting signals were compared to a standard curve of undigested probe and the concentrations of the mRNA in the samples calculated as described in section 2.6.1.6.

Of the five whole skin samples analysed, two samples showed the presence of CYP2A6 mRNA (fig 9.1.3). Six RNA samples from primary cultures of keratinocytes were analysed. Only two cultures had CYP2A6 mRNA, one of which was derived from a skin sample expressing CYP2A6 mRNA. The amount of CYP2A6 mRNA present in the samples of whole skin and primary keratinocyte cultures was <1 molecule/cell, which is much lower than that found in the human liver (approximately 20 molecules/cell) (fig 9.1.4). The values were determined as described in section 2.6.1.6.

9.2.2 Detection of CYP2B6

9.2.2.1 Northern blot hybridization analysis

A partial cDNA encoding CYP2B6, pBS7A22E, has been isolated and cloned previously (Santisteban *et al.*, 1988, Phillips *et al.*, 1985b). This clone could not be used for northern blot analysis because it contained *Alu* repetitive elements. Instead, a 450 bp *Hind* III subfragment from the cDNA clone, devoid of *Alu* sequences was used. This subfragment hybridized specifically to both human liver RNA samples on the northern blot (fig 9.2.1 and 9.2.2, lanes 8 and 9). At least four transcripts were observed. Of these, the most strongly hybridizing band was approximately 2.8 kb in length. The other three bands observed were larger than 2.8 kb and weakly hybridizing. The appearance of multiple transcripts was only observed in one of the human liver samples analysed (fig 9.2.1 and 9.2.2, lane 9). The other human liver sample had one weakly hybridizing band, approximately 2.8 kb in size. Three weakly hybridizing bands were observed in the RNA of human lung (lanes 2-5), the most strongly hybridizing band being approximately 2.8 kb in size. The remaining two weakly hybridizing bands were approximately 7.7 kb and 10 kb in length .

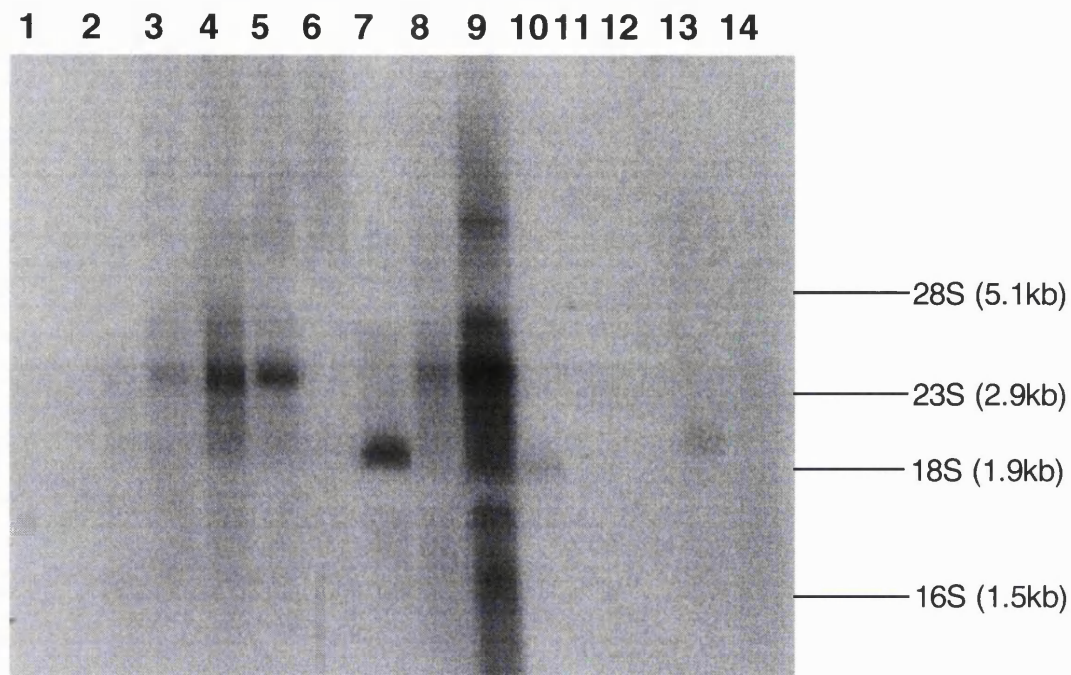


Fig 9.2.1 RNA samples (15 μ g) were electrophoresed on a 1% denaturing formaldehyde gel as described in section 2.5. RNA was from human lung (lanes 2-5), cynamologous monkey lung (lane 6), rabbit lung (lane 7), human liver (lanes 8 and 9), rabbit liver (lane 10), HaCaT cells (lane 13) and a primary culture of human epidermal keratinocytes (lane 14). Total *E. Coli* RNA (1 μ g) was electrophoresed (lanes 1 and 12) and used as size markers together with the 28S and 18S rRNA in the samples. The northern blot was hybridized with a 450 bp fragment derived from the CYP2B6 cDNA. Autoradiography was carried out for 3 weeks.

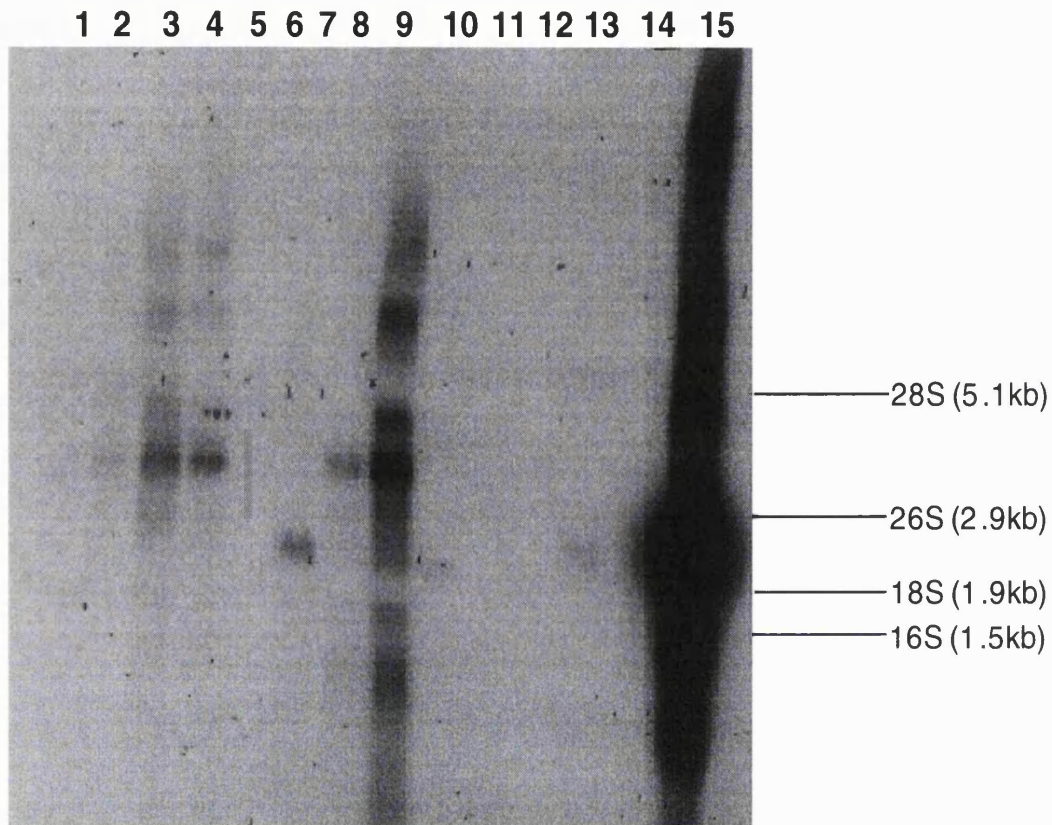


Fig 9.2.2 RNA samples (15 μ g) were electrophoresed on a denaturing formaldehyde agarose gel (1%). Samples were from human lung (lanes 2-5), cynamologous monkey lung (lane 6), rabbit lung (lane 7), human liver (lanes 8 and 9), rabbit liver (lane 10), HaCaT cells (lane 13), a primary culture of human epidermal keratinocytes (lane 14) and marmoset liver (lane 15). Total *E.Coli* RNA (1 μ g) was electrophoresed concurrently with the samples (lanes 1 and 12). These together with the 28S and 18S rRNA in the samples served as size markers. The blot was hybridized with a radiolabelled 450 bp fragment of the CYP2B6 cDNA. Autoradiography was carried out for 3 weeks.

The rabbit liver and rabbit lung samples on the other hand showed a single hybridizing band with the CYP2B6 fragment used in the analysis. The band observed was approximately 2 kb in length. A single, weakly hybridizing band was observed in the HaCaT cell RNA (lane 13). This band corresponded in size to that observed in the rabbit liver and lung, being 2 kb in size. No CYP2B6 mRNA was detected in the primary culture of human epidermal keratinocytes analysed.

9.2.2.2 RNase protection assay

The *Hind* III subfragment of a CYP2B6 cDNA clone (pBS7A22E) isolated in our laboratories (Santisteban *et al.*, 1988, Phillips *et al.*, 1985b) was used for RNase protection assay analysis (fig 9.2.3). Antisense transcripts, using T3 RNA polymerase were generated from this construct and used to assay CYP2B6 mRNA.

Fig 9.2.4 shows the results of an RNase protection assay using this probe. Human liver, lung and kidney samples, were used as positive controls and showed results corresponding to those found with the northern blot analysis. The human liver sample shows the highest expression of CYP2B6 mRNA (approximately 23 molecules/cell), followed by human lung (approximately 8 molecules/cell) and finally human kidney with <1 molecule per cell.

Three human skin samples were analysed. Of these only a single sample expressed CYP2B6 mRNA. None of the primary keratinocytes analysed showed the presence of CYP2B6 mRNA. The HaCaT cells expressed CYP2B6 but the concentration was <1 molecule/cell. The quantitative results obtained are shown in fig 9.2.5.

The smaller protected fragment observed in some of the samples could reflect a polymorphic variant or protection by a related mRNA e.g CYP2B7 or,

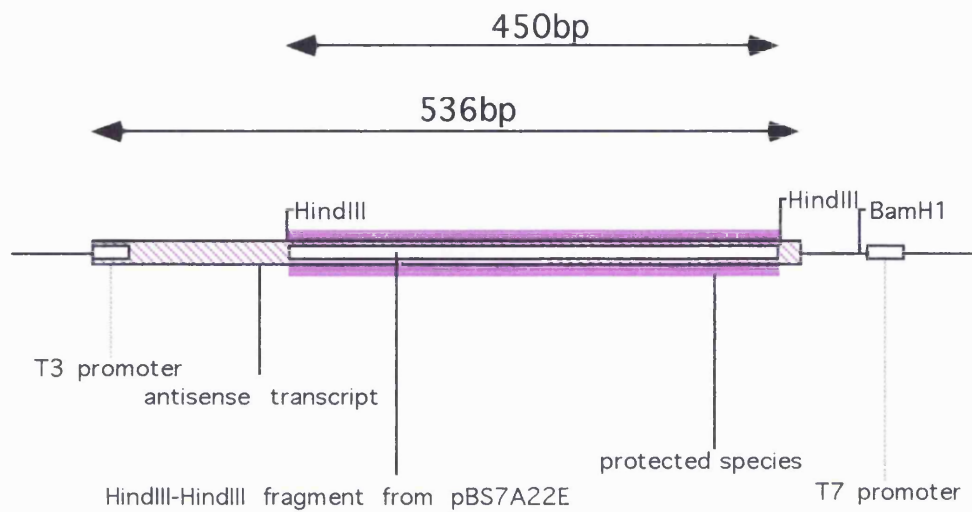


Fig 9.2.3 pBS2B(450); *Hind* III subfragment of CYP2B6 cDNA clone (pBS7A22E) and cloned into pBluescript.

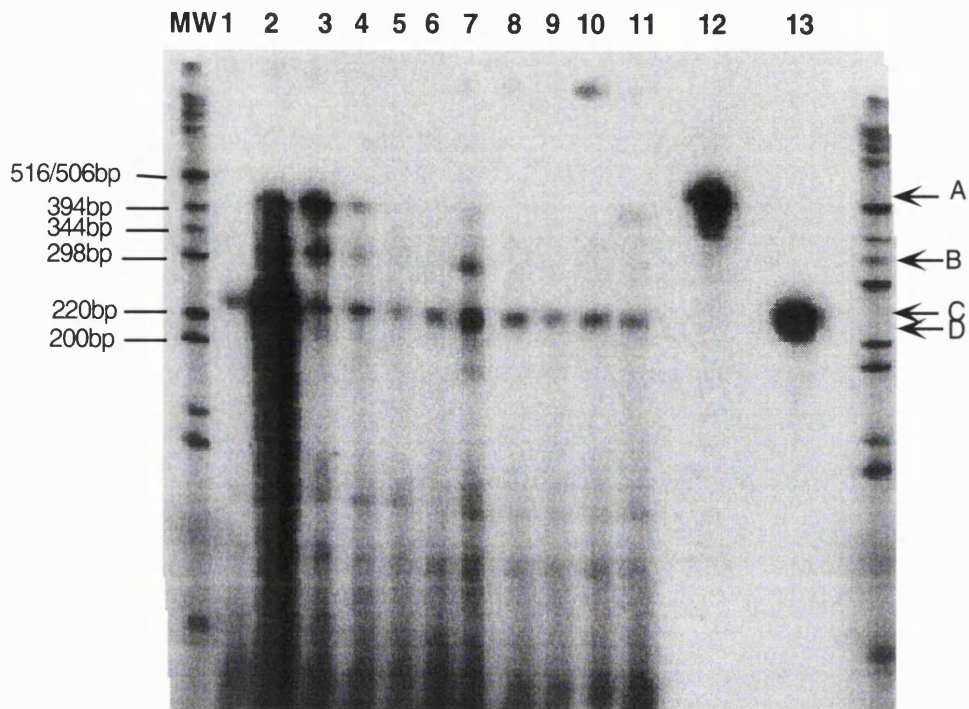


Fig 9.2.4 Analysis of CYP2B6 and CYP3A4 mRNAs by RNase protection. 30 μ g of total RNA was hybridized to antisense CYP2B6 and 3A4 mRNAs. Each reaction contained 1X10⁵cpm of each riboprobe. All assays were performed as described in section 2.6. RNA from human liver (5 μ g) (track 2), human lung (10 μ g) (track 3) and human kidney, (10 μ g) (track 4), were used as controls. RNA was from human skin (tracks 5, 7 and 9), primary cultures of human epidermal keratinocytes (tracks 6, 8 and 10) and HaCaT cells (track 11). Track 1 contains a control for digestion of the transcript, by RNase A/T1, in the presence of 30 μ g of tRNA. Tracks 12 and 13 contain undigested CYP2B6 and CYP3A4 antisense transcripts respectively. Molecular weight standards were ³⁵S-labelled fragments from the 1kb ladder set from Gibco BRL (section 2.6). The arrows indicate the length of the undigested CYP2B6 transcript (A, 536 bp), protected CYP2B6 hybrid (B, 450 bp), undigested CYP3A4 transcript (C, 250 bp) and protected CYP2B6 hybrid (D, 240 bp). Autoradiography was for 9 days.

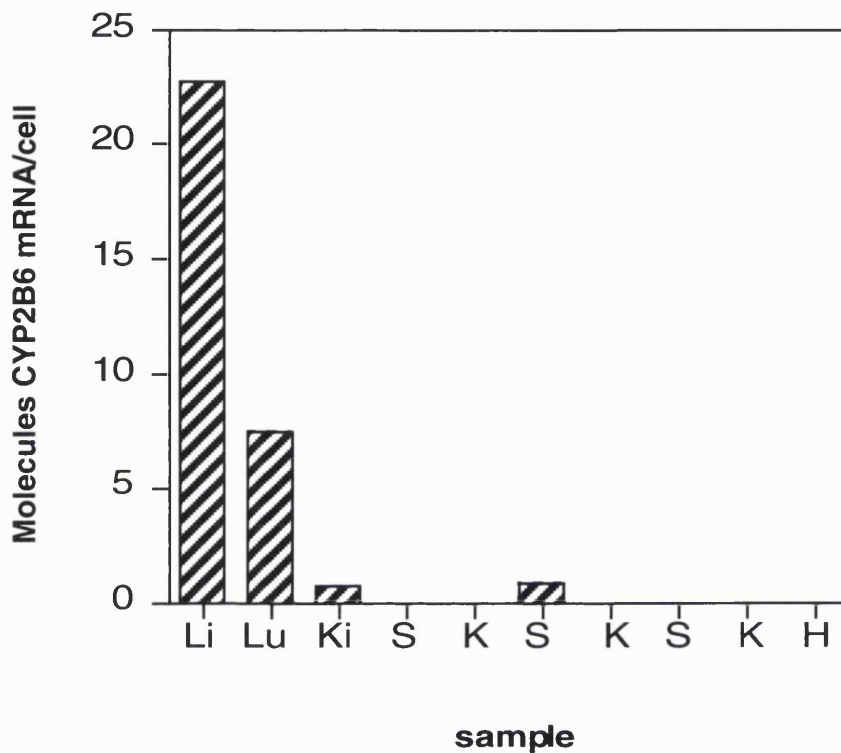


Fig 9.2.5 CYP2B6 mRNA concentrations in human liver (Li), human lung (Lu), human kidney (Ki), human skin (S), primary cultures of human epidermal keratinocytes (K) and HaCaT cells (H). Samples were analysed as described in section 2.6. The CYP2B6 antisense transcript was hybridized to human liver, human lung, human kidney, human skin, cultured primary human epidermal keratinocyte and HaCaT RNA and digested with a mixture of RNase A/T1. The digested RNA was electrophoresed and autoradiographed. The resulting signals were compared to a standard curve of undigested probe and the concentrations of the mRNA in the samples calculated as described in section 2.6.1.6.

be due to partial digestion of the legitimately hybridized probe. This smaller fragment is seen in samples that do not contain the 450 bp protected fragment or in the HaCaT sample.

9.2.3 Detection of CYP3A

9.2.3.1 Northern blot hybridization analysis

A 240 bp fragment from a cDNA clone encoding CYP3A4, pCYK, was used to probe northern blots of RNA from human liver and skin, marmoset liver, HaCaT cells and a culture of primary human epidermal keratinocytes (fig 9.3.1).

A strongly hybridizing band was observed in the human liver sample (lane 5). The size of this band was approximately 3.6 kb. A second but more weakly hybridizing band of 4.7 kb was also observed in the human liver RNA. There was considerable smearing below the lower band which indicates degradation of the RNA.

A weakly hybridizing band was observed in the marmoset liver RNA sample (lane 7). The size of this band corresponded to that observed in the human liver sample i.e 3.6 kb. None of the other samples of RNA, i.e the human skin, HaCaT or primary culture of human keratinocytes, hybridized to the CYP3A4 subfragment used in the analysis.

9.2.3.2 RNase protection assay

The structure of the construct used to synthesize a CYP3A4 antisense probe, for the analyses of CYP3A4 mRNA is shown in fig 9.3.2. This fragment distinguishes between the mRNAs encoding CYP3A3, CYP3A4 and CYP3A5.

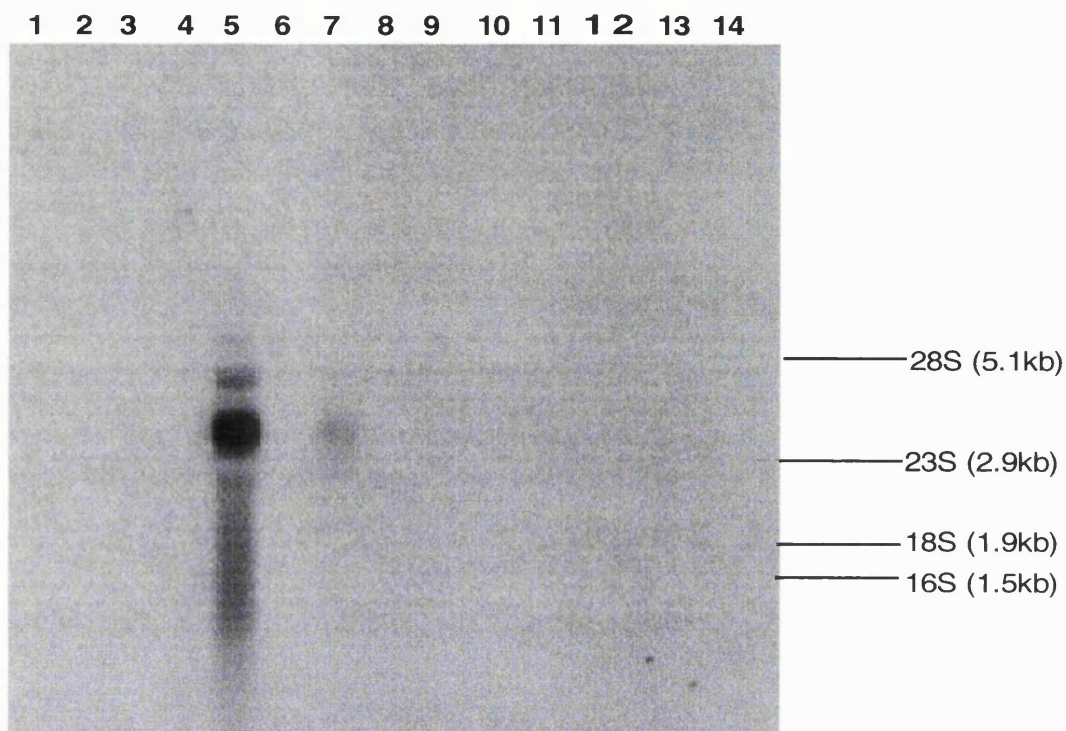


Fig 9.3.1 RNA samples (15µg) were electrophoresed on a 1% denaturing formaldehyde agarose gel detailed in section 2.5. Samples were from whole skin (lanes 2 and 3), adult human liver (lane 5), adult marmoset liver (lane 7), HaCaT cells (lanes 9-12) and a culture of primary human epidermal keratinocytes (lane 14). Lane 1 and 13, *E. coli* total RNA (1µg) was electrophoresed to serve as size markers together with the 28S and 18S rRNA in the samples and used for the subsequent estimation of the transcript size. The northern blot was hybridized with a 250 bp HindIII/SacI fragment of a cDNA clone encoding CYP3A4. Autoradiography was carried out for 48hours.

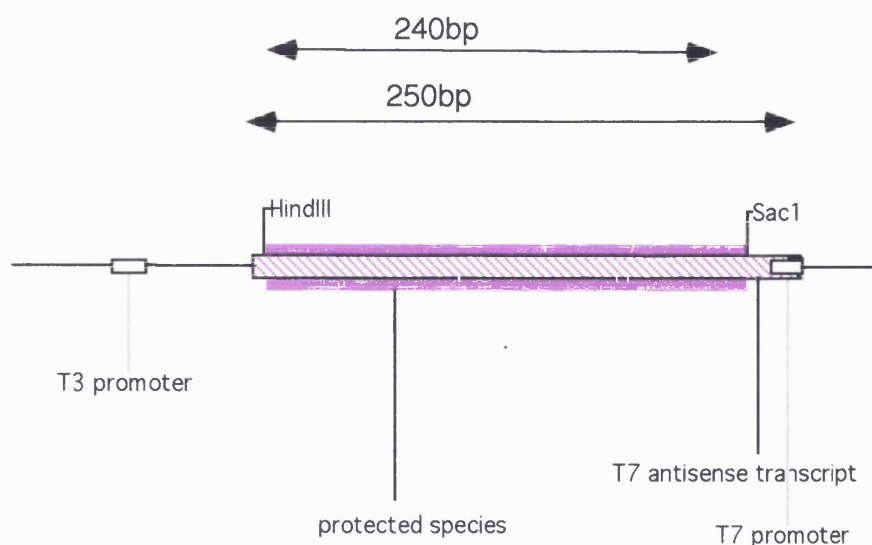


Fig 9.3.2 pBS3A(240); a 240bp *Hind* III/*Sac* I subfragment of pCYK cloned into pBluescript.

1519 (*Hind* III site)
3A3 |
3A4 AAGCTTAGGAGGACTTCTTCAACCAGAAAACCCGTTGTTCTAAAGTT
3A5 GA ACGCA A G

GAGTCAAGGGATGGCGATGGCACCGTAAGTGGAGCCTGAATTTTCCT-A
T A A C AA * G A T

AGGACTTCTGCTTTGCTCTTCAAGAAATCT-GTGCCTGAGAACACCA-G
A G G CC

AGACCTCAAATTACTTTGTGAATAGAACTCTGAAATGAAGATGGGCTTC
TT C GC---- A CT A A

ATCCAATGGACTGCATAAATAACCGGGGATTCTGTACATGCATTGAGCTC
T TA-----
End of 3A5 cDNA 1759 (*Sac* I site)

Fig 9.3.3 Sequence alignment of CYP3A4 with the corresponding regions of CYP3A3 and CYP3A5.

The above alignment of CYP3A3 and CYP3A5 cDNA sequences with position 1519 to 1759 of the CYP3A4 cDNA sequence, was compiled from Gonzalez *et al.* (1989) and Aoyama *et al.* (1990). The end of the protein coding sequence is denoted by *. Several deletions and multiple mismatches are present.

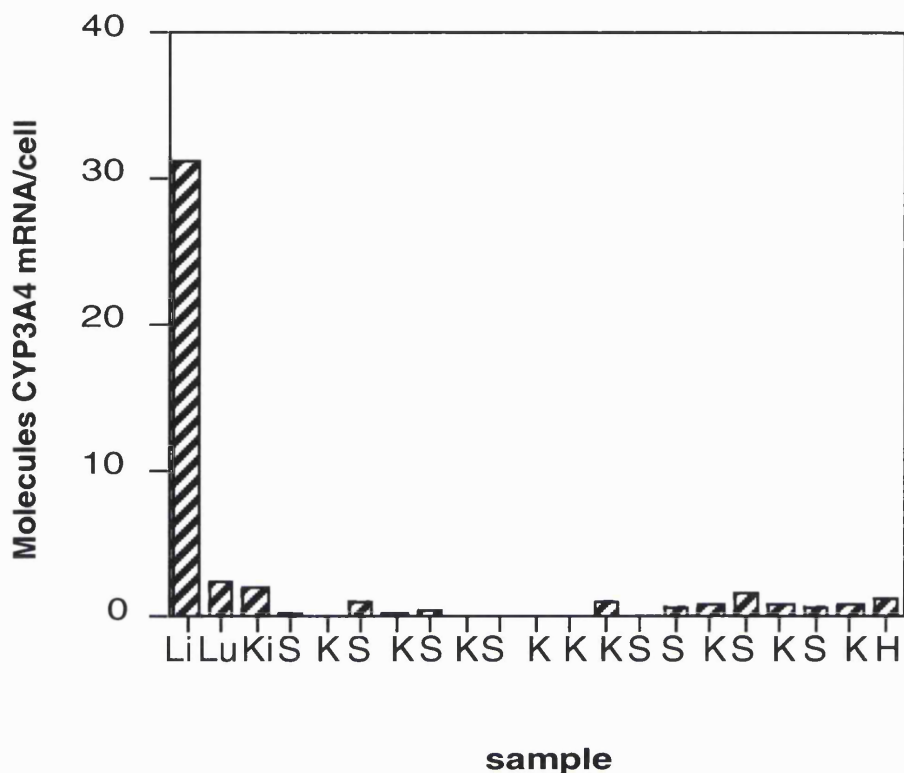


Fig 9.3.4 CYP3A4 mRNA concentrations in human liver (Li), human lung (Lu), human kidney (Ki), human skin (S), primary cultures of human epidermal keratinocytes (K) and HaCaT cells (H). Samples were analysed as described in section 2.6. The CYP3A4 antisense transcript was hybridized to human liver, human lung, human kidney, human skin, cultured primary human epidermal keratinocyte and HaCaT RNA and digested with a mixture of RNase A/T1. The digested RNA was electrophoresed and autoradiographed. The resulting signals were compared to a standard curve of undigested probe and the concentrations of the mRNA in the samples calculated as described in section 2.6.1.6.

The sequence alignment of the antisense transcript derived from this construct and CYP3A3 and 3A5 is shown in fig 9.3.3.

Figs 9.1.3 and 9.2.4 show the autoradiograms of the protected RNA species. Human liver, lung and kidney RNAs were used as controls. The highest amounts of CYP3A4 mRNA was observed in the human liver sample (31 molecules/cell), followed by the human lung (2 molecules/cell) and human kidney (2 molecules/cell). Of the eight human skin samples analysed, six had CYP3A4 mRNA. The amounts in these samples varied but on average was <1 molecule/cell. Nine primary keratinocyte cultures were analysed, of these, five showed the presence of CYP3A4 mRNA. CYP3A4 mRNA was also detected in the HaCaT cells. The results are summarized in fig 9.3.4.

CYP3A4 appears to be the most abundantly and widely expressed *CYP* in human skin. However, interindividual differences in the expression of *CYP3A4* are observed between different samples of skin.

9.3 Localisation of CYP2A6, 2B6 and 3A4 mRNA in human skin

Human skin samples were analysed as described in section 2.7. The sample for these investigations was from a single individual known to express *CYP2A6*, *2B6* and *CYP3A4*.

CYP2A6 and *CYP2B6* riboprobes hybridized strongly to the epidermis (fig 9.4A and 9.6A) and sebaceous gland (fig 9.5A and 9.7A) of the skin sample analysed. The hybridization with the *CYP2B6* antisense probe appeared to be greater than that observed with the *CYP2A6* probe, however this may be due to the higher specific activity of the probe. The control samples of sense probes showed only faint background staining of the epidermis (fig 9.4B and 9.6B) and sebaceous gland (fig 9.5B and 9.7B) implying that the signal observed in the experimental samples was specific.

Fig 9.4 Localisation of CYP2A6 mRNA to the epidermis of human skin.

Sections of human skin were incubated with ^{35}S -labelled antisense CYP2A6 RNA (A) or ^{35}S -labelled sense CYP2A6 RNA (B). The antisense probe hybridized to cells within the epidermis. Autoradiography was for 4 weeks. Magnification = X110

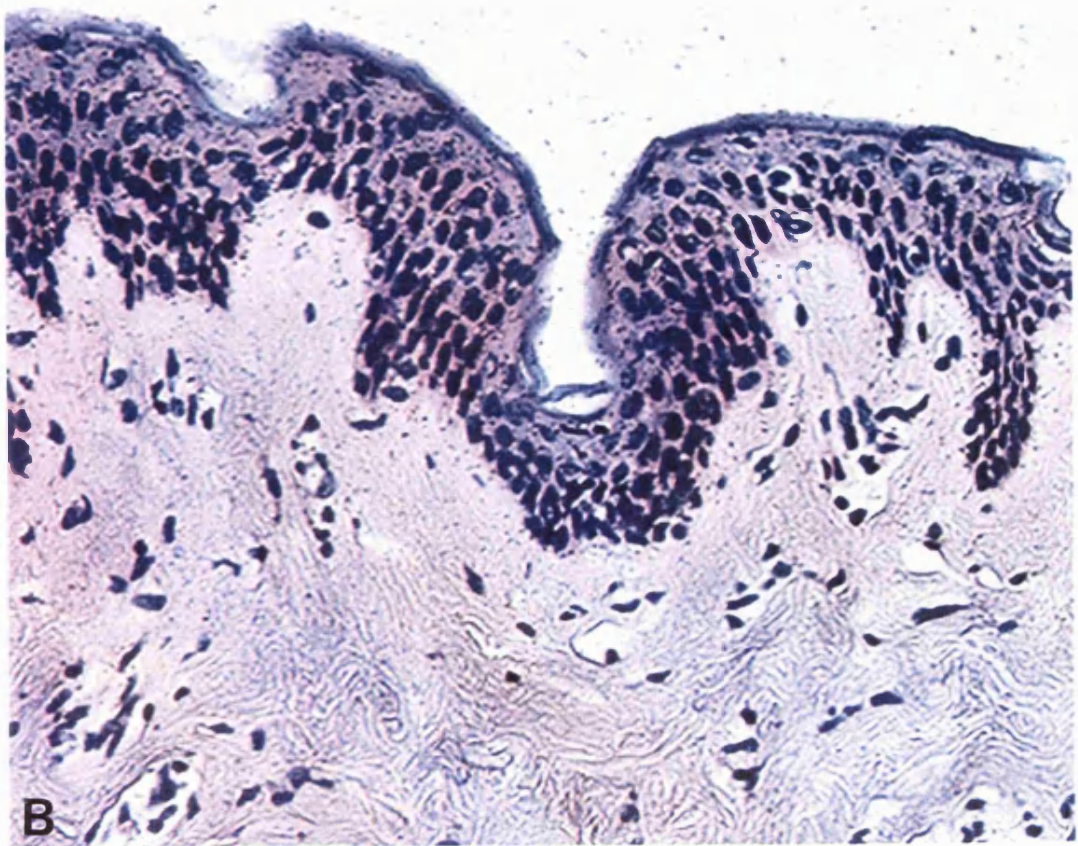
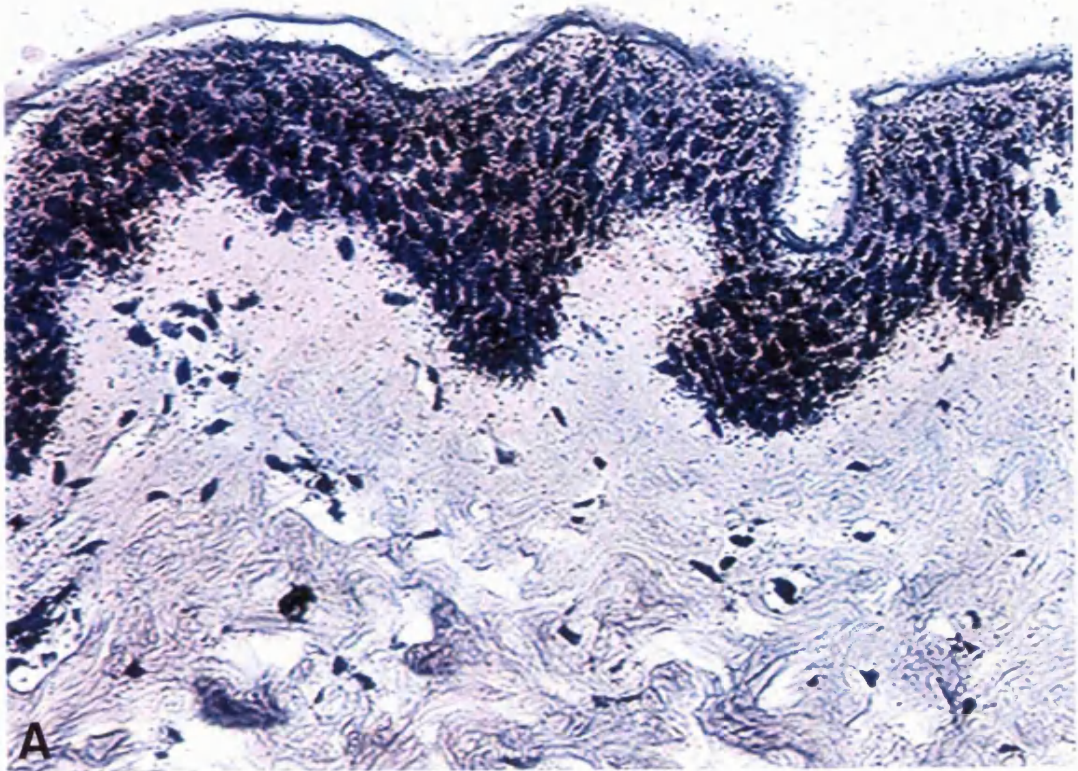


Fig 9.5 Localisation of CYP2A6 mRNA to the sebaceous gland of human skin.

Sections of human skin were incubated with ³⁵S-labelled antisense CYP2A6 RNA (A) or ³⁵S-labelled sense CYP2A6 RNA (B). The antisense probe hybridized to the sweat producing cells of the sebaceous gland. Autoradiography was for 4 weeks. Magnification = X110

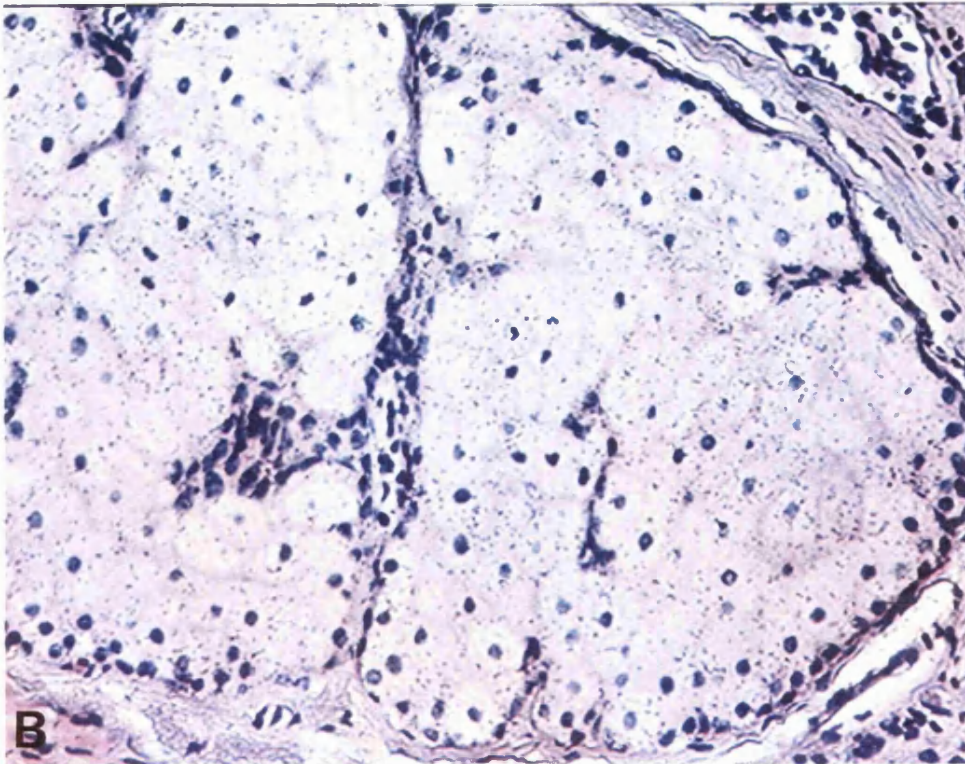
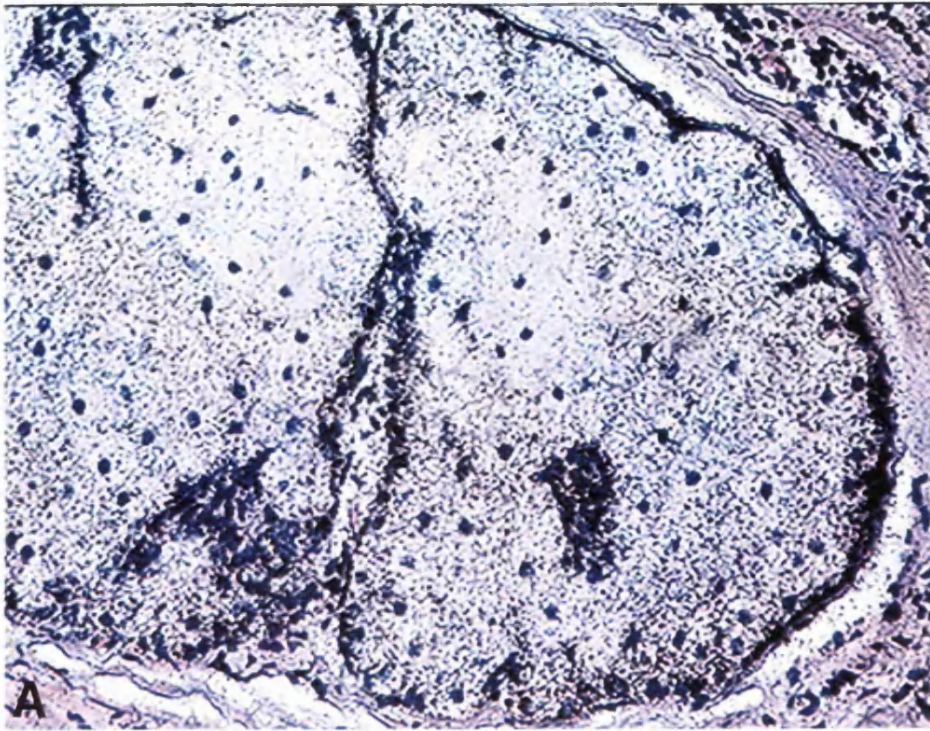


Fig 9.6 Localisation of CYP2B6 mRNA to the epidermis of human skin.

Sections of human skin were incubated with ^{35}S -labelled antisense CYP2B6 RNA (A) or ^{35}S -labelled sense CYP2B6 RNA (B). The antisense probe hybridized strongly to cells within the epidermis. Autoradiography was for 4 weeks. Magnification = X110

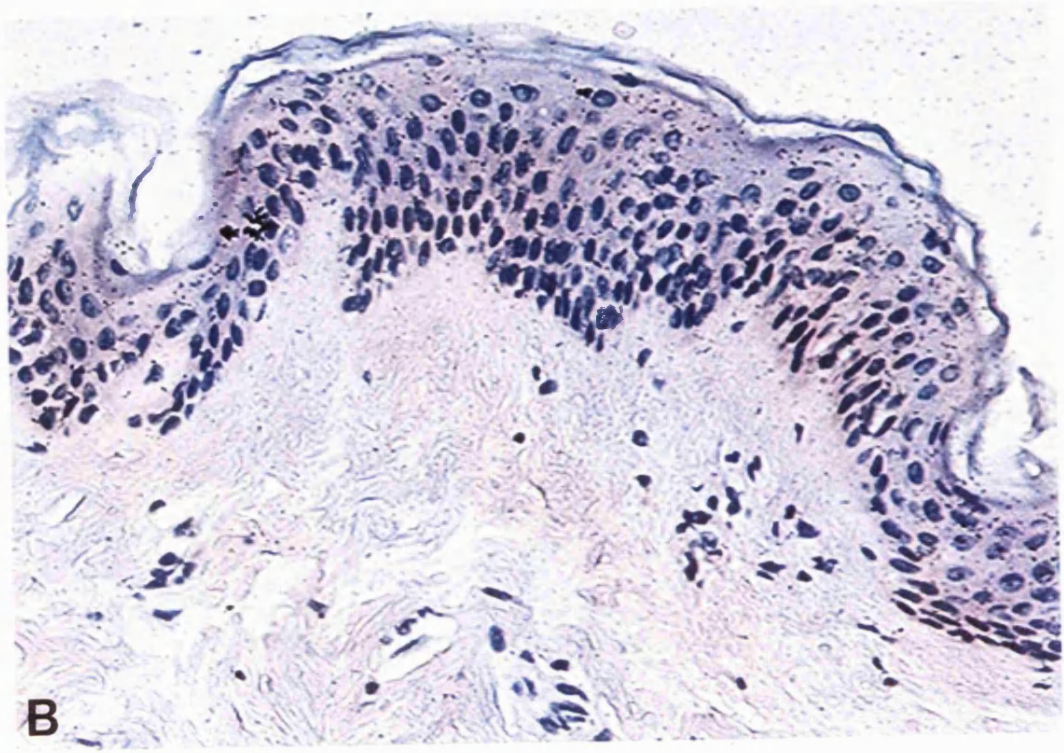
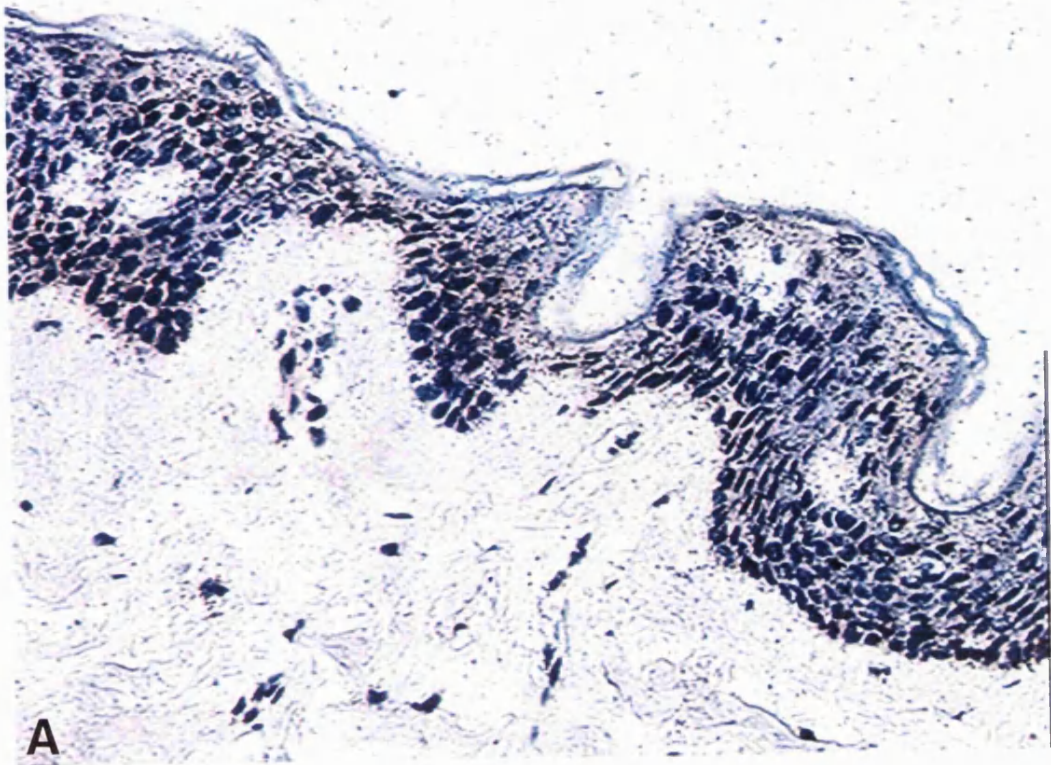


Fig 9.7 Localisation of CYP2B6 mRNA to the sebaceous gland of human skin.

Sections of human skin were incubated with ³⁵S-labelled antisense CYP2B6 RNA (A) or ³⁵S-labelled sense CYP2B6 RNA (B). The antisense probe hybridized to the sweat producing cells of the sebaceous gland. Autoradiography was for 4 weeks. Magnification = X110

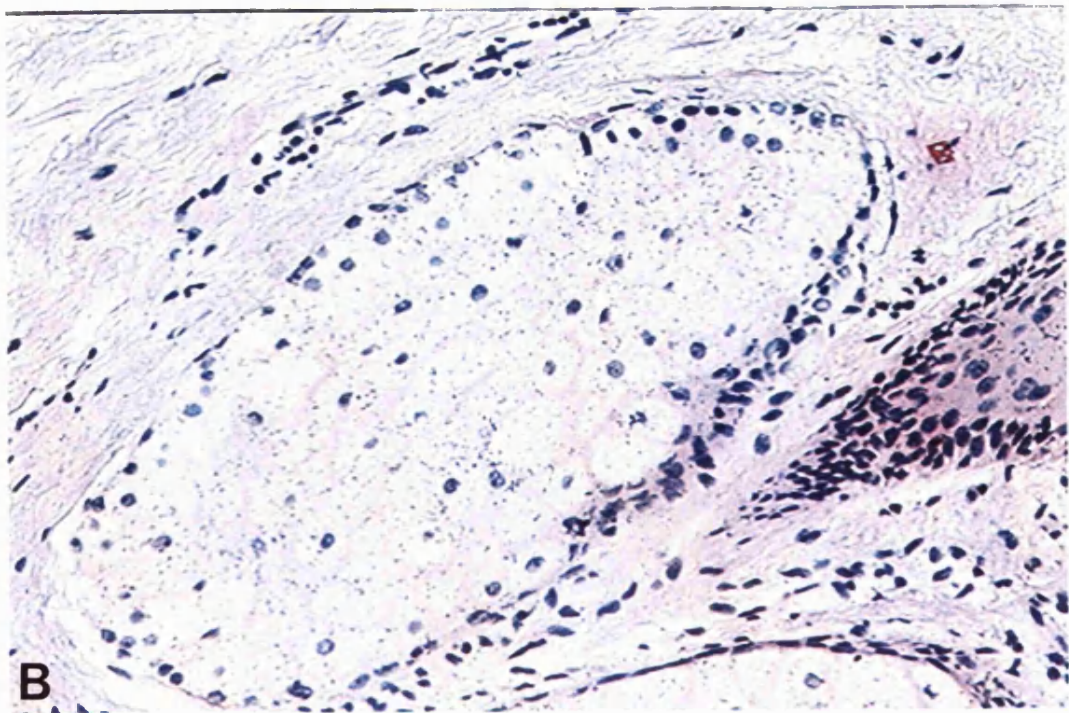
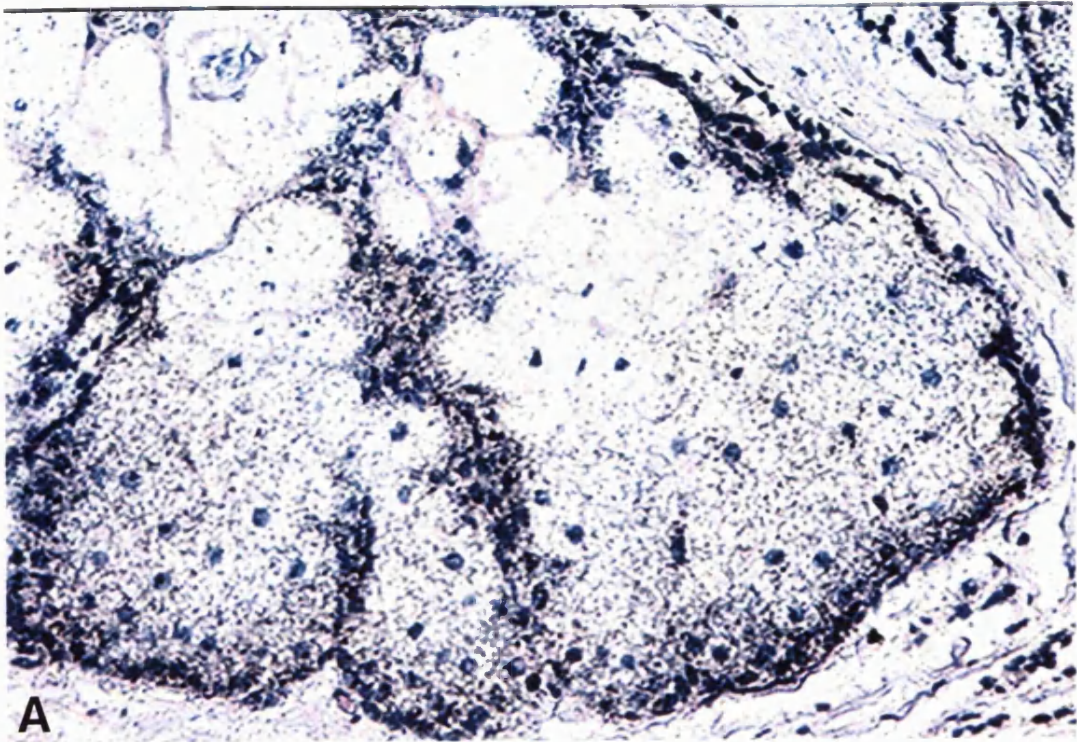


Fig 9.8 Localisation of CYP3A4 mRNA to the epidermis of human skin.

Sections of human skin were incubated with ^{35}S -labelled antisense CYP3A4 RNA (A) or ^{35}S -labelled sense CYP3A4 RNA (B). The antisense probe hybridized weakly to cells within the epidermis. Autoradiography was for 4 weeks. Magnification = X110

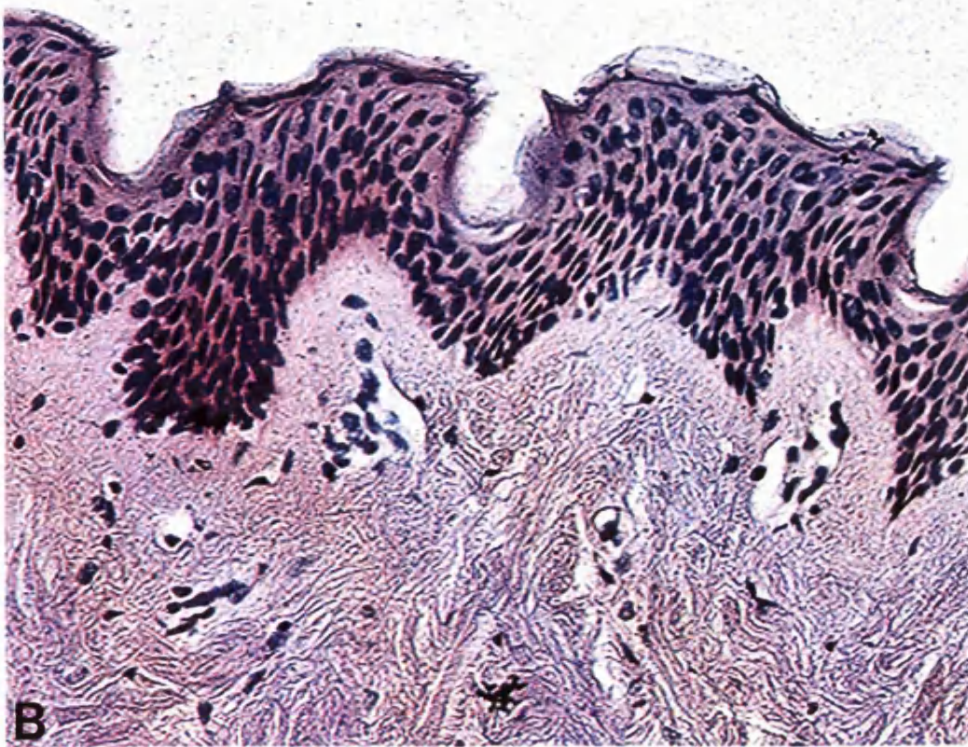
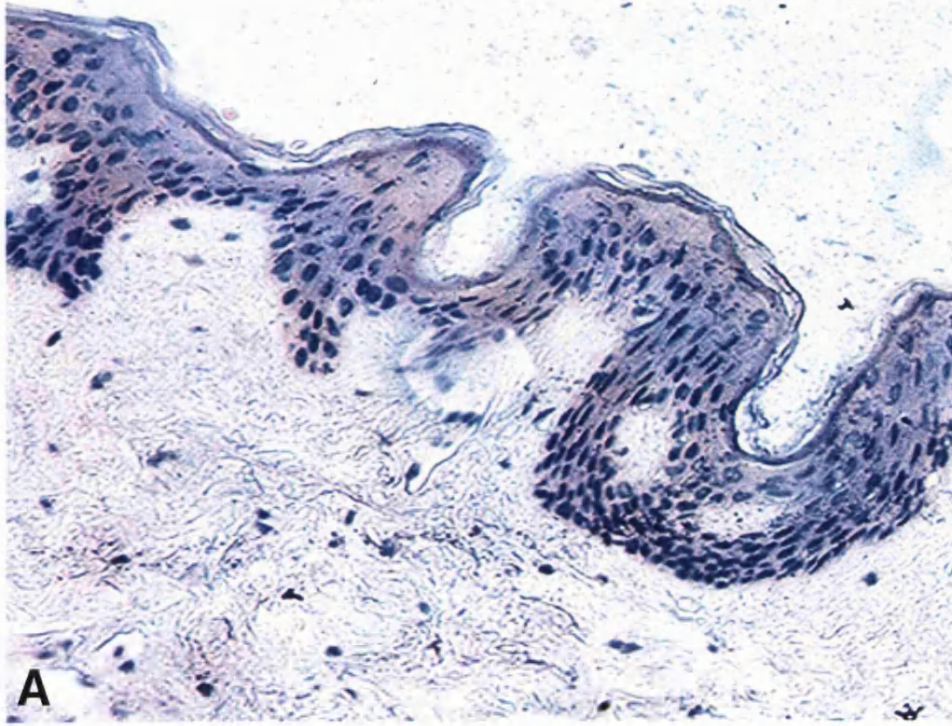
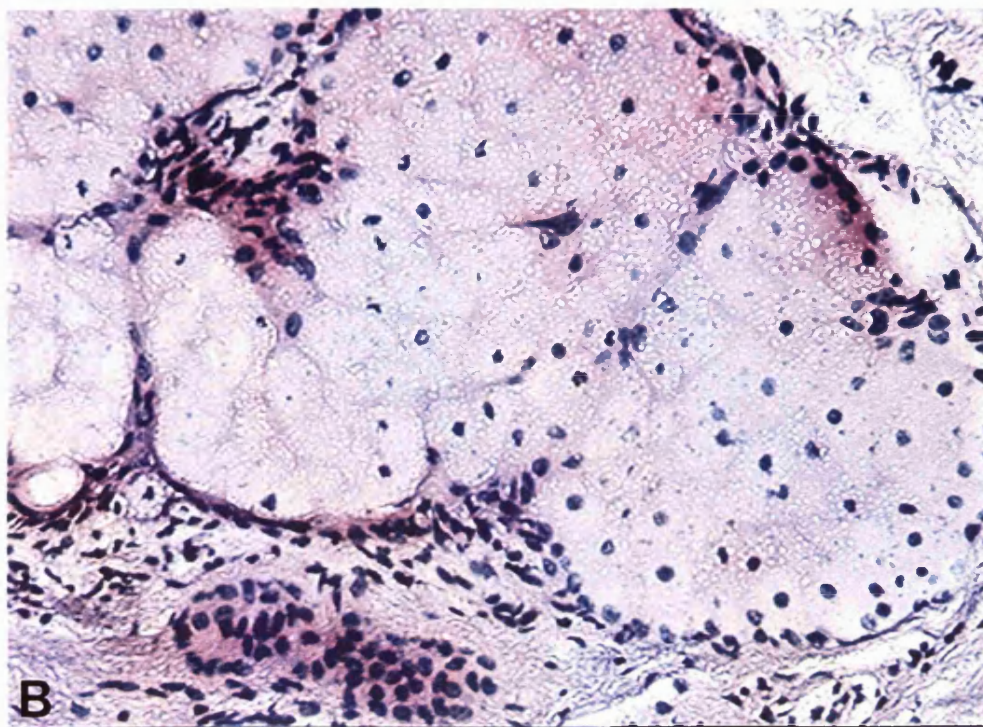
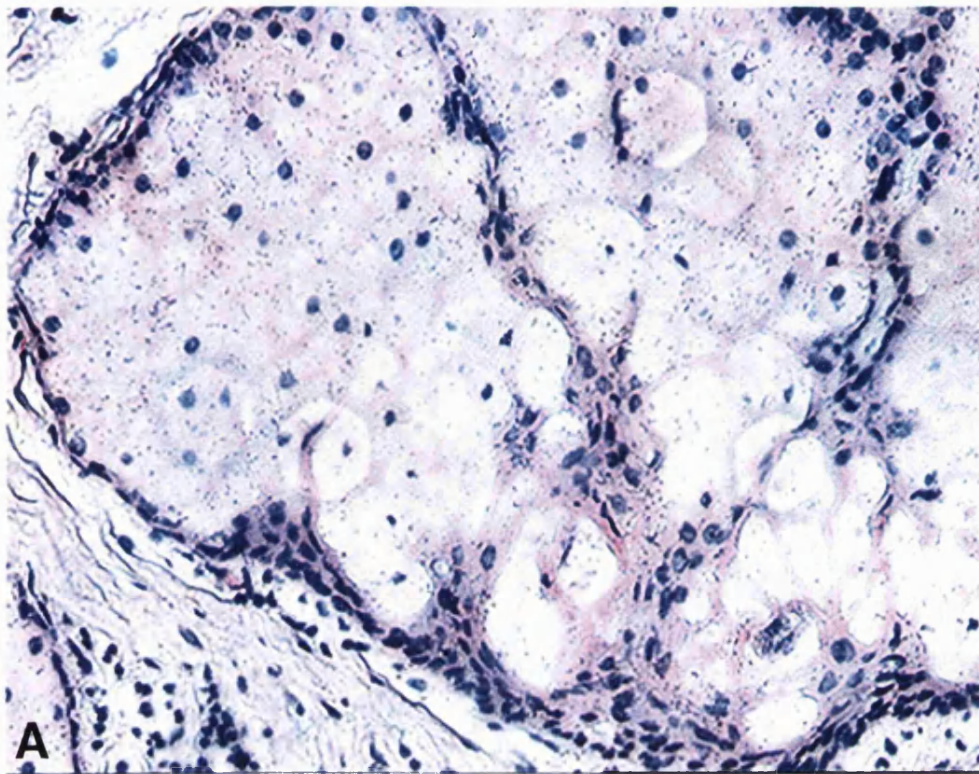


Fig 9.9 Localisation of CYP3A4 mRNA to the sebaceous gland of human skin.

Sections of human skin were incubated with ^{35}S -labelled antisense CYP3A4 RNA (A) or ^{35}S -labelled sense CYP3A4 RNA (B). The antisense probe hybridized very weakly to the cells of the sebaceous gland. Autoradiography was for 4 weeks. Magnification = X110



The CYP3A4 riboprobe showed weak hybridization relative to the control hybridization, although there was localisation of this probe to the epidermis and the sebaceous glands (figs 9.8 and 9.9). More probe hybridization was observed in the sweat gland (fig 9.9A) than in the epidermis (9.8A). The low signal intensity of CYP3A4 does not preclude the presence of another CYP3A family member such as CYP3A5 and CYP3A3 because the probe used for this analysis is specific to CYP3A4 (as detailed in section 9.2.3.2).

9.4 CYP protein expression

As detailed in section 6, numerous problems were encountered when polyclonal antibodies were used for western blot analyses of CYPs (section 6.1). Consequently, western blot analyses proved inconclusive due to the cross-reactivity of the polyclonal antibodies with keratins. Enzyme activity assays on samples of human skin microsomes could not be carried out to detect the presence of CYPs, due to the low yield of microsomes obtained and the general unavailability of sample.

Although the polyclonal antibodies used were probably cross-reacting with keratins during western blot analyses, it was hoped that IHC would at least give some indication of the regional localisation of the CYPs. This is because keratins are present only in the keratinocytes. Thus, other cells in the skin, such as those found in the sebaceous glands, which do not express keratin would only be stained if they expressed the relevant CYP protein. The immunohistochemical analyses would also confirm the results observed with the *in situ* hybridization analyses, i.e the presence of the CYPs in the epidermis and sebaceous glands.

Fig 9.10 shows the results of the IHC when antibodies to CYP2A (A and B), CYP2B (C and D) and CYP3A (E and F) were incubated with sections

of the human skin. Negative controls using pre-immune serum were also carried out (fig 9.11).

The anti-baboon CYP2A antibody cross-reacted to proteins in the lower layers of the epidermis and in the cells of the sebaceous gland. The staining of specific areas of the epidermis could indicate that the antibody cross-reacts with a class of keratins expressed only in these layers. These could be keratins 5 and 14, which are characteristic of stratified epithelia, or keratins 1 and 10, characteristic of epidermal differentiation (Sun *et al.*, 1983). The staining of these layers could also indicate the expression of CYP2A, however due to the non-specific background in the western blots this cannot be confirmed. The staining of the sebaceous glands (fig 9.10B) in the skin confirms the presence of this CYP in the skin. The areas stained using IHC correspond to areas to which the CYP2A6 probe hybridized strongly when *in situ* hybridization analyses was carried out.

The anti-rabbit CYP2B antibody strongly stained the epidermis (fig 9.10C) and the sebaceous glands (D) of the skin. Staining over the epidermis was uniform, but the stratum corneum was very strongly stained, indicating cross-reactivity with the keratinized cells in this layer. The cellular localisation of the CYP2B protein as determined by IHC, corresponds exactly to that observed with the *in situ* hybridization analyses.

Anti-rabbit CYP3A antibody strongly stained the epidermis (fig 9.10E) and sebaceous gland (F). The staining observed with this antibody was more significant when compared to that observed with CYP2A and CYP2B. The localisation of CYP3A protein in these areas of the skin corresponded to the localisation of the mRNA. However, the amount of protein observed in the sweat gland did not correlate to the amount of mRNA as seen by *in situ* hybridization analyses. This may be due to the presence in this particular sample of CYP3A5 or CYP3A3, both of which can be detected by the antibody. Thus, although the *in situ* hybridization analyses would not detect

Fig 9.10 Localisation of CYP2A, 2B and 3A to the epidermis and sebaceous gland of human skin.

Sections of human skin were incubated with an anti-baboon CYP2A antibody, (A and B) or an anti-rabbit CYP2B antibody (C and D) or an anti-rabbit CYP3A antibody (E and F). CYP2A, CYP2B and CYP3A were detected in both the epidermis and sebaceous gland. Mag = X110

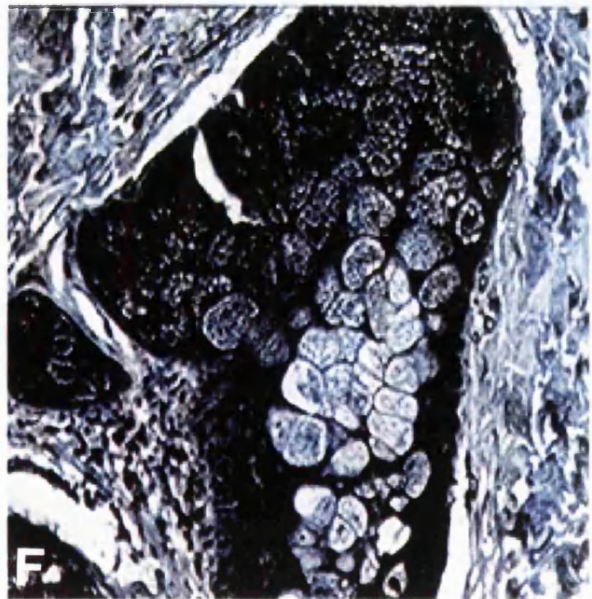
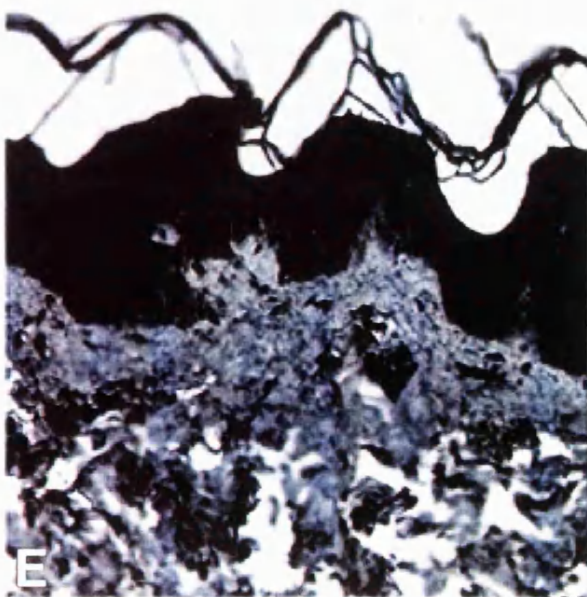
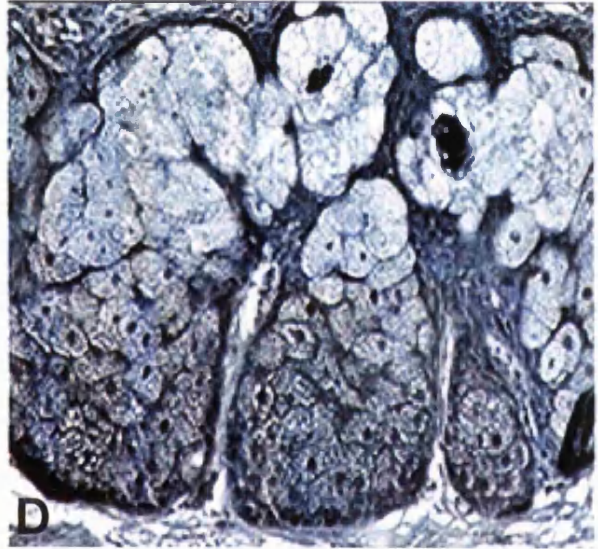
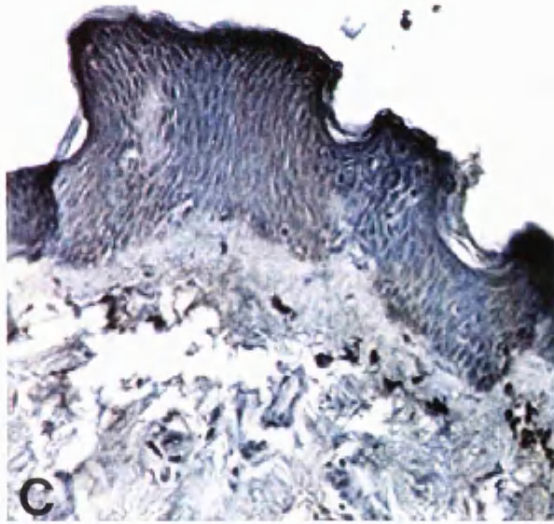
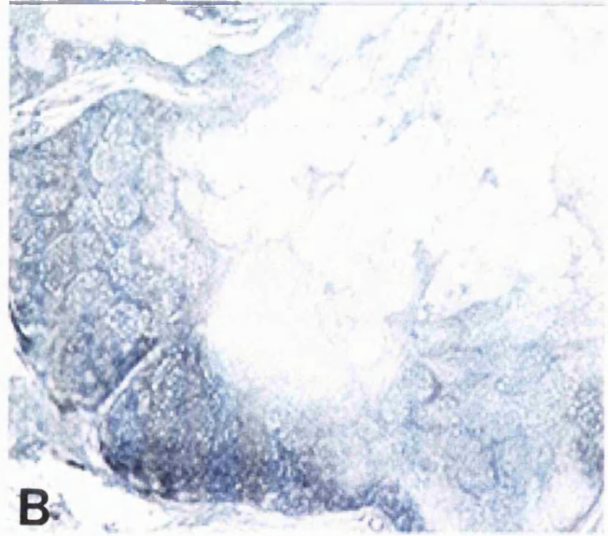
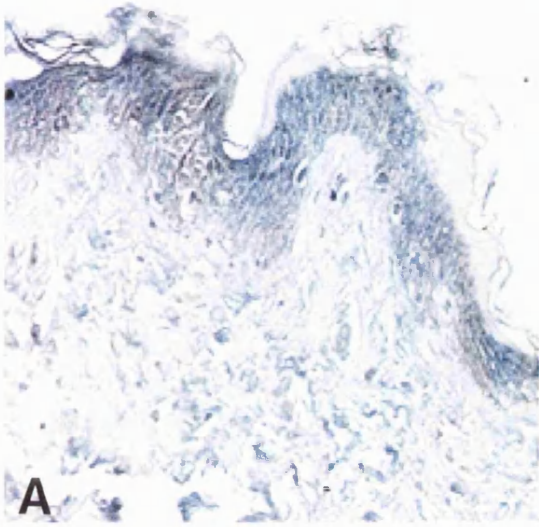
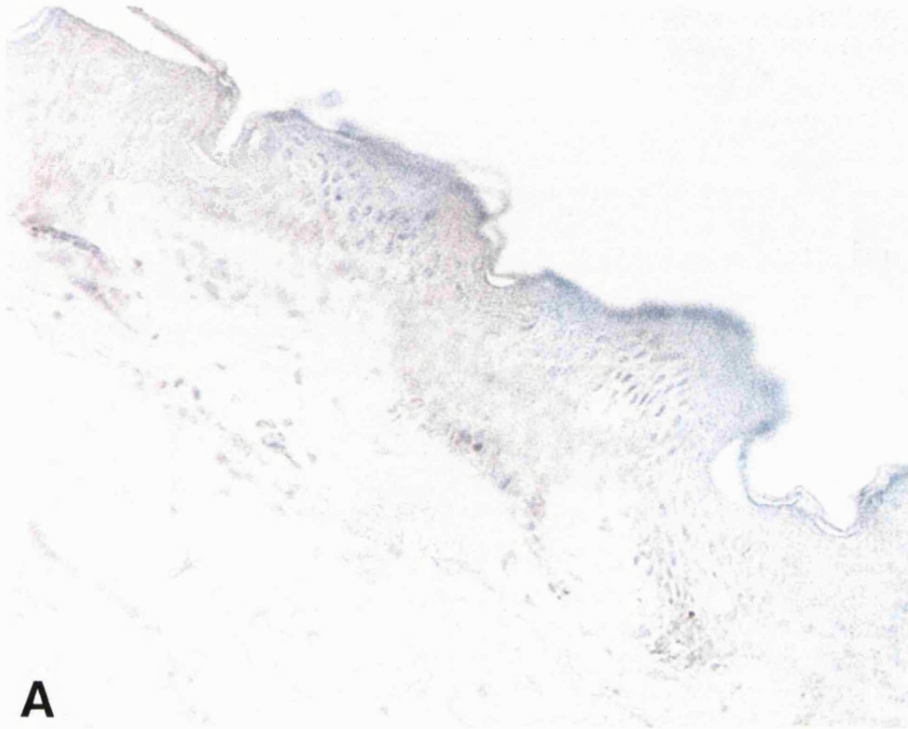
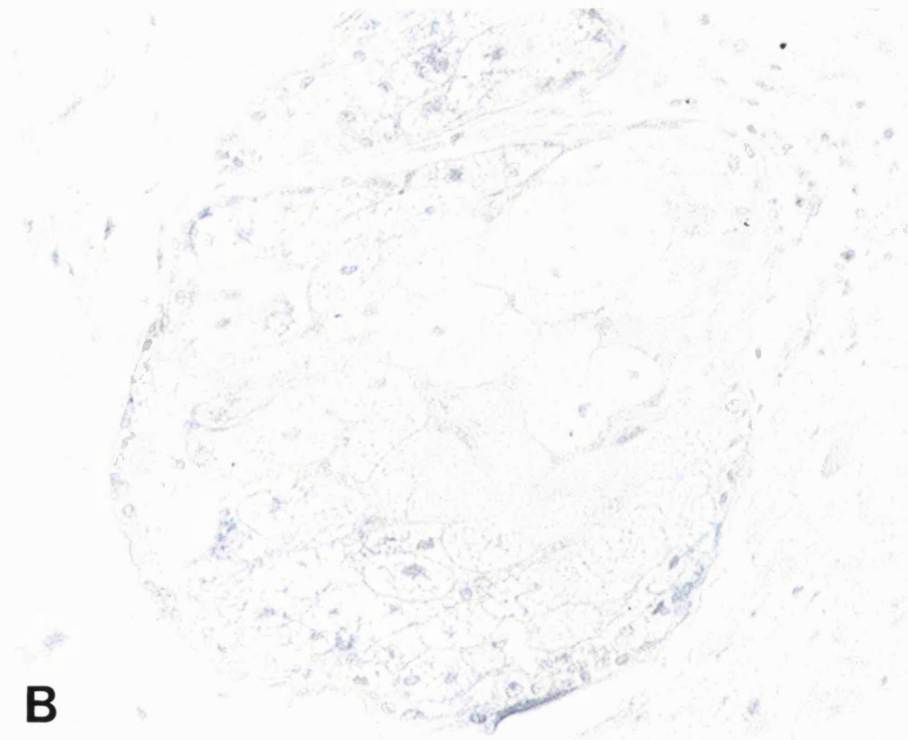


Fig 9.11 Negative staining with sheep pre-immune serum.

Sections of human skin were incubated with sheep pre-immune serum to serve as a negative control for the IHC using CYP2A, 2B and 3A antibodies. Very faint background staining was observed with the pre-immune serum in the sebaceous gland (B). In the epidermis, there was some cross-reactivity with proteins in the stratum corneum (A). Mag = X110



A



B

CYP3A5 or CYP3A3 mRNA, the antibody will detect all 3 forms of CYP3A subfamily.

9.5 Discussion

Studies on the expression of CYPs in skin have been largely restricted to rodent skin. The expression of CYPs in human skin has been limited by the unavailability of human skin samples and techniques to detect the low amounts of CYPs expressed in this tissue.

Our studies show the presence of members of the CYP2A, CYP2B and CYP3A subfamilies in the human skin. These three subfamilies have been shown to be important in the metabolism of xenobiotic compounds in laboratory animals, yet, few studies on their role and regulation of their genes in humans have been carried out due to the unavailability of human tissue.

RNase protection assays, which are more sensitive and are quantitative, have detected the presence of CYP2A6, CYP2B6 and CYP3A4 mRNAs in human skin samples. The amounts of these CYPs in the human skin are low (<1 molecule/cell) however, as mentioned in section 1.10.2 these small amounts may be significant in a tissue such as the skin which has reservoir characteristics, and is exposed to a wide variety of foreign compounds, either accidentally or intentionally.

Interindividual variation in the expression of the CYPs in the skin samples analysed shows that these enzymes illustrate the same variability in this tissue as they do in human liver. Thus, some of the regulatory mechanisms that control their expression in human liver are probably involved in the skin.

The co-localisation of the CYP mRNAs and proteins in human skin correlates to other studies carried out in rodent and human skin. In rodents, CYPs have been localised to the epidermis, sebaceous glands and hair

follicles. In human and rodent skin, phenobarbital inducible CYP isoforms have been localized to the epidermis, sebaceous glands and hair follicles (Baron *et al.*, 1986, Baron *et al.*, 1985). These studies have been carried out at the protein level using IHC techniques. We have shown the co-localisation of the mRNA and proteins encoding CYP2A, CYP2B and CYP3A in the epidermis and sebaceous glands of a sample of skin from a single individual. Unfortunately, the sample that was being used for analyses did not contain any hair follicles and thus we could not ascertain whether the CYPs were present in this particular skin appendage. The presence of these enzymes in the sebaceous gland and epidermis implies that this is probably a mechanism that the skin of animals has developed to combat the continuous challenge from environmental pollutants it faces on a day to day level.

The results obtained with the CYP3A4 *in situ* hybridization analyses and the IHC are probably because the individual from whom the skin sample was obtained did not express large quantities of CYP3A4 in the skin. Instead the individual probably expressed either CYP3A3 or CYP3A5. The riboprobe is not specific for these isoforms and will thus be digested by the RNase A/T1 cocktail. The anti-CYP3A antibody on the other hand recognises all three forms of this subfamily, thus the intense staining with the antibody. These results are similar to those obtained by Murray *et al.*, (1988). This group located members of the CYP3 family in the non-keratinized epidermis and epithelium of the sebaceous gland of human skin. The exact isoform that this antibody detected was not reported but it was probably a member of the human CYP3A subfamily. There have been reports of the high expression of CYP3A5 in human skin *in vivo*, relative to CYP3A3 and CYP3A4 (Li *et al.*, 1994). Another study suggests that CYP3A3 is expressed in the human skin too (Mercurio *et al.*, 1995).

The results obtained above suggest that interindividual variation in the expression of CYP2A, 2B and 3A occur in the human skin. Members of the

CYP3A family are the most highly expressed. The exact isoform probably varies from one individual to another. Further studies with probes specific to *CYP3A3* and *3A5* will probably help clarify the ambiguity of the present results. In addition to this, the development of specific monoclonal antibodies to these particular human isoforms will enable the complete range of isoforms in the human skin to be identified. With data such as this, individual risk assessment can be carried out especially with regards to cutaneous toxicity.

***IN VITRO* SYSTEMS
FOR TOXICOLOGICAL
STUDIES**

10.1 *In vitro* systems for the study of foreign compound metabolism

In the previous chapters, studies were described on the expression of *FMOs* and *CYPs* in human tissues such as the skin, liver, lung and kidney. The investigation of these enzymes in humans is severely limited due to the lack of human tissue available for experimentation. As a result, development of *in vitro* systems which would serve as *in vivo* models to study these enzymes is a growing field.

To date no studies on the expression of *FMOs* in primary keratinocytes or HaCaT cells have been published. Our aim was to investigate the range of *FMOs* and *CYPs* present in these culture systems and whether or not this correlated with those found in whole skin.

We have focused our studies on cultures of primary human epidermal keratinocytes and an immortalised human keratinocyte cell line (HaCaT). These culture systems have not been completely characterised in terms of their drug metabolising capabilities. It is important that before these systems can be used, for drug metabolism studies, the range of foreign compound metabolising enzymes expressed in them are identified. This would serve the dual purpose of knowing if such systems express the same range of foreign compound metabolising enzymes that are expressed in whole skin and whether these systems could be used for studies in the regulation of genes encoding these enzymes.

10.2 Primary human epidermal keratinocytes

As detailed in section 2.2.2, primary human keratinocytes were obtained from two different sources. One culture system was obtained commercially from Clonetic Corporation, USA. These primary keratinocytes

were established from a 26 year old Caucasian female. Our initial experiments using northern blot hybridization analysis used RNA isolated from these cells.

Northern blot hybridization analyses with FMOs1, 2, 3, 4 and 5 cDNA probes showed no hybridizing band with this sample. No hybridization occurred with CYP2A, CYP2B and CYP3A cDNA probes. To ascertain if this particular culture expressed mRNA for any drug metabolising enzymes, the northern blots containing this sample were hybridized with a 180 bp fragment from the human cytochrome P450-reductase cDNA (fig 10.1). All samples on the northern blot showed a hybridizing band with this fragment except the human keratinocytes. This proved that the culture provided to us by the company had an inherent deficiency in expressing any foreign compound metabolising enzymes. Due to the limited amount of this sample RNase protection assays could not be carried out to confirm the results of the northern blot hybridization analyses.

Primary cultures of human epidermal keratinocytes were instead established from whole skin samples obtained from breast reduction surgery, as detailed in section 2.2.2.2. These primary cultures were not passaged because the plating efficiency of primary keratinocytes is known to be low. For reasons unknown to us, keratinocytes derived from certain skin samples could not be cultured. Moreover, depending on the sample, several problems were encountered in trying to rid the culture of melanocytes. Although the tissue culture medium (KGM) is supposed to support only keratinocyte growth, in certain culture samples, both keratinocytes and melanocytes were present. Therefore, the numbers of cultures that could be used for experimentation were limited. All experiments were carried out on cultures that were grown until 90% confluent.

Only RNase protection assays were carried out on the RNA extracted from these cultures. Initially we decided to use the "Direct Protect [©]" (Ambion

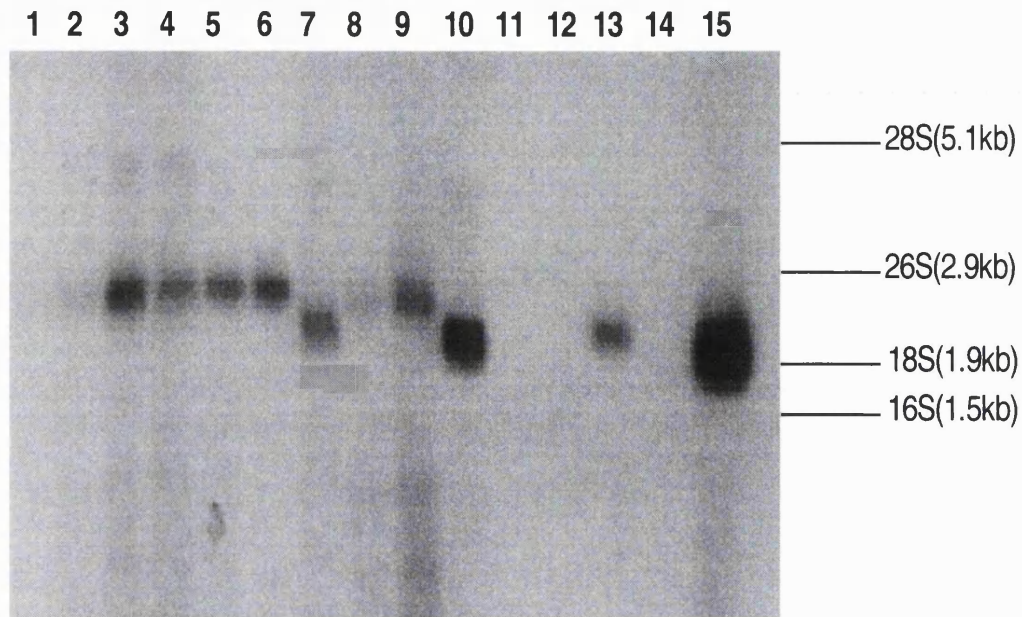


Fig 10.1 RNA samples (15 μ g) were electrophoresed on a denaturing agarose gel. Samples were from human lung (lanes 2-5), cynamologous monkey lung (lane 6), rabbit lung (lane 7), human liver (lanes 8 and 9), rabbit liver (lane 10), HaCaT cells (lane 13), primary culture of human epidermal keratinocytes (lane 14) and marmoset liver (lane 15). Total *E. Coli* RNA (1 μ g) electrophoresed concurrently with the samples (lanes 1 and 12) served as size markers with the 28S and 18S rRNA in the samples. The blot was hybridized with a radiolabelled 180bp fragment of a cDNA encoding cytochrome P450 reductase. Autoradiography was carried out for 3 weeks.

Inc., USA) kit and protocol, to enable us to carry out RNase protection assays without the need to extract the RNA from the cells. This however, gave a lot of background bands and no clear protected fragment was observed. As a result, it was decided to extract the RNA from the cells and carry out routine RNase protection analysis on these samples.

RNase protection assays using probes specific to FMOs1, 2, 3, 4 and 5 mRNAs showed that cultures derived from different individuals expressed a variety of FMOs. Only a single primary culture expressed FMO1 mRNA out of five different cultures analysed (fig 5.2.1, 5.2.2 and 5.2.3). The amount was comparable to that found in whole skin samples, although even then it was <1 molecule/cell.

FMO2 mRNA was the most widely expressed FMO in the primary cells. Of the four samples analysed, all expressed FMO2 mRNA (fig 5.2.2, 5.3.1 and 5.3.3). The whole skin from which these primary cultures were derived did not express *FMO2*. It is possible that FMO2 mRNA is only expressed in these cultures due to the addition of glucocorticoids to the culture medium. *FMO2* is known, in laboratory animals to be regulated by hormones (Lee *et al.*, 1993, Lee *et al.*, 1995).

Six different primary keratinocytes were analysed for the presence of FMO3 mRNA. Of these, three contained FMO3 mRNA (<1 molecule/cell). The primary keratinocyte samples which expressed this FMO were derived from whole skin samples that also expressed *FMO3*. However a single culture sample did not contain FMO3 mRNA although the skin from which it was derived did (fig 5.3.1, 5.4.1 and 5.4.2).

No FMO4 or FMO5 mRNAs were present in any of the primary keratinocyte samples analysed. FMO4 mRNA was not detected in any of the skin samples that these primary cultures were derived from, however FMO5 was detected in five out of eight skin samples (fig 5.4.1, 5.5.1 and 5.6). Therefore, in terms of expression of FMO4 mRNA, the primary cultures reflect

the situation in whole skin, but as for FMO5 mRNA, the situation is different, with the primary keratinocyte cultures losing the ability to express this isoform.

RNase protection assays were also used to detect the expression of CYP2A6, 2B6 and 3A4 in these cultures. Interindividual variation in the hepatic expression of these isoforms has been reported to occur (Fernandez Salguero and Gonzalez, 1995, Code *et al.*, 1997, Shimada *et al.*, 1994). The same was also apparent in cultures of primary keratinocytes.

Of the six primary cultures analysed for the presence of CYP2A6, two expressed CYP2A6 mRNA (fig 9.1.3 and 9.1.4). Primary keratinocyte cultures from skin samples that did not express CYP2A6 mRNA also did not express this isoform. However, a single sample derived from a skin sample that expressed CYP2A6 mRNA also expressed CYP2A6. A single keratinocyte sample did not express CYP2A6 although the skin from which it was derived did.

None of the primary keratinocyte RNAs analysed expressed CYP2B6 mRNA. This included a sample which was derived from a skin sample that expressed this isoform (fig 9.2.4 and 9.2.5).

CYP3A4 mRNA was expressed in five out of nine primary cultures analysed. Three cultures derived from skin samples expressing CYP3A4 mRNA also expressed this mRNA (fig 9.1.3, 9.2.4 and 9.3.4).

Detection of the relevant FMO and CYP proteins in these cultures was not possible due to the limited quantity of sample available. However, in early studies a few western blotting experiments were carried out on primary keratinocyte samples. But, the cross reactivity of the antibodies to the keratins in these cultures was apparent.

Attempts were made to detect the proteins using immunohistochemistry on the primary keratinocytes cultured on coverslips. This confirmed the cross-reactivity observed with the western blot analysis, because the cells were stained in the presence of pre-immune serum. Thus, it appeared that the

animal in which the antibodies were developed recognised a protein in these cells before being injected with the antigen.

10.3 HaCaT cells

The HaCaT cell line is a spontaneously transformed human epithelial cell line from adult skin (Boukamp *et al.*, 1988). The cell line maintains full epidermal differentiation and has been shown to reform an orderly structured and differentiated epidermal tissue when transplanted onto nude mice. The HaCaT cells derive their name from their origin i.e human adult skin propagated under low Ca²⁺ conditions and elevated temperature.

At the time they were provided to us, these cells were capable of clonal growth under normal culture conditions (37°C and independent of Ca²⁺ concentration). Morphologically the cells resemble primary keratinocytes (fig 10.2 and 10.3), however, these cells are aneuploid.

Northern blot hybridization analyses on RNA derived from these cells showed the presence of FMO4 (fig 4.5) and CYP2B mRNA (fig 9.2.1 and 9.2.2). Cytochrome P450 reductase mRNA was detected in the HaCaT cells.

RNase protection assays on the HaCaT cells confirmed the presence of FMO4 (fig 5.5.1 and 5.5.3) and CYP2B6 (fig 9.2.4 and 9.2.5) in these cells. In addition to these mRNAs, FMO1 (fig 5.2.1 and 5.2.3), FMO5 (fig 5.4.1, 5.5.1 and 5.6) and CYP3A4 (fig 9.1.3, 9.2.4 and 9.3.4) mRNA was also detected using this technique. The concentration of these mRNAs in the HaCaT cells is low (generally <1 molecule/cell).

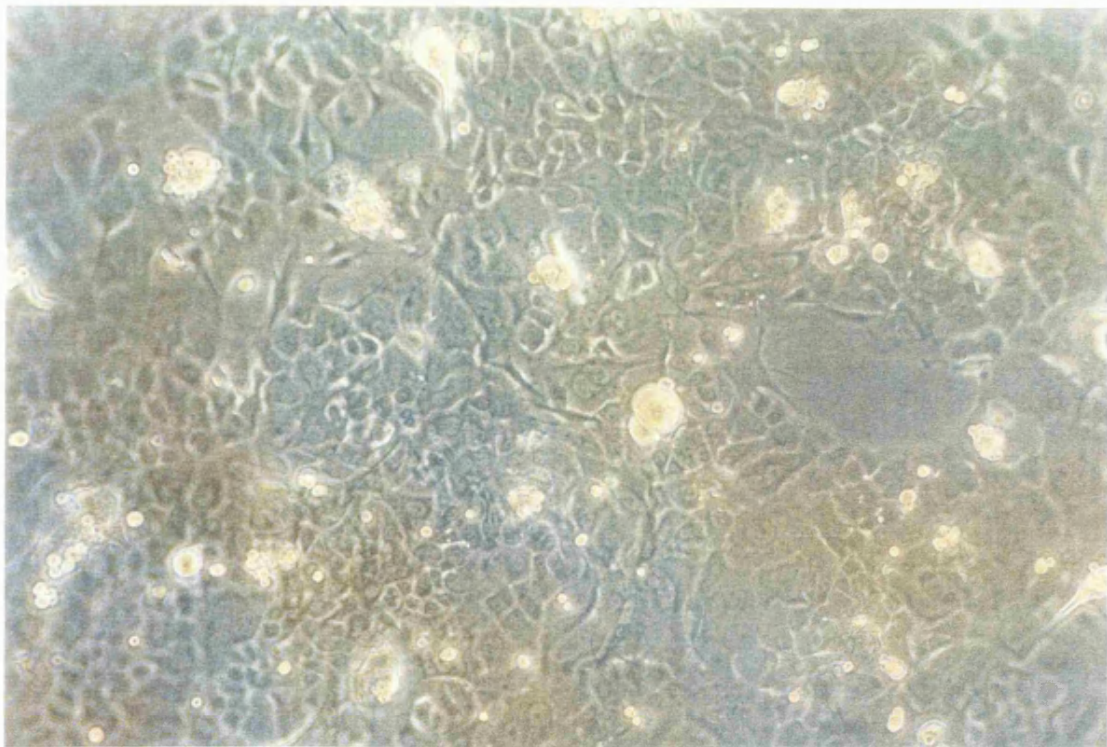
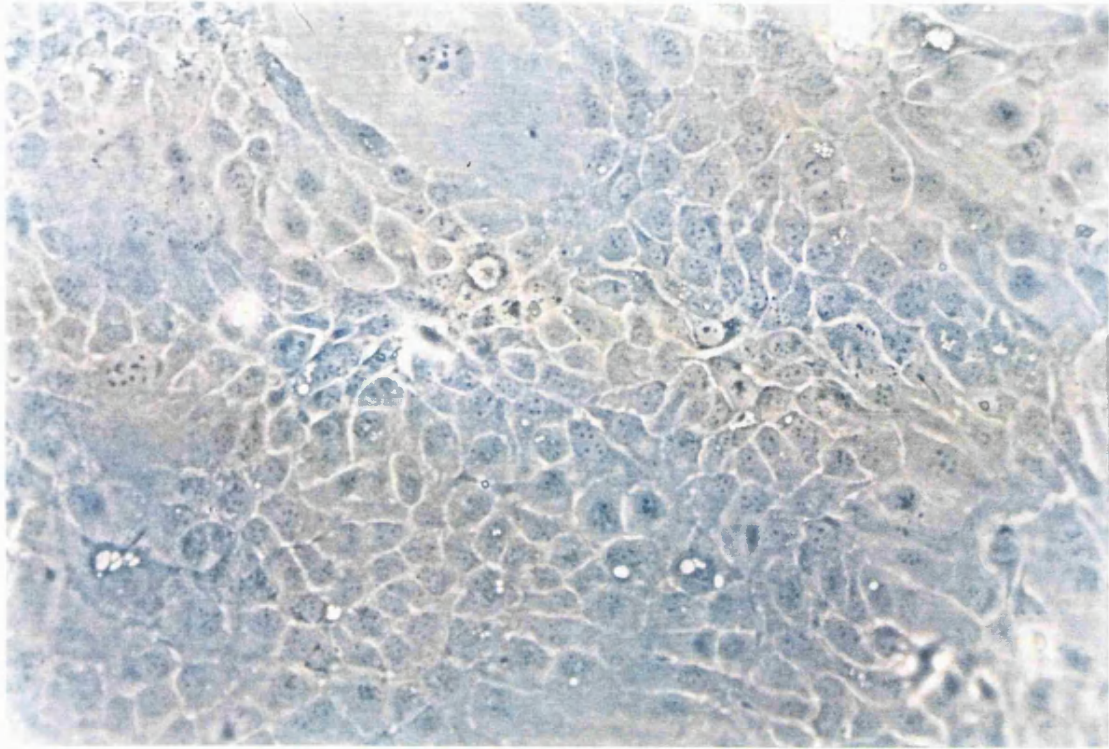
Extensive western blot analyses were carried out on this cell line. The problems encountered with this technique are described in section 6.1.

Fig 10.2 Confluent culture of primary human epidermal keratinocytes established from breast skin.

Primary cultures of human keratinocytes established from full thickness breast skin at 90% confluence. The cells were established as described in section 2.2.2.2.

Fig 10.3 Confluent culture of HaCaT cells.

HaCaT cells were cultured as described in section 2.2.1. Cells shown at approximately 75% confluence.



10.4 Discussion

From the data obtained using RNase protection assays, it is clear that primary keratinocyte cultures express CYP2A6 and 3A4, as well as FMOs 1, 2 and 3. The concentration of the mRNAs encoding these enzymes is low in these cells, but correspond relatively well to the concentration found in whole skin. Further studies on the metabolic capabilities of these cells is required to assess their ability to metabolize foreign compounds. However, one problem with primary cultures such as those that we have used is their ability to be influenced by a variety of factors such as serum and hormones in the media. Therefore, they might not be a true reflection of the *in vivo* situation. Their ability to express these enzymes in culture however could be important for studies on the regulation of both the *CYPs* and *FMOs* in humans. This is because, human samples for these investigations are difficult to obtain. Human skin is relatively more accessible than other organs and tissues. Skin samples may be obtained from plastic surgery, circumcisions, mastectomies and apronectomies.

However, ultimately, cell lines which have the ability to express a range of foreign compound metabolising enzymes would be a more viable prospect due to their availability and reproducibility of the results. Cell lines have a major limitation, because it is possible that during their transformation they do not retain all cellular functions and thus do not represent the true *in vivo* situation. Their transformation on the other hand can offer another advantage in that these cells sometimes can express genes that under normal conditions they would not. Such is the case with the HaCaT cells which we have shown to express *FMO4*. These cells can thus provide a model to study the regulation of this particular FMO which has proved to be difficult to characterise due to the inability to express it in heterologous expression systems.

Although the expression of both FMOs and CYPs in keratinocyte culture systems is low, these cells have the ability to express foreign compound metabolising enzyme mRNAs. More definitive studies are required to assess their metabolic capabilities together with the development of sensitive techniques to detect these enzymes. Ultimately the ability to use cultures such as the above to test individual risks to chemicals would prove invaluable in the study of the role and regulation of the human FMOs and CYPs.

SUMMARY

11 Summary of results

This thesis presents data on the expression of *FMOs* and *CYPs* in human skin and keratinocyte culture systems. Until recently the *CYPs* have been studied more widely than the *FMOs*, in terms of their xenobiotic metabolising capabilities. Recently however, the importance of *FMOs* as xenobiotic metabolising enzymes have led to further investigations into their role and expression.

There have been very few reports on the expression of *FMOs* in the human tissues, particularly the skin. Most of the work carried out on the skin has been focused either on the activity or localization of *FMOs* in the skin of laboratory animals. No data on the expression *FMO* mRNAs in human skin or their cellular localization in this tissue have been published.

Our studies also extended to the investigation of the *FMOs* in keratinocyte culture systems. Not only have these culture systems not been completely characterised in terms of their drug metabolizing capabilities, but no studies have been carried out on the expression of *FMOs* in keratinocyte cultures. We focused our studies on primary cultures of human epidermal keratinocytes derived from human skin and on an immortalized human keratinocyte cell line (HaCaT). These systems were assessed for their ability to express the *FMOs* and *CYPs* relative to whole skin.

Southern blot hybridization analysis of genes encoding human *FMOs* 2, 3, 4 and 5 in Chapter 3 suggest that the *FMOs* are encoded for by single genes that have a minimum size of 25 kb. This result is similar to that obtained by Dolphin *et al.*, (1997b) who showed, through the use of vectorette-PCR, that *FMO3* is encoded for by a single gene, of minimum size 22.5 kb. To confirm that there is a single gene for each of the *FMOs* requires Southern blot analysis, of human genomic DNA, with exon specific probes for each of the four cDNAs.

The expression of FMO mRNAs in human skin, primary human epidermal keratinocytes and HaCaT cells was investigated using two methods. These were northern blot hybridization analyses (Chapter 4) and RNase protection assays (Chapter 5). Northern blots proved to be relatively insensitive in the detection of FMO mRNAs in these samples. Using this method, only FMO1 mRNA was detected in the human skin. No FMOs were detected in the commercially obtained primary culture of human epidermal keratinocytes, while only FMO4 mRNA could be detected in the HaCaT cells. Using RNase protection assays which are more specific, sensitive and quantitative, a clearer picture of the FMO mRNA expression in the skin and culture samples was obtained. FMOs 1, 3 and 5 mRNAs are expressed in various human skin samples and there is a considerable degree of interindividual variation in their expression. The amounts of the FMO mRNAs were approximately <1 molecule/cell. *FMO1* was the most highly expressed *FMO* form in the skin samples. No correlation between the ages of the individuals and the expression of *FMOs* was observed. The primary keratinocytes also showed a variation in the expression of FMOs, with some samples expressing FMO2 or FMO3 mRNAs or both or none. There was no correlation between the expression of FMO3 mRNA in the primary culture of human epidermal keratinocytes with the expression of this mRNA in the individual from whom the skin was obtained. FMO 1, 4 and 5 mRNAs were detected in the HaCaT cells at a concentration of < 1 molecule/cell.

Analyses on the expression of FMO proteins was carried out using western blot analyses (Chapter 6) and enzyme activity assays (Chapter 7). Western blot analyses were done using antibodies specific to FMOs 1, 3 and 5. Analyses of FMO2 were not carried out because it has recently been found (Dolphin *et al.*, 1998; submitted) that the human *FMO2* gene has a premature termination codon within the FMO2 protein coding sequence. Consequently, although the mRNA is transcribed, the protein is not detectable. Analyses

using western blotting was unsuccessful due to the cross-reactivity of the antibodies to non-specific proteins within the skin microsomes and cytosol. These non-specific cross-reacting proteins are probably keratins. Moreover, the amounts of FMOs in the human skin are probably very low. As such antibodies with higher titres will be required to detect the FMOs present.

Human skin microsomes were assayed for their activity towards methimazole which is a substrate for FMOs 1, 2, 3 and 4. Inconclusive results were obtained when we carried out these enzyme activity assay studies. The addition of enhancers of FMO activity, Emulgen 911 and *n*- octylamine, did not lead to any observable increase in the activity of FMOs in the skin. A non-linear curve was obtained when the assay was carried out. This is probably due to the presence of contaminating proteins in the microsomes. The lack of any activity towards methimazole may be because it is FMO5 that is the major FMO present in this tissue. FMO5 has been shown to exhibit either low or no activity towards methimazole. Unfortunately, due to the limited availability of human skin samples, further activity studies on specific substrates for FMO5 could not be carried out. Additional experiments using these substrates should be carried out to fully understand if any FMO protein is present in the human skin and what the role of this FMO might be. Activity assays on primary cultures of human epidermal keratinocytes and HaCaT cells were not carried out. This was mainly due to the limited quantity of sample, in the case of the primary cultures, and the inability to obtain microsomes from the HaCaT cells. Another reason for the lack of activity in the skin microsomal samples could be the extreme lability of the FMOs. The extraction procedures during microsomal preparation, although carried out as close to 4°C as possible, are harsh and have been optimised for the retention of CYP related enzyme activity. The conditions for the preparation of microsomes for the analyses of FMOs probably need to take into consideration the lability of these enzymes and thus need modification.

Cellular localisation of the FMOs was carried out on a sample of skin obtained from a single individual (Chapter 8). Localisation was investigated using IHC and *in situ* hybridization analyses. IHC was unsuccessful due to the cross reactivity of the antibodies to the keratins and the low titres of the antibodies being used by us. *In situ* hybridization analyses localised FMOs 1, 3, 4 and 5 mRNAs to the epidermis and sebaceous glands in the skin. The signals obtained with the different riboprobes varied, with FMO5 giving the highest signal, followed by FMO1, then FMO3 and finally FMO4. These results are different to those obtained with the RNase protection assays. This may be because in the RNase protection assays total mRNA is detected. Whilst in the *in situ* experiments it is possible to localise an mRNA to a specific cell type. Another reason for the different signal intensities could be that the specific activities of the riboprobes differed.

Numerous studies on the expression of CYPs in the skin have been carried out. However, of these, few have been carried out on human skin. To investigate the range of CYPs expressed in human skin, we looked at the expression of *CYP2A*, *CYP2B* and *CYP3A* (Chapter 9). The same techniques that were used to investigate FMO expression in the skin were used. In addition to human skin, we extended our studies to the expression of members of these subfamilies in primary cultures of human epidermal keratinocytes and HaCaT cells. Northern blot hybridization analyses detected the presence of *CYP2B6* mRNA in the HaCaT cells. RNase protection assay showed the presence of *CYP2A6*, *2B6* and *3A4* mRNAs in some of the skin samples analysed. In the primary cultures of human epidermal keratinocytes, some samples had *CYP2A6* and *CYP3A4* mRNAs. None contained *CYP2B6* mRNA. This was however detected in the HaCaT cells. There was no correlation between the expression of the *CYP2A*, *2B* and *3A* mRNAs in the skin samples and the primary epidermal keratinocyte cultures derived from the skin samples. Therefore, it could not be determined whether in this

culture system the cells retain the ability to express the same CYPs as are expressed in the whole skin.

Western blot analyses, of CYPs, in microsomes from human skin could not be carried out, however, studies on HaCaT cells and a few primary cultures, showed non-specific cross-reactivity with proteins within these cells. Cellular localisation of CYP2A, CYP2B and CYP3A proteins using IHC indicated that the cause of the cross-reactivity on western blots was probably due to the keratins in the epidermal layers, because the epidermis was darkly stained with antibodies to CYP2A, CYP2B or CYP3A. Interestingly however, the cells of the sebaceous glands were deeply stained with these antibodies, indicating the presence of members of these subfamilies in these cells.

CYP2A6, 2B6 and CYP3A4 mRNAs were localised to the epidermis and sebaceous gland by *in situ* hybridization. CYP2A6 and 2B6 mRNAs were more highly expressed than CYP3A4 mRNA. The amount of CYP3A protein detected by IHC as compared to the amount of mRNA detected by *in situ* hybridization analyses can be explained, because, the antibody can detect all three forms of CYP3A, whereas, the probe used in the *in situ* hybridization analyses would only be able to detect CYP3A4. Further studies with probes specific to CYP3A3 and CYP3A5 will help clarify the isoforms of the CYP3A subfamily present in the human skin.

From the results obtained in this thesis, it can be seen that a range of xenobiotic metabolising enzymes are expressed in the human skin, primary cultures derived from them and the immortalised cell line, HaCaT. The expression of a range of FMOs and CYPs in this tissue and their localisation to the epidermis and sebaceous glands, indicates that these enzymes probably serve to protect the body from harmful chemicals that it comes into contact via the skin. The expression of these enzymes in cultures derived from the skin and especially in a cell line allows for the use of such systems for further studies into their role and regulation in humans. However, these

systems would not be suitable for drug metabolism studies because they do not express the same range of FMOs and CYPs that are present in human skin *in vivo*.

BIBLIOGRAPHY

Agarwal, R., Jugert, F. K., Khan, S. G., Bickers, D. R., Merk, H. F. and Mukhtar, H. (1994) *Biochem Biophys Res Commun*, **199**, 1400-1406.

Ahmad, N., Agarwal, R. and Mukhtar, H. (1996) *Skin Pharmacol.*, **9**, 231-241.

Akin, F. J. and Norred, W. P. (1976) *J-Invest-Dermatol*, **67**, 709-712.

Al Waiz, M., Ayesh, R., Mitchell, S. C., Idle, J. R. and Smith, R. L. (1987a) *Lancet*, **1**, 634-635.

Al Waiz, M., Mitchell, S. C., Idle, J. R. and Smith, R. L. (1987b) *Xenobiotica*, **17**, 551-558.

Al Waiz, M., Mitchell, S. C., Idle, J. R. and Smith, R. L. (1987c) *Toxicology*, **43**, 117-121.

Al-Waiz, M., Ayesh, R., Mitchell, S. C., Idle, J. R. and Smith, R. L. (1987) *Clin Pharmacol Ther*, **42**, 588-594.

Al-Waiz, M., Ayesh, R., Mitchell, S. C., Idle, J. R. and Smith, R. L. (1989) *J Inherit Metab Dis*, **12**, 80-85.

Allen Hoffmann, B. L. and Rheinwald, J. G. (1984) *Proc-Natl-Acad-Sci-U-S-A*, **81**, 7802-7806.

Angerer, L. M., Cox, K. H. and Angerer, R. C. (1987) *Methods Enzymol*, **152**, 649-661.

Atta Asafo Adjei, E., Lawton, M. P. and Philpot, R. M. (1993) *J-Biol-Chem*, **268**, 9681-9689.

Ayesh, R., Al-Waiz, M. and Crother, N. J. (1988) *Br J Clin Pharmacol*, **25**, 664.

Ayesh, R., Mitchell, S. C., Zhang, A. and Smith, R. L. (1993) *Bmj*, **307**, 655-657.

Baden, H. P. (1980) *Curr Probl Dermatol*, **10**, 345-363.

Baron, J., Voigt, J. M., Whitter, T. B., Kawabata, T. T., Knapp, S. A., Guengerich, F. P. and Jakoby, W. B. (1985) In *Biological Reactive Intermediates III: Mechanisms of Action in Animal Models and Human Disease.*, Vol. 197 (Eds, Kocsis, J. J., Jollow, D. J., Witmer, C. M., Nelson, J. O. and Snyder, R.) Plenum Press, New York, pp. 119-144.

Baron, J., Voigt, J. M., Whitter, T. B., Kawabata, T. T., Knapp, S. A., Guengerich, F. P. and Jakoby, W. B. (1986) *Adv Exp Med Biol*, **197**, 119-144.

Bartek, M. J., LaBudde, J. A. and Maibach, H. I. (1972) *J-Invest-Dermatol*, **58**, 114-123.

Beaty, N. B. and Ballou, D. P. (1980) *J Biol Chem*, **255**, 3817-3819.

Bejjani, B. A., Lewis, R. A., Tomey, K. F., Anderson, K. L., Dueker, D. K., Jabak, M., Astle, W. F., Otterud, B., Leppert, M. and Lupski, J. R. (1998) *Am-J-Hum-Genet*, **62**, 325-333.

Belpaire, F. M., and Bogaert, M. G., (1996) *Acta-Clinica- Belgica* **51**(4): 254-260.

Bhamre, S., Shankar, S. K., Bhagwat, S. V. and Ravindranath, V. (1993) *Life Sci*, **52**, 1601-1607.

Bickel, M. H. (1971) *Xenobiotica*, **1**, 313-319.

Bickers, D. R., Dutta Choudhury, T. and Mukhtar, H. (1982a) *Mol-Pharmacol*, **21**, 239-247.

Bickers, D. R. and Kappas, A. (1978) *J-Clin-Invest*, **62**, 1061-1068.

Bickers, D. R., Wroblewski, D., Tapu Dutta, C. and Mukhtar, H. (1982b) *J-Invest-Dermatol*, **78**, 227-229.

Bork, R. W., Muto, T., Beaune, P. H., Srivastava, P. K., Lloyd, R. S. and Guengerich, F. P. (1989) *J-Biol-Chem*, **264**, 910-919.

Bouclier, M., Cavey, D., Kail, N. and Hensby, C. (1990) *Pharmacol-Rev*, **42**, 127-154.

Boukamp, P., Petrussevska, R. T., Breitkreutz, D., Hornung, J., Markham, A. and Fusenig, N. E. (1988) *J-Cell-Biol*, **106**, 761-771

Breitbart, R. E., Andreadis, A. and Nadal Ginard, B. (1987) *Annu Rev Biochem*, **56**, 467-495.

Burnett, V. L., Lawton, M. P. and Philpot, R. M. (1994) *Journal Of Biological Chemistry*, **269**, 14314-14322.

Cashman, J. R. and Hanzlik, R. P. (1981) *Biochem Biophys Res Commun*, **98**, 147-153.

Cashman, J. R. and Ziegler, D. M. (1986) *Mol-Pharmacol*, **29**, 163-167.

Cathala, G., Savouret, J. F., Mendez, B., West, B. L., Karin, M., Martial, J. A. and Baxter, J. D. (1983) *DNA*, **2**, 329-335.

Chang, T. K., Yu, L., Maurel, P. and Waxman, D. J. (1997) *Cancer-Res*, **57**, 1946-1954.

Chen, H. and Aiello, F. (1993) *Am J Med Genet*, **45**, 335-339.

Chiba, K., Horii, H., Kubota, E., Ishizaki, T. and Kato, Y. (1990) *Eur J Pharmacol*, **180**, 59-67.

Chiba, K., Kubota, E., Miyakawa, T., Kato, Y. and Ishizaki, T. (1988) *J Pharmacol Exp Ther*, **246**, 1108-1115.

Chirgwin, J. M., Przybyla, A. E., MacDonald, R. J. and Rutter, W. J. (1979) *Biochemistry*, **18**, 5294-5299.

Cholerton, S. and Smith, R. L. (1991) In *N-Oxidation of Drugs: Biochemistry, Pharmacology, Toxicology*. (Eds, Hlavic, P. and Damani, L. A.) Chapman & Hall, London, pp. 107-131.

Christophers, E., Schubert, C. and Goos, M. (1989) In *Pharmacology of the Skin I* (Eds, Greaves, M. W. and Shuster, S.) Springer-Verlag, Berlin, pp. 3-31.

Code, E. L., Crespi, C. L., Penman, B. W., Gonzalez, F. J., Chang, T. K. and Waxman, D. J. (1997) *Drug-Metab-Dispos*, **25**, 985-993.

Coecke, S., Mertens, K., Segaert, A., Callaerts, A., Vercruyssen, A. and Rogiers, V. (1992) *Anal Biochem*, **205**, 285-288.

Coutts, R. T. and Beckett, A. H. (1977) *Drug Metab. Rev.*, **6**, 51-104.

Damen, F. J. and Mier, P. D. (1982) *Br-J-Pharmacol*, **75**, 123-127.

deBethizy, J. D. and Hayes, J. R. (1994) In *Principles and Methods of Toxicology* (Ed, Hayes, A. W.) Raven Press, Ltd., New York, pp. 59-100.

de la Hueraga, J. and Popper, H. (1951) *J Clin Invest*, **30**, 463-470.

Demlehner, M. P., Schafer, S., Grund, C. and Franke, W. W. (1995) *J-Cell-Biol*, **131**, 745-760.

Denhardt, D. T. (1966) *Biochem-Biophys-Res-Commun*, **23**, 641-646.

Di Monte, D., Shinka, T., Sandy, M. S., Castagnoli, N., Jr. and Smith, M. T. (1988) *Drug-Metab-Dispos*, **16**, 250-255.

Ding, S., Lake, B. G., Friedberg, T. and Wolf, C. R. (1995) *Biochem-J*, **306**, 161-166.

Dixit, A. and Roche, T. E. (1984) *Arch-Biochem-Biophys*, **233**, 50-63.

Dolphin, C., Cullingford, T.E, Janmohamed, A., Shephard, E. A., Smith, R. L. and Phillips, I. R. (1998) submitted.

Dolphin, C., Shephard, E. A., Povey, S., Palmer, C. N., Ziegler, D. M., Ayesh, R., Smith, R. L. and Phillips, I. R. (1991) *J Biol Chem*, **266**, 12379-12385.

Dolphin, C. T., Cullingford, T. E., Shephard, E. A., Smith, R. L. and Phillips, I. R. (1996) *Eur-J-Biochem*, **235**, 683-689.

Dolphin, C. T., Janmohamed, A., Smith, R. L., Shephard, E. A. and Phillips, I. R. (1997a) *Nat-Genet*, **17**, 491-494.

Dolphin, C. T., Riley, J. H., Smith, R. L., Shephard, E. A. and Phillips, I. R. (1997b) *Genomics*, **46**, 260-267.

Dolphin, C. T., Shephard, E. A., Povey, S., Smith, R. L. and Phillips, I. R. (1992) *Biochem-J*, **287**, 261-267.

Eichler, G., Rubben, A., Frankenberg, S., Jugert, F. and Merk, H. F. (1996) *Skin Pharmacol.*, **9**, 147.

Falls, J. G., Blake, B. L., Cao, Y., Levi, P. E. and Hodgson, E. (1995) *J-Biochem-Toxicol*, **10**, 171-177.

Falls, J. G., Cherrington, N. J., Clements, K. M., Philpot, R. M., Levi, P. E., Rose, R. L. and Hodgson, E. (1997) *Arch-Biochem-Biophys*, **347**, 9-18.

Feinberg, A. P. and Vogelstein, B. (1983) *Anal-Biochem*, **132**, 6-13.

Fernandez Salguero, P. and Gonzalez, F. J. (1995) *Pharmacogenetics*, **5**, S123-S128.

Fourney, R. M., Miyakoshi, J., Day, R. S. and Paterson, M. C. (1988) *Focus (BRL)*, **10**, 5-7.

Finnen, M. J., Herdman, M. L. and Shuster, S. (1984) *J Steroid Biochem*, **20**, 1169-1173.

Finnen, M. J., Herdman, M. L. and Shuster, S. (1985) *Br-J-Dermatol*, **113**, 713-721.

Flammang, A. M., Gelboin, H. V., Aoyama, T., Gonzalez, F. J. and McCoy, G. D. (1992) *Biochem. Arch.*, **8**, 1.

Gasser, R., Tynes, R. E., Lawton, M. P., Korsmeyer, K. K., Ziegler, D. M. and Philpot, R. M. (1990) *Biochemistry*, **29**, 119-124.

Ged, C., Umbenhauer, D. R., Bellew, T. M., Bork, R. W., Srivastava, P. K., Shinriki, N., Lloyd, R. S. and Guengerich, F. P. (1988) *Biochemistry*, **27**, 6929-6940.

Gibson, G. and Skett, P. (1994) *Introduction to drug metabolism*, Chapman and Hall.

Gillette, J. R. and Kamin, J. J. (1960) *J. Pharmacol. Exp. Ther.*, **130**, 262-267.

Giudicelli, J. F. and Tillement, J. P. (1977) *Clin-Pharmacokinet*, **2**, 157-166.

Gonzalez, F. J., Skoda, R. C., Kimura, S., Umeno, M., Zanger, U. M. Nebert, D. W., Gelboin, H. V., Hardwick, J. P., and Meyer, U. A., (1988) *Nature* , **331**: 442-446

Gonzalez, F. J. and Gelboin, H. V. (1993) *J-Toxicol-Environ-Health*, **40**, 289-308.

Gonzalez, F. J., Mackenzie, P. I., Kimura, S. and Nebert, D. W. (1984) *Gene*, **29**, 281-292.

Gorski, J. C., Hall, S. D., Jones, D. R., VandenBranden, M. and Wrighton, S. A. (1994) *Biochem-Pharmacol*, **47**, 1643-1653.

Guengerich, F. P., Muller Enoch, D. and Blair, I. A. (1986) *Mol-Pharmacol*, **30**, 287-295.

Guengerich, F. P. and Shimada, T. (1991) *Chem-Res-Toxicol*, **4**, 391-407.

Guy, R. H., Hadgraft, J. and Bucks, D. A. (1987) *Xenobiotica*, **17**, 325-343.

Hajjar, N. P. and Hodgson, E. (1980) *Science*, **209**, 1134-1136.

Hajjar, N. P. and Hodgson, E. (1982) *Biochem Pharmacol*, **31**, 745-752.

Hakkola, J., Pasanen, M., Pelkonen, O., Hukkanen, J., Evisalmi, S., Anttila, S., Rane, A., Mantyla, M., Purkunen, R., Saarikoski, S., Tooming, M. and Raunio, H. (1997) *Carcinogenesis*, **18**, 391-397.

Hlavica, P. and Kehl, M. (1977) *Biochem J*, **164**, 487-496.

Hotchkiss, S. A. M. (1992) In *Progress in Drug Metabolism.*, Vol. 13 (Ed, Gibson, G. G.) Taylor and Francis, London, pp. 217-262.

Huss, J. M. and Kasper, C. B. (1998) *J- Biol- Chem* **273**(26): 16155-16162.

Humbert, J. A., Hammond, K. B. and Hathaway, W. E. (1970) *Lancet*, **2**, 770-771.

Imaoka, S., Yamada, T., Hiroi, T., Hayashi, K., Sakaki, T., Yabusaki, Y. and Funae, Y. (1996) *Biochem-Pharmacol*, **51**, 1041-1050.

Itagaki, K., Carver, G. T. and Philpot, R. M. (1996) *J-Biol-Chem*, **271**, 20102-20107.

Jaiswal, A. K., Gonzalez, F. J. and Nebert, D. W. (1985) *Science*, **228**, 80-83.

Jaiswal, A. K., Nebert, D. W. and Gonzalez, F. J. (1986) *Nucleic-Acids-Res*, **14**, 6773-6774.

Jenner, P. (1971) *Xenobiotica*, **1**, 399-418.

Jugert, F. K., Agarwal, R., Kuhn, A., Bickers, D. R., Merk, H. F. and Mukhtar, H. (1994a) *J Invest Dermatol*, **102**, 970-975.

Jugert, F. K., Agarwal, R., Mukhtar, H., Bickers, D. R. and Merk, H. F. (1994b) *J. Invest. Dermatol*, **102**, 647.

Kadlubar, F. F., McKee, E. M. and Ziegler, D. M. (1973) *Arch Biochem Biophys*, **156**, 46-57.

Kadlubar, F. F., Miller, J. A. and Miller, E. C. (1976) *Cancer-Res*, **36**, 1196-1206.

Kao, J. and Carver, M. P. (1990) *Drug Metab Rev*, **22**, 363-410.

Kimura, S., Umeno, M., Skoda, R. C., Meyer, U.A., and Gonzalez, F. J., (1989)
Am- J - Hum- Genet **45**: 889-904.

Khan, I. U., Bickers, D. R., Haqqi, T. M. and Mukhtar, H. (1992) *Drug Metab Dispos*, **20**, 620-624.

Khan, W. A., Park, S. S., Gelboin, H. V., Bickers, D. R. and Mukhtar, H. (1989a) *J-Pharmacol-Exp-Ther*, **249**, 921-927.

Khan, W. A., Park, S. S., Gelboin, H. V., Bickers, D. R. and Mukhtar, H. (1989b) *J-Invest-Dermatol*, **93**, 40-45.

Kinsler, S., Levi, P. E. and Hodgson, E. (1988) *Pest. Biochem. Physiol.*, **31**, 54.

Kitada, M. and Kamataki, T. (1979) *Biochem-Pharmacol*, **28**, 793-797.

Kitada, M. and Kamataki, T. (1994) *Drug Metab Rev*, **26**, 305-323.

Kitada, M., Kamataki, T., Itahashi, K., Rikihisa, T., Kato, R. and Kanakubo, Y. (1985) *Arch-Biochem-Biophys*, **241**, 275-280.

Kulkarni, A. P. and Hodgson, E. (1980) *Pharmacology and Therapeutics*, **8**, 379-475.

Lawton, M. P., Cashman, J. R., Cresteil, T., Dolphin, C. T., Elfarra, A. A., Hines, R. N., Hodgson, E., Kimura, T., Ozols, J., Phillips, I. R., Philpot, R. M., Poulsen, L. L., Rettie, A. E., Shephard, E. A., Williams, D. E. and Ziegler, D. M. (1994) *Arch Biochem Biophys*, **308**, 254-257.

Lawton, M. P., Gasser, R., Tynes, R. E., Hodgson, E. and Philpot, R. M. (1990) *J-Biol-Chem*, **265**, 5855-5861.

Lawton, M. P., Kronbach, T., Johnson, E. F. and Philpot, R. M. (1991) *Mol-Pharmacol*, **40**, 692-698.

Lee, M. Y., Clark, J. E. and Williams, D. E. (1993) *Arch-Biochem-Biophys*, **302**, 332-336.

Lee, M. Y., Smiley, S., Kadkhodayan, S., Hines, R. N. and Williams, D. E. (1995) *Chem-Biol-Interact*, **96**, 75-85.

Lenoir, M. C., Bernard, B. A., Ferracin, J., Shroot, B. and Vermorken, A. J. (1985) *Arch Dermatol Res*, **278**, 120-125.

Lenoir, V. M., Galup, C., Darmon, M. and Bernard, B. A. (1993) *Arch Dermatol Res*, **285**, 197-204.

Levi, P. E. and Hodgson, E. (1988) *Xenobiotica*, **8**, 29-39.

Li, X. Y., Duell, E., Qin, L., Watkins, P. B. and Voorhees, J. J. (1994) *J. Invest. Dermatol.*, **102**, 624.

Light, D. R., Waxman, D. J. and Walsh, C. (1982) *Biochemistry*, **21**, 2490-2498.

Lintzel, W. (1934) *Biochem Z*, **273**, 243.

Little, P. F. R. and Jackson, I. J. (1987) In *DNA cloning*, Vol. III (Ed, Glover, D. M.) IRL Press, Oxford, pp. 1-18.

Lomri, N., Gu, Q. and Cashman, J. R. (1992) *Proc-Natl-Acad-Sci-U-S-A*, **89**, 1685-1689.

Longin Sauvageon, C., Lattard, V., Lilaz Michel, C., Buronfosse, T. and Benoit, E. (1998) *Drug-Metab-Dispos*, **26**, 284-287.

Lowry, O. H., Rosebrough, N. J., Farr, A. L. and Randall, R. J. (1951) *J. Biol. Chem*, **193**, 265-275.

Luo, Z. and Hines, R. N. (1996) *Arch-Biochem-Biophys*, **336**, 251-260.

Luo, Z. and Hines, R. N. (1997) *Arch-Biochem-Biophys*, **346**, 96-104.

Maloney, S. J., Fromson, J. M. and Bridges, J. W. (1982) *Biochem. Pharmacol.*, **31**, 4011.

Masters, B. S. and Ziegler, D. M. (1971) *Arch Biochem Biophys*, **145**, 358-364.

McKusick, V. A. (1983) *Mendelian Inheritance in Man*, John Hopkins University Press, Baltimore.

Mercurio, M. G., Bickers, D. R. and Sassa, S. (1995) *J. Invest. Dermatol.*, **104**, 676A.

Merk, H. F., Mukhtar, H., Kaufmann, I., Das, M. and Bickers, D. R. (1987) *J Invest Dermatol*, **88**, 71-76.

Miles, J. S., McLaren, A. W., Forrester, L. M., Glancey, M. J., Lang, M. A. and Wolf, C. R. (1990) *Biochem. J.*, **267**, 365.

Miles, J. S., Spurr, N. K., Gough, A. C., Jowett, T., McLaren, A. W., Brook, J. D. and Wolf, C. R. (1988) *Nucleic-Acids-Res*, **16**, 5783-5795.

Mimura, M., Baba, T., Yamazaki, H., Ohmori, S., Inui, Y., Gonzalez, F. J., Guengerich, F. P. and Shimada, T. (1993) *Drug-Metab-Dispos*, **21**, 1048-1056.

Miners, J. O., Birkett, D. J., (1998) *Br- J- Clin- Pharmacol.* **45** (6): 525-538.
Morgan, E. T. and Coon, M. J. (1984) *Drug-Metab-Dispos*, **12**, 358-364.

Mukhtar, H. and Bickers, D. R. (1981) *Drug Metab Dispos*, **9**, 311-314.

Mukhtar, H. and Bickers, D. R. (1983) *Drug Metab Dispos*, **11**, 562-567.

Murray, G. I., Barnes, T. S., Sewell, H. F., Ewen, S. W. B., Melvin, W. T. and Burke, M. D. (1988) *Br. J. Clin. Pharmacol.*, **25**, 465.

Nebert, D. W. and Gielen, J. E. (1972) *Fed-Proc*, **31**, 1315-1325.

Nebert, D. W. and Jones, J. E. (1989) *Int J Biochem*, **21**, 243-252.

Nebert, D. W., Nelson, D. R., Adesnik, M., Coon, M. J., Estabrook, R. W., Gonzalez, F. J., Guengerich, F. P., Gunsalus, I. C., Johnson, E. F., Kemper, B. and *et al.* (1989) *DNA*, **8**, 1-13.

Ortiz de Montellano, P. R. (Ed.) (1995) Cytochrome P450: Structure, Mechanism and Biochemistry, Plenum Press, Plenum Press, San Francisco.

Nelson, D. R., Kamataki, T., Waxman, D. J., Guengerich, F. P., Estabrook, R. W., Feyereisen, R., Gonzalez, F. J., Coon, M. J., Gunsalus, I. C., Gotoh, O. and *et al.* (1993) *DNA-Cell-Biol*, **12**, 1-51.

Nelson, D. R., Koymans, L., Kamataki, T., Stegeman, J. J., Feyereisen, R., Waxman, D. J., Waterman, M. R., Gotoh, O., Coon, M. J., Estabrook, R. W., Gunsalus, I. C. and Nebert, D. W. (1996) *Pharmacogenetics*, **6**, 1-42.

Nikbakht, K. N., Lawton, M. P. and Philpot, R. M. (1992) *Pharmacogenetics*, **2**, 207-216.

Odland, G. F. (1983) In *Biochemistry and Physiology of the skin.*, Vol. 1 (Ed, Goldsmith, L. A.) Oxford University Press, New York, pp. 3-63.

Overby, L., Nishio, S. J., Lawton, M. P., Plopper, C. G. and Philpot, R. M. (1992) *Exp Lung Res*, **18**, 131-144.

Overby, L. H., Buckpitt, A. R., Lawton, M. P., Atta Asafo Adjei, E., Schulze, J. and Philpot, R. M. (1995) *Arch-Biochem-Biophys*, **317**, 275-284.

Overby, L. H., Carver, G. C. and Philpot, R. M. (1997) *Chem-Biol-Interact*, **106**, 29-45.

Ozols, J. (1989) *Biochem Biophys Res Commun*, **163**, 49-55.

Pannatier, A., Testa, B. and Etter, J. C. (1982) *Experientia*, **38**, 604-605.

Pereira, T. M., CarlstedtDuke, J., Leckner, M. C., Gustafsson, J. A., (1998)
DNA-Cell-Biol 17(1): 39-49.

Park, S. B., Howald, W. N. and Cashman, J. R. (1994) *Chem Res Toxicol*, **7**, 191-198.

Pendington, R. U., Williams, D. L., Naik, J. T. and Sharma, R. K. (1994) *Toxicology in vitro*, **8**, 525-527.

Pettit, F. H., Orme Johnson, W. and Ziegler, D. M. (1964) *Biochem Biophys Res Commun*, **16**, 444-448.

Pham, M. A., Magdalou, J., Totis, M., Fournel Gignoux, S., Siest, G. and Hammock, B. D. (1989) *Biochem-Pharmacol*, **38**, 2187-2194.

Phillips, I. R., Shephard, E. A., Ashworth, A. and Rabin, B. R. (1985a) *Proc-Natl-Acad-Sci-U-S-A*, **82**, 983-987.

Phillips, I. R., Shephard, E. A., Povey, S., Davis, M. B., Kelsey, G., Monteiro, M., West, L. F. and Cowell, J. (1985b) *Ann-Hum-Genet*, **49**, 267-274.

Phillips, I. R., Dolphin, C. T., Clair, P., Hadley, M. R., Hutt, A. J., McCombie, R. R., Smith, R. L. and Shephard, E. A. (1995) *Chem-Biol-Interact*, **96**, 17-32.

Pichard, L., Gillet, G., Fabre, I., Dalet Beluche, I., Bonfils, C., Thenot, J. P. and Maurel, P. (1990) *Drug-Metab-Dispos*, **18**, 711-719.

Pohl, R. J., Philpot, R. M. and Fouts, J. R. (1976) *Drug-Metab-Dispos*, **4**, 442-450.

Poulsen, L. L., Hyslop, R. M. and Ziegler, D. M. (1974a) *Biochem Pharmacol*, **23**, 3431-3440.

Poulsen, L. L., Kadlubar, F. F. and Ziegler, D. M. (1974b) *Arch Biochem Biophys*, **164**, 774-775.

Poulsen, L. L., Taylor, K., Williams, D. E., Masters, B. S. and Ziegler, D. M. (1986) *Mol-Pharmacol*, **30**, 680-685.

Poulsen, L. L. and Ziegler, D. M. (1977) *Arch Biochem Biophys*, **183**, 563-570.

Poulsen, L. L. and Ziegler, D. M. (1979) *J Biol Chem*, **254**, 6449-6455.

Prough, R. A. (1973) *Arch-Biochem-Biophys*, **158**, 442-444.

Quattrochi, L. C., Okino, S. T., Pendurthi, U. R. and Tukey, R. H. (1985) *DNA*, **4**, 395-400.

Raza, H., Agarwal, R., Bickers, D. R. and Mukhtar, H. (1992) *J Invest Dermatol*, **98**, 233-240.

Regnier, M., Asselineau, D. and Lenoir, M. C. (1990) *Skin Pharmacol*, **3**, 70-85.

Regnier, M. and Darmon, M. (1989) *In-Vitro-Cell-Dev-Biol*, **25**, 1000-1008.

Reiners, J. J., Cantu, A. R., Thai, G. and Scholler, A. (1992) *Drug Metab Dispos*, **20**, 360-366.

Rettie, A. E., Williams, F. M. and Rawlins, M. D. (1986) *Xenobiotica*, **16**, 205-211.

Rheinwald, J. G. and Beckett, M. A. (1980) *Cell*, **22**, 629-632.

Riddles, P. W., Blakeley, R. L. and Zerner, B. (1983) *Methods in Enzymology*, **91**, 49-60.

Rongone, E. L. (1983) In *Dermatotoxicology* (Eds, Marzulli, F. N. and Maibach, H. I.) Hemisphere, New York, pp. 1-70.

Sadek, C. M. and Allen, H. B. (1994) *J Biol Chem*, **269**, 16067-16074.

Sambrook, J., Fritsch, E. F. and Maniatis, T. (1989) *Molecular Cloning: A laboratory Manual*, Cold Spring Harbour Laboratory Press.

Santisteban, I., Povey, S., Shephard, E. A. and Phillips, I. R. (1988) *Ann-Hum-Genet*, **52**, 129-135.

Sarforazi, M. (1997) *Hum Mol Genet*, **6**, 1667-1677.

Schuetz, E. G., Schuetz, J. D., Strom, S. C., Thompson, M. T., Fisher, R. A., Molowa, D. T., Li, D. and Guzelian, P. S. (1993a) *Hepatology*, **18**, 1254-1262.

Schuetz, J. D., Kauma, S. and Guzelian, P. S. (1993b) *J-Clin-Invest*, **92**, 1018-1024.

Schweikl, H., Taylor, J. A., Kitareewan, S., Linko, P., Nagorney, D. and Goldstein, J. A. (1993) *Pharmacogenetics*, **3**, 239-249.

Shehin Johnson, S., Williams, D. E., Larsen Su, S., Stresser, D. M. and Hines, R. N. (1995) *J Pharmacol Exp Ther*, **272**, 1293-1299.

Shimada, T., Gillam, E. M., Sutter, T. R., Strickland, P. T., Guengerich, F. P. and Yamazaki, H. (1997) *Drug-Metab-Dispos*, **25**, 617-622.

Shimada, T., Yamazaki, H., Mimura, M., Inui, Y. and Guengerich, F. P. (1994) *J-Pharmacol-Exp-Ther*, **270**, 414-423.

Skerrow, D. (1974) *Biochem-Biophys-Res-Commun*, **59**, 1311-1316.

Smyser, B. P. and Hodgson, E. (1985) *Biochem Pharmacol*, **34**, 1145-1150.

Sogawa, K., Gotoh, O., Kawajiri, K., Harada, T. and Fujii Kuriyama, Y. (1985) *J-Biol-Chem*, **260**, 5026-5032.

Stauber, K. L., Laskin, J. D., Yurkow, E. J., Thomas, P. E., Laskin, D. L. and Conney, A. H. (1995) *J Pharmacol Exp Ther*, **273**, 967-976.

Steinert, P. M. and Idler, W. W. (1975) *Biochem-J*, **151**, 603-614.

Stoilov, I., Akarsu, A. N., Alozie, I., Child, A., Barsoum Homsy, M., Turacli, M. E., Or, M., Lewis, R. A., Ozdemir, N., Brice, G., Aktan, S. G., Chevrette, L., Coca Prados, M. and Sarfarazi, M. (1998) *Am-J-Hum-Genet*, **62**, 573-584.

Stoilov, I., Akarsu, A. N. and Sarfarazi, M. (1997) *Hum-Mol-Genet*, **6**, 641-647.

Uematsu, F., Kikuchi, H., Motomiya, M., Abe, T., Ishioka, C., Kanamaru, R., Sagami, I., and Watanabe, M., (1992) *Tohoku- J-Exp- Med.*, **168**: 113-117.

Sun, T. T., Eichner, R., Nelson, W. G., Vidrich, A. and Woodcock-Mitchell, J. (1983) In *Normal and Abnormal Epidermal Differentiation*(Eds, Seiji, M. and Bernstein, J. A.) University of Tokyo Press, Tokyo, pp. 277-291

Sutter, T. R., Tang, Y. M., Hayes, C. L., Wo, Y. Y., Jabs, E. W., Li, X., Yin, H., Cody, C. W. and Greenlee, W. F. (1994) *J-Biol-Chem*, **269**, 13092-13099.

Taylor, K. L. and Ziegler, D. M. (1987) *Biochem-Pharmacol*, **36**, 141-146.

Thibodeau, G. A. and Patton, K. T. (1996) *Anatomy and Physiology*, Mosby-Year Book, Inc.

Thompson, S. and Slaga, T. J. (1976) *J-Invest-Dermatol*, **66**, 108-111.

Tynes, R. E. and Hodgson, E. (1985) *Arch-Biochem-Biophys*, **240**, 77-93.

Tynes, R. E. and Philpot, R. M. (1987) *Mol-Pharmacol*, **31**, 569-574.

Tynes, R. E., Sabourin, P. J. and Hodgson, E. (1985) *Biochem-Biophys-Res-Commun*, **126**, 1069-1075.

Tynes, R. E., Sabourin, P. J., Hodgson, E. and Philpot, R. M. (1986) *Arch-Biochem-Biophys*, **251**, 654-664.

Umbenhauer, D. R., Martin, M. V., Lloyd, R. S. and Guengerich, F. P. (1987) *Biochemistry*, **26**, 1094-1099.

Van Pelt, F. N., Meierink, Y. J., Blaauboer, B. J. and Weterings, P. J. (1990) *J-Histochem-Cytochem*, **38**, 1847-1851.

Vecchini, F., Mace, K., Magdalou, J., Mahe, Y., Bernard, B. A. and Shroot, B. (1995) *Br-J-Dermatol*, **132**, 14-21.

Venkatesh, K., Levi, P. K., Inman, A. O., Monteiro-Riviere, N. A., Misra, R. and Hodgson, E. (1992) *Pesticide Biochemistry and Physiology*, **43**, 53-66.

Vermilion, J. L. and Coon, M. J. (1974) *Biochem-Biophys-Res-Commun*, **60**, 1315-1322.

Vizethum, W., Ruzicka, T. and Goerz, G. (1980) *Chem-Biol-Interact*, **31**, 215-219.

Watkins, P. B., Wrighton, S. A., Schuetz, E. G., Molowa, D. T. and Guzelian, P. S. (1987) *J-Clin-Invest*, **80**, 1029-1036.

Waxman, D. J., Light, D. R. and Walsh, C. (1982) *Biochemistry*, **21**, 2499-2507.

Welch, P. and Scopes, R. K. (1981) *Anal-Biochem*, **112**, 154-157.

Wessel, D. and Flugge, U. I. (1984) *Anal-Biochem*, **138**, 141-143.

Whitlock, J. J. (1986) *Annu Rev Pharmacol Toxicol*, **26**, 333-369.

Williams, C. H. and Kamin, H. (1962) *J. Biol. Chem*, **237**, 587-595.

Williams, D. E., Hale, S. E., Muerhoff, A. S. and Masters, B. S. (1985) *Mol-Pharmacol*, **28**, 381-390.

Yamazaki, H., Inoue, K., Chiba, K., Ozawa, N., Kawai, T., Suzuki, Y., Goldstein, J. A., Guengerich, F. P., Shimada, T., (1998) *Biochem- Pharmacol.*, **56** (2): 243-251.

Williams, D. E., Kelly, J. and Dutchuk, M. (1990) In *8th International Symposium on microsomes and drug oxidations* Stockholm, Sweden.

Williams, D. E., Meyer, H. H. and Dutchuk, M. S. (1989) *Comp Biochem Physiol B*, **93**, 465-470.

Williams, D. E., Ziegler, D. M., Nordin, D. J., Hale, S. E. and Masters, B. S. (1984) *Biochem-Biophys-Res-Commun*, **125**, 116-122.

Wrighton, S. A., Brian, W. R., Sari, M. A., Iwasaki, M., Guengerich, F. P., Raucy, J. L., Molowa, D. T. and Vandenbranden, M. (1990) *Mol-Pharmacol*, **38**, 207-213.

Wrighton, S. A., Campanile, C., Thomas, P. E., Maines, S. L., Watkins, P. B., Parker, G., Mendez-Picon, G., Haniu, M., Shively, J. E., Levin, W. and Guzelian, P. S. (1986) *Mol. Pharmacol.*, **29**, 405.

Wrighton, S. A., Ring, B. J., Watkins, P. B. and VandenBranden, M. (1989) *Mol-Pharmacol*, **36**, 97-105.

Wyatt, M. K., Philpot, R. M., Carver, G., Lawton, M. P. and Nikbakht, K. N. (1996) *Drug-Metab-Dispos*, **24**, 1320-1327.

Yamano, S., Nhamburo, P. T., Aoyama, T., Meyer, U. A., Inaba, T., Kalow, W., Gelboin, H. V., McBride, O. W. and Gonzalez, F. J. (1989) *Biochemistry*, **28**, 7340.

Yamano, S., Tatsuno, J. and Gonzalez, F. J. (1990) *Biochemistry*, **29**, 1322-1329.

Yang, C. S., Yoo, J. S. H., Ishizaki, H., and HONG, J., (1990) *Drug-Metab- Rev.*, **22**:147-159.

Yokoi, T., and Kamataki, T., (1998) *Pharma- Res.*, **15** (4): 517-524.

Yamazaki, H., Inui, Y., Yun, C. H., Guengerich, F. P. and Shimada, T. (1992) *Carcinogenesis*, **13**, 1789-1794.

Yueh, M. F., Krueger, S. K. and Williams, D. E. (1997) *Biochim-Biophys-Acta*, **1350**, 267-271.

Yun, C. H., Shimada, T. and Guengerich, F. P. (1991) *Mol. Pharmacol.*, **40**, 679.

Yun, C. H., Shimada, T. and Guengerich, F. P. (1992) *Carcinogenesis*, **13**, 217-222.

Ziegler (1980) In *Enzymatic basis of detoxification*, Vol. 1 (Ed, Jakoby, W. B.) Academic Press, , pp. 201-227.

Ziegler, D. M. (1988) *Drug Metab Rev*, **19**, 1-32.

Ziegler, D. M. (1990) *Trends Pharmacol Sci*, **11**, 321-324.

Ziegler, D. M. (1993) *Annu Rev Pharmacol Toxicol*, **33**, 179-199.

Ziegler, D. M., McKee, E. M. and Poulsen, L. L. (1973) *Drug Metab Dispos*, **1**, 314-321.

Ziegler, D. M. and Mitchell, C. H. (1972) *Arch Biochem Biophys*, **150**, 116-125.

Ziegler, D. M. and Poulsen, L. L. (1977) *Trends Biochem Sci*, **2**, 79-81.

PUBLICATIONS

Missense mutation in flavin-containing mono-oxygenase 3 gene, *FMO3*, underlies fish-odour syndrome

Colin T. Dolphin¹, Azara Janmohamed², Robert L. Smith³, Elizabeth A. Shephard² & Ian R. Phillips¹

Individuals with primary trimethylaminuria exhibit a body odour reminiscent of rotting fish, due to excessive excretion of trimethylamine (TMA; refs 1–3). The disorder, colloquially known as fish-odour syndrome, is inherited recessively as a defect in hepatic *N*-oxidation of dietary-derived TMA^{4–6} and cannot be considered benign, as sufferers may display a variety of psychosocial reactions, ranging from social isolation to clinical depression and attempted suicide⁶. TMA oxidation is catalyzed by flavin-containing mono-oxygenase (FMO; refs 7,8), and tissue localization^{9,10} and functional studies¹¹ have established *FMO3* as the form most likely to be defective in fish-odour syndrome. Direct sequencing of the coding exons of *FMO3* amplified from a patient with fish-odour syndrome identified two missense mutations. Although one of these represented a common polymorphism, the other, a C→T transition in exon 4, was found only in an affected pedigree, in which it segregated with the disorder. The latter mutation predicts a proline→leucine substitution at residue 153 and abolishes *FMO3* catalytic activity. Our results indicate that defects in *FMO3* underlie fish-odour syndrome and that the Pro153→Leu153 mutation described here is a cause of this distressing condition.

Of the five known forms of mammalian *FMO*¹², *FMO3* represents the major hepatic FMO in humans^{9,10} and displays a distinct substrate preference for tertiary amines¹¹. As TMA is cleared substantially by hepatic first-pass metabolism¹³, *FMO3* is thus likely to catalyze most TMA *N*-oxidation *in vivo*. The *FMO3* gene is located on chromosome 1q (ref. 14) in the region 1q23–24 (R.R. McCombie, E.A.S. & I.R.P., unpublished data) and contains one non-coding and eight coding exons¹⁵.

Knowledge of the internal organization of the gene enabled each exon and its flanking intronic sequences to be amplified from genomic DNA and directly sequenced. Comparison of sequences amplified from the proband, PR, of a fish-odour syndrome pedigree (see Methods) with those of a normal individual revealed no deletions and no differences in acceptor or donor splice sites. However, a C→T missense mutation, corresponding to nucleotide 551 in the cDNA¹⁰, was identified in exon 4 of both *FMO3* alleles of PR (Fig. 1a). This mutation changes a CCC proline triplet at codon 153 to a CTC leucine triplet (Pro153→Leu153). The second affected sibling, CR, was also homozygous for the CTC triplet at codon 153, whereas the father (Fig. 1b), mother and third sibling, JR (data not shown), were heterozygotes. Four unrelated, non-trimethylaminuric individuals were each homozygous for a CCC triplet at this position (Fig. 1c and data not shown). In addition, the father and JR were identified as heterozygous for GAG glutamate and AAG lysine triplets at codon 158 (Fig. 1b), whereas the mother and PR (Fig. 1a) and CR were homozygous for the GAG codon. Three of the four normal individuals analysed were GAG homozygotes (data not shown), and the other was an AAG homozygote (Fig. 1c). Glu158 and Lys158 variants have previously been detected in *FMO3* cDNA sequences^{10,16}.

To determine the frequencies of Pro153, Leu153, Glu158 and Lys158 *FMO3* variants, we devised a genotyping method that employs restriction enzyme digestion of a PCR-amplified region of the gene encompassing both variant codons (Fig. 2a). The ability of the method to accurately predict the sequence at the variant position within each codon was confirmed by analysis of

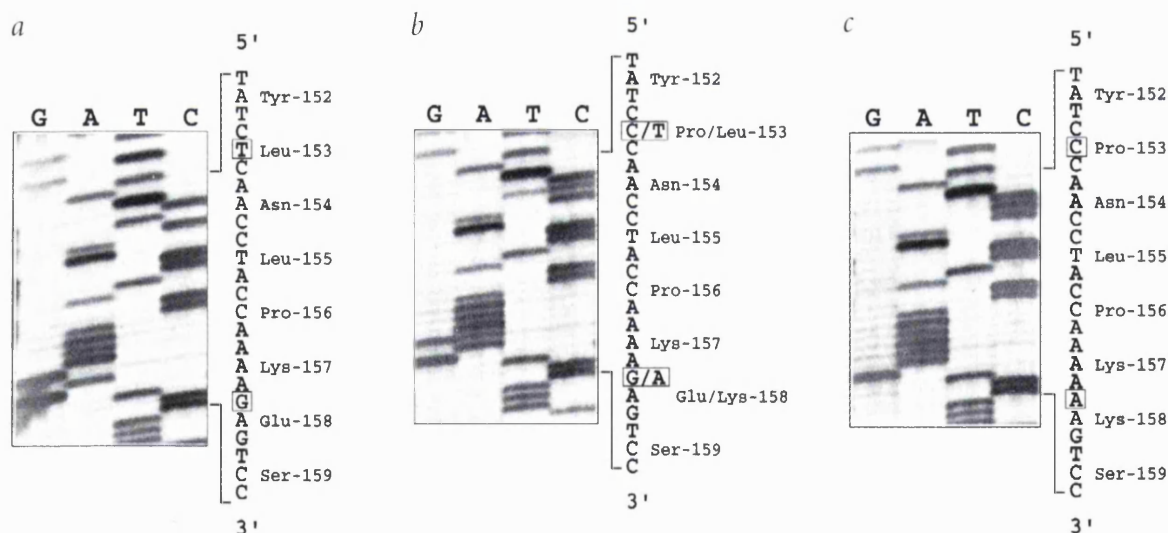


Fig. 1 Identification of mutations within exon 4 of the *FMO3* gene. Exon 4 of the gene was amplified from genomic DNA isolated from the proband, PR (**a**), and father (**b**) of a fish-odour syndrome pedigree and from a non-trimethylaminuric control (**c**). Nucleotide sequences and deduced amino-acid sequences are shown to the right of each sequencing gel. Variant nucleotides are boxed.

¹Laboratory of Molecular Biology, Department of Biochemistry, Queen Mary & Westfield College, University of London, Mile End Road, London E1 4NS, UK. ²Department of Biochemistry and Molecular Biology, University College London, Gower Street, London WC1E 6BT, UK. ³Molecular Toxicology, Imperial College School of Medicine, Norfolk Place, London W2 1PG, UK. Correspondence should be addressed to I.R.P.

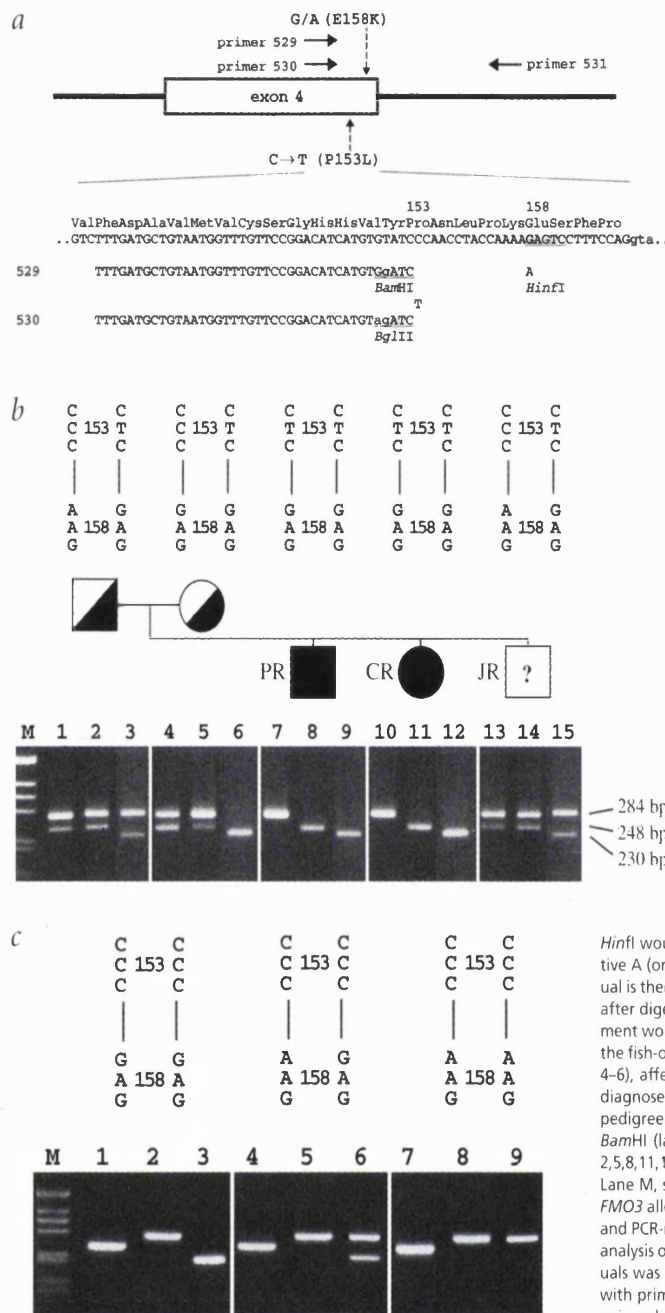


Fig. 2 Determination of Pro153/Leu153 and Glu158/Lys158 variants of *FMO3* by means of a PCR/restriction enzyme-based method. **a**, Schematic representation. Annealing positions of primers (solid arrows) and positions of codons 153 and 158 (dashed arrows) are shown in relation to the structure of *FMO3*. Partial DNA sequence is shown for the 3' end of exon 4 (capitals), with the deduced amino-acid sequence shown above, and for the 5' end of intron 4 (lower case). Below this are shown the sequences of primers 529 and 530, used in conjunction with a single reverse primer, 531 (5'-GGCAGTTTGAGTCATATATTTAAACAAAGAC-3'), and the single nucleotide differences within codons 153 and 158. The positions of incomplete *Bam*HI and *Bgl*II restriction sites within primers 529 and 530 allowed the generation in the 284-bp amplification products of different and unique restriction sites, depending on the identity of the nucleotide present immediately 3' of the primer end. Thus, if both copies of *FMO3* contained a C at the second position of codon 153, *Bam*HI digestion of the PCR product derived from the 529/531 primer pair would yield a fragment of 248 bp. As amplification is possible only if a C is present at the first position of codon 153, and as the third position of the proline codon is fully degenerate, such individuals would therefore be homozygous for the Pro153 allele. This would be confirmed by the failure of *Bgl*II to cut the PCR product derived from the 530/531 primer pair. In contrast, if both copies of *FMO3* contained the alternative, CTC, triplet at this position, the amplification product derived from the 530/531 primer pair would be cut by *Bgl*II, whereas that derived from the 529/531 pair would not be cut by *Bam*HI. As the third position of a leucine codon is also fully degenerate, this pattern of digestion would be indicative of individuals homozygous for the Leu153 allele. The presence, after digestion with either enzyme, of both undigested PCR product and the 248-bp fragment would indicate that the individual is heterozygous for Pro153 and Leu153. The Glu158/Lys158 alleles of the *FMO3* gene can be distinguished by digestion of either the 529/531 or 530/531 PCR products with *Hin*fi, as a cleavage site for this enzyme is present in the amplified DNA only when a G is present at the first, variant, position of codon 158. Thus, *Hin*fi digestion of either PCR product amplified from an individual homozygous for G at this position would yield a DNA fragment of 230 bp, indicating that the individual is homozygous for the GAG glutamate triplet. In contrast, failure to cut with *Hin*fi would indicate that both copies of the *FMO3* gene contained the alternative A (or another, unidentified nucleotide) at this position and that the individual is therefore likely to be homozygous for the AAG lysine triplet. The presence, after digestion with *Hin*fi, of both undigested PCR product and the 230-bp fragment would indicate that the individual is heterozygous. **b**, Genotype analysis of the fish-odour syndrome kindred. DNA from the father (lanes 1-3), mother (lanes 4-6), affected son, PR (lanes 7-9), affected daughter, CR (lanes 10-12), and the diagnosed sibling, JR (lanes 13-15), of a fish-odour syndrome kindred, whose pedigree is illustrated, was amplified with primers 529/531 and digested with *Bam*HI (lanes 1,4,7,10,13), with primers 530/531 and digested with *Bgl*II (lanes 2,5,8,11,14) or with either primer pair and digested with *Hin*fi (lanes 3,6,9,12,15). Lane M, size markers (1-kb ladder). The sequence of codons 153 and 158 in the *FMO3* alleles present in each individual (based on the results of DNA sequencing and PCR-restriction digestion analysis) is shown above the pedigree. **c**, Genotype analysis of unrelated, non-trimethylaminuric individuals. DNA from three individuals was amplified with primers 529/531 and digested with *Bam*HI (lanes 1,4,7), with primers 530/531 and digested with *Bgl*II (lanes 2,5,8) or with either primer pair and digested with *Hin*fi (lanes 3,6,9). Lane M, size markers (1-kb ladder).

individuals of known genotype (Fig. 2b,c). Analysis of 30 unrelated, non-trimethylaminuric individuals (Fig. 2c and data not shown) established that all were Pro153 homozygotes, whereas Glu158 and Lys158 occur with frequencies of approximately 50% each. The Glu158 and Lys158 alleles thus represent a common *FMO3* polymorphism, indicating that neither can underlie fish-odour syndrome. In contrast, Leu153 was detected only in the affected kindred, in which it co-segregated with the disorder (Figs 1,2b). The results indicate that the Leu153 mutation occurred on a Glu158 allele. Leu153 has subsequently been detected in two other fish-odour kindreds, in which it also co-segregated with the disorder (data not shown).

To determine the functional effect of the Leu153 mutation, cDNAs encoding native and mutant *FMO3*s were expressed in a baculovirus-insect-cell system. The concentrations of the expressed proteins in insect-cell microsomal membranes, determined by immunoblotting, were 55 pmol/mg protein for Pro153Glu158 and Pro153Lys158 cDNA expression constructs

and 70 pmol/mg protein for the Leu153Glu158 construct (Fig. 3a). Immunoreactive protein was undetectable in microsomal membranes from non-infected cells or from cells infected with wild-type virus (Fig. 3a). The two polymorphic variants catalyze the *N*-oxidation of TMA (Fig. 3b) and the *S*-oxidation of methimazole (Fig. 3c), Pro153Glu158 being more effective in catalyzing both *N*-oxidation ($k_{cat}^{app} \approx 60 \text{ min}^{-1}$) and *S*-oxidation ($k_{cat}^{app} \approx 36 \text{ min}^{-1}$) than Pro153Lys158 ($k_{cat}^{app} \approx 29 \text{ min}^{-1}$ for *N*-oxidation and $k_{cat}^{app} \approx 15 \text{ min}^{-1}$ for *S*-oxidation). In contrast, the Leu153Glu158 mutant failed to catalyze the oxidation of either substrate (Fig. 3b,c).

The marked effect of the Pro→Leu substitution on both the *N*- and *S*-oxidation activities of *FMO3* clearly identifies Pro153 as important for the structure or function of the enzyme. Pro153 is the first residue of a PXXP motif located between the fingerprint sequences¹⁷ identifying the $\beta\alpha\beta$ -folds of the FAD- and NADP-binding domains, 33 residues *N*-terminal of the start of the latter sequence. The sequence and location of this motif are

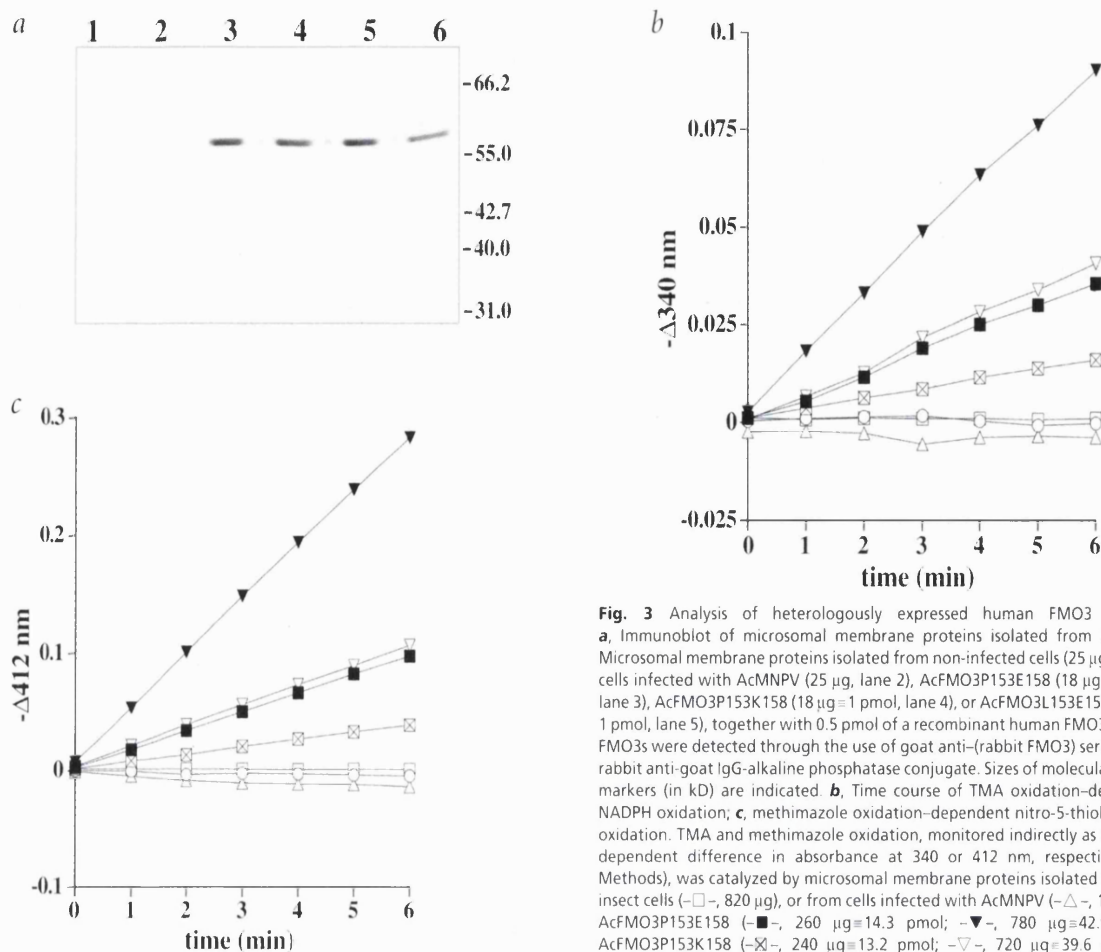


Fig. 3 Analysis of heterologously expressed human FMO3 variants. **a**, Immunoblot of microsomal membrane proteins isolated from *T.ni* cells. Microsomal membrane proteins isolated from non-infected cells (25 μg, lane 1), cells infected with AcMNPV (25 μg, lane 2), AcFMO3P153E158 (18 μg=1 pmol, lane 3), AcFMO3P153K158 (18 μg=1 pmol, lane 4), or AcFMO3L153E158 (14 μg=1 pmol, lane 5), together with 0.5 pmol of a recombinant human FMO3 (lane 6). FMO3s were detected through the use of goat anti-(rabbit FMO3) serum and a rabbit anti-goat IgG-alkaline phosphatase conjugate. Sizes of molecular weight markers (in kD) are indicated. **b**, Time course of TMA oxidation-dependent NADPH oxidation; **c**, methimazole oxidation-dependent nitro-5-thiobenzoate oxidation. TMA and methimazole oxidation, monitored indirectly as the time-dependent difference in absorbance at 340 or 412 nm, respectively (see Methods), was catalyzed by microsomal membrane proteins isolated from *T.ni* insect cells (-□-, 820 μg), or from cells infected with AcMNPV (-Δ-, 1,500 μg), AcFMO3P153E158 (-■-, 260 μg=14.3 pmol; -▼-, 780 μg=42.9 pmol), AcFMO3P153K158 (-X-, 240 μg=13.2 pmol; -▽-, 720 μg=39.6 pmol) or AcFMO3L153E158 (-○-, 650 μg=45.5 pmol).

conserved in all known mammalian FMOs except FMO5, which contains an alanine at this position and exhibits markedly reduced catalytic activities towards typical FMO substrates¹⁸. A PXXP motif is also found, at approximately the same location with respect to the FAD- and NAD(P)-binding domains, in an FMO-like protein of yeast¹⁹, in cyclohexanone mono-oxygenase²⁰ (a bacterial mono-oxygenase related to FMOs) and in each of the two polypeptide chains of several flavoprotein disulphide oxidoreductases^{21–24}, suggesting that it plays an important role in the structure or function of enzymes containing dinucleotide-binding βαβ-folds.

In conclusion, we have identified a missense mutation, 551C→T, in FMO3, which segregates with impaired TMA oxidation in a fish-odour syndrome pedigree and, by substituting a highly conserved proline at residue 153 with a leucine, essentially abolishes FMO3 catalytic activity. Individuals homozygous for the Leu153 allele are thus unable to support the metabolism of dietary-derived TMA and, consequently, excrete the malodorous amine rather than its non-odorous *N*-oxide and hence display the associated and often highly distressing symptoms of fish-odour syndrome. In addition to TMA, FMOs catalyze the oxidation of a range of structurally diverse compounds, including drugs, pesticides and other xenobiotics⁸. Although patients with fish-odour syndrome are apparently deficient in nicotine *N*-oxidation²⁵, a reaction catalyzed predominantly by FMO3 (ref. 26), the pharmacological and toxicological significance of an inherited block in FMO3-mediated oxidative metabolism is unclear.

Methods

Patients. The pedigree investigated in this study was previously described⁶. The probands, PR and CR, had, since birth, exhibited classical symptoms of severe fish-odour syndrome, which, particularly in the case of PR, had resulted in significant adverse psychosocial reactions. In contrast, neither parent nor the third sibling, IR, was clinically affected.

FMO3 amplification. Individual coding exons and associated splice sites were amplified from 100 ng of genomic DNA (isolated from whole blood) by PCR as described¹⁰. Respective sense and antisense primer sequences, designed from the FMO3 gene sequence¹⁵, were as follows: exon 2: 5'-GTGAGCTACCATCTCAGCCAGTG-3', 5'-CACAGTGTGCTCTTATACACTTCCC-3'; exon 3: 5'-GACCTGATCAGTATACTCAITTTACC-3', 5'-AGTAGTAGACATAGACTTCTTCAGC-3'; exon 4: 5'-CTTTTCTTTTTCATACTGTATCTGC-3', 5'-AAAAAGAAGACATATCAAGATATT-3'; exon 5: 5'-TATGCTTGGTGTGTTAAATAGCAC-3', 5'-CACACCTTCAAACGATAATAACTC-3'; exon 6: 5'-CAGAAIATCCACTACAAATGGTCAC-3', 5'-GCTTACAGGACATTAAGGGTTGTTG-3'; exon 7: 5'-GCCTCCCATCAATTTTGTCTTCAG-3', 5'-CAAAGATCCAAAGTATTGTCACTG-3'; exon 8: 5'-GGAAAATACAGGCTGGTCCCTATGC-3', 5'-ATAGCTTGTAGTTGTCATTCCAAIG-3'; exon 9: 5'-TTCCTGTTCTGTTCTACACAGAG-3', 5'-CCCTGTCTGGGTATTGTCAGTAAAC-3'. Reaction mixtures were incubated for 36 cycles at 94 °C for 1 min, 56 °C for 1 min and 72 °C for 1 min.

DNA sequencing. Purified PCR products were sequenced directly, either by cycle sequencing²⁷ or after preparation of single-stranded DNA²⁸.

Genotyping. Genomic DNA was amplified by PCR with primer pairs 529 and 531 or 530 and 531 (Fig. 2a). Conditions were as described¹⁰, except that the reaction mixtures were incubated for 3 cycles of 94 °C for 1 min,

51 °C for 1 min and 72 °C for 1 min, followed by 38 cycles of 94 °C for 1 min, 56 °C for 1 min and 72 °C for 1 min, then for an additional 5 min at 72 °C. Aliquots (15 µl) of the 529/531 and 530/531 amplification products were incubated with *Bam*HI and *Bgl*II, respectively. An additional aliquot (15 µl) of either product was incubated with *Hinf*I. Digested samples were analysed by electrophoresis through a 3% (w/v) agarose (Metaphor, FMC) gel with a 1-kb ladder (GIBCO BRL) as a size marker.

Recombinant baculovirus construction and heterologous expression. A Leu153Glu158 *FMO3* cDNA was constructed by substituting a *Bsp*EI/*Bcl*II restriction fragment of the native cDNA¹⁰ with an equivalent PCR-generated fragment containing CTC at codon 153. Reaction mixtures, containing 15 pmol each of primers 542 (5'-GTTTGTTCGGACATCATGTG-TATCICAACCTACC-3'; mismatch underlined) and 418 (5'-ATCAC-CCAGGAGCGAATTCGGAACTGATC-3'), 10 ng of p1D16A (ref. 10) and 5 U of *Pfu* polymerase (Stratagene), were cycled 35 times at 94 °C for 1 min, 52 °C for 1 min and 72 °C for 4 min. The product was ligated into *Eco*RV-linearized pBluescript (Stratagene) to give p(418-542). After incubation of p1D16A and p(418-542) with *Bsp*EI and *Bcl*II, the larger, vector, fragment of p1D16A and the smaller, restriction, fragment of p(418-542) were ligated to give p1D16A(C-T). cDNA inserts were released from p1D16A and p1D16A(C-T) by digestion with *Bam*HI and *Pst*I and inserted into *Bam*HI/*Pst*I-digested pFastBac1 (GIBCO BRL) to produce pFastFMO3P153E158 and pFastFMO3L153E158, respectively. The Lys158 wild-type variant was generated by direct mutagenesis (QuickChange, Stratagene) of pFastFMO3P153E158 to give pFastFMO3P153K158. All constructs were fully sequenced. Recombinant baculoviruses were generated with the Bac-to-Bac system (GIBCO BRL).

Sf9 and *T.ni* cells were passaged, respectively, in Sf-900II (GIBCO BRL) or Excell 405 (JRH Biosciences) media containing amphotericin B (5 µg/ml), penicillin-G (100 U/ml) and streptomycin sulphate (50 µg/ml). Virus was amplified in Sf9 cells with a multiplicity of infection (MOI) of ≤0.1. For expression, *T.ni* cells (500 ml at 10⁶ cells/ml) were infected at an MOI of 5 and incubated at 28 °C for 72 h in medium supplemented with 2% fetal calf serum in spinner flasks (Bellco). Cells were pelleted, re-suspended in 120 ml of homogenization buffer (0.154 M KCl, 50 mM Tris, pH 7.4, 0.2 mM phenylmethanesulphonyl flu-

oride) and sonicated on ice for three 30-s bursts (Dyna-tech). Microsomes were obtained by differential centrifugation²⁹, re-suspended in 20 ml of storage buffer (0.154 M KCl, 10 mM HEPES, pH 7.5, 1 mM EDTA, 20% glycerol) and stored in aliquots at -80 °C. Protein concentration was determined by the BCA method (Pierce).

Western blotting. Proteins were electrophoresed through a 10% polyacrylamide-SDS gel and electroblotted to nitrocellulose. The filter was incubated sequentially with goat anti-(rabbit FMO3) serum (1/3,000 dilution) and rabbit anti-goat IgG-alkaline phosphatase (Sigma), and the antigen visualized (Color Development Kit, Bio-Rad). Concentrations of expressed proteins were determined by densitometry using a standard curve of authentic human FMO3.

FMO assays. TMA and methimazole oxidation activities were determined spectrophotometrically (Cary 1) in the split-beam mode. TMA *N*-oxidation was measured by monitoring oxidation of NADPH at 340 nm, whereas methimazole *S*-oxidation was determined indirectly by monitoring consumption of nitro-5-thiobenzoate at 412 nm as described³⁰. Assays were performed in a volume of 1 ml at 37 °C in aerated 0.1 M tricine (pH 8.4). Reactions were initiated by addition of TMA or methimazole to provide essentially saturating concentrations of substrate (5 mM and 2 mM, respectively).

Acknowledgements

We thank R. Philpot for authentic human FMO3 and anti-(rabbit FMO3) serum, R. Ayesch for collecting blood from the affected family, S. Povey for supplying blood from non-trimethylaminuric individuals, R. Harris and D. Miller for advice on baculovirus-mediated expression and K. Brocklehurst for advice on enzyme assays and for use of equipment. A.J. is a recipient of an Overseas Research Studentship from the Committee of Vice-Chancellors and Principals of the U.K. This work was supported by grants from the Wellcome Trust (ref. Nos 036025 and 045229).

Received 24 July; accepted 21 October 1997.

- Mitchell, S.C. The fish-odour syndrome. *Perspect. Biol. Med.* **39**, 514-526 (1996).
- Shelley, E.D. & Shelley, W.D. The fish-odour syndrome: trimethylaminuria. *JAMA* **251**, 253-255 (1984).
- Spellacy, E., Watts, R.W.E. & Gollamali, S.K. Trimethylaminuria. *J. Inherited Metab. Dis.* **2**, 85-88 (1979).
- al-Waiz, M., Ayesch, R., Mitchell, S.C., Idle, J.R., & Smith, R.L. Trimethylaminuria (fish-odour syndrome): an inborn error of oxidative metabolism. *Lancet* **i**, 634-635 (1987).
- al-Waiz, M., Ayesch, R., Mitchell, S.C., Idle, J.R., & Smith, R.L. Trimethylaminuria ('fish-odour syndrome'): a study of an affected family. *Clin. Sci.* **74**, 231-236 (1988).
- Ayesch, R., Mitchell, S.C., Zhang, A. & Smith, R.L. The fish-odour syndrome: biochemical, familial and clinical aspects. *Br. Med. J.* **307**, 655-657 (1993).
- Gut, I. & Conney, A.H. Trimethylamine *N*-oxygenation and *N*-demethylation in rat liver microsomes. *Biochem. Pharmacol.* **46**, 239-244 (1993).
- Ziegler, D.M. Flavin-containing monooxygenases: enzymes adapted for multisubstrate specificity. *Trends Pharmacol. Sci.* **11**, 321-324 (1990).
- Phillips, I.R. et al. The molecular biology of the flavin-containing monooxygenases of man. *Chem.-Biol. Interact.* **96**, 17-32 (1995).
- Dolphin, C.T., Cullingford, T.E., Shephard, E.A., Smith, R.L. & Phillips, I.R. Differential developmental and tissue-specific regulation of expression of the genes encoding three members of the flavin-containing monooxygenase family of man, FMO1, FMO3 and FMO4. *Eur. J. Biochem.* **235**, 683-689 (1996).
- Lomri, N., Yang, Z. & Cashman, J.R. Expression in *Escherichia coli* of the flavin-containing monooxygenase D (form II) from adult human liver: determination of a distinct tertiary amine substrate specificity. *Chem. Res. Toxicol.* **6**, 425-429 (1993).
- Lawton, M.P. et al. A nomenclature for the mammalian flavin-containing monooxygenase gene family based on amino acid sequence identities. *Arch. Biochem. Biophys.* **308**, 254-257 (1994).
- al-Waiz, M., Ayesch, R., Mitchell, S.C., Idle, J.R., & Smith, R.L. Disclosure of the metabolic retroversion of trimethylamine *N*-oxide in humans: a pharmacogenetic approach. *Clin. Pharm. Ther.* **42**, 608-612 (1987).
- Shephard, E.A. et al. Localization of genes encoding three distinct flavin-containing monooxygenases to human chromosome 1q. *Genomics* **16**, 85-89 (1993).
- Dolphin, C.T., Riley, J.R., Smith, R.L., Shephard, E.A. & Phillips, I.R. Structural organization of the human flavin-containing monooxygenase 3 gene (*FMO3*), the favored candidate for fish-odour syndrome, determined directly from genomic DNA. *Genomics* (in the press).
- Itagaki, K., Carver, G.T. & Philpot, R.M. Expression and characterization of a modified flavin-containing monooxygenase 4 from humans. *J. Biol. Chem.* **271**, 20102-20107 (1996).
- Wierenga, R.K., Terpstra, P. & Hol, W.G.J. Prediction of the occurrence of the ADP-binding βαβ-fold in proteins using an amino acid sequence fingerprint. *J. Mol. Biol.* **187**, 101-107 (1986).
- Overby, L.H. et al. Characterization of flavin-containing monooxygenase 5 (FMO5) cloned from human and guinea pig: evidence that the unique catalytic properties of FMO5 are not confined to the rabbit ortholog. *Arch. Biochem. Biophys.* **317**, 275-284 (1995).
- Suh, J.K., Poulsen, L.L., Ziegler, D.M. & Robertus, J.D. Molecular cloning and kinetic characterization of a flavin-containing monooxygenase from *Saccharomyces cerevisiae*. *Arch. Biochem. Biophys.* **336**, 268-274 (1996).
- Chen, Y.C.J., Peoples, O.P. & Walsh, C.T. Acinetobacter cyclohexanone monooxygenase: gene cloning and sequence determination. *J. Bacteriol.* **170**, 781-789 (1988).
- Tutic, M., Lu, X., Schirmer, R.H. & Werner, D. Cloning and sequencing of a mammalian glutathione reductase cDNA. *Eur. J. Biochem.* **188**, 523-528 (1990).
- Greer, S. & Perham, R.N. Glutathione reductase from *Escherichia coli*: cloning and sequence analysis of the gene and relationship to other flavoprotein disulphide oxidoreductases. *Biochemistry* **25**, 2736-2742 (1986).
- Laddaga, R.A., Chu, L., Misra, T.K. & Silver, S. Nucleotide sequence and expression of the mercurial-resistance operon from *Staphylococcus aureus* plasmid p1258. *Proc. Natl. Acad. Sci. USA* **84**, 5106-5110 (1987).
- Aboagye-Kwarteng, T., Smith, K. & Fairlamb, A.H. Molecular characterization of the trypanothione reductase gene from *Crithidia fasciculata* and *Trypanosoma brucei*: comparison with other flavoprotein disulphide oxidoreductases with respect to substrate specificity and catalytic mechanism. *Mol. Microbiol.* **6**, 3089-3099 (1992).
- Ayesch, R. et al. Deficient nicotine *N*-oxidation in two sisters with trimethylaminuria. *Br. J. Clin. Pharmacol.* **25**, P664-P665 (1988).
- Park, S.B., Jacob, P.J., Benowitz, N.L. & Cashman, J.R. Stereoselective metabolism of (S)-(-)-nicotine in humans: formation of *trans*-(S)-(-)-nicotine *N*-1-oxide. *Chem. Res. Toxicol.* **6**, 880-888 (1993).
- Murray, V. Improved double-stranded DNA sequencing using the linear polymerase chain reaction. *Nucleic Acids Res.* **17**, 8889 (1989).
- Higuchi, R.G. & Ochman, H. Production of single-stranded DNA templates by exonuclease treatment following the polymerase chain reaction. *Nucleic Acids Res.* **17**, 5865 (1989).
- Lake, B.G. Preparation and characterisation of microsomal fractions for studies of xenobiotic metabolism. in *Biochemical Toxicology: A Practical Approach* (eds Snell, K. & Mullock, B.) 183-215 (IRL, Oxford, 1987).
- Dixit, A. & Roche, T.E. Spectrophotometric assay of the flavin-containing monooxygenase and changes in its activity in female mouse liver with nutritional and diurnal conditions. *Arch. Biochem. Biophys.* **233**, 50-63 (1984).